Genetic studies into the origin and transcriptional regulation of midbrain dopaminergic neurons in mice

Hiu Mei Carol Yan

Presented for the degree of Doctor of Philosophy

August 2008

Division of Developmental Neurobiology

National Institute for Medical Research

The Ridgeway, Mill Hill

London NW7 1AA

United Kingdom

Department of Anatomy and Developmental Biology

University College London

University of London

ProQuest LLC
789 East Eisenhower Parkway
P.O. Box 1346
Ann Arbor, MI 48106-1346

Declaration of Authenticity

I, **Hiu Mei Carol Yan**, confirm that the work presented in this thesis is my own. Where information has been derived from other sources, I confirm that this has been indicated in the thesis.

Hiu Mei Carol Yan
1st August 2008

Abstract

The midbrain dopaminergic (mDA) neurons, consisting of anatomically and functionally heterogeneous cell populations, are the major source of dopamine in the central nervous system. They are involved in diverse psychiatric and neurological disorders, including Parkinson's disease (PD), which is marked by the specific degeneration of mDA neurons in the substantia nigra pars compacta. Therefore, understanding the origin and the development of this specific subpopulation will greatly facilitate the development of cell replacement therapy for PD.

Using genetic fate mapping studies, we suggest that mDA neurons originate from the floor plate of midbrain and caudal diencephalon. Unlike the popular believe that the different mDA populations are generated from spatially distinct progenitors, our data have ruled out the medial versus lateral correlation between progenitors and neuronal populations. We provide evidence that medial progenitors can develop into both medial and lateral mDA populations, and late born mDA neurons from lateral progenitors predominantly populate the medial nuclei, suggesting a complex mechanism for the generation of different mDA subpopulations.

The LIM-homeodomain transcription factors, Lmx1a and Lmx1b, are expressed in both mDA progenitors and neurons. *Lmx1a* mutant *dreher* displays a moderate reduction of correctly specified mDA neurons. Previously, Lmx1b has been shown to be essential for the specification and maintenance of mDA neurons. However, these mice have lost the isthmic organiser, which is essential for the induction of mDA neurons. Here, we investigated the specific functions of Lmx1b in the ventral neural tube by a Shh^{cre} mediated conditional deletion of *Lmx1b*. *Lmx1b* conditional mutants show no defect in mDA neuron specification and maintenance, thus arguing against the central role of Lmx1b in mDA neuron development. Nevertheless, double mutant analyses demonstrate that Lmx1a/b regulate the specification and proliferation of mDA progenitors, and their differentiation into mDA neurons in a gene dosage dependent manner. Thus, Lmx1a/b play essential roles throughout the development of mDA neurons.

Acknowledgement

I would like to thank my supervisor Dr Siew-Lan Ang for the wonderful training through the exploration on different projects and the acquisition of a wide range of techniques. It has been great opportunity to work in the stimulating environment of NIMR, to meet many wonderful people, and to learn how to surf over the difficult times of research and life.

I have to thank my mid-term report examiners Drs James Briscoe and Francois Guillemot for inspiring discussions and insightful comments regarding my projects.

I am indebted to Drs. Yannis Mavromatakis, Anna Ferri and Martin Cheung, who have taught me various techniques and given me suggestions on my projects. I would not have achieved this thesis without their guidance and support, and surely not without Dr Yannis Mavromatakis who commented on my thesis in a fortnight.

I would also like to thank Dr Simon Stott for providing me with his beautiful TH staining on horizontal brain section for the introduction, and Dr Wei Lin for sharing his Lmx1a/b gain-of-function data for the discussion of this thesis.

Finally, I would like to thank Dr Shuk Han Cheng for her philosophy, which helped to keep my faith. "We do science not because it is easy, but because it is difficult."

Table of contents

List of figures

List of tables

List of abbreviations

+/+	wildtype
β-gal	β-galactosidase
aa	amino acid
AADC	aromatic L-amino acid decarboxylase
ADHD	Attention deficient hyperactivity disorder
ak	*aphakia*
Ap	Apterous (*Drosophila* Lhx2 orthologue)
AP	anteroposterior
BP	basal plate
BrdU	5-bromo-2'-deoxyuridine
BSA	bovine serum albumin
CA	catecholamine
CB	calbindin
CLi	caudal linear nucleus of raphe
CNS	central nervous system
DA	dopamine / dopaminergic
DAB	diaminobenzidine
DAT	dopamine transporter
DBH	dopamine β-hydroxylase
DCC	deleted in colorectal cancer
dr	*dreher*
DV	dorsoventral
E	embryonic day
EMSA	electrophoretic mobility shift assays
En1	Engrailed 1
En2	Engrailed 2
ER	estrogen receptor
Fgf8	Fibroblast growth factor 8
FP	floor plate
Fz	Frizzled
GFP	green fluorescent protein
Girk2	G-protein-gated inwardly rectifying K+ channel
h	hour
HD	homeodomain
IF	interfascicular nucleus
IP	interpeduncular
Isl1	Islet-1
Isl2	Islet-2
IsO	Isthmic Organiser
L-DOPA	L-dihydroxyphenylalanine

LGE	lateral ganglionic eminence
Li	linear nucleus of raphe
LID	LIM interacting domain
LIM-HD	LIM-homeodomain
LMCl	lateral subset of lateral motor column
LMO	LIM-only
mDA	midbrain dopaminergic
MFB	medial forebrain bundle
MGE	medial ganglionic eminence
MHB	midbrain-hindbrain boundary
min	minutes
$MMCm^{v}$	medial motor column innervating ventral body wall muscles
MN	motor neuron
NMR	nuclear magnetic resonance
OHT	4-hydroxytamoxifen
P	postnatal day
PAG	periaqueductal gray
PBS	phosphate-buffered saline
PBT	PBS, 0.1% (v/v) Triton X-100
PCR	polymerase chain reaction
PD	Parkinson's disease
PFA	paraformaldehyde
PN	paranigral nucleus
PNMT	phenylethanolamine N-methyltransferase
R26R	ROSA26 reporter
RP	roof plate
RR	retrorubral field
Shh	Sonic hedgehog
SNc	substantia nigra, pars compacta
SNl	substantia nigra, pars lateralis
SNr	substantia nigra, pars reticulata
Tam	tamoxifen
TGF-β	Transforming growth factor-beta
TH	tyrosine hydroxylase
Toto	Toto-3-iodide
TSH-β	thyroid-stimulating hormone β-subunit
VMAT	vesicular monoamine transporter type 2
VP	vaginal plug
VTA	ventral tegmental area
wt	wild type
X-gal	5-Bromo-4-chloro-3-indolyl-β-D-galactopyranoside

Chapter 1
Introduction

1.1 Midbrain dopaminergic neuron

Dopamine (DA) belongs to a family of chemicals know as the catecholamines (CA), which also include adrenaline (epinephrine) and noradrenaline (norepinephrine). It was first visualised in neurons along with other CA in formaldehyde histofluorescence studies (Falck et al., 1962). Seventeen CA cell groups (A1 to A17) distributed from the medulla oblongata to the olfactory bulb and retina have been outlined (Figure 1-1) (Dahlström and Fuxe, 1964; Hökfelt et al., 1984). Most of these groups are not confined to single anatomical structures.

The availability of immunohistochemical techniques for the visualisation of molecules and enzymes involved in the synthesis of CA allowed differentiation between various types of CA neurons (Figure 1-2) (Geffard et al., 1984; Goridis and Rohrer, 2002; Hökfelt et al., 1984). Dopaminergic neurons are defined by the expression of tyrosine hydroxylase (TH) and aromatic L-amino acid decarboxylase (AADC), but not dopamine β-hydroxylase (DBH) and phenylethanolamine N-methyltransferase (PNMT). They are found in groups A8-A16 in the midbrain, hypothalamus and olfactory bulb (Hökfelt et al., 1984). The most prominent groups of dopaminergic neurons are the A8-A10 groups located in the ventral midbrain of the central nervous system (CNS), and are collectively referred to as midbrain dopaminergic (mDA) neurons.

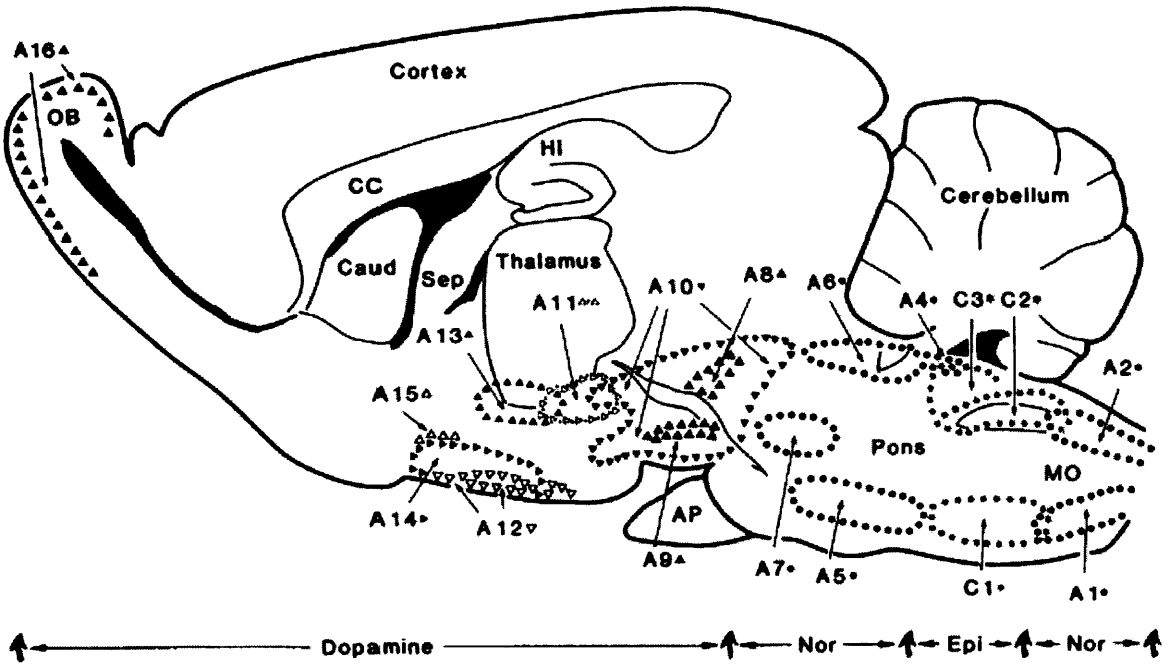

Figure 1-1 Schematic drawing of a sagittal section of the rat brain showing the catecholamine populations 1.4 millimeters lateral to the midline.

The approximate distribution of dopamine (triangles), norepinephrine (dots), and epinephrine (asterisks) cell groups are shown. Each catecholamine principally has its own domain in the brain with dopamine cell bodies (A8 to A16) in the rostral parts of the brain (mesencephalon, hypothalamus, and olfactory bulb) and norepinephrine cells at the pontine (A5 and A6) and lower medullary (Al and A2) levels, whereas the epinephrine cells lie between the rostral and caudal norepinephrine complexes. Abbreviations: AP, anterior pituitary; Caud, caudate nucleus; CC, crus cerebri; HI, hippocampal complex; MO, medulla oblongata; OB, olfactory bulb; and Sep, septum. Diagram taken from Hökfelt et al., 1984.

1.1.1 The neurotransmitter dopamine

The CA neurotransmitters DA, noradrenalin and adrenalin are all synthesized form the amino acid tyrosine in a common biosynthetic pathway (Figure 1-2). Tyrosine is first converted into L-dihydroxyphenylalanine (L-DOPA) by TH in the rate limiting step of DA synthesis (Levitt et al., 1965; Nagatsu et al., 1964a; Nagatsu et al., 1964b). L-DOPA is then decarboxylated to form dopamine by AADC, which also catalyses the biosynthesis of serotonin. DA can then be further converted into noradrenalin by the enzymes DBH, and then to adrenalin by PNMT (reviewed by Goridis and Rohrer, 2002). DA neurons do not produce DBH; therefore, the synthesis of CA terminates at DA.

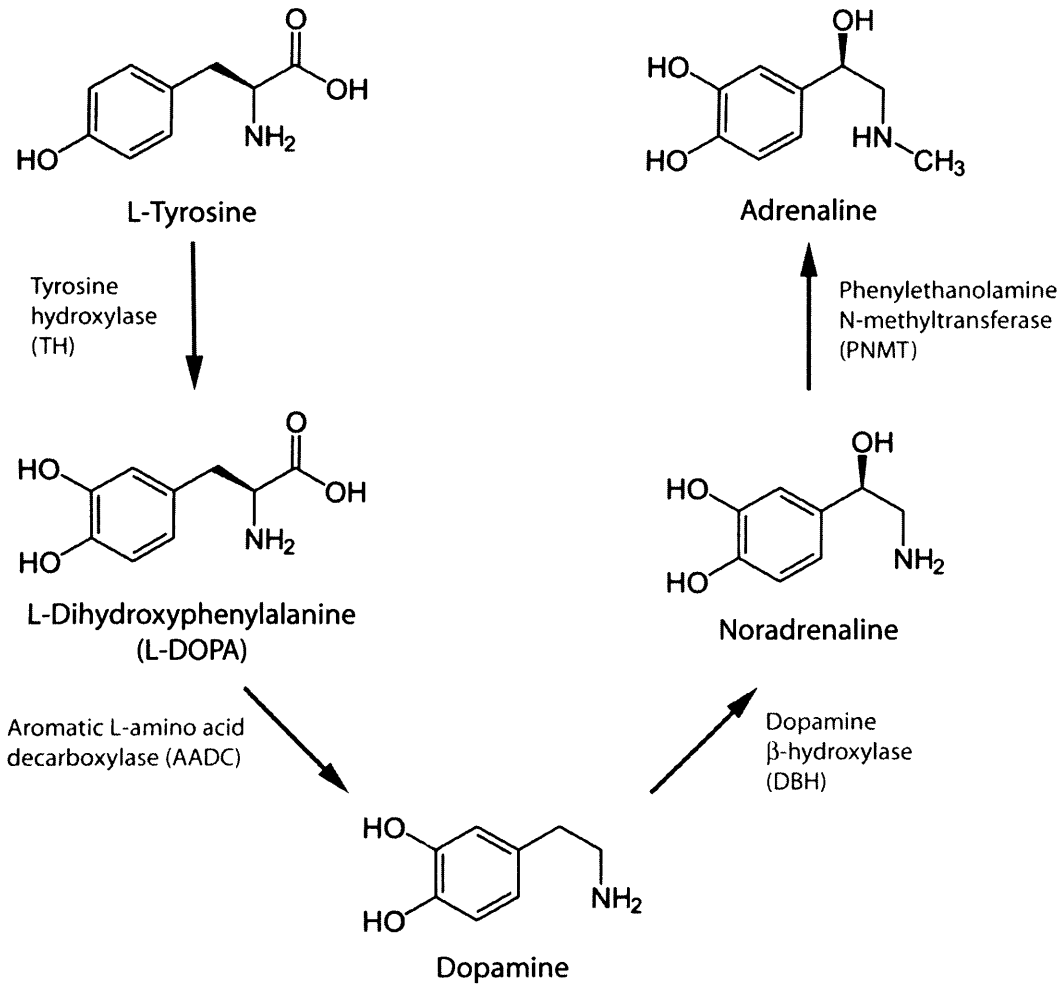

Figure 1-2 The enzymatic pathway of catecholamine synthesis.

Catecholamines are produced from the enzymatic modifications of the amino acid precursor tyrosine.

In DA neurons, DA produced in the cytoplasm is concentrated into synaptic vesicles by the vesicular monoamine transporter type 2 (VMAT). When an action potential arrives at the terminus of the pre-synaptic axon, the vesicles containing DA fuse with the cytoplasm membrane and release DA into the synaptic cleft (Figure 1-3). DA then acts by binding to specific DA receptors on the postsynaptic membrane (Eells, 2003). The synaptic DA can be removed by (1) diffusion from the synapse, (2) enzymatic degradation, and/or (3) recycling via uptake into the pre-synaptic terminal by the DA transporter (DAT) (Giros and Caron, 1993; Horn, 1990).

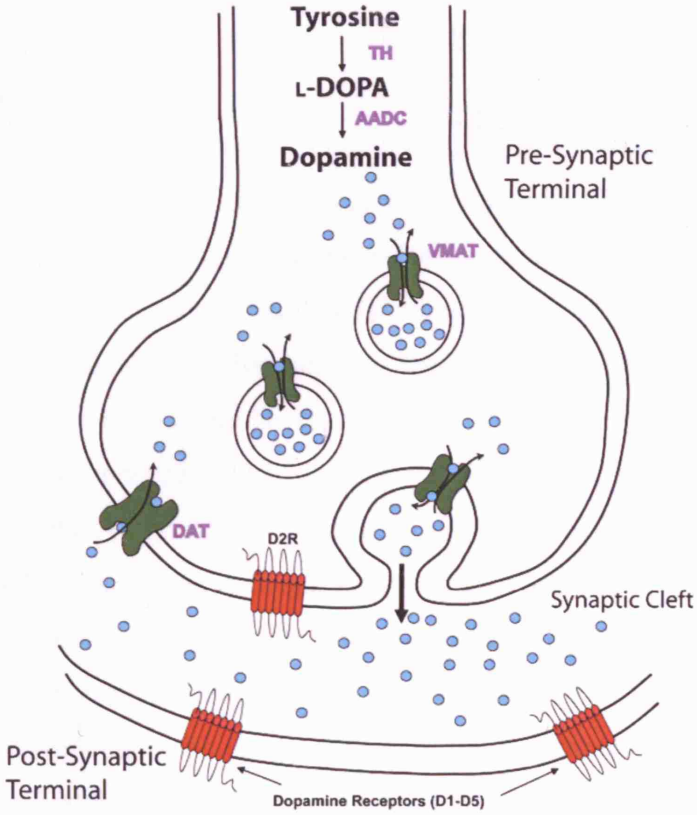

Figure 1-3 Schematic representation of the dopaminergic synapse.

Newly synthesised dopamine in accumulated in the cytoplasm and is then packaged into vesicles by the vesicular monoamine transporter type 2 (VMAT). When an action potential arrives at the pre-synaptic terminal of the neuron, the vesicles containing the dopamine fuse to the cytoplasmic membrane of the pre-synaptic neuron releasing dopamine into the synaptic cleft. Dopamine then binds to its specialised receptors on either the pre- or post-synaptic membrane. Dopamine binding to the pre-synaptic membrane receptors allows the neuron to regulate extracellular dopamine levels. Diagram taken from Mavromatakis, 2006.

1.1.2 The subpopulations of mDA neurons

1.1.2.1 The A8 to A10 groups of mDA neurons

The anatomically and functionally heterogeneous mDA neurons are historically divided into three cell groups: A8 nucleus in the retrorubral field (RR), A9 nucleus in the substantia nigra (SN), and A10 nucleus in the ventral tegmental area (VTA) and related nuclei (Dahlström and Fuxe, 1964; Hökfelt et al., 1984). There is no distinct boundary between these cell groups (Figure 1-4A, S. Stott, unpublished) (Dahlström and Fuxe, 1964). The subpopulations of mDA neurons are distinguished by the anatomical structures, the size and morphology of their somata, as well as their axon projections. The distrubution and innervation of these populations are depicted in Figure 1-4B (Björklund and Dunnett, 2007).

Approximately 11% of the mDA neurons are located in A8, 38% in A9 and 51% in A10 groups in both C57BL/6 and FVB/N mouse strains, although the number of neurons varies between different strains of mice (Nelson et al., 1996).

The A8 group in rat consists mainly of medium-sized cells and some small cells. They are round to oval in shape. The medium-sized cells are often clearly multipolar, and have coarse, intensely stained Nissl granules. The small cells have only fine, moderately stained Nissl granules (Dahlström and Fuxe, 1964). In a mouse study, the neurons in the RR of the A8 group were reported to be large (Nelson et al., 1996). The A8 cells project predominantly to the dorsal striatal matrix (Gerfen et al., 1987).

In the A9 group, the majority of the DA neurons are located in the substantia nigra pars compacta (SNc), and only a small number of the DA neurons reside in the substantia nigra pars reticulata (SNr) and substantia nigra pars lateralis (SNl) (German and Manaye, 1993; Nelson et al., 1996). Neurons from the SNc are large and have prominent projections to the dorsal striatum constituting the nigrostriatal pathway (German and Manaye, 1993; Golden, 1972). The nigrostriatal projection plays an essential role in the control of voluntary motor movement (Chinta and Andersen, 2005).

The DA neurons in the SNc are further sub-divided into two distinct dorsal and ventral populations. The more abundant ventral population contains pyramidal neurons with dendrites projecting ventrally and laterally into the adjacent SNr and axons projecting to the neostriatum. The other population located along the dorsal margin of the SNc contains cells fusiform in shape with dendrites confined to the SNc and axons projecting to the basal forebrain (Fallon et al., 1978).

The A10 group consists mainly of the medium-sized cells in the VTA, parabrachial pigmented nucleus (PBP), paranigral nucleus (PN), some small oval-shaped cells in the interfascicular nucleus (IF) and the linear nucleus of raphe (Li), and large multipolar cells in periaqueductal gray (PAG) (Dahlström and Fuxe, 1964; Flores et al., 2005; Hasue and Shammah-Lagnado, 2002; Nelson et al., 1996; Paxinos and Franklin, 2001). The VTA neurons project into the nucleus accumbens, olfactory tubercle, septum, amygdala and hippocampus giving rise to the mesolimbic and mesocortical pathways to the limbic system and the neocortex respectively (Björklund and Lindvall, 1984; Chinta and Andersen, 2005; Van den Heuvel and Pasterkamp, 2008). The mesolimbic and mesocortical systems are involved in the regulation of emotions and rewards (Di Chiara et al., 2004; Tzschentke, 2000; Van den Heuvel and Pasterkamp, 2008).

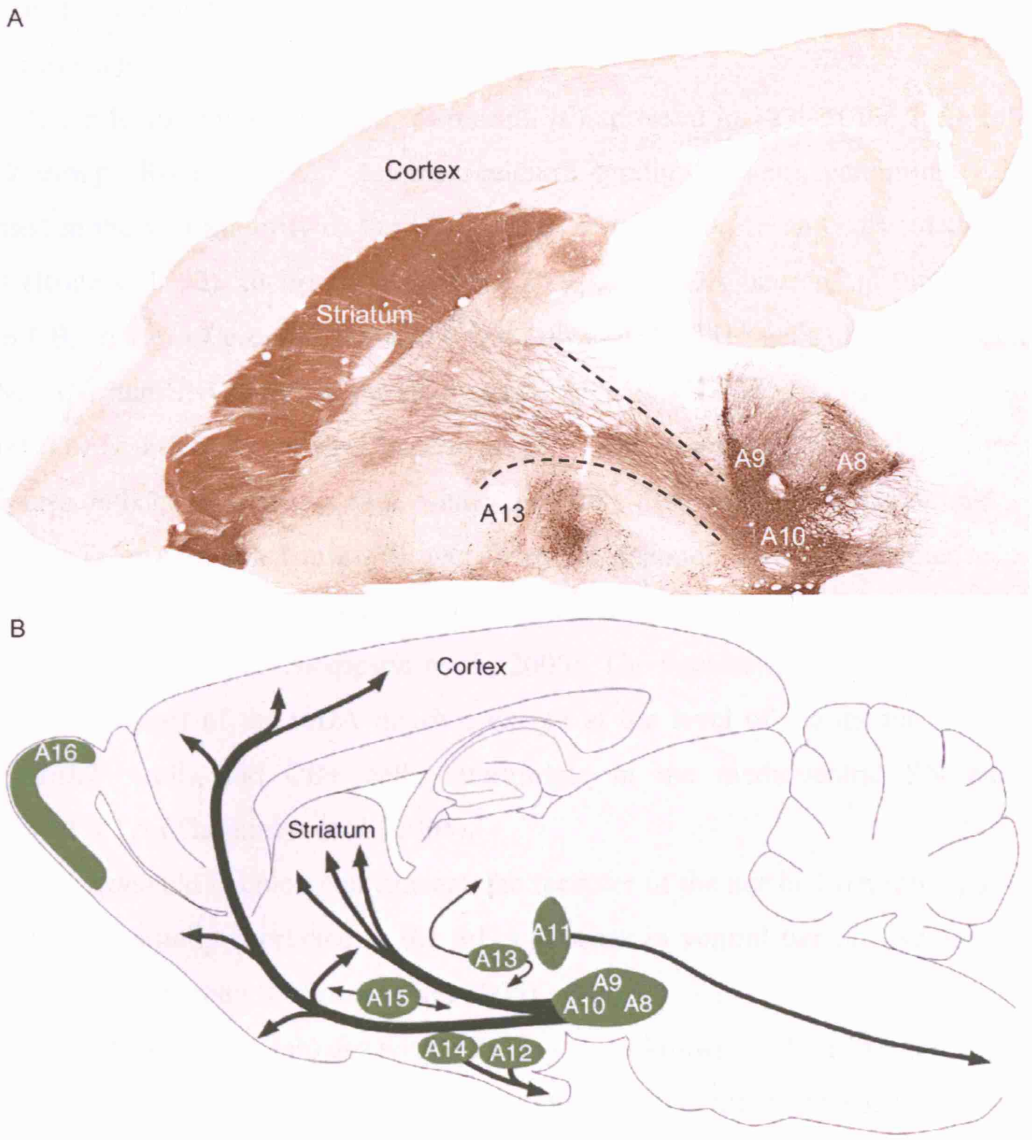

Figure 1-4 Distribution of DA cell groups in the adult rat brain.

(A) A horizontal section stained with an antibody raised against TH, illustrating the A8, A9, A10 and A13 DA cell groups, and the nigrostriatal pathway. The nigrostriatal pathway begins just medial to the SNc forming a dense bundle of fibers projecting rostrolaterally (dashed lines). Picture kindly provided by Simon Stott.

(B) A schematic diagram for the sagittal view of adult rat brain illustrating the localizations of nine distinctive cell groups (A8 to A16) distributed from the mesencephalon to the olfactory bulb. The principal projections of the DA cell groups are illustrated by arrows. Diagram taken from Björklund and Dunnett, 2007.

1.1.2.2 Heterogeneous expression of molecular markers

Studies on the molecular markers expressed by mDA neurons provide increasing evidence that the mDA neurons are more heterogeneous than suggested by the early anatomical studies.

The calcium binding protein, calretinin, is expressed in 72% of the TH+ cells in the A9 group (Rogers, 1992). Another calcium binding protein, calbindin (CB), is expressed in the vast majority of the DA neurons in the VTA, IF and parts of the SN in the rat (Rogers, 1992). In the mouse, about 30% of the DA neurons in the A8 group contain CB. In the A9 group, 21.7%, 0% and 100% of the TH+ cells also express CB in the SNc, SNr and SNl show. In the A10 group, 55% of VTA, 85.7% of Li, 97% of PN and 100% of IF DA cells are double positive for CB (Liang et al., 1996). Therefore, the CB expression is heterogeneous even within the finely divided DA subpopulations.

The G-protein-gated inwardly rectifying K+ channel, Girk2, is detected in SNc, SNr, the lateral aspects of the VTA and in some cells of the A8 group (Inanobe et al., 1999; Schein et al., 1998; Thompson et al., 2005). The expression of Girk2 and CB do not overlap in most of the mDA neurons except at the level of the medial lemniscus, where Girk2+ cells and CB+ cells intermingle in the medioventral SN and the laterodorsal VTA (Thompson et al., 2005).

DCC (deleted in colorectal cancer), the receptor of the netrin-1 neuronal guidance factor, is differentially expressed in the mDA neurons in ventral tier of SNc and the IF nucleus in the A10 group (Osborne et al., 2005).

The retinaldehyde dehydrogenase Raldh1 (also known as Aldh1a1 and Adh2) is mainly expressed in the SNc (A9) subpopulation of the mDA neurons, with minor contribution to the ventral portions of A8 and A10 subpopulations (McCaffery and Dräger, 1994).

Taken together, although preferential expression of particular genes has been observed in certain mDA subpopulations, none of the identified molecular markers is exclusively expressed in any of the mDA subpopulation.

1.1.3 Functional significance of mDA neurons

The importance of the DA neurotransmitter in movement and feeding was highlighted by DA-deficient mice, in which TH gene was inactivated in DA neurons and TH function was restored in noradrenalinergic cells (Zhou and Palmiter, 1995). Moreover, different subpopulations of mDA neurons are implicated in different functions and diseases.

1.1.3.1 Parkinson's disease and the striatal DA system

Parkinson's disease (PD) is a progressive neurodegenerative disorder affecting over 1 million people in North America, with the cardinal clinical symptoms of bradykinesia, resting tremor, rigidity, and postural instability (Lang and Lozano, 1998a; Moore et al., 2005). The onset of PD occurs with the selective degeneration of pigmented DA neurons in the SNc leading to a severe deficiency of DA neurotransmission in the striatum (Hirsch et al., 1988). There is a more severe cell loss in the lightly pigmented cells of the ventral tier of SNc than the heavily pigmented dorsal tier and the paranigral nucleus (Gibb and Lees, 1991). In monkey, PD symptoms appearance is associated with critical thresholds of DA depletion, with 43.2% loss in the TH expressing neurons at the nigral level, and 80.3% and 81.6% reduction in DAT binding and DA content respectively at the striatal level (Bezard et al., 2001).

Due to the degenerative nature of PD, patients lose their response to the symptomatic drug treatment by levodopa, which is readily converted to DA by the remaining neurons (Lang and Lozano, 1998b). Clinical trials for the restorative cell replacement therapy for PD with intrastriatal transplants of fetal midbrain tissue have been proven successful in restoring regulated DA release and significant symptomatic relief, albeit without complications and variability in the clinical benefit (Astradsson et al., 2008; Lindvall and Björklund, 2004; Mendez et al., 2005). The differentiation of DA neurons from pluripotent embryonic stem (ES) cells can potentially allow access to the specific DA cell type at various stages of maturation for the best transplantation effect.

1.1.3.2 Schizophrenia and the cortical DA system

Schizophrenia is a severe, chronic and complex neurological disorder with either psychotic or deficit symptoms. The psychotic symptoms are characterised by hallucinations and delusions, whilst the deficit symptoms are characterised by major

cognitive defects such as poverty of speech and dramatic functional impairment (Egan and Weinberger, 1997; Wong and Van Tol, 2003). The aetiology of schizophrenia remains unclear, but the general consensus is that at least some of the cognitive deficits are related to dysfunction in the prefrontal cortex DA system (Durstewitz and Seamans, 2008). Subcortical DA release has been implicated as an important site of dysregulation in schizophrenia based on the observations that DA agonists amphetamine can elicit psychosis in normal individuals, and that antipsychotic drugs positively correlate with their affinity for the D2 DA receptor (Abi-Dargham et al., 2000; Agid et al., 2007; Angrist et al., 1974; Berry et al., 2003; Egan and Weinberger, 1997; Seeman et al., 1976).

1.1.3.3 Addiction and the limbic DA system

The DA projections from the VTA to the nucleus accumbens of the limbic area have been implicated in the rewarding effects of drug abuse (Pierce and Kumaresan, 2006). The extracellular DA in the nucleus accumbens is preferentially increased by addictive drugs (Bradberry et al., 2000; Di Chiara et al., 2004). Conversely, depletion of DA in this region severely attenuates the rewarding effects of cocaine or amphetamine (Gerrits et al., 2002; Gerrits and Van Ree, 1996).

1.1.3.4 Attention deficient hyperactivity disorder (ADHD) and the prefrontal cortex DA system

ADHD is characterised by symptoms including motor impaired behavioural inhibition, increased motor activity and inattention (Brennan and Arnsten, 2008). Two parallel prefrontal-striatal-thalamic-cortical circuits are involved in the pathophysiology of ADHD (Castellanos, 1997). The first (direct) pathway runs from the prefrontal cortex through the internal segment of the globus pallidus through thalamus, feeding back to exert a net amplification of the original cortical output. A depletion of DA within this pathway results in the difficulty in initiating movement (Rubia et al., 1999). The second (indirect) pathway projects through the external segment of the globus pallidus, and synapses on inhibitory projections from the subthalamic nucleus to the internal globus pallidus to produce a net inhibition of cortical output. A lack of DA activity in this pathway results in excessive motor output (Solanto, 2002).

1.2 The development of mDA neurons

1.2.1 Development of the midbrain

The CNS derives from the dorsal region of the ectoderm of vertebrate embryos to form the neural plate, which subsequently rolls up on its anteroposterior (AP) axis to form the neural tube (Lumsden and Krumlauf, 1996; Wilson and Hemmati-Brivanlou, 1997). The anterior end of the neural tube expands and partitions into a series of vesicles representing the anlagen of forebrain, midbrain and hindbrain. The posterior regions of the neural tube do not undergo an extensive expansion in size and remain as a long narrow tube giving rise to the spinal cord. Subsequently, the forebrain is further subdivided to yield the telencephalon and the diencephalon, while the midbrain does not undergo any further subdivision. The hindbrain also undergoes a further subdivision into the metencephalon and the rhombencephalon (Gilbert, 2003).

The developing neural tube is patterned along the AP and dorsoventral (DV) axes by inductive signals emanating from local signalling centres (Lumsden and Krumlauf, 1996; Simon et al., 1995; Tanabe and Jessell, 1996). The regional fate in the CNS is determined along the AP axis before and independently of fate restriction of the DV axis (Lumsden and Krumlauf, 1996). Stereotypically arranged neurons are then developed from neural progenitors that assume distinct cell fates according to their locations on a Cartesian grid of positional information along these axes (Hynes and Rosenthal, 1999; Lumsden and Krumlauf, 1996).

In the midbrain, local AP pattern is generated by the signalling activities from the Isthmic Organiser (IsO) located at the midbrain-hindbrain boundary (MHB), which is formed some distance anterior to the isthmic constriction (Lumsden and Krumlauf, 1996). The position of the MHB is governed by the opposing interactions of two homeodomain (HD) transcription factors Otx2 and Gbx2 (Simeone, 2000). Along the DV axis, two signalling centres, one located dorsally in the roof plate (RP) and the other located ventrally in the floor plate (FP), are the sources of signalling molecules that pattern cell types along this axis (Jessell, 2000; Lee and Jessell, 1999).

1.2.2 Induction of mDA neurons by signalling molecules

1.2.2.1 Sonic hedgehog (Shh)

The secreted molecule Shh is first expressed in the midline mesoderm of the head process at the late streak stages of gastrulation, and then extends to the notochord (Echelard et al., 1993). The CNS expression of Shh initiates at the ventral midline of the midbrain at 8-somite stage, and rapidly extends rostrally into the forebrain and caudally into the hindbrain and spinal cord. In the hindbrain and spinal cord, Shh expression is restricted to the FP, whereas it extends ventrolaterally in the midbrain (Echelard et al., 1993).

In the developing midbrain, DA neurons were first suggested to develop in close proximity to the FP, which is sufficient for the induction of DA neurons in midbrain explant cultures and in the dorsal midbrain with an ectopic FP (Hynes et al., 1995b). Shh is subsequently demonstrated to be the inductive signal derived from the FP that is responsible for the induction of DA neurons (Hynes et al., 1995a).

1.2.2.2 Fibroblast growth factor 8 (Fgf8)

It was later shown that the intersection of Shh from the FP and Fgf8 from the IsO is responsible for the induction of mDA neurons (Hynes et al., 1995a; Wang et al., 1995; Ye et al., 1998). Moreover, FGF8 blocking experiments show that the level of FGF8 correlates with the number of DA neurons generated in ventral midbrain explants (Ye et al., 1998).

Fgf8 expression is detected in the prospective MHB between E8.0 and E8.5, and becomes restricted to the isthmic constriction at around E9.0 to E9.5 (Crossley and Martin, 1995). The Fgf8 protein has been shown to produce the same midbrain-inducing and polarising effect as the isthmic tissue (Crossley et al., 1996). Since Fgf8 is shown to regulate the expression of Wnt1, Engrailed 1 (En1) and Engrailed 2 (En2) in the MHB that are also implicated in mDA neuron development (Crossley et al., 1996; Shamim et al., 1999), it was not clear if Fgf signalling played a direct role in mDA neurons development. A recent study showed that Fgf receptors (Fgfrs) acted redundantly to regulate the development of mDA progenitors and the maturation of mDA neurons without affecting Wnt and Shh signalling as well as neurogenic gene expression in the

ventral midbrain (Saarimaki-Vire et al., 2007). This suggests a more direct role for Fgf signalling in the development of mDA neurons.

1.2.2.3 Wnts

Wnt1 (originally named Int-1) is expressed in the presumptive midbrain throughout the neural plate stages, and gradually becomes restricted to a tight circle lying just anterior to the isthmus by neural tube closure (McMahon et al., 1992; Parr et al., 1993; Wilkinson et al., 1987). Wnt1 has been shown to regulate midbrain development by maintaining En1 expression (Danielian and McMahon, 1996; McMahon et al., 1992; Wurst et al., 1994).

In the developing midbrain, thirteen out of nineteen members of the Wnt secreted molecule and all ten Frizzled (Fz) receptors have been shown to be expressed by quantitative polymerase chain reaction (PCR) (Rawal et al., 2006). Among the members of the Wnt family, Wnt1 and Wnt5a are highly expressed in the ventral midbrain, while Wnt3a is expressed at higher levels in the dorsal midbrain during mDA neuron generation (Castelo-Branco et al., 2003). In addition to the expression anterior to the isthmus, Wnt1 is also detected in two stripes adjacent to the floor plate of the midbrain and overlaps with the region where mDA progenitors first appear (Prakash et al., 2006).

The functions of these three Wnt proteins in mDA neuron development have been shown by both *in vitro* and *in vivo* studies. Treatment of rat ventral midbrain cultures with Wnt conditioned media show that Wnts are key regulators for the proliferation and differentiation of mDA progenitors, and that each Wnt has different functions in DA neuron development (Castelo-Branco et al., 2003). Wnt1 enhances the production of DA neurons by regulating the proliferation of DA precursors. It up-regulates the expressions of cyclins D1 and D3, which promote cell cycle progression, and down-regulates the expression of cell cycle inhibitors p27 and p57. Wnt5a primarily promotes the maturation of DA precursors into DA neurons, and up-regulates the expression of Pitx3 and c-ret mRNA. Wnt3a is able to promote the proliferation of mDA precursor cells, but it does not increase the number of TH+ neurons.

Besides playing a role in mDA precursor proliferation *in vitro*, Wnt1 is also required for the proper differentiation of mDA neurons. In *Wnt1*$^{-/-}$ mutant embryos, only very few DA neurons expressing the mature mDA markers Nurr1 and TH were generated, and these cells fail to express Pitx3 (Prakash et al., 2006).

1.2.2.4 Transforming growth factor-beta (TGF-β)

In the midbrain, TGF-β2 and TGFβ-3 are expressed in the ventral marginal and mantle zones where differentiating neurons, glial cells and their processes are located at E12 mouse embryos (Flanders et al., 1991), and their location coincides with the TH expressing region.

Treatment of E12 rat ventral midbrain dissociated cultures with TGF-β3 for 24 hours (h) increases the number of TH+ cells without affecting cell proliferation and survival (Farkas et al., 2003). In a similar study, treatment of ventral midbrain dissociated neurospheres with TGF-β can induce the number of Nurr1+ and TH+ cells, and the induction is enhanced by a combined treatment with TGF-β, Shh and Fgf8 (Roussa et al., 2006). Interestingly, the expression of another mDA marker Pitx3 is not induced in these treatments. On the other hand, reducing the endogenous TGF-β by neutralising antibody reduces the production of TH+ neurons in chick during the induction of mDA neuron at E2-E3 (Farkas et al., 2003). Double knockout mice studies show that TGF-β2 and TGF-β3 are also required for the differentiation of mDA neurons (Roussa et al., 2006). Furthermore, neutralising TGF-β after the acquisition of the TH phenotype results in significant loss of TH+ neurons (Farkas et al., 2003). Thus, TGF-β is required for induction, differentiation and survival of mDA neurons.

1.2.3 Molecular specification of mDA neurons

The positional information laid down by these extrinsic factors is then translated into cell intrinsic determinants to specify mitotically active progenitor cells to postmitotic differentiating immature DA neurons and finally to mature differentiated neurons. The progressive restriction of cell fate relies on an array of transcription factors that act at distinct steps to control the precise timing and location for the expression of downstream target genes that control cell proliferation, neurogenesis, cell morphology, neurotransmitter phenotype, cell migration, axon pathfinding, synaptic specificities, survival, and so on.

Although the molecular mechanisms underlying mDA neuron development is still poorly understood, several key molecules have been identified and are presented below in their rough chronology of expression in the mDA system.

1.2.3.1 Foxa1 and Foxa2

In the CNS, the Forkhead box transcription factors Foxa1 and Foxa2 (previously know as HNF-3α and HNF-3β respectively) are expressed in the ventral midline of the neural tube, and it is spread more dorsally in the midbrain than in the posterior neural tube (Lai et al., 1990; Lai et al., 1991; Sasaki and Hogan, 1993). Ectopic expression of Foxa2 in the dorsal midbrain and rostral hindbrain by the En2 promoter is sufficient to induce the expression of Shh as well as the generation of TH expressing DA neurons in the dorsal midbrain (Hynes et al., 1995b). This study however cannot dissociate if Foxa2 can induce mDA development independent of Shh.

It is later shown that Foxa2 together with Foxa1 are expressed in both the mDA progenitors and postmitotic neurons (Ferri et al., 2007). Double mutant studies on *Foxa1*$^{-/-}$ and a conditional mutant of Foxa2, in which Foxa2 is inactivated from E10.5 so that mDA progenitors are unaffected, have demonstrated that Foxa1/2 positively regulate the expression of Ngn2, thus neurogenesis (Ferri et al., 2007). Moreover, Foxa1/2 are also required for the acquisition of mDA neuronal fate by regulating the expression of the mDA postmitotic markers Nurr1, En1, AADC and TH (Ferri et al., 2007).

A recent study shows that Foxa2 is also expressed in the adult mDA neurons and that a reduced level of Foxa2 protein leads to a progressive loss of mDA neurons and a motor behavioural deficit that spontaneously appears in old age (Kittappa et al., 2007). These studies show that Foxa2 plays important roles in the generation and maintenance of mDA neurons.

1.2.3.2 Lmx1a and Lmx1b

Lmx1a and Lmx1b, members of the LIM-homeodomain (LIM-HD) transcription factor family, are both expressed in the ventral mesencephalon and caudal diencephalon where mDA neurons are thought to be generated (Andersson et al., 2006b). Lmx1a transcript and protein are first detected in the ventral midbrain at E8.5 and E9 respectively (Andersson et al., 2006b; Millen et al., 2004). Lmx1a is specifically expressed in mDA progenitors and maintained in mDA postmitotic neurons (Andersson et al., 2006b), and its expression persisted in the ventral midbrain at least until E16.5 (Failli et al., 2002). Lmx1b is expressed broadly around the presumptive midbrain-hindbrain boundary at E8.5, and becomes restricted to the ventral midbrain and caudal diencephalon at E9.5 (Guo et al., 2007). This early expression of Lmx1b is not restricted to mDA progenitors. Lmx1b expression become downregulated in mDA progenitors at

E11.5 (Andersson et al., 2006b). *Lmx1b* RNA expression is maintained in the SNc and VTA throughout adulthood (Smidt et al., 2000).

Lmx1b plays an early essential role in the development of the midbrain development by regulating the expression of genes such as *Fgf8*, *Wnt1*, *En1* and *Pax2* that are required for the midbrain and hindbrain development (Guo et al., 2007; Matsunaga et al., 2002). In the mDA system, Lmx1b is proposed to be required for the differentiation and maintenance of mDA neurons without affecting the neurotransmitter phenotype (Smidt et al., 2000). *Lmx1b* null mutants initially develop a reduced field of TH+ mDA neurons, which lack the expression of a key mDA neuronal marker Pitx3. After E16, TH expression is no longer detectable. The presence of TH but loss of Pitx3 expression in *Lmx1b*$^{-/-}$ mutants at early stages has led the authors to propose an Lmx1b-Pitx3 pathway in mDA neuron specification independent of the neurotransmitter phenotype.

During this thesis, two groups have reported on the roles of Lmx1a in mDA neuron development. In chick embryos, Lmx1a is both required and sufficient for DA neuron generation in the ventral midbrain (Andersson et al., 2006b). Mis-expression of Lmx1a in chick midbrain at HH stage 10 extensively induces ectopic DA neurons in the ventral midbrain region, whereas siRNA knockdown of Lmx1a drastically reduce postmitotic DA neurons. Lmx1a is both sufficient and required for the expression of Msx1 in mDA progenitors. Knockdown of Lmx1a does not affect the progenitor expression of Lmx1b, which cannot compensate for the loss of Lmx1a in DA neuron generation. Furthermore, Lmx1a is a much more potent inducer of TH+ neurons than Lmx1b when transfected into mouse embryonic stem (mES) cells ventralised by Shh. Contrary to the striking phenotype in *Lmx1b*$^{-/-}$ mouse embryos, Lmx1b does not appear to be a key determinant in mDA specification in the chick model.

The other group reported the involvement of Lmx1a in mDA neuron specification using the spontaneous mouse mutant *dreher* (*Lmx1a*$^{dr/dr}$). In contrast to the almost complete loss of DA neurons in chick *Lmx1a* knockdown, the *Lmx1a*$^{dr/dr}$ mutants only show a 32% reduction of Lmx1b+ neurons per section at E13.5 (Ono et al., 2007). Consistent with the reduction in mDA neurons, Ngn2+ and Mash1+ cells are reduced to approximately 70%. Interestingly, the authors claimed no significant change in the total number of Lmx1a+ progenitors in the *Lmx1a*$^{dr/dr}$ mutant despite showing a decrease in BrdU incorporation. The reduction of BrdU incorporation is similar to those of Ngn2 and Mash1 expressing cells. Apart from the reduction in Ngn2 and Mash expression, the specification of progenitors appears normal. The expressions of mDA neuronal markers

are mostly normal, except for the ectopic expression of Lim1/2 in some lateral Lmx1b+ neurons, which do not express TH and Pitx3. The projections of TH+ axons to the striatum are also normal. Taken together, Lmx1a is required for mDA neurogenesis and correct differentiation of mDA neurons.

1.2.3.3 Engrailed 1 (En1) & Engrailed 2 (En2)

Two closely related homeobox transcription factors En1 and En2 have been identified in vertebrates (Joyner et al., 1985; Joyner and Martin, 1987). En1 starts to be expressed in the presumptive MHB region at the 1-somite stage, followed by the expression of En2 at the 5-somite stage (Davis and Joyner, 1988). *En* genes play an early role in maintaining the expression of Fgf8 in the MHB (Liu and Joyner, 2001).

In the mDA system, En1/2 are expressed in the mDA neurons during embryonic stages and in the SN, VTA and PAG at postnatal day 0 (P0). En1 is highly expressed by essentially all DA neurons in the SN and VTA, whereas En2 is highly expressed by a subset of them and weakly expressed in the remaining cells. In the adult brain, En1/2 are co-ordinately expressed in the SN and VTA (Simon et al., 2001). In the development of mDA neurons, En1/2 substantially compensate for the loss of one another such that single mutants of either *En1* or *En2* display a relatively normal appearance of SN and VTA (Simon et al., 2001). In *En1/2* double mutants, despite the general deletion of the midbrain and hindbrain region, a small population of mDA neurons are generated at E11, exhibit a lack of TH axonal outgrowth towards the basal forebrain, and these neurons disappear by E14 (Alberi et al., 2004; Liu and Joyner, 2001; Simon et al., 2001).

It has also been shown that *En* genes are required to prevent apoptosis in mDA neurons in a cell-autonomous manner (Alberi et al., 2004). Moreover, the expression of α-synuclein, which has been genetically linked to PD in humans, is lost in *En1/2* double mutants (Simon et al., 2001).

1.2.3.4 Msx1

Muscle segment homeobox gene *Msx1* is first expressed in mDA progenitors at E9.5, and remains restricted to a medial mDA progenitors domain slightly smaller than that of *Lmx1a* at least until E12.5 (Andersson et al., 2006b). Although electroporation of Lmx1a into the chick ventral midbrain can induce Msx1 expression and DA fate, overexpression studies show that Msx1 is insufficient to induce ectopic DA neurons in

the midbrain (Andersson et al., 2006b). Similarly, transfection of Msx1 driven by the Nestin enhancer is insufficient to induce DA fate in mouse embryonic stem cells. Instead of mediating the induction of mDA fate by Lmx1a, Msx1 functions to suppress alternative cell fate by repressing Nkx6.1, and to promote pan-neuronal differentiation. Because premature expression of Msx1 in the ventral midbrain induces differentiation of mDA progenitors, the authors suggested that Msx1 controls the timing of DA cell neurogenesis. However, in *Msx1* knockout embryos, there is only 40% reduction in Ngn2+ progenitor cells and Nurr1+ DA neurons, suggesting that other factors, possibly *Msx2*, may compensate for the loss of *Msx1* in DA neuron generation (Andersson et al., 2006b).

1.2.3.5 Neurogenin 2 (Ngn2)

The proneural basic helix-loop-helix (bHLH) transcription factor Ngn2 regulate neural cell fate as well as specifying neuronal subtype identities (Bertrand et al., 2002; Brunet and Ghysen, 1999; Guillemot, 1999). In the ventral midbrain, three proneural bHLH genes have distinct expression profiles. Of these, Mash1 and Ngn2 are expressed in a fraction of the mDA progenitors, whereas Ngn2 is also expressed in some Nurr1 expressing postmitotic neurons in the intermediate zone (Kele et al., 2006).

Mutational studies in mouse have shown that that Ngn2 is the major proneural factor required for the development of mDA neurons. Ngn2 null mice have a substantial loss of mDA neurons at early stages of mDA development that only thin stripes of TH+ cells are present in the lateral edges of the mDA neuron domain, but this loss is partially and gradually recovered during embryonic development (Andersson et al., 2006a; Kele et al., 2006). This is due to a partial compensation by Mash1 based on the observation that *Mash1*;*Ngn2* double mutant embryos show a stronger reduction of mDA neurons and that substituting *Mash1* allele into the *Ngn2* locus can partially accelerate the differentiation of DA precursors in *Ngn2* mutants (Kele et al., 2006). Therefore, Ngn2 is uniquely required for the development of mDA neurons.

1.2.3.6 Nurr1

The orphan nuclear receptor Nurr1 (also known as Nr4a2) is widely expressed in the CNS including mDA neurons. During embryonic development, Nurr1 is expressed when mDA neurons become postmitotic (Wallén et al., 1999). In the adult, Nurr1 is

expressed in the majority of the TH+ neurons in the SN, VTA, RR, Li and central grey area (Bäckman et al., 1999).

Knockout mice studies have shown that Nurr1 is not required for the neuronal differentiation of mDA and the expression of the mDA marker genes En1/2, Pitx3 and Raldh1 (Wallén et al., 1999). Instead, it plays critical roles in the maturation, migration, striatal target area innervation, and survival of differentiating mDA cells by regulating the expression of TH, AADC, DAT and VMAT-2 (Hermanson et al., 2003; Kim et al., 2007; Sacchetti et al., 2001; Sakurada et al., 1999; Saucedo-Cardenas et al., 1998; Schimmel et al., 1999; Wallén et al., 1999).

A Nurr1 response element has been identified in the proximal region of the TH promoter that mediates a moderate activation of the promoter suggesting a direct regulation (Iwawaki et al., 2000; Sakurada et al., 1999). Furthermore, the identification of Nurr1 mutations in patients with familial PD has underscore its clinical significance (Le et al., 2003).

1.2.3.7 Pitx3

The paired-like homeodomain transcription factor Pitx3 (also known as Ptx3) is expressed in the postmitotic mDA neurons from E11.5 and restricted in the mDA system until adulthood (Holland and Takahashi, 2005; Smidt et al., 1997; Zhao et al., 2004). A double immunohistochemistry study shows that Pitx3 are preferentially expressed in the ventral but not the dorsal tier of the SNc, and about half of those in the VTA in the adult (van den Munckhof et al., 2003). However, a knock-in GFP reporter of Pitx3 shows overlapping expression of GFP and TH in the vast majority of the mDA neurons in the SN and VTA (Zhao et al., 2004).

The functions of Pitx3 have been studied in the spontaneous *aphakia* (*ak*) mutant mice. In these Pitx3-deficient mice, mDA neurons are born and differentiated, but the TH+ cells in the SN fail to survive and undergo apoptosis during the fetal period (van den Munckhof et al., 2003). This leads to a dramatic reduction of DA innervation in the dorsolateral striatum. The VTA is only reduced by half at P100, and its innervation into the ventral striatum is less severely affected (van den Munckhof et al., 2003). The TH immunoreactivity in A8 group of *ak* mice is comparable to wild type mice (Nunes et al., 2003). These demonstrate a specific requirement of Pitx3 for the development of the mDA neurons in the SN.

1.2.3.8 Raldh1

The retinaldehyde dehydrogenase Raldh1 (also known as Adh2) mediates the oxidation of retinaldehyde to retinoic acid. In mouse embryos, Raldh1 expression is detected in the ventral midbrain from E9.5 in a rostral caudal gradient where its expression is stronger in the more caudal parts (Wallén et al., 1999). Raldh1 is also expressed in postmitotic mDA neurons co-localising with Nurr1 and TH.

Raldh1 is expressed in mDA neurons from E13, and is also present in axons and terminals of a subpopulation of DA neurons projecting from the ventral midbrain to the corpus striatum and the shell of the nucleus accumbens via the mesostriatal and mesolimbic pathway respectively (McCaffery and Dräger, 1994). In the adult, Raldh1 is mainly expressed in the SNc (A9) subpopulation of the mDA neurons, with minor contribution to the ventral portions of A8 and A10 subpopulations (McCaffery and Dräger, 1994).

Pitx3 is suggested to activate Raldh1 transcription by interacting with a highly conserved enhancer region in intron 1 of *Raldh1* gene (Jacobs et al., 2007). This regulation is supported by a severe reduction of Raldh1 expression in *Pitx3*-deficient mice. In these mice, Raldh1 expression is lost at E13.5, and is complete absent in the SNc and lateral VTA, while only maintained in some mDA neurons in the caudal VTA. Maternal supplementation of RA can compensate for the loss of Raldh1 expression caused by *Pitx3* deficiency. These data thus link RA synthesis to the differentiation and maintenance of a specific mDA neuronal subpopulation.

1.2.3.9 Tyrosine hydroxylase

TH is the rate limit enzyme in the biosynthesis of the catecholamine (Section 1.1.1, Figure 1-2), thus a major determinant for the DA neurotransmitter phenotype. TH expression has been studied in different species (Marín et al., 2005; Puelles and Verney, 1998; Specht et al., 1981a; Vitalis et al., 2000). During mouse embryogenesis, TH transcript can be detected from E10 in the floor plate of the most rostral midbrain and in the caudal diencephalon up to the mammillary recess, corresponding to the mDA anlage (Marín et al., 2005). At E11, this domain reaching the ventricular surface expands laterally into the mantle layer of the midbrain and diencephalic basal plate in a rostral to caudal gradient. By E12, the TH labelling in the floor plate disappears from the proliferative zone and move to the mantle layer reaching down to the isthmic region

(Marín et al., 2005). In rat embryos, TH protein is reported to be first detected in migrating and cytologically immature neurons from E12.5 (Specht et al., 1981a). In the mouse, TH protein is only observed in the mantle zone and serves as a marker for mature mDA neurons (Andersson et al., 2006a; Ferri et al., 2007; Kele et al., 2006).

According to Marin et al., 2005, the TH expressing cells in ventral midbrain and caudal diencephalon show an incipient mediolateral subdivision into the A8, A9 and A10 group as early as E12.5-13.5 (Figure 1-5).

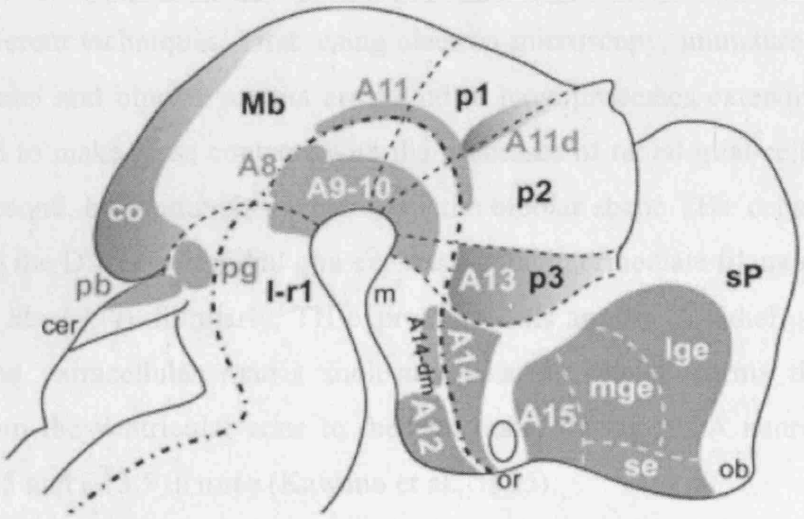

Figure 1-5 Schemetic diagram of *TH* RNA expression in embryos ranging from E12.5 to E14.5.

The dopaminergic groups are represented in relation to the neuromeric map (subdivision into isthmic region [I-r1], midbrain [Mb], prosomeres 1 to 3 (p1-3), and secondary prosencephalon [sP]) and the subdivision between alar and basal plates. The *TH* profile is basically maintained from E12.5 to E14.5 with the exception of the dissipation of dorsal A11 (A11d) after E13. The A16 group located in the olfactory bulb, with no expression at these stages, and A17, whose expression in the retina was present from E10.5 are not shown. The dorsomedial hypothalamus is included as part of A14 (A14-dm). cer, cerebellum; co, inferior colliculus; ob, olfactory bulb; pb, parabrachial nucleus; pg, parabigeminal nucleus. Diagram taken from Marín et al., 2005.

1.2.4 Late differentiation processes of mDA neurons

1.2.4.1 Migration of mDA neurons

The mDA neurons are hypothesized to migrate in three sequential phases (Figure 1-6) (Kawano et al., 1995; Nishikawa et al., 2003; Ohyama et al., 1998). First, newly born DA neurons migrate ventrally from the ventricular surface along radial glial fibres. Then, they migrate laterally along the ventral pial surface along tangentially arranged fibres. Finally, they migrate farther laterally leaving the tangential fibres or the VTA cell group to the SN region.

The theory on radial migration of young neurons is based on the observations from two different techniques. First, using electron microscopy, immature neurons with elongated nuclei and bipolar somata are found to have processes extending in the DV direction, and to make close contacts with the processes of radial glial cells (Kawano et al., 1995). Second, by immunohistochemistry, the bipolar shape TH+ cells are observed to align along the DV axis of radial glia expressing the intermediate filament vimentin in rat (Shults et al., 1990). Similarly, TH expressing cells appose to radial glial processes expressing the extracellular matrix molecule tenascin, which forms thin processes extending from the ventricular zone to the pial mater during mDA neuron generation between E10.5 and E13.5 in mice (Kawano et al., 1995).

Further from the ventricular zone, the majority of the more mature TH positive neurons are oriented parallel to the ventral pial surface, and align along the horizontal fibre bundles expressing neurofilament (Kawano et al., 1995). The chondroitin sulfate proteoglycan, 6B4 proteoglycan, is expressed on the cell bodies of migratory DA neurons immediately before they translocate on the tangential fibres from E11.5 to 13.5 (Ohyama et al., 1998). These cells are closely apposed to tangentially arranged nerve fibres expressing the cell adhesion molecule L1. Since these molecules have been shown to interact *in vitro*, it has been suggested that the heterophilic interaction between 6B4 proteoglycan on mDA neurons and L1 on the fibres is involved in the lateral migration of mDA neurons. The role of L1 in the migration of mDA neurons has subsequently been demonstrated in knockout mice. These mice display an altered rostrocaudal distribution of DA neurons in the SN and VTA, where fewer TH+ neurons are present in the rostral midbrain, while more TH+ cells are found in caudal regions (Demyanenko et al., 2001).

The third phase of migration was suggested by the study on the Reelin mutants. The secreted glycoprotein Reelin is encoded by *reeler* gene and is essential for the correct positioning of neurons (Rice and Curran, 2001). Reelin transcripts are detected in the striatum but not in the ventral midbrain, while its protein is suggested to be axonally transported from the striatal primordium to the ventral midbrain. Reelin is required for the tangential migration of DA neurons in the SN, such that DA neurons in the SN fail to migrate laterally and become clustered just lateral to the VTA in *reeler* mutants (Nishikawa et al., 2003). Interestingly, the number of DA neurons and their projections to the striatum are both unaffected by this mutation.

In rat, the distribution and appearance of the mDA neuronal structures at E18 resemble that in the adult brain, where E1 is the day of vaginal plug detection (Specht et al., 1981b). It is then extrapolated to the mouse time table that mDA neurons are probably settled by E15.5, where the detection of vaginal plug is designated as E0.5 (Bayer et al., 1995).

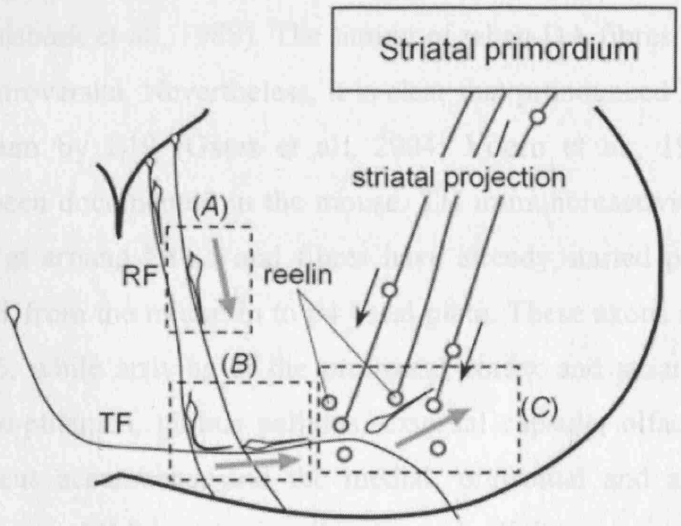

Figure 1-6 Schematic diagram of the hypothetical role of Reelin in the lateral migration of nigral DA neurons.

The nigral DA neurons are proposed to migrate to their given positions in the adult brain in three sequential phases. First [phase (A)], they migrate toward the ventromedial mesencephalon along radial glial fibers (RF) with the DA neurons destined for the VTA. Second [phase (B)], they migrate laterally in the basal part of the mesencephalon along tangentially arranged nerve fibers (TF) with the VTA neurons. In the final phase (C), they migrate farther laterally, leaving from the TF or the VTA cell group. Because the VTA is almost normally formed but the nigral DA neurons are anomalously clustered just lateral to the VTA in *reeler* mutants, Reelin is proposed to derive from the striatal primordium and to play a role in the more lateral migration of nigral DA neurons found in phase (C). Diagram taken from Nishikawa et al., 2003.

1.2.4.2 Axon projections of mDA neurons

The ultimate goal of a neuron is to form a functional circuit by projecting axons, connecting to the target cells and conveying messages through its specific neurotransmitter.

The mDA neurons start to develop their circuit soon after they are generated. In the rat, mDA neurons start to express TH at around early E12. About 6 h later, they have already begun to extend their axons dorsally before re-orienting their growth rostrally towards the developing forebrain by E13 (Nakamura et al., 2000). By E14, these axons continue to project rostrally along the ventral forebrain along the immature medial forebrain bundle (MFB) to a point just ventral and slightly caudal to the lateral ganglionic eminence (LGE) (Gates et al., 2004). The amount of TH+ axons in the region continues to increase over the next few days. DA fibres have passed through the developing striatum to reach the cortical regions in the ventral part of the lateral wall of the frontal hemisphere at E15, to reach the medial wall at E17, to arrive at the most dorsal part of the cortex on E18, and to distribute throughout the greater part of the cortex by E19 (Kalsbeek et al., 1988). The timing of when DA fibres begin to innervate the striatum is controversial. Nevertheless, it is clear that pronounced DA projection has reached the striatum by E19 (Gates et al., 2004; Voorn et al., 1988). Similar DA projections have been documented in the mouse. TH immunoreactivity is first detected in the mDA area at around E11.5 and fibres have already started projection rostrally following the MFB from the midbrain to p4 basal plate. These axons reach the caudate-putamen by E14.5, while arriving at the prefrontal cortex and striatum by E15.5. By E18.5, the caudate-putamen, globus pallidus, external capsule, olfactory tubercle and ventrolateral nucleus accumbens, and the medial, prefrontal and anterior cingulated cortices have all received DA innervation (Vitalis et al., 2000).

The axonal outgrowth of mDA neurons is dependent on the graded directional cue along the rostrocaudal axis (Nakamura et al., 2000). Moreover, these axons display a temporal and graded chemoattractive response to the MFB and LGE/striatal regions, while showing a chemorepulsive response to the embryonic cortex and brain stem, or unresponsive to thalamic tissue (Gates et al., 2004). It is conceivable that the mDA neurons project to their target area via complex set of attractive and repulsive guidance molecules in the environment. For example, in *Pax6* mutant mice, except for a small population of fibres that follows the normal route of the MFB, most of the mDA axons are misrouted dorsally at the presumptive p1/p2 boundary, looping at the roof of p2,

plunging mediolaterally after the presumptive p2/p3 border, and finally turning rostroventrally in p3 basal plate to follow the original MFB in p4 and p5 (Vitalis et al., 2000). In these mutants, there are general aberrant fibre pathways in the diencephalon shown by the ectopic expression of general axonal pathway markers NCAM and L1. The authors further suggested a link between the dorsal expansion of the laminin-related secreted protein Netrin-1 and the tangential migration and pathfindings of mDA neurons.

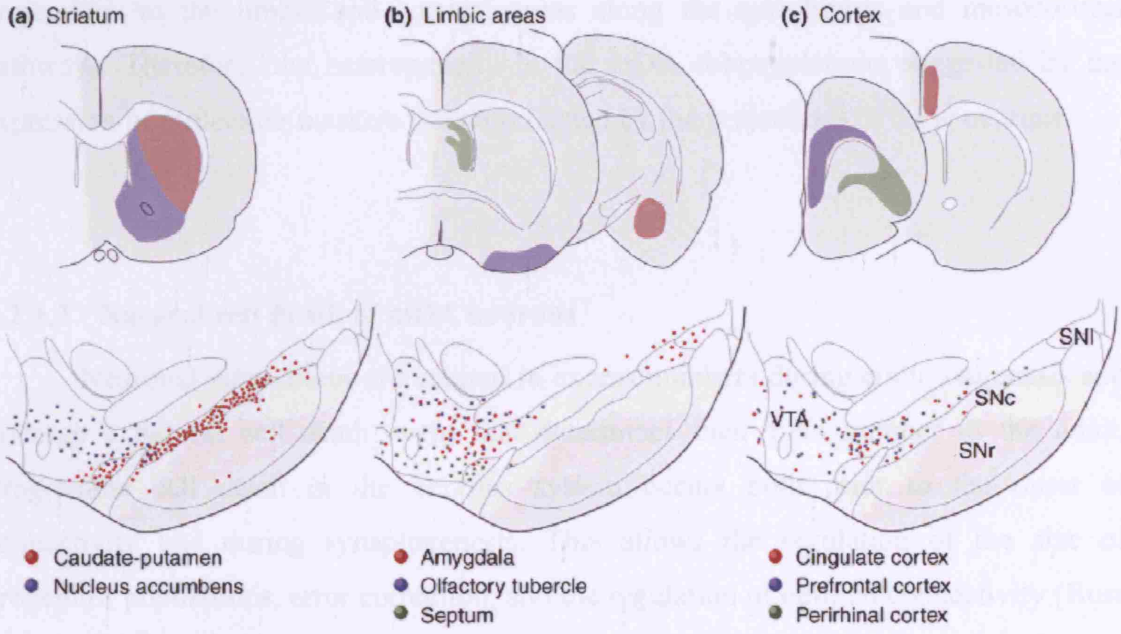

Figure 1-7 Cells of origin of the mesostriatal, mesolimbic and mesocortical pathways in the rat.

The DA neurons projecting to (a) striatal, (b) limbic and (c) cortical areas are partly intermixed: The cells located in the ventral tier of the SNc [red dots in (a)] innervate, probably exclusively, the sensorimotor part of the caudate-putamen [red area in the inset in (a)], whereas the cells of the dorsal tier comprise neurons that project widely to both limbic and cortical forebrain regions, as illustrated in (b) and (c), respectively. Abbreviations: SNc, substantia nigra pars compacta; SNl, substantia nigra pars lateralis; SNr, substantia nigra pars reticulata; VTA, ventral tegmental area. Taken from Björklund and Dunnet, 2007.

Three distinct mDA projection pathways (the nigrostriatal, mesolimbic and mesocortical pathways) have been suggested by early histofluorescence studies (Fallon and Moore, 1978; Lindvall et al., 1977). Retrograde labelling studies have supported that

the three DA projection systems are both anatomically and functionally distinct, but that their cells of origin are intermixed (Figure 1-7) (Björklund and Dunnett, 2007). Because of that, the authors suggested that the nigrostriatal pathway is more accurately referred to as the mesostriatal pathway. The interdigitated neurons dispersed throughout the midbrain project widely to diverse forebrain targets. The A8 cell group project to the striatal, limbic and cortical areas. The A9 neurons project to the striatum as well as innervating the cortical and limbic areas. The A10 group targets the ventral striatum and the ventromedial part of the head of the caudate-putamen in rodents in addition to the projections to the limbic and cortical areas along the mesolimbic and mesocortical pathways. Therefore, the heterogeneity in the mDA subpopulations suggested by the expression of molecular markers is also reflected by the projections of these neurons.

1.2.4.3 Natural cell death of mDA neurons

Neuronal populations are created in excess numbers during embryongenesis and undergo a natural cell death event that determines their final number in the adult. Programme cell death in the nervous system occurs both prior to the onset of connectivity and during synaptogenesis. This allows the regulation of the size of progenitor populations, error correction, and the regulation of optimal connectivity (Buss et al., 2006).

The mDA neurons in the SNc undergo biphasic postnatal natural cell death in both rat and mouse. Both species show the same time course of apoptosis with an initial major peak at P2 and a second minor peak at P14 (Jackson-Lewis et al., 2000; Janec and Burke, 1993; Oo and Burke, 1997). In the rat, the cell death of SN begins on E20 and ceases on P28 (Oo and Burke, 1997). The initiation of this process has not been studied in the mouse, while apoptotic neurons are no longer detected by P32 (Jackson-Lewis et al., 2000). It has been suggested that the developmental cell death in mDA neurons is regulated by target interaction. Glial-cell-line-derived neurotrophic factor (GDNF) in the striatum serves as a physiological limiting neurotrophic factor for mDA neuron during the first but not the second phase of natural cell death (Burke, 2003; Oo et al., 2003).

1.3 Aim of project

The mDA neurons constitute a highly heterogeneous population of cells having different properties, innervating different target tissues and performing different functions. In order to develop a long-term therapy for PD, in which mDA neurons in the SNc are selectively degenerated, the first essential step is to understand how this population is developed within the highly heterogeneous mDA neurons. The first aim of this study is understand the origin of different subpopulations of mDA neurons. The second aim is to characterise the functions of the Lmx family of transcription factors, which are the first known factors to be specifically expressed in the mDA progenitors.

Chapter 2
Materials and methods

2.1 Animals and tissue preparation

2.1.1 Mouse lines

The following mouse lines or embryos were used in the present study: ArxLacZ mice (Kitamura et al., 2002), *Lmx1a* mutant mice (B6C3Fe-*a/a-Lmx1a*$^{dr\text{-}J}$, dreher, *Lmx1a*^{dr} or *dr*^{J}, The Jackson Laboratory), BAC transgenic Lmx1aCre embryos and brains (A.G. Lindgren and K.J. Millen, unpublished), Lmx1bFlox mice (Collombat et al., 2003), Lmx1b knockout embryos (Chen et al., 1998a), Msx1-nLacZ embryos (Houzelstein et al., 1997), BAC transgenic Nkx2.2CreER^{T2} mice (R. Taveira-Marques, N. Tekki-Kessaris and W.D. Richardson, unpublished), R26RLacZ mice (Soriano, 1999), R26REYFP mice (Srinivas *et al.*, 2001), and ShhGFPCre (Shh^{cre}) and ShhCreER^{T2} (Harfe et al., 2004). All the mice were maintained in a mixed background. ArxLacZ animals were maintained as heterozygous females.

2.1.2 Mating

Conventional mating was set up after 4pm in the afternoon and the presence of a vaginal plug (VP) was checked the next morning. Mating was assumed to have occurred at midnight, and 12:00 noon at the day of VP detection was defined as embryonic days (E) E0.5 *post-coitum.*

Timed mating was set between ShhCreER^{T2};R26RLacZ males and R26RLacZ females for lineage tracing studies, and *Lmx1a*$^{dr/+}$;*Shh*^{cre};*Lmx1b*$^{f/+}$ males and *Lmx1a*$^{dr/+}$;*Lmx1b*$^{f/f}$ females for *Lmx1a/b* double mutant studies. Mating was set up at 7a.m. and the presence of a VP was checked at 10a.m., after which the mice were separated. The embryos were staged as E0 when a VP was detected at 10a.m.

2.1.3 Tamoxifen and progesterone treatments

Tamoxifen (T-5648, Sigma) stock solutions of either 10 mg/ml or 50 mg/ml were made by dissolving tamoxifen in one volume of absolute ethanol to nine volumes of sunflower oil (Tesco Ltd., UK). Tamoxifen was administered to time-pregnant females by oral gavage at various embryonic stages from E6.5 to E11.5 using a mouse feeding needle (18061-22, Fine Science Tool). Repeats were performed from at least three separate tamoxifen administrations.

Progesterone (P-3972, Sigma) was dissolved in corn oil (Sigma) and delivered together with tamoxifen by oral gavage to pregnant females at 0.375-0.5 mg per gram body weight to overcome high doses tamoxifen toxicity (Joyner and Zervas, 2006).

2.1.4 BrdU injections

Pregnant females were injected intraperitonealy with a solution of BrdU (B-5002, Sigma, stock solution of 10mg/ml in phosphate-buffered saline [PBS]) at 100 μg per gram body weight. For short pulse labelling, embryos were harvested one hour after a single injection. For birth dating studies, timed mating was set up for 3 hours. Three pulses of BrdU were injected to time-mated females 2 hours before, at and 2 hours after the indicated time.

2.1.5 Perfusion and tissue treatment

Adult mice were anesthetised by intraperitoneal injection of 0.1 ml of Hypnorm (fentanyl citrate 0.315 mg/ml and fluanisone 10 mg/ml, Vetapharma Ltd, UK) per 10g body weight, and then perfused intracardially with chilled 4% (w/v) paraformaldehyde (PFA) in PBS.

Adult brains were dissected out from the skull, fixed in 4% PFA at 4°C overnight. Embryos were collected from pregnant female mice killed by a Schedule One method. Brains were dissected out from E18.5 embryos. Embryos or E18.5 brains were fixed in 4% PFA (w/v) in PBS at 4°C for 2 hours. Fixed tissues were washed in PBS twice, sunken in 15% and then 30% sucrose in PBS, and embedded in O.C.T. compound (BDH, UK). All samples were cut at 12 μm thickness using Leica CM3050S cryostat (Leica, Germany).

2.1.6 Genotyping

Ear or tail biopsy were digested with 200 mg/μl of proteinase K in DNA extraction buffer (100mM Tris-HCl pH8.5, 5mM EDTA pH8.0, 200mM NaCl, 0.2% SDS) overnight at 56°C. Digested samples were incubated with 200μl of 6M ammonium acetate on ice for 15 minutes, centrifuged at 13,200 rpm for 15 minutes to remove debris. Genomic DNA was precipitated by isopropanol extraction, washed in 70% ethanol and resuspended in TE buffer.

The Cre allele was detected using primers listed in Table 2-1 using the following PCR program: 94°C for 30 seconds, 55°C for 30 seconds, 72°C for 30 seconds repeated for 34 cycles. R26R mice were genotyped as described (Soriano, 1999).

The genotyping of *dreher* allele involves a PCR with primers listed in Table 2-1 using a programme of 94°C for 7 minutes, 35 cycles of 55°C for 30 seconds, 72°C for 30 seconds, and then 72°C for 10 mins. The PCR products were then digested with HypCH4V (New England Biolab, UK) at 37°C for at least two hours and run on 10% acrylamide gel. The *dreher* mutant allele was detected as a 90bp fragment, and wild type allele was detected as two fragments of 40bp and 50bp. Lmx1bFlox mice were genotyped as previously described (Zhao et al., 2006c).

Transgene	Primers
Cre	ATCCGAAAAGAAAACGTTGA
	ATCCAGGTTACGGATATAGT
Rosa26R	AAAGTCGCTCTGAGTTGTTAT
	GCGAAGAGTTTGTCCTCAACC
	GGAGCGGGAGAAATGGATATG
LacZ	GCACATCCCCCTTTCGCCAGCTGGCGTAAT
	CGCGTCTGGCCTTCCTGTAGCCAGCTTTCA
Dreher	GGCAACATCTGTTGCTGTTG
	GAAGCAGGCACTTACTTCTC
Lmx1b Flox	AGGCTCCATCCATTCTTCTC
	CCACAATAAGCAAGAGGCAC
Lmx1b Null	CCCTGGGGTCATCTTAGTGGTGTT
	GCAGGGAAGGCAGAATGGGTAAG

Table 2-1 List of PCR primers used in the genotyping.

2.2 Staining

2.2.1 5-Bromo-4-chloro-3-indolyl-β-D-galactopyranoside (X-gal) staining

Embryos were fixed in 1% (v/v) formalin in PBS with 0.2% (v/v) glutaraldehyde, 5mM EGTA, 2mM $MgCl_2$ and 0.02% (v/v) NP-40, and then washed in 0.02% (v/v) NP-40 in PBS for 3 x 20 min. Samples were then allowed to develop in the dark at 37°C in staining solution (0.1% X-gal in DMF, 5mM $K_3Fe(CN)_6$, 5mM $K_4Fe(CN)_6$, 2mM $MgCl_2$ and 0.02% NP-40 in PBS). The staining reaction was stopped by washing samples in 0.02% NP-40 in PBS for 3 x 15 min and then fixed in 4% PFA. Whole mount embryos were cleared in a series of 25%, 50%, 75% and 100% Glycerol in PBS. Images were collected on a Zeiss LSM510 microscope (Oberkochen, Germany).

2.2.2 Immunohistochemistry

Slides were incubated in 1% (w/v) bovine serum albumin (BSA) diluted in PBS with 0.1% (v/v) Triton X-100 (PBT) for three minutes. Primary antibodies (listed in Table 2-2) were diluted in PBT and slides incubated overnight at 4°C. Slides were then washed in PBS for 3 x 5 min and incubated with conjugated secondary antibodies diluted in PBT for 2 hours at room temperature. Secondary antibodies conjugated with FITC, Cy3 or CY5 raised in donkey against goat, guinea pig, mouse, rabbit, rat and sheep were used (1:250, Jackson ImmunoResearch Laboratories, Inc.). Slides were washed in PBS for 3 x 5 min and mounted using Vectashield® mounting medium for fluorescence (H-1000, Vector Laboratory Inx, Burlingame). Cell nuclei were detected by either mounting slides in Vectorshield® mounting medium for fluorescence with DAPI (H-1200, Vector Laboratory Inx, Burlingame), or incubating with Toto-3-iodide (1:1000, Molecular Probes) for 1 hour at room temperature prior to slides mounting. Images were collected on a Leica TCS SP2 confocal microscope.

TH immunohistochemistry on X-gal stained sections were performed as the fluorescent method with the substitution of fluorescent conjugated secondary antibody by horseradish peroxidase conjugated donkey anti-rabbit IgG (1:250, Jackson ImmunoResearch Laboratories, Inc.) and subsequent detect with 0.3mg/ml diaminobenzidine (DAB, Sigma D-5636) and 0.03% (v/v) H_2O_2 in water.

Antibody	Host, isotype	Concentration	Source
β-gal	Rabbit IgG	1:200	Biogenesis Ltd., UK (4600-1509)
β-gal	Goat IgG	1:500	Biogenesis Ltd., UK (4600-1409)
AADC	Rabbit IgG	1:500	Novus Biologicals, Inc., USA (NB300-174)
BrdU*	Rat IgG2a	1:20	AbD Serotec, UK (OBT0030S)
Brn3a	Mouse IgG2b	1:100	Santa Cruz Biotechnology, USA (sc-8429)
Cyclin D2	Rabbit IgG	1:200	Santa Cruz Biotechnology, USA (sc-181)
GFP	Sheep IgG	1:200	Biogenesis, UK (4745-1051)
Isl1	Mouse IgG2b	1:5	DSHB, University of Iowa, USA (39.4D5)
Ki67	Rat IgG	1:50	DAKO, USA
Lim1/2	Mouse IgG1	1:20	DSHB, University of Iowa, USA (4F2)
Lmx1a	Rabbit IgG	1:500	gift from M German, University of California San Francisco Diabetes Center, USA
Lmx1b	Guinea pig	1:2000	gift from T. Müeller and C. Birchmeir, Max-Delbruck-Center for Molecular Medicine, Germany
Mash1	Mouse IgG	1:200	gift from Dr. David Anderson, California Institute of Technology, USA
Nestin	Mouse IgG	1:100	Chemicon, USA (MAB353)
Ngn2	Mouse IgG	1:20	gift from Dr. David Anderson, California Institute of Technology, USA
Nkx2.2	Mouse IgG2b	1:5	DSHB, University of Iowa, USA (74.5A5)
Nkx6.1	Rabbit IgG	1:1500	gift from Martyn Goulding, Salk Institute, USA
Nurr1	Rabbit IgG	1:200	Santa Cruz Biotechnology, USA (sc-990)
p27	MouseIgG1	1:200	BD Biosciences, USA (554069)
Pax7	Mouse IgG1	1:10	DSHB, University of Iowa, USA
p-Caspase 3	Rabbit IgG	1:500	Abcam, UK (ab4051)
Sox2	Rabbit IgG	1:500	Chemicon, USA (AB5603)
TH	Rabbit IgG	1:200	Chemicon, USA (AB152)
TH	Sheep IgG	1:200	Chemicon, USA (AB1542)
VMAT	Rabbit IgG	1:100	Chemicon, USA (AB1767)

Table 2-2 List of primary antibodies used in this study.

* Staining of BrdU involves pre-treatment of sections with 2N HCl at 37°C for 30 minutes (Ferri et al., 2004).

2.2.3 *In situ* hybridization

For whole mount *in situ* hybridization, embryos were dissected and fixed in 4% PFA in PBS at 4°C for 2 hours, washed in PBS, stored at -20°C in 100% methanol, and staining was performed as previously described (Rosen and Beddington, 1994; Rosen and Beddington, 1993).

The procedure for *in situ* hybridization on brain sections has been described previously (Conlon and Herrmann, 1993), and the following mouse antisense RNA probes that were used: *Arx* (Colombo et al., 2004), *Bmp7* (Arkell and Beddington, 1997), *Dll1* (Bettenhausen et al., 1995), *Delta3* (Campos et al., 2001), *En1* (Danielian and McMahon, 1996), *Hes5* (Akazawa et al., 1992), *Id3* (Bai et al., 2007), *Lmx1a* (Millonig et al., 2000), *Lmx1b* (320 base pair long over exons 4-6 of *Lmx1b* gene encoding for the HD), *Msx1* (Catron et al., 1996; Hill et al., 1989), *Pitx3* (Puelles et al., 2003; Smidt et al., 1997), *Raldh1* (Niederreither et al., 2002), *Shh* (Echelard et al., 1993), and *Wnt1* (McMahon and Bradley, 1990).

2.2.4 Cell counting

Quantifications of cells were performed on confocal images acquired after immunohistochemistry. For E12.5 embryos, cells from half of the sections separated at the ventral midline were counted on every sixth section at 12μm thickness, and total number of cells of the mDA region were obtained by multiplying raw counts by 12. For E10.5 embryos, the total number of cells was obtained by counting cells from every fourth sections at 12μm thickness and multiplying raw counts by 4.

Chapter 3
The origin of midbrain DA neurons

3.1 Introduction

3.1.1 The origin of mDA neurons

The existing theories for the origin of mDA neurons have been evolving with the advance in techniques. The early studies mainly focused on the origin of the SN subset of mDA neurons. Many contradicting theories were speculated based on histofluorescence and the cytoarchitecture of the brain. These include their origins from the basal plate (BP), the alar plate, the middle third of the BP of the midbrain, the diencephalon, the fovea isthmi at the midbrain/hindbrain junction and isthmus rhombencephali (the narrow segment of neural tube extending between the level of the fovea isthmi and the cerebellar plate) [reviewed by (Marchand and Poirier, 1983)].

Since the development of immunohistochemical techniques, more precise locations of the TH positive mDA neurons have been reported. In human embryos, mDA neurons were detected and thought to be generated mainly in the FP and collaterally in the BP across the caudal diencephalon, midbrain and isthmus (Verney, 1999; Verney et al., 2001). Similar patterns of TH protein expression were observed in the mouse described in section 1.2.3.9 (Marín et al., 2005; Vitalis et al., 2000). Hence, the predominant belief was that mDA neurons are generated in the BP and FP of the ventral midbrain and caudal diencephalon (Smits et al., 2006).

3.1.2 Theories on the origin of of mDA subpopulations

3.1.2.1 Spatial model

It has been suggested that neuronal cell fate specification depends on a Cartesian grid of positional information along the AP and DV axes of the neural tube (Lumsden and Krumlauf, 1996). This is exemplified in the generation of spinal cord neuronal subtypes from spatially distinct progenitor domains along the dorsoventral axis (Helms and Johnson, 2003; Jessell, 2000; Lee and Pfaff, 2001). A cellular and molecular organisation similar to that in the spinal cord is observed along the dorsoventral axis of the ventral midbrain. In the ventral midbrain, distinct groups of cells expressing different molecules are arranged in arcuate shape columns accentuated by the curve of the cephalic flexure in both the ventricular and mantle zones established by the positional signal of Shh (Agarwala and Ragsdale, 2002; Agarwala et al., 2001; Sanders et al., 2002).

Early studies using tritiated thymidine to follow the spatial and temporal origins of neurons from the SN and VTA in the rat suggested that SN and VTA originated from the middle third of the BP and the medial third of the BP respectively (Hanaway et al., 1971). It has also been suggested that mDA neurons initially migrate radially along radial glia before migrating tangentially to their final destinations (Kawano et al., 1995; Shults et al., 1990). In *Pitx3*-deficient mice, TH expression is reported to be absent in the rostrolateral mDA region from E12.5, and in the SNc located in the corresponding region of the adult mice (Smidt et al., 2004). These studies suggest that the subpopulations of mDA neuron may be generated from spatially distinct domains. Therefore, the spatial difference for the origin of mDA subpopulations has been the predominant theory in the field with minor modification. Recently, it has been proposed that the VTA is derived from the FP, and that the SN and RR are generated from the BP (Puelles, 2007). Smits et al. proposed an AP code along the ventricular zone of FP and BP in the midbrain and caudal diencephalon where mDA neurons are generated (Figure 3-1) (Smits et al., 2006).

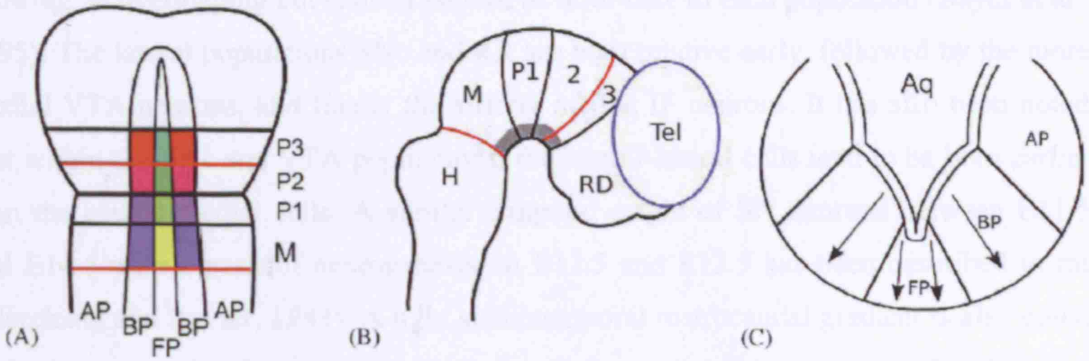

Figure 3-1 Schematic representation of the origin of mDA neurons.

(A) A drawing of a flattened embryo brain. The putative domains where mDA neurons may arise during development are indicated by different colored boxes. (B) A sagittal representation with mDA neurons indicated in gray. (C) A coronal representation. The specific regions are indicated according the prosomeric model. The radial and inverted fountain migration is indicated by arrows. Aq: aqueduct; AP: alar plate; BP: basal plate; FP: floor plate; M: midbrain; P1–3: prosomere 1–3; RD: rostral diencephalon; Tel: telencephalon. The boundaries indicated in red are important organizing regions, caudal the isthmus and rostral the zona limitans. Diagram taken from Smits et al., 2006.

3.1.2.2 Temporal model

In some parts of the nervous system, different neuronal subtypes are generated from multipotent progenitors in stereotyped chronological order (Pearson and Doe, 2004). This is evident in the histogenesis of the mammalian cerebral cortex. Multipotent progenitors, under the influence of extrinsic and intrinsic factors, generate different types of neurons in a specific order (Molyneaux et al., 2007; Shen et al., 2006). Moreover, temporal cross-repressive interactions between transcription factors has also been shown to direct a different cell fate in the same progenitor domain (Jacob et al., 2007).

The timing of origin for different mDA populations in mice has been studied by combining TH immunostaining with [^{3}H]thymidine autoradiography. The four populations of mDA neurons (IF, VTA, SNc and RR) are born between E9.5 and E13.5, showing an overlapping but distinct pattern of birth-date in each population (Bayer et al., 1995). The lateral populations SNc and RR are born relative early, followed by the more medial VTA neurons, and finally the strictly medial IF neurons. It has also been noted that within the SNc and VTA populations, the rostral-lateral cells tend to be born earlier than the caudal-medial cells. A similar temporal origin of SN neurons between E11.5 and E14.5 with a peak of neurogenesis on E12.5 and E13.5 has been described in rat (Marchand and Poirier, 1983). A light spatiotemporal rostrocaudal gradient is also noted in the neurogenesis of rat SN, where neurons in the rostral SN are generated earlier than those in the caudal SN (Marchand and Poirier, 1983).

It is hypothesized that a single germinal source of progenitors at the junction between the third ventricle and the cerebral aqueduct produces neurons settling in the RR, SN, VTA and IF (Figure 3-2) (Bayer et al., 1995). It is postulated that early born mDA neurons mainly destined for the SN and RR migrate ventrolaterally and posterolaterally from the source and settle along the entire extent from the future rostral SN to the caudal RR (Figure 3-2A). During the middle stage (Figure 3-2B), newly born mDA neurons giving rise mainly to RR, SN and VTA are generated from the same source and settle just medial to the early born neurons. The DA progenitor source is displaced to a more caudal position due to an extensive growth of the diencephalic neuroepithelium, thereby leaving the earlier generated neurons in the rostral SN. At late stage (Figure 3-2C), the DA progenitor source is further displaced caudally, and the neurons born are destined for the VTA and IF, migrate ventrally to settle in a concentrated region just medial to the middle-generated neurons. This theory incorporates a combined effect of caudal displacement of mDA progenitor domain, and the sequential migration of young neurons settling in a lateral to medial pattern to explain the distribution of mDA populations in the adult mouse brain (Figure 3-2D).

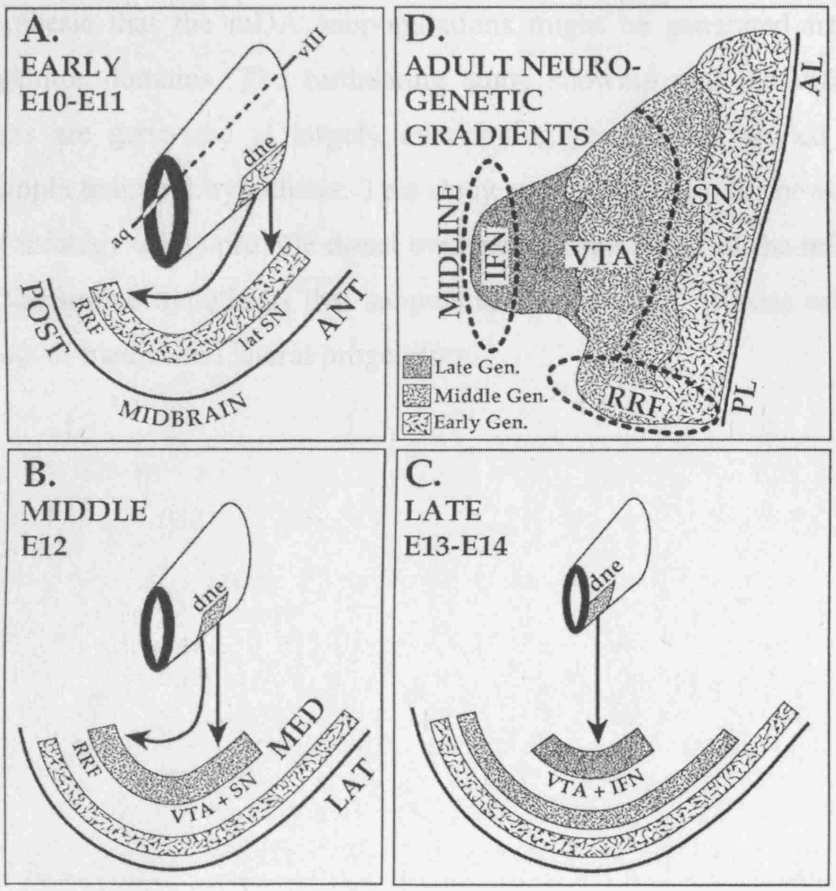

Figure 3-2 Schematic diagram on the combined processes of sequential DA neurogenesis, successive migratory waves of young DA neurons, and sequential cell settling during embryonic development (A-C) shape the adult midbrain DA system (D).

E1 is designated as the day after mating. AL, anterolateral; ANT, anterior; aq, cerebral aqueduct; dne, DA neuroepithelium; IFN, interfascicular nucleus (IF); LAT, lateral; MED, medial; PL, posterolateral; POST, posterior; RRF, retrorubral field (RR), SN, substantia nigra; VTA, ventral tegmental area, vIII, third ventricle. Taken from Bayer et al., 1995.

3.2 Aim

At the beginning of this study, it was believed that mDA neurons were generated in both the FP and BP of the midbrain and caudal diencephalon. This has led to the popular hypothesis that the mDA subpopulations might be generated from spatially distinct progenitor domains. The birthdating study showing that the different mDA subpopulations are generated at largely overlapping periods has argued against the alternative simple temporal hypothesis. This study attempted to use the powerful genetic fate mapping strategy to (1) provide direct evidence for the origin of the mDA neurons, and (2) test the simple hypothesis that subpopulations of mDA neurons originate from distinct subsets of medial and lateral progenitors.

3.3 Results

3.3.1 The anterior limit of mDA progenitors lies at the boundary between the rostral and caudal diencephalon

Lmx1a was expressed in the mDA region in the ventral midbrain and ventral diencephalon among other regions in the developing mouse embryos at E10.5 (Figure 3-3A). In a collaboration with K.J. Millen, Lmx1aCre animals (A.G. Lindgren and K.J. Millen, unpublished) were crossed with the R26RLacZ reporter animals (Soriano, 1999) to allow permanent labelling of Lmx1a expressing cells, which could be visualised either by enzymatic reactions towards X-gal or by immunohistochemical detection with antibodies against β-galactosidase (β-gal).

An Lmx1aCre transgenic mouse line made from a BAC clone containing about 100kb sequences including region 5' to the Lmx1a coding region up to the first intron showed a lack of Cre activity in the ventral midbrain and caudal diencephalon at E10.5 (Figure 3-3B). This allowed us to test if the border of Cre activity between the ventral midbrain and diencephalic corresponds to the anterior limit of the mDA progenitor domain. Therefore, the long-term fate of the ventral rostral diencephalic progenitors in these Lmx1aCre;R26RLacZ animals was followed to adulthood. Preliminary data showed that the β-gal positive cells were detected in the hypothalamic region but excluded from the TH+ mDA population except for two cells in the most rostral part of the adult midbrain (Figure 3-4). This serves as indirect evidence that the anterior border of mDA progenitors lies at the boundary between the rostral and caudal diencephalon, although more experiments will be required to confirm this observation.

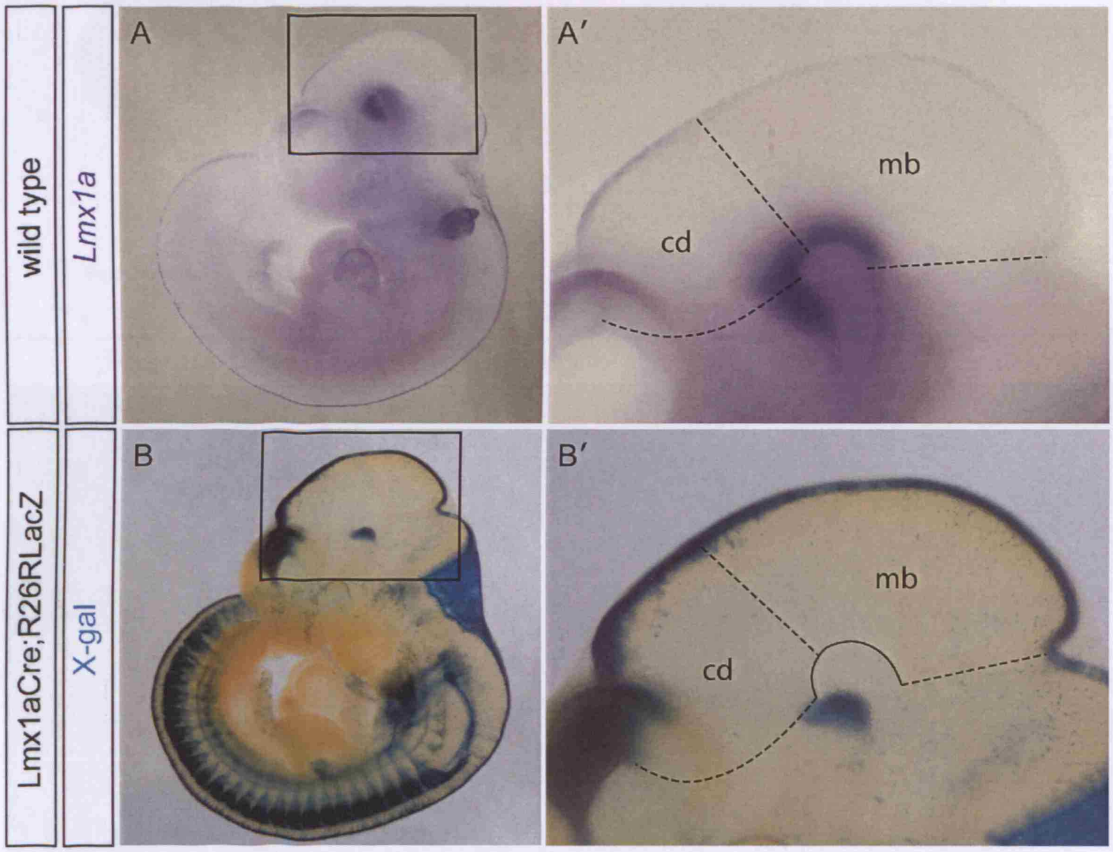

Figure 3-3 Cre activity in Lmx1aCre mouse line is excluded from the ventral midbrain and caudal diencephalon.

(A) Endogenous Lmx1a is expressed in the ventral midbrain and diencephalon shown by whole-mount *in situ* hybridisation of in wild type embryos at E10.5. (B) Whole-mount X-gal staining in Lmx1aCre;R26RLacZ embryos at E10.5 demonstrate a lack of Cre ectivity in the Lmx1aCre mouse line. Abbreviations: mb, midbrain; cd, caudal diencephalon.

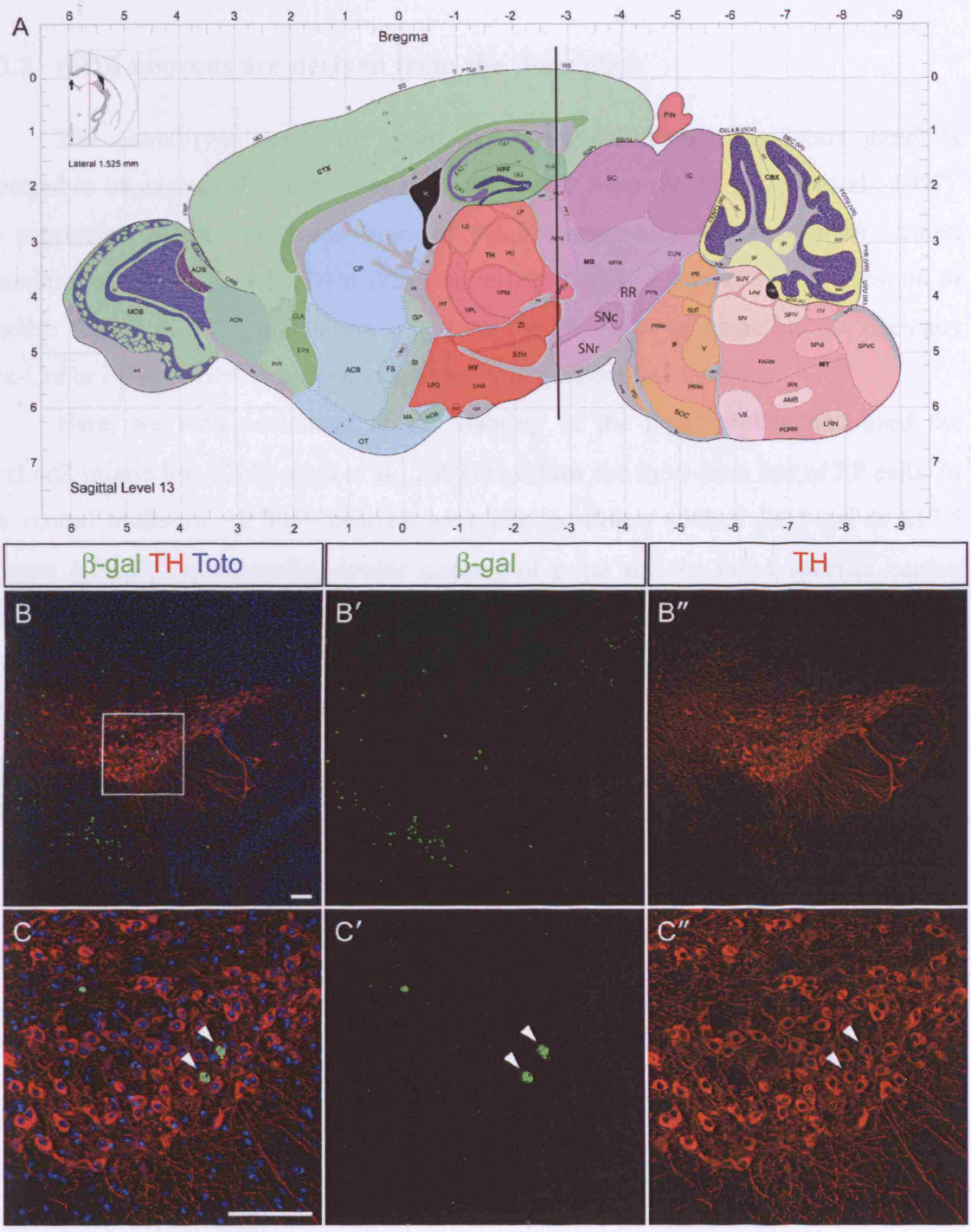

Figure 3-4 Cells in the rostral diencephalon labelled by Lmx1aCre are almost completely excluded from mDA neurons.

(A) A sagittal plane at the lateral 1.525mm level of the adult mouse brain shows the midbrain in pink and anatomical structures including RR, SNc and SNr (modified from the Allen Brain Atlas). (B,C) Double staining of β-gal and TH on a coronal section of adult Lmx1aCre;R26RLacZ mouse brain taken at the rostral midbrain level indicated by a black solid line in (A). Scale bars correspond to 100μm.

3.3.2 mDA neurons are derived from the floor plate

The paired-type homeobox gene *Arx* (aristaless related homeobox gene) is reported to be expressed in the FP of mouse embryos from E9-9.5 (Miura et al., 1997). Its expression in the ventricular zone of the FP prior to and during mDA neuron generation (Figure 3-5, 3-7C,D) makes it a perfect candidate to address the question of whether the whole mDA population arise from the FP. However, there has not been any Arx-Cre or FP specific Cre animal available for permanent fate mapping.

Here, we took advantage of the stability of the β-gal protein and used the ArxLacZ mouse line (Collombat et al., 2003) to follow the short-term fate of FP cells. In the ventral midbrain, all TH+ neurons were also positively stained for β-gal at E12.5 (Figure 3-6A,B). Additionally, double staining of β-gal and the mDA specific marker Lmx1a showed a complete overlap of the two domains in the ventral midbrain at E12.5 (Figure 3-6D,E). In the caudal diencephalon, bilateral streams of β-gal+TH+ (Figure 3-6C) and β-gal+Lmx1a+ (Figure 3-6F) cells had extended from the FP to the mantle zone of the BP. These provide direct evidence that TH+ mDA neurons are derived from the FP, and that the TH+ cells observed in the BP are migrated from the FP.

In the most rostral part of the caudal diencephalon, cells that weakly expressed TH did not co-express β-gal (Figure 3-6C). The expression of Lmx1a extended more rostrally in the diencephalon than β-gal (Figure 3-6F). This suggests that ArxLacZ may not be expressed in the most rostral progenitors of mDA neurons.

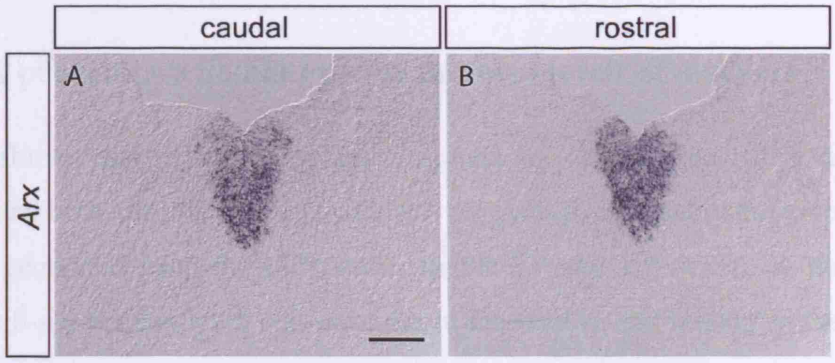

Figure 3-5 *Arx* RNA is expressed in the ventricular zone of the midbrain FP of wild type embryos at E12.5.

Scale bar corresponds to 100μm.

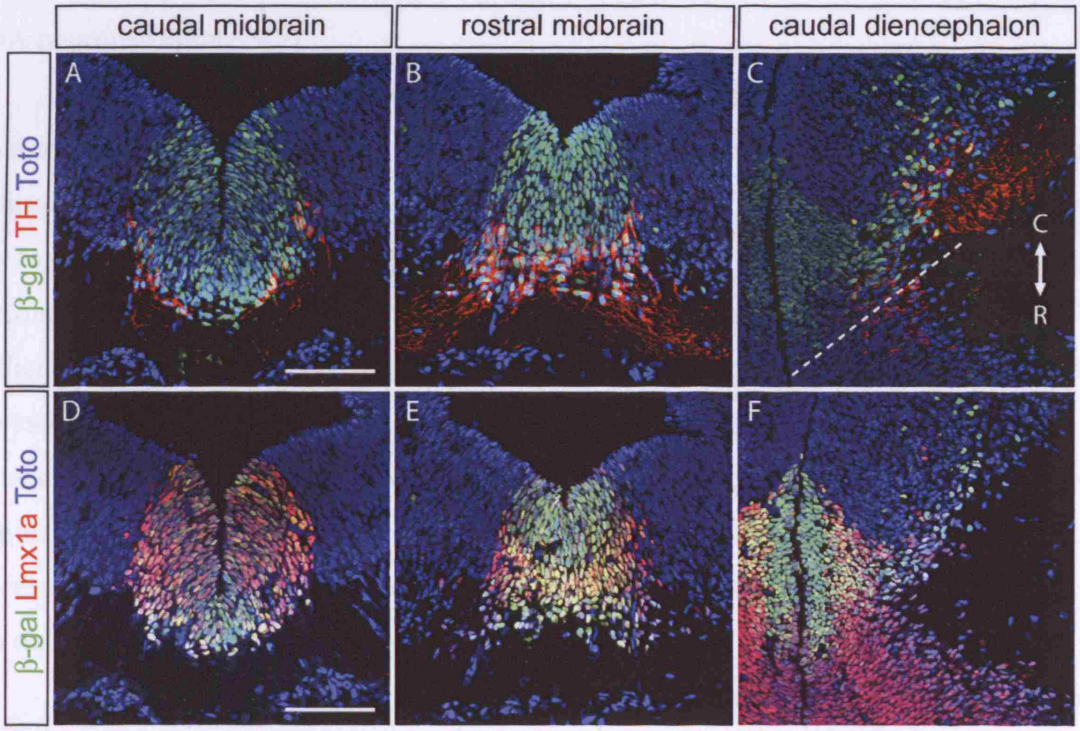

Figure 3-6 The majority of the mDA neurons are derived from ArxLacZ positive cells.

Double staining of β-gal/TH (A-C) and β-gal/Lmx1a (D-F) on coronal sections of E12.5 ArxLacZ embryos at the levels of caudal midbrain (A,D), rostral midbrain (B,E) and caudal diencephalon (C,F) representing the caudal, middle and rostral parts of the mDA population respectively. In C, dashed line marks the boundary of β-gal expressing cells, and the rostral (R) – caudal (C) axis is indicated. Scale bars correspond to 100μm.

3.3.3 mDA progenitors do not express uniform levels of markers

The above data provides evidence against the theory that mDA neurons are generated from both the FP and BP, and the suggestion that subpopulations of mDA neurons are generated from the differences in the FP and BP origin. In the ArxLacZ embryos, the β-gal protein level was stronger in the medial and weaker in the lateral FP cells at E12.5. At both E10.5 (Figure 3-7C,D) and E12.5 (Figure 3-5), a similar light gradient of stronger medial and weaker lateral Arx transcript level was observed in the caudal but not the rostral midbrain. This led us to hypothesize a medial-lateral difference in gene expression within the midbrain FP, which may generate different subpopulations of mDA neurons. We started by screening for differences in gene expression within the Lmx1a+ mDA progenitor domain at E10.5 that might specify different populations of mDA neurons (Figure 3-7).

At E10.5, *Lmx1a* and *Lmx1b* expression indicated the mDA domain, which consisted mainly of progenitors with some early postmitotic neurons in the rostral midbrain (Figure 3-7A,B and data not shown). *Arx* was expressed in the same pattern as *Lmx1a*, except for the lack of expression in the very thin mantle zone in the most rostrolateral part of the midbrain (Figure 3-7C,D). Interestingly, *Bmp7* displayed a gradient of expression along the rostrocaudal extent of the ventral midbrain. It was expressed in the same region as *Lmx1a* and *Arx* in the caudal midbrain, in which it showed a stronger medial and weaker lateral pattern (Figure 3-7E). This expression diminished towards the rostral level (Figure 3-7F). Comparing adjacent sections expressing *Lmx1a* rostral to and *Arx* caudal to that of *Bmp7*, it was evident that *Bmp7* was only detected at a low level in the medial part within the mDA domain.

Wnt1 expression has been shown to be restricted to the lateral mDA progenitors (Zervas et al., 2004). The same lateral expression of *Wnt1* was observed at E10.5 (Figure 3-7G,H) and other stages from E8.5 to E12.5 (data not shown). The expression of *Raldh1* showed both rostrocaudal and mediolateral differences at E10.5. It was expressed more strongly in the lateral than in the medial mDA domain, and the level of its expression became very weak towards the rostral midbrain (Figure 3-7I,J). *Shh* expression was detected in both the FP and BP along the ventral midbrain at E10.5 (Figure 3-7K,L).

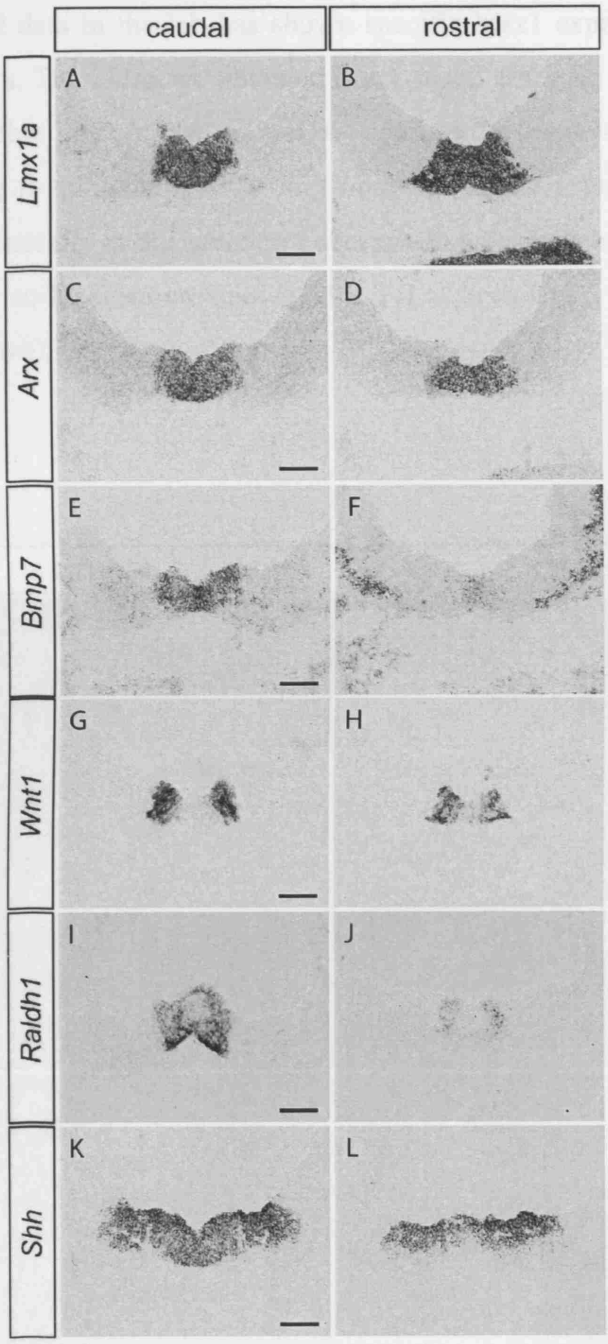

Figure 3-7 Genes expressed in the ventral midbrain progenitors of wild type embryosdisplay medial and lateral differences at E10.5.

A,C,E,K and B,D,F,L are adjacent sections in the caudal and rostral midbrain respectively. *Lmx1a* (A,B) and *Arx* (C,D) displayed similar expression patterns. (E,F) *Bmp7* was expressed in the same domain as *Lmx1a* and *Arx* in the caudal midbrain, but only in the medial region in the rostral midbrain. (G,H) *Wnt1* was expressed in the lateral region at all levels in the midbrain. (I) In the caudal midbrain, *Raldh1* was expressed more strongly in the lateral than medial mDA domain. (J) In the rostral midbrain, *Raldh1* was expressed very weakly in the lateral and absent in the medial mDA domain. (K,L) *Shh* expression was detected in both FP and BP in the midbrain. Scale bars correspond to 100μm.

Unpublished data in the lab has shown specific Msx1 expression in the ventral midbrain progenitors. Therefore, we obtained Msx1-nlacZ embryos (Bach et al., 2003) in an attempt to define the origin of mDA neurons by short-term fate mapping. Surprisingly, strong β-gal staining was only observed in the ventricular zone, and the level declined dramatically in the immature neurons and was beyond detectable levels in mature neurons for co-localisation studies with TH at both E12.5 (Figure 3-8A,B) and E14.5 (data not shown).

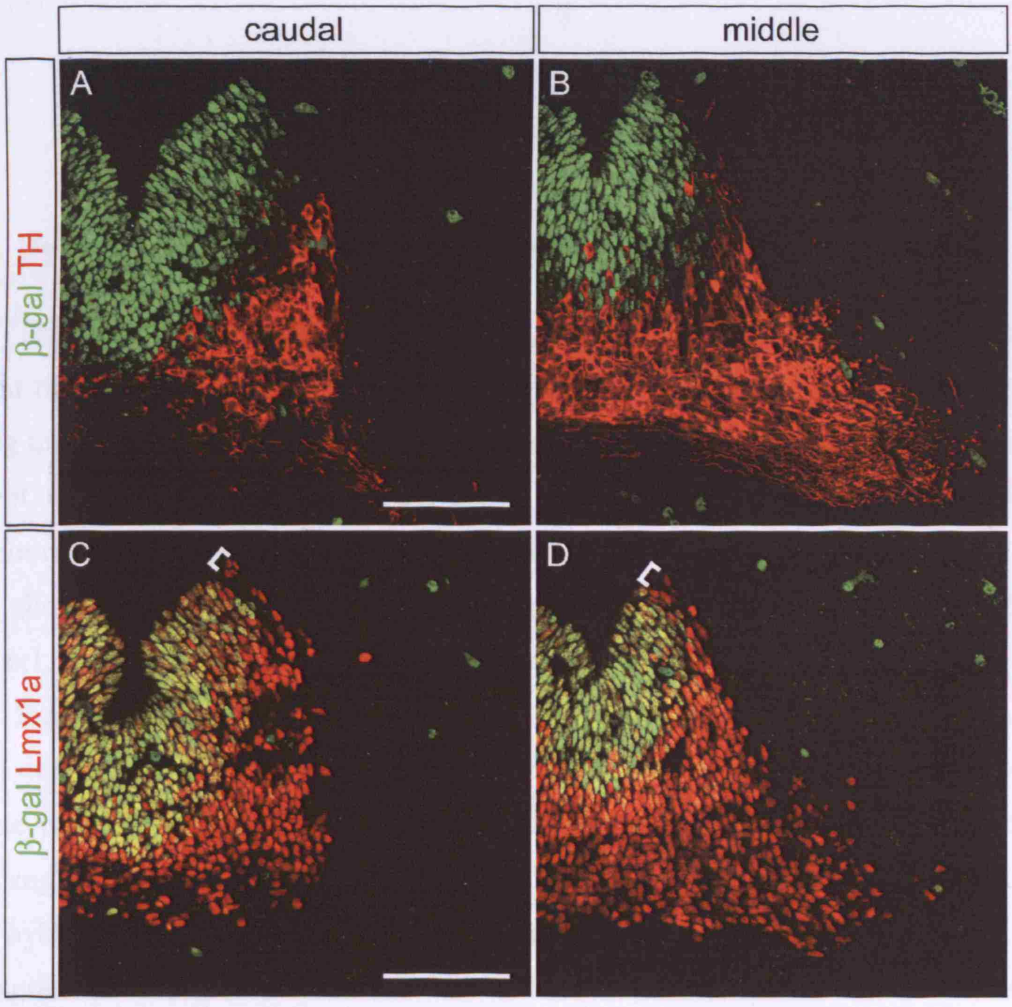

Figure 3-8 Msx1-nLacZ is not expressed in the lateral mDA progenitor domain.

Double staining of β-gal/TH (A,B) and β-gal/Lmx1a (C,D) at E12.5. Brackets in C and D indicate a lack of β-gal expression in the most lateral region of the Lmx1a+ domain. Scale bars correspond to 100μm.

Double staining of β-gal with Lmx1a in the Msx1-nlacZ embryos however showed that Msx1 was not expressed in the entire Lmx1a+ domain at both E12.5 (Figure 3-8C,D) and E14.5 (data not shown). Andersson et al. independently showed that Msx1 protein is expressed in the medial subset of Lmx1a+ progenitor domain (Andersson et al., 2006b). Unfortunately, the LacZ reporter expression did not persist in postmitotic neurons. Thus, it is not possible to investigate if Msx1 expressing cells develop into a subset of mDA neurons.

Taken together, the differential expressions of *Bmp7*, *Wnt1*, *Raldh1* and Msx1LacZ demonstrate heterogeneity within the mDA progenitor domain along the mediolateral and rostrocaudal axes.

3.3.4 Dynamic Shh expression in the ventral midbrain

The above data showing that mDA neurons are generated in the FP but not the BP, and that the FP cells display differential gene expression had led us to modify the existing theory of spatial origin of mDA subpopulations. We made a new hypothesis that different mDA subpopulations are generated from spatially and genetically distinct progenitors in the medial and lateral FP regions. We then searched for mouse lines that would allow us to trace the fate of mDA progenitors expressing Bmp7, Wnt1, Raldh1 and Msx1. However, there has not been useful tool available (see discussions).

From the information that Shh protein is detected in a dynamic pattern in the ventral midbrain from E8.75 to E12.5 (Mavromatakis, 2006), we turned our attention to examine if the dynamic patterns of Shh protein arise from spatial differences in cells expressing it or by diffusion. The distribution of Shh-expressing cells was examined by *in situ* hybridisation from the 5-somite (5s) stage to E12.5 (Figure 3-9). It is reported that Shh expression in the CNS initiates at the ventral midline of the midbrain at 8s stage (Echelard et al., 1993). However, in this study we showed that a narrow band of Shh transcripts can be detected very weakly in this region at 5s (Figure 3-9A). This Shh expression domain remained narrow, but the signal intensified at 8s (Figure 3-9B). At 10s stage (E8.5), the expression of Shh appeared to have expanded (compare Figure 3-9B, C), and remained roughly the same until E9.0 at neural tube closure (Figure 3-9D). The Shh expression greatly expanded laterally, presumably to the basal plate by E9.5

(22s) (Figure 3-9E), and remained broad until E12.5 (Figures 3-9F-H). From E10.5 (37s), Shh began to be downregulated in the medial region (Figure 3-9D), and this downregulation became more evident at E11.5 (Figure 3-9G) and E12.5 (Figure 3-9H).

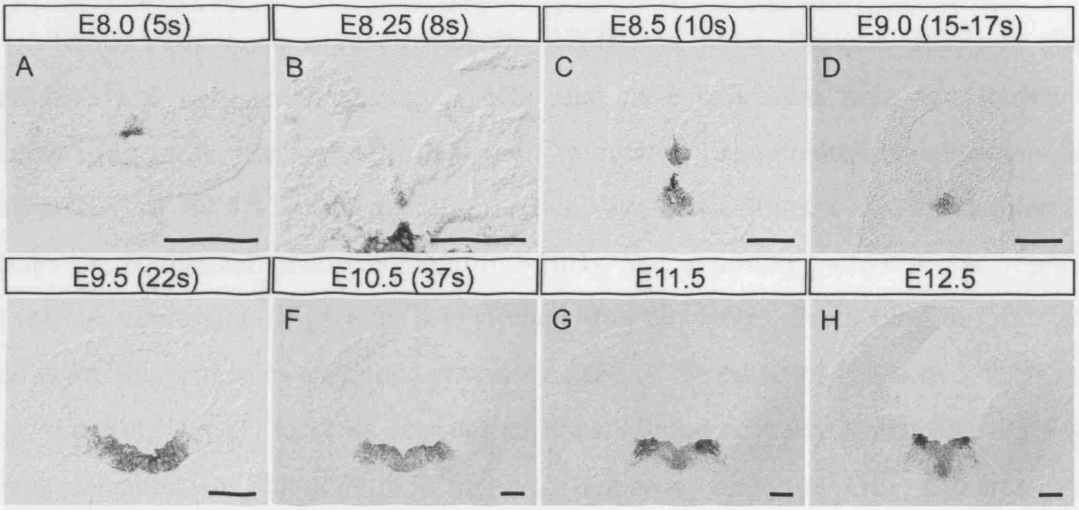

Figure 3-9 *Shh* is dynamically expressed by cells in the ventral midbrain.

(A) A narrow band of *Shh* RNA started to be detected weakly at 5-somite (5s) stage (E8.0). (B) A similar narrow *Shh* expression domain was detected at 8s. *Shh* expression appeared slightly broader at E8.5 (C) and E9.0 (D). By E9.5, the expression of *Shh* had further expanded. It started to be downregulated in the medial region from E10.5 (F). This downregulation became more evident at E11.5 (G) and E12.5 (H). Scale bars correspond to 100μm.

3.3.5 Shh progenies contributed to all subpopulations of mDA neurons

The initial expansion of Shh expression and later downregulation in the medial region can be exploited to map the fate of medially and laterally located cells in the ventral midbrain with the tamoxifen inducible ShhCreER^{T2} mouse line (Harfe et al., 2004). A ShhGFPCre mouse line, which contains an in-frame fusion of GFP and Cre recombinase, and a nuclear localization signal made in the same manner as the ShhCreER^{T2} (Harfe et al., 2004), was first used to demonstrate the efficacy of tracing Shh expressing cells to mDA fate.

ShhGFPCre mice were crossed the R26RLacZ mice (Soriano, 1999) to allow cumulative and permanent tracing of cells that have expressed Shh. We started by characterising these mice to confirm if the Cre activity recapitulated endogeneous Shh expression. At E9.5, Shh progenies, shown by whole mount X-gal staining on ShhGFPCre;R26RLacZ embryos (Figure 3-10B), had a similar pattern as the reported *Shh* mRNA expression (Figure 3-10A) (Echelard et al., 1993). From E9.5 to E12.5, the cumulative Shh progenies expanded at various parts of the embryos (Figures 3-10B-E).

Looking closely at cross sections of the midbrain revealed a delay in the β-gal protein detection in ShhGFPCre;R26RLacZ embryos. Shh and GFP proteins were strongly expressed in the ventral midline at E9.0, whereas the β-gal protein was only marginally detected (Figures 3-10F,K). The delay may be attributed to the time required for the sufficient accumulation of Cre recombinase to remove the stop sequence, flanked by LoxP sites, in the reporter allele and to allow the expression of β-gal. At E9.5 and E10.5, mosaic β-gal expression was detected in the same domain as the GFP, with a more mosaic pattern and a weaker expression level at the lateral edges (Figures 3-10L,M). The same expression patterns were observed on adjacent sections visualising the β-gal enzymatic activity using X-gal substrate at all stages from E9.5 to E12.5 (Figures 3-10G-J,L-O). Thus, it is not a technical artefact. At the medial region of the ventral midline, a downregulation of GFP protein level started to be observed at E11.5 and became evident at E12.5, while β-gal staining was still strongly detected (Figure 3-10N,O). Therefore, the ShhGFPCre line faithfully and permanently labels the Shh expressing cells in ventral midbrain.

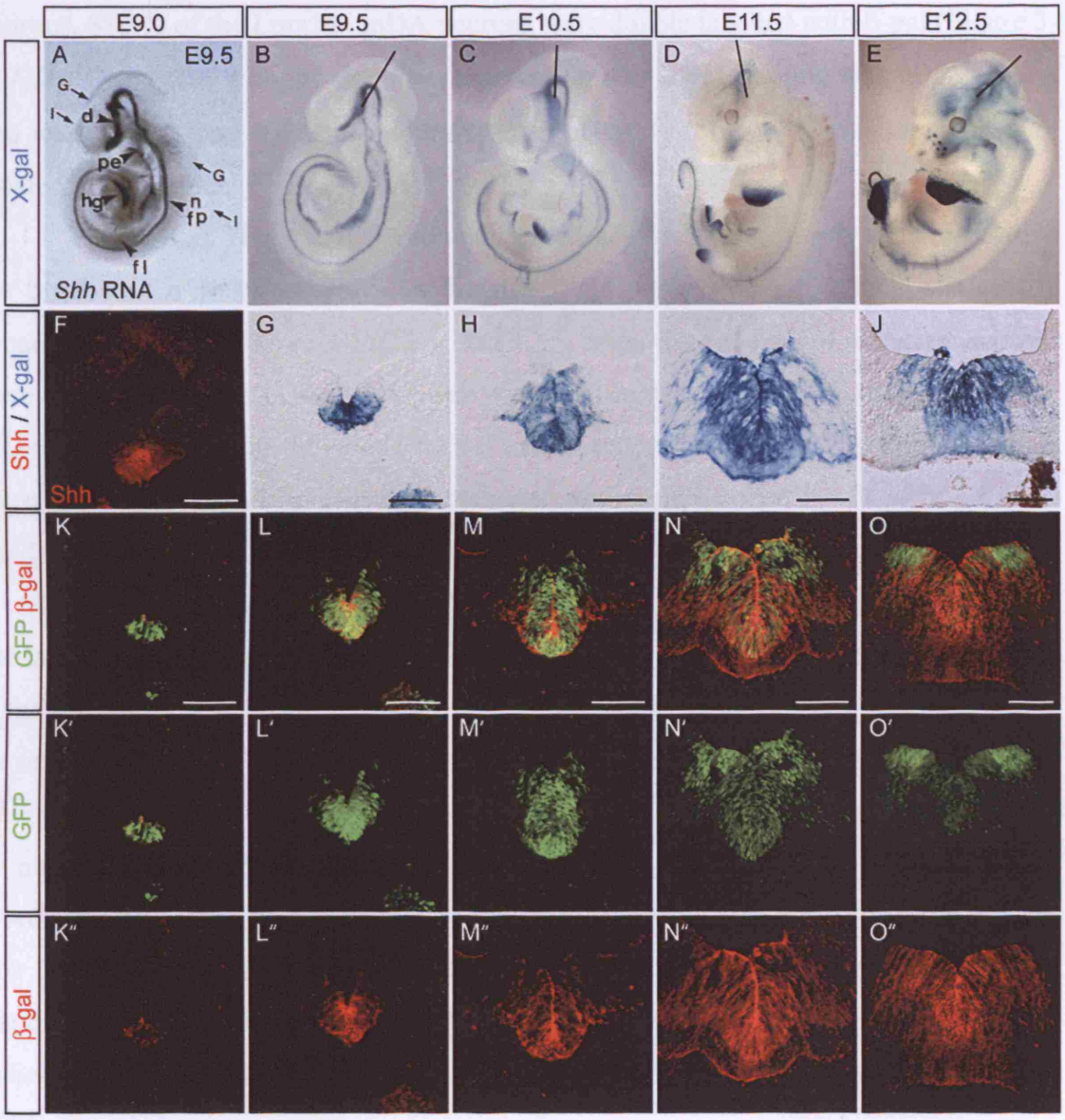

Figure 3-10 ShhGFPCre;R26RLacZ mouse line faithfully and permanently label Shh expressing cells in the ventral midbrain.

(A) *Shh* RNA expression in whole mount mouse embryo at E9.5 taken from Echelard et al., 1993. (B-E) Shh progenies were detected by whole mount X-gal staining. (F) Shh protein at E9.0 (Y.E. Mavromatakis, unpublished data). (G-O) Cross sections of the midbrain were taken at the levels shown in the whole embryos at the respective stages. (G-J) Detection of β-galactosidase activity by X-gal staining. (K-O) Double immunostaining with GFP and β-gal on adjacent sections of G-J where applicable. Scale bars correspond to 100μm.

After establishing the fidelity of the Cre activity, we investigated if mDA neurons are derived from Shh expressing cells. At E10.5, before the generation of mature mDA neurons, 88.3% of the Lmx1a+ mDA neurons were double labelled with β-gal (Figure 3-11A,B). Consistent with the previous observation that β-gal staining was more mosaic and weaker in the caudolateral midbrain, most of the Lmx1a single positive cells were located in this region (Figure 3-11A).

The earliest TH+ mDA neurons observed at E11.5 were mostly double positive for β-gal, and were all generated within the β-gal positive region, which was clearly broader than the FP (Figure 3-11C,D). At E12.5, when the majority of the mDA neurons have been born (Bayer et al., 1995), Shh progenies contributed vast majority of the TH+ mDA neurons covering the whole rostral caudal extent (Figure 3-11E,F). Again, there were fewer TH expressing cells that were also positively labelled for β-gal in the most caudal section of the midbrain (Figure 3-11E).

It has been suggested that mDA neurons in the RR subpopulation originate from the lateral position in the caudal midbrain (Marín et al., 2005). We therefore investigated if the less robust labelling in the caudolateral midbrain by ShhGFPCre;R26RLacZ would be reflected in this mDA subpopulation. However, there was no bias in the distribution of β-gal positive cells in the adult mDA populations (Figure 3-12). Shh progenies settled in all anatomically distinct mDA subpopulations including the periaqueductal gray (PAG, Figure 3-12C), linear nucleus of raphe (Li, Figure 3-12D,E), RR (Figure 3-12F), SNr (Figure 3-12G), interfascicular nucleus (IF, Figure 3-12H), paranigral nucleus (PN, Figure 3-12I), VTA (Figure 3-12J), SNc (Figure 3-12K), and SNl (Figure 3-12L). This indicates that the mosaic Cre activity in the ShhGFPCre mouse line does not specifically affect any mDA subpopulation.

As expected from the broad expression of Shh in both the FP and BP of the midbrain, Shh expressing cells also developed into other neuronal cell types such as the oculomotor neurons expressing Isl1 (Figure 6-1A), Brn3a positive red nucleus neurons (Figure 6-1B) and Pax7 expressing neurons in the interpeduncular fossa (Figure 6-1C).

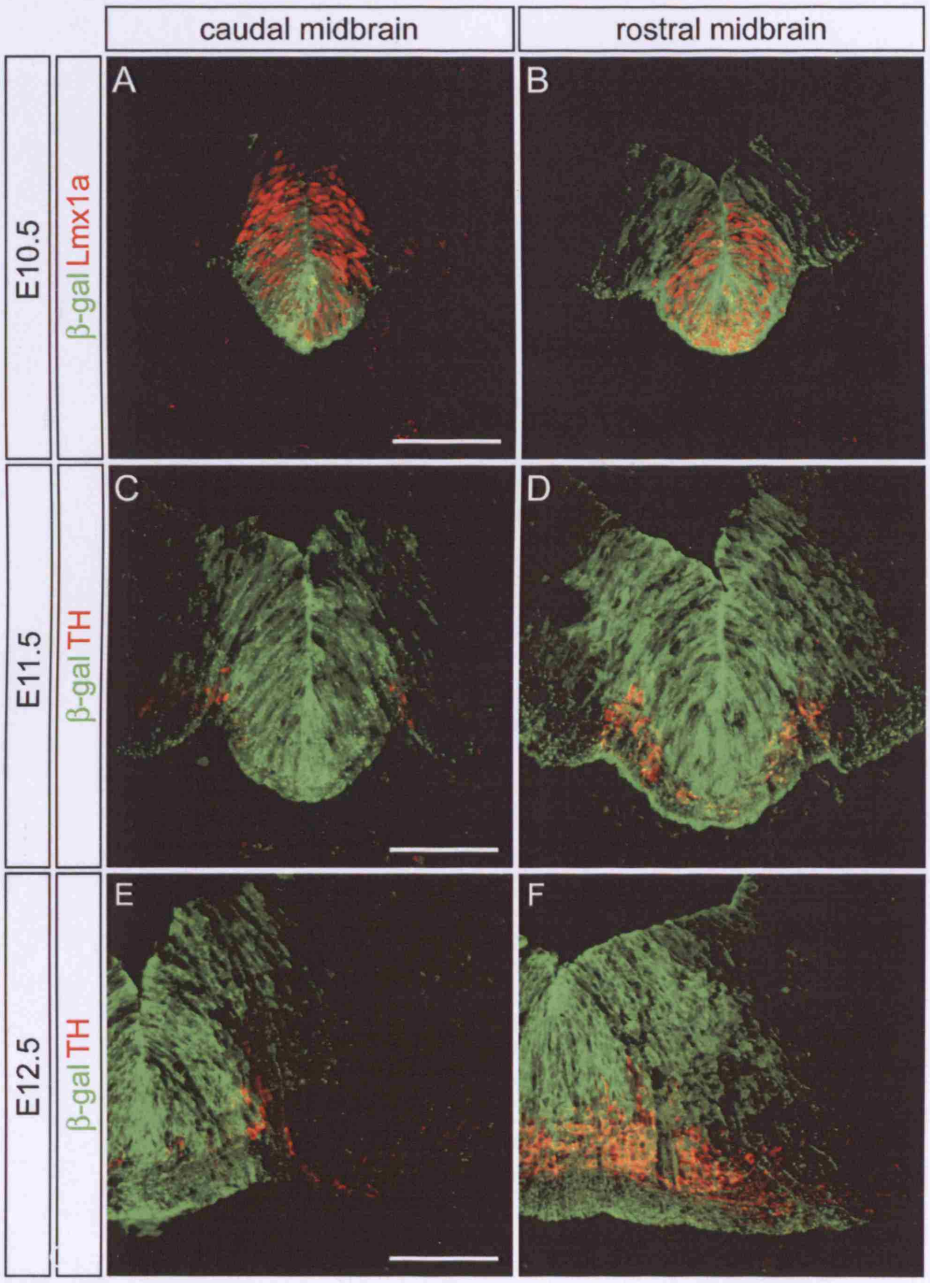

Figure 3-11 ShhGFPCre;R26RLacZ mouse line labels the majority of the embryonic mDA progenitors and neurons.

Double immunostaining of β-gal/Lmx1a at E10.5 (A,B), and β-gal/TH at E11.5 (C,D) and E12.5 (E-F) in the caudal (A,C,E) and rostral (B,D,F) midbrain. Scale bars correspond to 100μm.

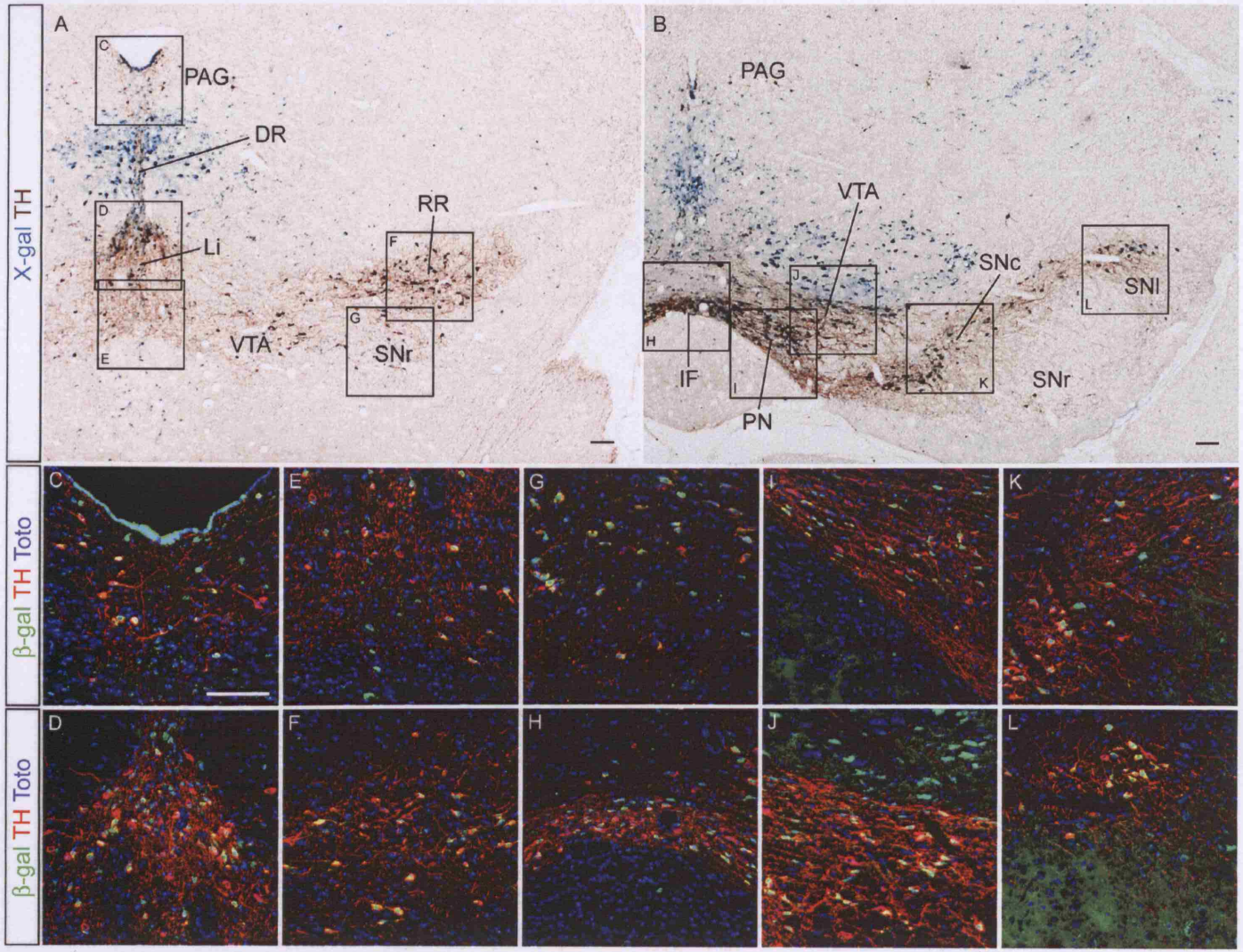
X-gal TH
A
B
C
PAG
DR
D
Li
E
RR
F
G
SNr
VTA
PAG
VTA
SNc
SNl
H
IF
I
J
K
L
SNr
PN
β-gal TH Toto
β-gal TH Toto

Figure 3-12 Shh progenies give rise to all adult mDA subpopulations.

Coronal sections of adult ShhGFPCre;R26RLacZ animals at mid-caudal (A) and mid-rostral (B) levels in the midbrain, stained with X-gal and anti-TH antibody to reveal Shh progenies and mDA neurons respectively. Cells double positive for β-gal and TH were identified in all TH+ nuclei in the midbrain: (C) PAG, periaqueductal gray; (D,E) Li, linear nucleus of raphe; (F) RR, retrobrual fieldd, (G) SNr, substantia nigra pars reticular; (H) IF, interfascicular nucleus; (I) PN, paranigral nucleus; (J) VTA, ventral tegmental area; (K) SNc, substantia nigra pars compacta; (L) SNl, substantia nigra pars lateralis. Scale bars correspond to 100μm.

3.3.6 Tracing the medial and lateral ventral midbrain progenitors by tamoxifen induced fate mapping

Based on the dramatic expansion of Shh expression from E8.0 to E9.5 (Figure 3-9) and a lack of BrdU incorporation in the midbrain FP region at E9.5 (Y.E. Mavromatakis, unpublished), we made an assumption that this occurs by Shh expanding into the dorsal domain instead of by proliferation. We then attempted to label the Shh expression domains at different time with the tamoxifen inducible ShhCreER^{T2} mice crossed with either the R26RLacZ or R26REYFP (Srinivas et al., 2001) reporter mice.

The ShhCreER^{T2} mice carry the Cre fusion protein with a tamoxifen-responsive mutant form of human estrogen receptor ligand binding domain (Feil et al., 1997; Indra et al., 1999). The CreER^{T2} is sequestered in the cytoplasm by heat shock protein 90 until a conformational change is induced by the synthetic estrogen antagonist 4-OH-tamoxifen, allowing its translocation into the nucleus to induce recombination between loxP sites (Branda and Dymecki, 2004; Joyner and Zervas, 2006). Tamoxifen administered into mice is converted by the liver to the active inducer 4-OH-tamoxifen (Branda and Dymecki, 2004). The tamoxifen induced Cre recombinase activity starts at around 6 hours (h), increases markedly from 6 h to 12 h, peaks between 12 and 24 h, and lasts up to 36 to 48 h postinjection (Hayashi and McMahon, 2002; Zervas et al., 2004). Therefore, we define the tamoxifen induced labelling period as 6 to 48 h with a peak at 12 to 24h after tamoxifen administration.

Conventional mating was set up after 4pm in the afternoon and the presence of a vaginal plug (VP) was checked the next morning. Noon on the day of VP detection was defined as E0.5. Tamoxifen was administered by oral gavage at 12:00 noon at E7.5, 8.5, 9.5 and 10.5 to pregnant females to obtain peak labelling at E8.0-8.5, E9.0-9.5, 10.0-10.5 and E11.0-11.5 respectively. The embryos were harvested at E12.5, and cross-sections of the midbrains were stained with antibodies against TH and β-gal for R26RLacZ or GFP for R26REYFP. From our assumption, we had expected a progressively broader domain of labelling by administering tamoxifen from E7.5 to 9.5, and a lateral domain from administration of the tamoxifen at E10.5. However, no consistent pattern of labelling has been obtained from 5 litters of embryos with tamoxifen administered at E7.5, 14 litters at E8.5, 10 litters at E9.5 and 1 litter at E10.5 using either R26RLacZ or R26REYFP reporter mice (Figure 3-13B-E). A narrow stream of medially labelled cells was

observed in only 1 litter from tamoxifen administered at E7.5, which appeared much younger than E12.5 at harvest (Figure 3-13A). Then, we tried to administer tamoxifen at 7a.m. (about E7.25), and the medial labelling described above could not be reproduced (data not shown). There was no observable difference in the domain labelled with different doses of tamoxifen or by either R26RLacZ or R26REYFP reporter mice.

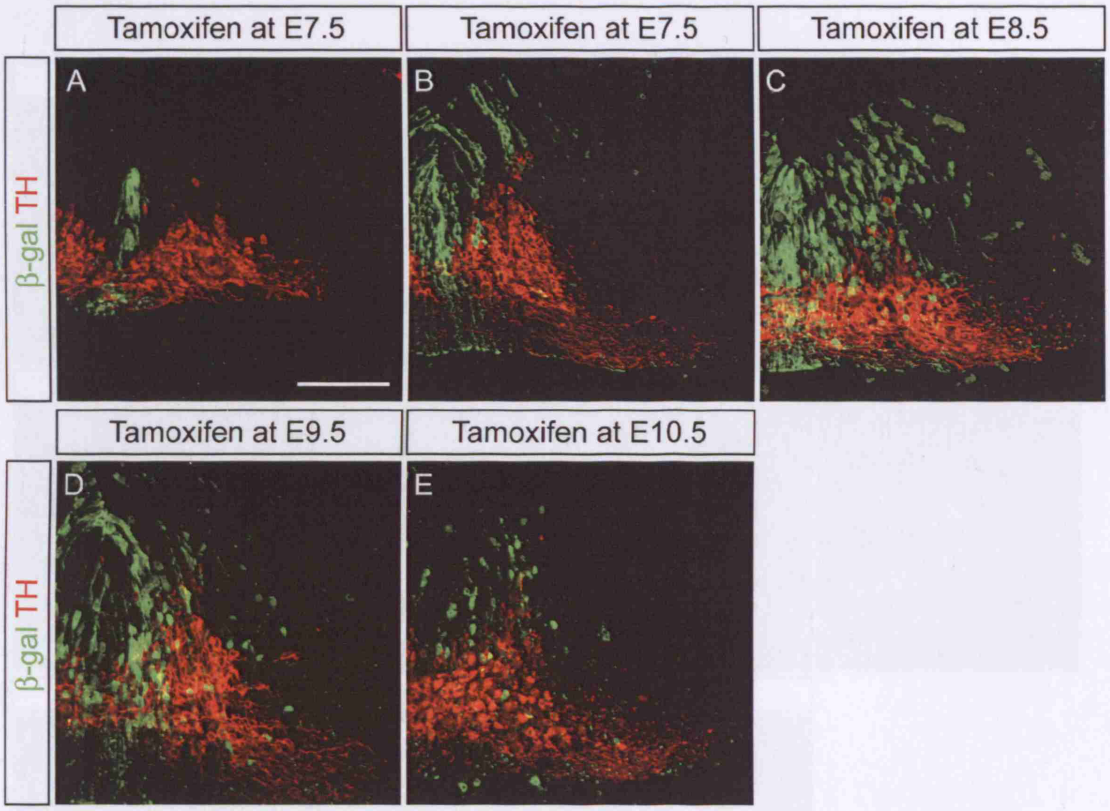

Figure 3-13 No consistent and distinct pattern of labelling by ShhCreER^{T2};R26RLacZ with conventional mating.

Double immunostaining of β-gal and TH on rostral midbrain cross sections of E12.5 embryos with tamoxifen administration at E7.5 (A,B), E8.5 (C), E9.5 (D) and E10.5 (E). Scale bars correspond to 100μm.

Since the expansion in *Shh* expression occurred in a very short period between E8.5-9.5, and that medial labelling had only been observed in the young litter with tamoxifen gavage at E7.5. We reason that the variation in the timing of mating by conventional mating would be too large. We then attempted to precisely control the mating time, and thus the stage of embryos. Timed mating between

ShhCreER^{T2};R26RLacZ males and R26RLacZ females were set up at 7a.m. and the presence of a VP was check at 10a.m., after which the mice were separated. The embryos were staged as E0 when VP was detected 10a.m., and harvested at 10p.m. at E10.5, E12.5, E13.5 or E18.5. Tamoxifen was administered to pregnant mice at various time points summarised in Figure 3-14 to determine the timing and domain labelled with ShhCreER^{T2};R26RLacZ.

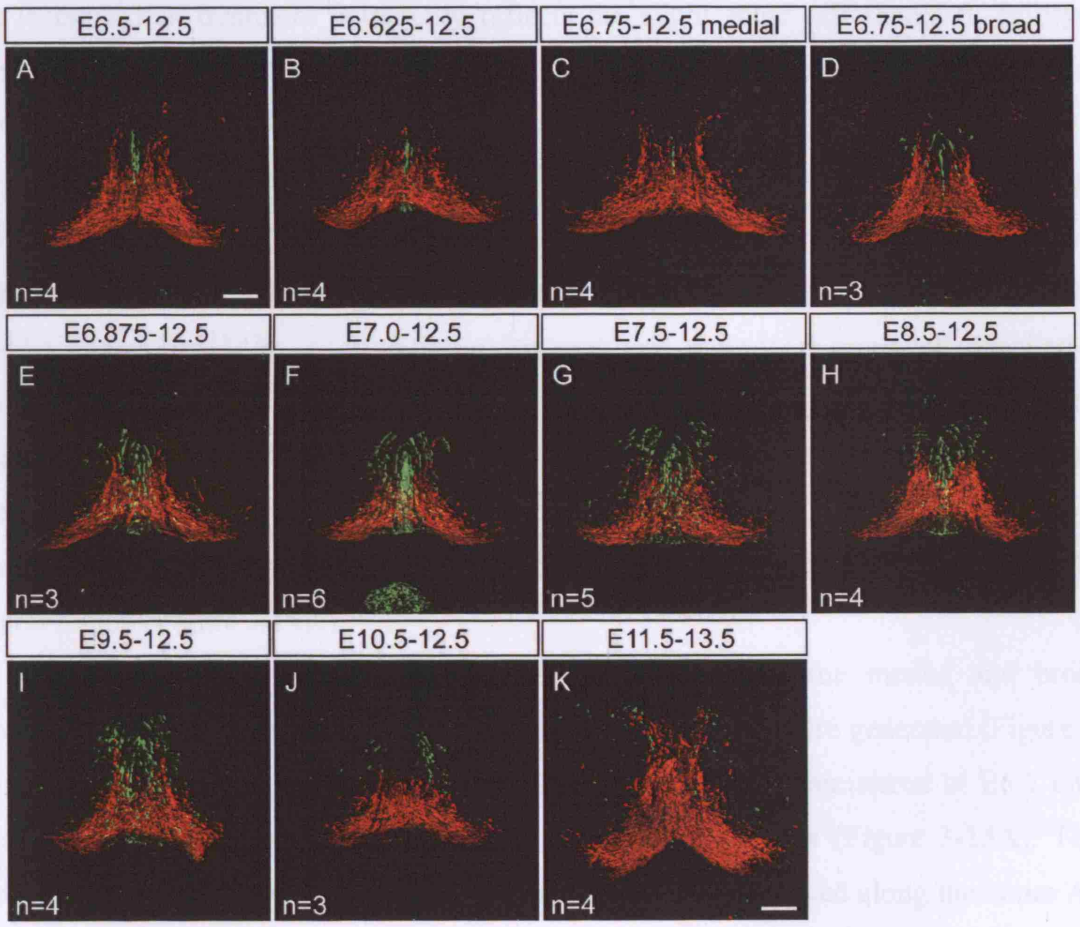

Figure 3-14 Distinct pattern of temporal mediated labelling of ventral midline cells obtained in tamoxifen treated ShhCreER^{T2};R26RLacZ embryos with 3 hour timed mating.

Double immunohistochemistry of β-gal (green) and TH (red) on rostral midbrain sections from ShhCreER^{T2};R26RLacZ embryos harvested at E12.5 (A-J) or at E13.5 (K). Tamoxifen was administered to timed pregnant females between E6.5 and E11.5 as indicated. Tamoxifen administration at E6.5, E7.5, E8.5, E9.5, E10.5 and E11.5 corresponded to oral gavage at 10p.m. on the respective days, whereas E6.625, E6.75, E6.875 and E7.0 corresponded to oral gavage at 1a.m., 4a.m., 7a.m. and 10a.m. respectively. The numbers of experiments from independent tamoxifen administrations are indicated as n. Scale bars correspond to 100μm.

We were finally able to obtain distinct and consistent patterns of labelling. Very narrow medial labelling was obtained when tamoxifen was administered at E6.5 (Figure 3-14A) and E6.625 (Figure 3-14B). Interestingly, when tamoxifen was given at E6.75, either medial narrow (Figure 3-14C) or broad (Figure 3-14D) labelling was observed. Due to the variable and mosaic nature of tamoxifen induced fate mapping, embryos were classified as having broad labelling when any β-gal positive cells were found beyond the TH+ mDA region. In the embryos defined as having broad labelling, labelled cells were predominantly found in the medial region. The different labelling pattern obtained in the E6.75 tamoxifen treatment potentially reflects the slight stage differences in embryos obtained from different time of conception within the 3 hours timed mating. Broad labelling was obtained from E6.875 to E9.5 (Figures 3-14E-I). The β-gal+ cells tend to be more densely populated in the medial than lateral region at E6.875 (Figure 3-14E) and E7.0 (Figure 3-14F) tamoxifen stages. The labelling was more evenly spread throughout the Shh expression domain when tamoxifen was administered at E7.5 (Figure 3-14G) and E8.5 (Figure 3-14H). At E9.5 tamoxifen treatment, there were more cells labelled in the lateral region (Figure 3-14I). At E10.5 tamoxifen administration, labelled cells were exclusively located in the rostrolateral midbrain, while predominantly but not exclusively situated in the caudolateral midbrain (Figure 3-14J). When tamoxifen was given at E11.5 and embryos harvested at E13.5, labelling was only observed in the lateral region (Figure 3-14K).

We then captured the progenitor domain marked in the medial and broad labelling by harvesting embryos at E10.5 before mDA neurons were generated (Figure 3-15). Consistent with the data obtained at E12.5, tamoxifen administered at E6.5 only labelled a narrow medial part of the Lmx1a+ mDA progenitors (Figure 3-15A). This medial labelling was usually very sparse, and might not be observed along the entire AP axis. Broad area of β-gal positive cells encompassing both Lmx1a+ FP and Lmx1a- BP regions were repeatedly found in E7.5 tamoxifen treatments (Figure 3-15D). Tamoxifen treatment at E6.75 again resulted in either medial (Figure 3-15B) or broad (Figure 3-15C) labelling. Taken together, three different patterns of labelling are obtained by temporal control of Cre activities in ShhCreER^{T2} mice: (1) medial from E6.5 to E6.625, (2) broad from E6.875 to E9.5, and (3) lateral at E11.5.

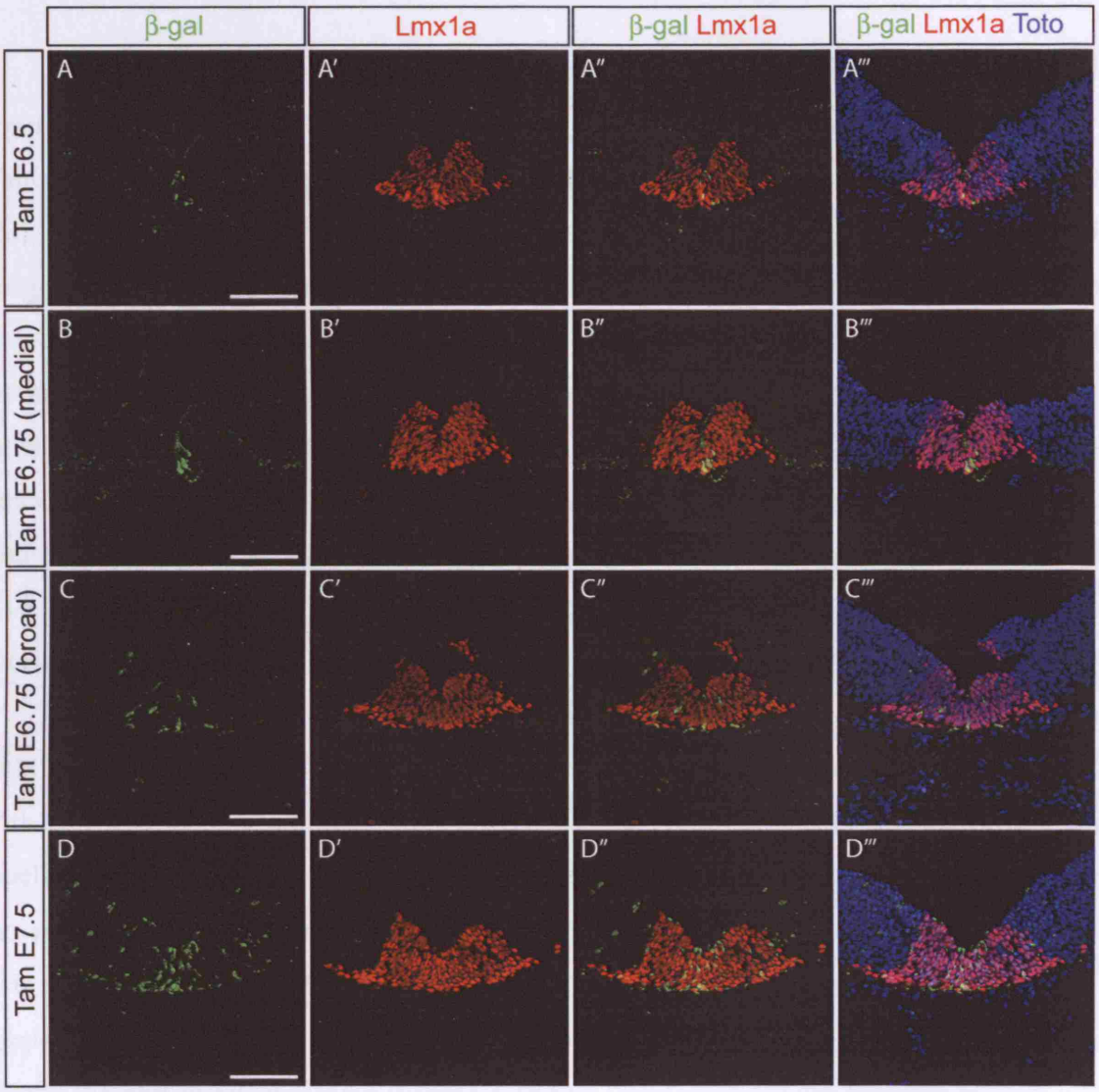

Figure 3-15 Either medial or broad pattern instead of progressive expansion in Shh-expressing progenitors is labelled by tamoxifen treatment of ShhCreER^{T2};R26RLacZ embryos.

Double immunohistochemistry of β-gal and Lmx1a in E10.5 ShhCreER^{T2};R26RLacZ embryos. Tamoxifen (Tam)was administered to timed pregnant females from E6.5 to E7.5. Medial Lmx1a+ progenitors were labelled by E6.5 (A) and some cases of E6.75 (B). Broad progenitor labelling was achieved by tamoxifen treatment at E7.5 and occasionally at E6.75. Scale bars correspond to 100μm.

3.3.7 No medial versus lateral correlation between mDA progenitors and neurons

Shh-expressing cells labelled at different stages from E6.5 to E10.5 all had contributions to the TH+ mDA neurons at E12.5 (Figure 3-16). Cells labelled by ShhGFPCre, which corresponded to the cumulative Shh expression domain from E8.0 (5s), gave rise to the vast majority of the mDA neurons (Figures 3-16A,G). The medial progenitors labelled between E8.0 and E8.5 with tamoxifen administration at E6.5 were found as a stream of medially located cells along the ventral midline, and extended laterally at the ventral part of the mantle zone (Figures 3-16B,H). Broad scattered cells labelled from E8.0 to E11.5 by tamoxifen treatment from E7.5 to E9.5 were distributed randomly within and beyond the TH+ mDA neuronal domain (Figures 3-16C-E, I-K). Shh-expressing cells labelled between E10.75 and E12.5 by tamoxifen administration at E10.5 (Figures 3-16F,L) extended from the lateral progenitor region to the mDA neurons located laterally.

We then followed the long-term fates of the early medial progenitors labelled by ShhCreER^{T2} with tamoxifen treatment at E6.5 and late lateral labelling by ShhCreER^{T2} with E11.5 tamoxifen administration. At E18.5, the cumulative Shh progenitor domain labelled by ShhGFPCre maintained a high level of β-gal expression in a broad region at the ventricular zone (Figures 3-17A1, 3-18A1). Similar to the findings in the adult, the TH+ mDA neurons were mostly double positive for β-gal in the PAG, Li and RR subpopulations located in the mid-caudal midbrain (Figure 3-17A), and in the VTA and SNc in the mid-rostral midbrain (Figure 3-18A).

Contrary to the hypothesis that subpopulations of mDA neurons are generated from spatially distinct progenitors located in the respective medial and lateral locations, the narrow medial progenitor domain labelled by E6.5 tamoxifen, remained in the medial region at E18.5, but gave rise to mDA neurons in PAG, Li and RR populations in the mid-caudal midbrain (Figure 3-17B), and VTA and SNc populations in the mid-rostral midbrain (Figure 3-18B). However, the lateral progenitors marked by late tamoxifen treatment at E11.5 mainly destined to the medial mDA populations in the Li (Figure 3-17C2) and VTA (Figure 3-18C2), with very few cells in the medial SN region. The lateral TH+ cells in the RR (Figure 3-17C3) and SN (Figure 3-18C3), and medial PAG neurons (Figure 3-17C1) were devoid of β-gal immunoreactivity.

Taken together, the narrow medial progenitor domain has the potential to generate all major subpopulations of mDA throughout the midbrain, whereas the fate of lateral mDA progenitors labelled at a later stage are only confined to the Li, VTA and medial SN populations.

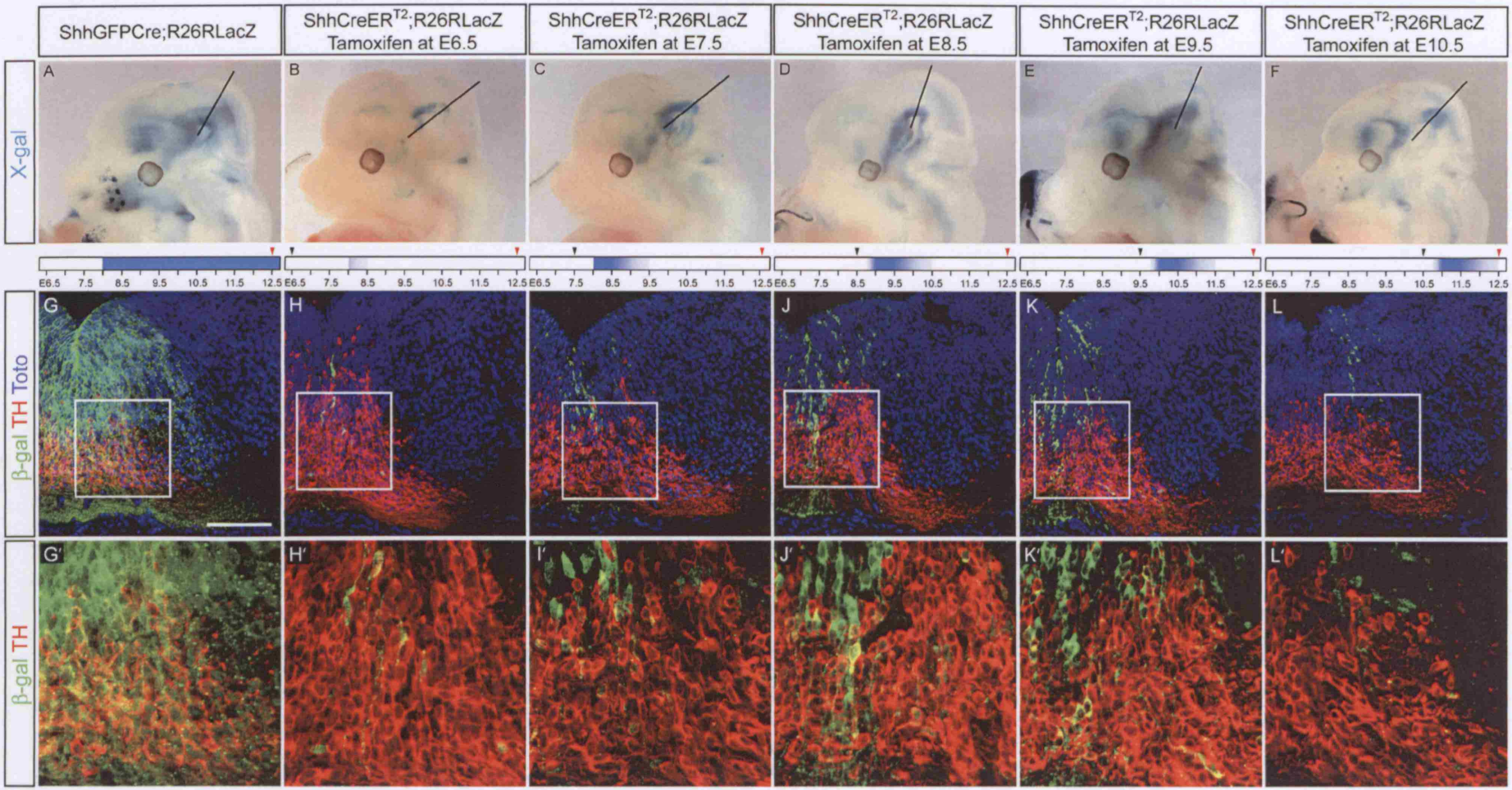
ShhGFPCre;R26RLacZ
ShhCreER^{T2};R26RLacZ Tamoxifen at E6.5
ShhCreER^{T2};R26RLacZ Tamoxifen at E7.5
ShhCreER^{T2};R26RLacZ Tamoxifen at E8.5
ShhCreER^{T2};R26RLacZ Tamoxifen at E9.5
ShhCreER^{T2};R26RLacZ Tamoxifen at E10.5
X-gal
A
B
C
D
E
F
E6.5 7.5 8.5 9.5 10.5 11.5 12.5
β-gal TH Toto
G
H
J
K
L
β-gal TH
G'
H'
I'
J'
K'
L'

Figure 3-16 Shh progenies labelled at different stages contribute to mDA neurons.

Whole mount X-gal staining of ShhGFPCre;R26RLacZ (A) and ShhCreER^{T2};R26RLacZ (B-F) embryos with tamoxifen administered at the stages indicated by black arrowheads and harvested at E12.5 (red arrowheads). The time scales in blue indicate the period of recombination events that activate the LacZ reporter allele. (G-L) The contributions of Shh progenies to the mDA neurons on cross-sections of the rostral midbrain. The level and angle of sections taken in G-L are designated by black lines in A-F. Scale bar corresponds to 100μm.

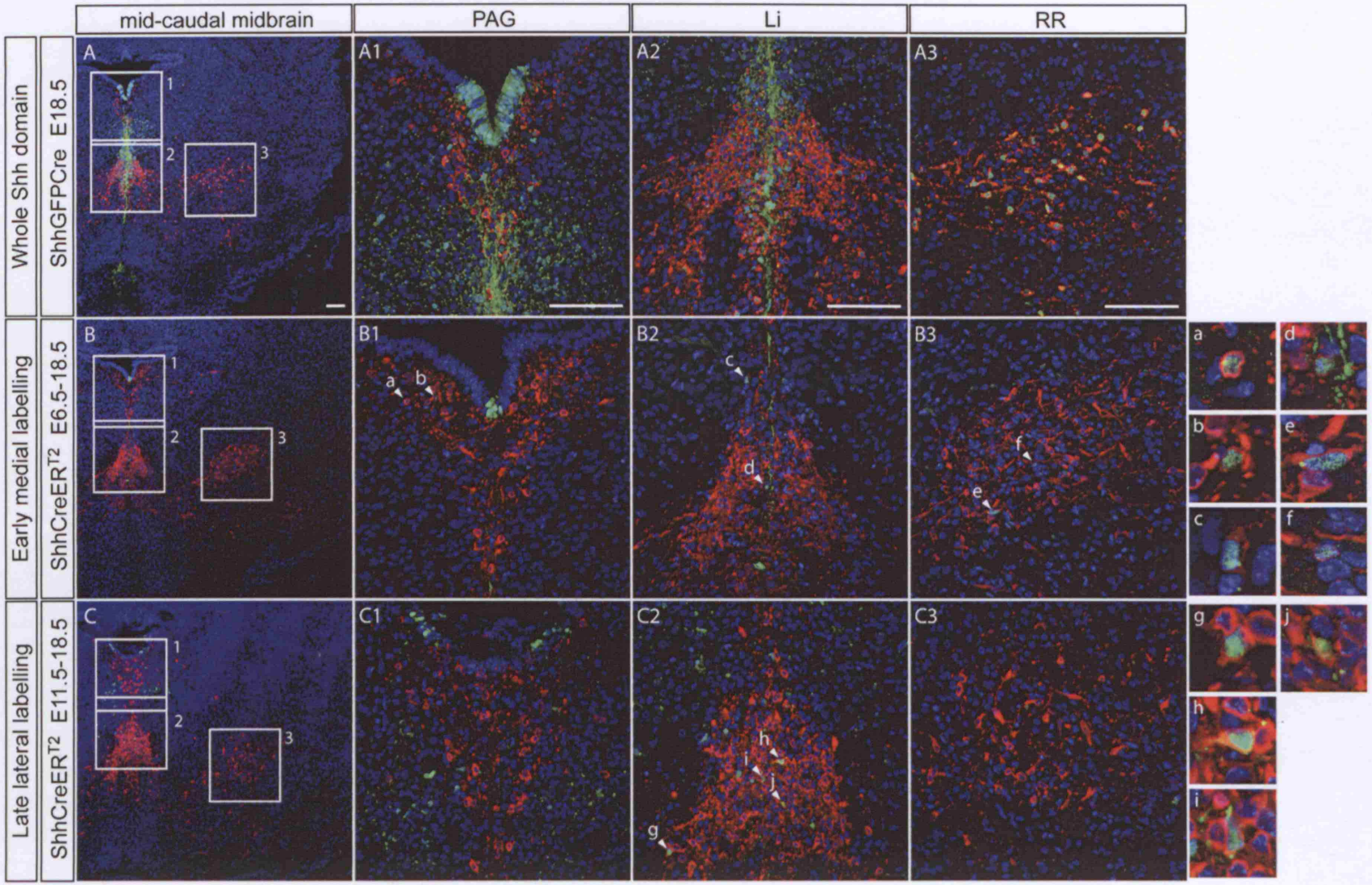
mid-caudal midbrain
PAG
Li
RR
Whole Shh domain
ShhGFPCre E18.5
Early medial labelling
ShhCreER^{T2} E6.5-18.5
Late lateral labelling
ShhCreER^{T2} E11.5-18.5
A
A1
A2
A3
B
B1
B2
B3
C
C1
C2
C3
1
2
3
a
b
c
d
e
f
g
h
i
j

Figure 3-17 Early labelled medial progenitors contribute to all mDA populations, whereas late lateral progenitors mainly contribute to medial mDA populations in the mid-caudal midbrain from long-term fate mapping of Shh expressing cells.

Coronal sections of E18.5 ShhGFPCre;R26RLacZ (A) and ShhCreER^{T2};R26RLacZ (B,C) embryos at the mid-caudal level in the midbrain were double labelled with β-gal and TH. Cells double positive for β-gal and TH are indicated by arrowheads in each of the PAG (1), Li (2) and RR (3) subpopulations of mDA neurons, and further magnified in (a) to (j). Scale bars correspond to 100μm.

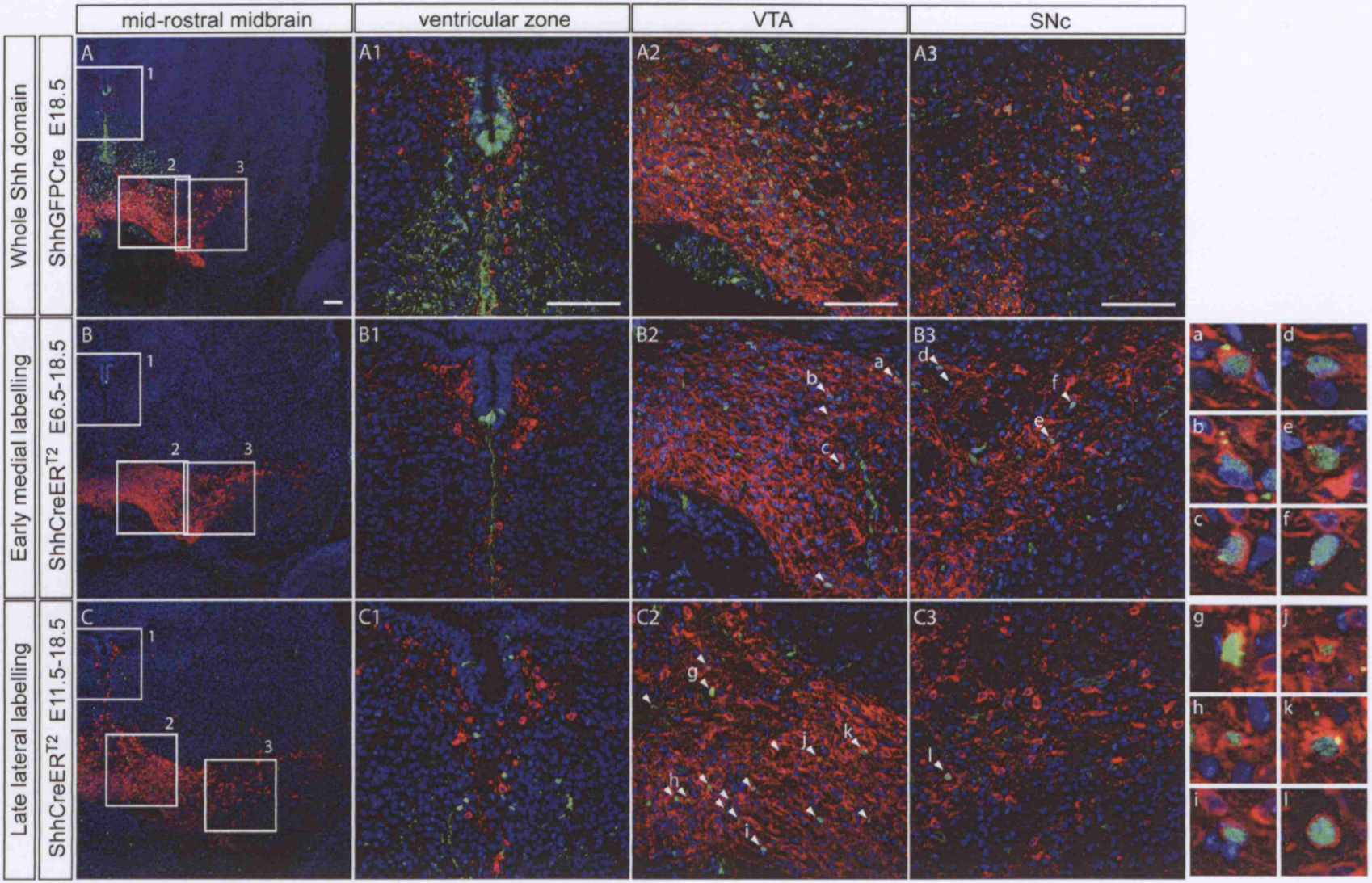
mid-rostral midbrain
ventricular zone
VTA
SNc
Whole Shh domain
ShhGFPCre E18.5
Early medial labelling
ShhCreER^{T2} E6.5-18.5
Late lateral labelling
ShhCreER^{T2} E11.5-18.5
A
A1
A2
A3
B
B1
B2
B3
C
C1
C2
C3
1
2
3
a
b
c
d
e
f
g
h
i
j
k
l

Figure 3-18 Early labelled medial progenitors contribute to all mDA populations, whereas late lateral progenitors mainly contribute to medial mDA populations in the mid-rostral midbrain from long-term fate mapping of Shh expressing cells.

Coronal sections of E18.5 ShhGFPCre;R26RLacZ (A) and ShhCreER^{T2};R26RLacZ (B,C) embryos at the mid-rostral level in the midbrain were double labelled with β-gal and TH. The origin of the β-gal positive cells in the ventricular zone is shown in (1). Cells double positive for β-gal and TH are indicated by arrowheads in the each of the VTA (2) and SNc (3) subpopulations of mDA neurons. Selected double positive cells are further magnified in (a) to (l). Scale bars correspond to 100μm.

3.4 Discussion

3.4.1 mDA neurons are generated in the FP of the midbrain and caudal diencephalon

Based on the expression pattern of the key mDA neuronal marker, TH, it was believed that mDA neurons originate from both the FP and BP of the midbrain and caudal diencephalon (Marín et al., 2005; Smits et al., 2006; Verney, 1999; Verney et al., 2001; Vitalis et al., 2000).

3.4.1.1 The anteroposterior limit of mDA neurons

In this study, we have used a BAC transgenic Lmx1aCre;R26RLacZ mouse line to provide indirect evidence that the anterior limit of mDA progenitors lies at the boundary between rostral and caudal diencephalon. Evidence that mDA neurons are not generated in the isthmus region comes from a study on a transgenic midbrain-hindbrain boundary (MHB)-Cre mouse line. In this line, Cre recombinase is expressed briefly at around E10.5 in the MHB area (Kala et al., 2008). When crossed with R26RLacZ mice, a narrow band of β-gal positive cells is detected in the MHB in whole mount embryos at E10.5. These cells contribute to the dorsal MHB area, a portion of the anterior rhombomere 1, a few scattered cells in the dorsal midbrain and the ventral isthmus region at E11.5. Some of these cells develop into bilateral streams of cells in the ventral midbrain in the adult, intermingling with mDA neuronal fibres but not expressing TH (Kala et al., 2008).

3.4.1.2 mDA neurons are derived exclusively from the floor plate

During the preparation of this thesis, two recent studies have revolutionised the theory on both FP and BP origin of mDA neurons by suggesting a single FP origin (Andersson et al., 2006b; Ono et al., 2007). Andersson et al. identified two mDA progenitor markers Lmx1a and Msx1. They suggested that Lmx1a was able to induce Msx1 expression, which in turn suppressed the non-neurogenic FP characteristics by inducing Ngn2 expression and mDA neuronal differentiation (Andersson et al., 2006b).

In the other study, Ono et al. showed that the Lmx1a expression domain completely overlapped with that of the FP marker FP4 in rat. They also identified the transmembrane domain-containing cell-surface protease, Corin, which was expressed in an identical region as FP4 in the midbrain and hindbrain. The fate of Corin positive E13.5 rat FP cells isolated by fluorescence-activated cell sorting (FACS) was followed *in vitro*. Corin+ cells isolated during the neurogenesis stage can generate neurons, of which 53.6% express TH, and 80% of these TH+ cells coexpress Pitx3, which is suggestive of correct mDA identity. Together with data showing that Lmx1a was involved in the generation of mDA neurons in loss-of-function studies, the authors suggested that mDA neurons originate from ventral midline cells with FP like characteristics in the midbrain (Ono et al., 2007).

At the same time, we used an *in vivo* transient genetic fate mapping approach to follow Arx expressing FP progenitors with the ArxLacZ mouse line. Consistent with the other two studies, we found that the β-gal expression of Arx progenies from the FP completely overlapped with that of Lmx1a and TH in the ventral midbrain. Moreover, we observed that the β-gal+TH+ mDA neurons had already migrated laterally into the BP region of the caudal diencephalon at E12.5. We have also ruled out the BP origin of mDA neurons by showing that BP cells labelled by *-8.4ngn1:gfp* and Nkx2.2CreER^{T2} mouse lines do not generate mDA neurons. Using a transgenic mouse line made from the 8.4kb upstream sequence of the zebrafish *ngn1* (*-8.4ngn1:gfp*) (Blader et al., 2003), the GFP positive domain in the BP abutted the Lmx1a+ mDA progenitors at E10.5 and E11.5 (Figures 6-3A,B), and the TH+ mDA neurons at E12.5 and E13.5 (Figures 6-3C and data not shown). The ventrolateral region of mDA neurons partially overlapped with the GFP positive domain, but no co-localisation between the cell bodies was observed. Moreover, the BP cells labelled by tamoxifen treatment of Nkx2.2CreER^{T2} mouse line (R. Taveira-Marques, N. Tekki-Kessaris and W.D. Richardson, unpublished) from E7.5 to E9.5 did not give rise to mDA neurons at E12.5 (Figures 6-2B-D), and no labelling was obtained in the midbrain by administering tamoxifen at E6.5 (data not shown). Taken together, our data provide direct evidence for an exclusive FP origin of mDA neurons (Figure 3-19 A-B).

3.4.1.3 Further experiments for confirming the origin of mDA neurons

In pursuing the anterior limit of mDA progenitors, we can provide stronger evidence by requesting more BAC transgenic Lmx1aCre;R26RLacZ embryos and adult

brains for sagittal studies. First, we can characterise the precise location of the Lmx1aCre activity at E10.5 with molecular markers such as Nkx2.1, which is expressed in the rostral ventral diencephalon. Second, we can check on E12.5 sagittal sections to see if β-gal and TH expression domains abut each other. Then, the final distribution of the Lmx1aCre progenies and mDA neurons can be better examined on sagittal sections of E18.5 embryos or postnatal brains.

An ideal solution is to generate a Cre line that is expressed in the ventricular zone of the FP in the midbrain and caudal diencephalon. There appears to be enhancer regions that can potentially drive the expression of Lmx1a, Shh and Wnt1 in this domain.

3.4.1.4 Ventral midbrain and caudal diencephalon specific enhancers

The lack of Cre activity in the ventral midbrain and caudal ventral diencephalon of the Lmx1aCre animals indicates that Lmx1a has an mDA specific enhancer outside of the 100kb region 5' to its coding region. Sequences in the intronic, 5' and 3' regions of Lmx1a can be further explored to identify this mDA specific enhancer, which can be used to drive the expression of Cre recombinase in transgenic animals for lineage tracing studies. However, it is necessary to investigate if the enhancer is only active in mDA progenitor domain. The presence of enhancer activity in postmitotic mDA neurons will not be useful in locating their origin.

Moreover, midbrain and caudal diencephalon specific enhancers have been identified in *Shh* and *Wnt1*. A 532bp Shh brain enhancer (SBE1), located within the second intron of *Shh*, specifically drives reporter activity in the ventral region in the rostral midbrain and caudal diencephalon at E9.5 (Epstein et al., 1999; Jeong and Epstein, 2003). Furthermore, two Foxa2 binding sites within this SBE1 enhancer are required for the midline but not the lateral expression of Shh in the midbrain and caudal diencephalon (Epstein et al., 1999). This suggests that the midline and lateral Shh expressions in the midbrain and caudal diencephalon are regulated by different mechanisms.

A 110 bp cis-regulatory element of *Wnt1*, in which the putative Pax sites are deleted, drives reporter expression solely in the ventral diencephalon after neural tube closure. From the data presented, it appears that the reporter expression extends to the ventral midbrain as well (Rowitch et al., 1998). Since Wnt1 is expressed in the lateral mDA progenitors, this enhancer will allow specific tracing of the fate of lateral mDA progenitors. However, Wnt1 is also expressed in one layer of cells just outside the FP

ventricular zone at E12.5 (data not shown). Therefore, it is also necessary to investigate whether this Wnt1 enhancer is active in these newly born cells.

Besides lineage tracing studies, these enhancers will allow further studies on factors that bind to them for the activation of mDA specific expressions. This will be of paramount importance for understanding the genetic cascade leading to mDA neuron development.

3.4.2 The development of tools to label the heterogeneous mDA progenitors

In this study, we have shown that the Lmx1a+Arx+ mDA progenitor domain displays differential mediolateral expressions of Bmp7, Wnt1, Raldh1 and Msx1. Bmp7 and Raldh1 also show different levels of expression along the rostrocaudal extent. This heterogeneity within the mDA progenitor domain provided the basis for our hypothesis that subpopulations of mDA neurons are generated from spatially and genetically distinct progenitors.

3.4.2.1 The search for suitable mouse lines

Msx1 expression is excluded from the very thin lateral margin of the mDA progenitor domain (Figure 3-8, Andersson et al., 2006). Unfortunately, our attempts to follow the short-term fate of Msx1 expressing progenitors with Msx1-nlacZ embryos at both E12.5 and E14.5 were unsuccessful. The nlacZ reporter gene in the Msx1-nLacZ mouse line was inserted into the homeobox of Msx1 gene. Therefore, it is highly likely that the Msx1-nLacZ fusion protein is subjected to the same mechanisms that rapidly degrade the endogenous Msx1 protein in postmitotic neurons. In view of this, an Msx1Cre mouse line is being generated in the lab to allow permanent fate mapping of this subset of Lmx1a expressing cells.

We then investigated the possibility of adopting other strategies to follow subsets of mDA progenitors. Although a knock-in $Bmp7^{Cre}$ line has been reported (Oxburgh et al., 2004), it is not suitable for mDA progenitor fate mapping because *Bmp7* is broadly expressed in postmitotic neurons close to the mDA domain at E10.5 (Figure 3-7F), as well as in postmitotic mDA neurons at E12.5 (data not shown).

Wnt1 expressing cells have been reported to develop into mDA neurons with the Wnt1-CreER^{T};R26R mice (Zervas et al., 2004). This mouse line should be very useful for investigating the fate of lateral mDA progenitors, as well as their contributions to the various subpopulations at different embryonic stages. In fact, this group is actively pursuing this issue. This further demonstrates the popularity of the theory that mDA subpopulations are generated from distinct progenitor domains.

To date, there has not been any description on reporter mice for Raldh1. Nevertheless, Raldh1 is strongly expressed in a subset of postmitotic mDA neurons [Figure 4-28 and (Jacobs et al., 2007)]. Therefore, unless an inducible Cre line or a reporter driven by an mDA progenitor specific enhancer is available, it will not be suitable for testing our hypothesis.

Studies by a former student in the lab showed changes in the pattern of Shh protein in the ventral midbrain during mDA neuron development (Mavromatakis, 2006). These have provided insights into the possible changes in spatial and temporal expression of Shh by mDA progenitors, and are corroborated by our *Shh* RNA expression studies. We started by thoroughly characterised the ShhGFPCre;R26RLacZ mouse line, which cumulatively label Shh expressing cells. We showed that the vast majority of mDA progenitors in the embryos and mDA neurons in the adult are derived from Shh expressing cells.

3.4.2.2 Optimising conditions for tamoxifen induced fate mapping

We then used the tamoxifen inducible ShhCreER^{T2} mice to test our hypothesis. Although theoretically simple to perform, this technique proved difficult for us to perfect and retrieve consistent results. Firstly, the labelling efficiency was extremely poor with the dosage of tamoxifen used in the published work (Hayashi and McMahon, 2002; Zervas et al., 2004). During the optimisation of dose that would balance the recombination efficiency with the toxicity of tamoxifen leading to lethality and growth retardation of the embryos, we had faced unexpected problems that some batches of tamoxifen purchased from Sigma caused serious abortion problem when administered to pregnant females. The inconsistent qualities of the tamoxifen batches had hindered our ability to make a successful series of titrations for the optimal tamoxifen dosage. Efficient recombination was finally achieved by tracking the lot number of tamoxifen and using a high dosage that would also allow a reasonable viability for the embryos. It was later found that the problem might be attributed to the neo cassette in the

ShhCreER^{T2} targeting construct, which has not been removed in the transgenic mice. This has probably reduced the efficiency of the ShhCreER^{T2} allele. S. Blaess and A. Joyner have experienced the same problem, and overcome it by removing the frt-flanked neo cassette (personal communication).

Secondly, the expected expansion of ShhCreER^{T2} labelling could not be achieved in the initial experiments. Despite a trend in the expected labelling pattern, scattered cells in the broad Shh expression domain were inevitable. One of the reasons for this is that we assumed to obtain the pattern of the peak labelling period, which did not turn out to be the case. The weaker Cre activities were sufficient to induce recombination, albeit in a more mosaic manner. The other reason is that the expansion of Shh into the more dorsal domain was not progressive, and occurred at an earlier stage than expected. We were finally able to consistently label a smaller Shh expression domain when we took the radical approach to precisely limit the mating time to 3 h and perform a thorough study on the changes in Shh-labelling patterns. Using 3 h timed mating for the ShhCreER^{T2} mouse line, we managed to label early medial mDA progenitors, the entire Shh domain in the FP and BP, or late lateral mDA progenitors.

Finally, when we tried to trace the ultimate fate of the medial and lateral progenitors into adulthood, the viability problem struck again. Due to the high dosage of tamoxifen used, none of the embryos from the E11.5 tamoxifen treatment survived the parturition process. We had tried to improve the viability by delivering progesterone with tamoxifen to pregnant females (Joyner and Zervas, 2006), but without success. Although it is known that the mDA neurons undergo natural cell death during the first postnatal month (Jackson-Lewis et al., 2000), it has also been suggested that the migration of mDA neurons in mouse has been completed by E15.5 based on an extrapolation of their development in rat (Bayer et al., 1995). Therefore, we decided to analyse the long-term fate of the medial and lateral labelling at E18.5, just before birth. In fact, the pattern of the mDA system is the same as that in the adult. This allowed us to distinguish the subpopulations by their position, despite not being able to use many of the molecular markers expressed at postnatal stages. The postnatal survival problem was finally overcome by fostering pups dissected at E18.5. However, due to the time constrain, we are not able to analyse the adult specimens yet.

3.4.2.3 Early labelling of lateral mDA progenitors cannot be achieved

Since we were unable to mark lateral mDA progenitors at an early stage with ShhCreER^{T2} coupled with the unavailability of the Wnt1-CreER^{T} mouse line, we sought to trace the lateral cells with other mouse lines. The expression of Nkx2.2 abuts the small Shh expression domain as revealed by the nuclear GFP in ShhGFPCre embryos at E9.0 (Figure 6-2A). We hypothesized that the early Nkx2.2 expression domain might correspond to the prospective lateral mDA progenitor domain. Therefore, we attempted to follow the fate of Nkx2.2 expressing cells using the BAC transgenic Nkx2.2CreER^{T2} mouse line. This mouse line has very high recombination efficiency comparing with the ShhCreER^{T2} line. However, only BP cells, which do not generate mDA neurons, were labelled.

The Nkx2.2 progenies labelled from E7.5 to E9.5 appeared to shift slightly dorsally from not overlapping to partially overlapping with the endogenous Nkx2.2 domain in the BP at E12.5 (Figures 6-2E-G). From these data, we can speculate on two possibilities. First, Shh expression has already reached the broad domain at E9.0. In light of this, we can make use of the nuclear GFP in the ShhGFPCre to study the expression of Shh relative to Nkx2.2 and possibly other markers in greater details. We can also compare the Shh and Nkx2.2 domains with the mDA specific Lmx1a expression, which is reported to begin at E9. Second, it is possible that the BAC transgene does not contain all the regulatory sequences to reflect the endogenous Nkx2.2 expression in the ventral midbrain. Therefore, it is necessary to correlate the endogenous Nkx2.2 expression with the Cre activities of Nkx2.2CreER^{T2} line in the ventral midbrain before drawing any conclusion.

Taken together, there is currently no available tool that allows us to label lateral mDA progenitors at early stages. The information will be made available once M. Zervas' group publishes their data. In this study, we are only able to test our hypothesis on the origin of mDA subpopulations by following the fate of medial progenitors during the whole course of mDA neuron production and lateral mDA progenitors from E10.75 onwards.

3.4.3 Subpopulations of mDA neurons are not distinguished by their medial-lateral position in the mDA progenitor domain

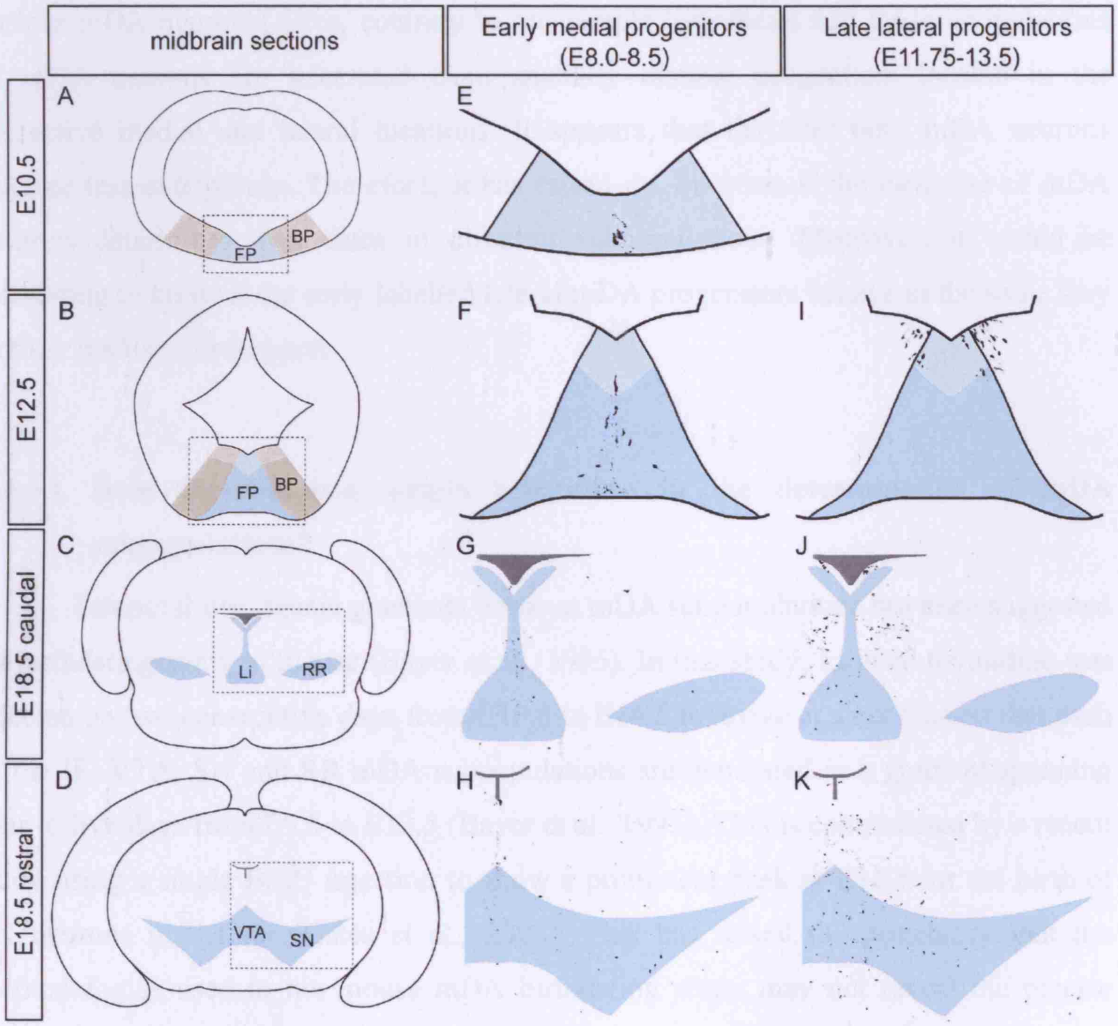

Figure 3-19 Schematic diagram showing the origin of mDA neurons from the midbrain floor plate region.

(A-D) The midbrain FP progenitors (blue) but not the BP progenitors (brown) generate mDA neurons. Medial mDA progenitors labelled in ShhCreER^{T2};R26RLacZ embryos by tamoxifen administration at E6.5 remain in the medial progenitor domain at E10.5 (E), become postmitotic and start to migrate laterally in the mantle zone at E12.5, and settle at different mDA subpopulations in the Li and RRF in the caudal midbrain (G), and in the VTA and SN nucleus in the rostral midbrain (H) at E18.5. Lateral progenitors labelled in ShhCreER^{T2};R26RLacZ embryos by tamoxifen administration at E11.5 (I) mainly contribute to the medial mDA populations in the Li (J) and VTA (K) at E18.5.

The narrow medial mDA progenitors sparsely labelled by tamoxifen treatment at E6.5 are found to give rise to all the anatomically distinct mDA subpopulations (Figure 3-19 E-H), whereas the late born neurons derived from the lateral mDA progenitors labelled by tamoxifen treatment at E11.5 settle at the medial mDA subpopulation (Figure 3-19 I-K). This strongly suggests that medial progenitors have the potential to generate various mDA neuronal fates, contrary to our simple hypothesis that the subpopulations of mDA neurons are generated from spatially distinct progenitors located in the respective medial and lateral locations. It appears that the later born mDA neurons migrate less extensively. Therefore, it has raised the question if the birthdate of mDA neurons determines their fates in different subpopulations. Moreover, it would be interesting to know if the early labelled lateral mDA progenitors behave in the same way as their medial counterparts.

3.4.3.1 Does the temporal origin contribute to the determination of mDA subpopulations?

Temporal neurogenic gradients between mDA subpopulations has been suggested by birthdating study in mouse (Bayer et al., 1995). In this study, tritiated thymidine was injected on two consecutive days from E10.5 to E14.5 to arrive at a conclusion that each of the IF, VTA, SN and RR mDA subpopulations are generated in a gradient spanning four to five days from E9.5 to E13.5 (Bayer et al., 1995). This is contradicted by a recent study using a single BrdU injection to show a prominent peak at E11.5 for the birth of SN neurons in the rat (Gates et al., 2006). This has raised the possibility that the methodologies used in the mouse mDA birthdating study may not reveal the precise timing of mDA origin. Therefore, we decided to re-examine the birthdates of the mouse mDA subpopulations, and to investigate whether the medial progenitors develop into different subpopulations at different time points by combining the E6.5 tamoxifen treatment with BrdU birthdating studies.

We used the 3h timed mating set-up to control the embryonic staging precisely. Three pulses of BrdU were given to pregnant females at 2 h intervals for each stage of E9.5, E10.5, E11.5 and E12.5. Preliminary data on embryos collected at E18.5 (Figures 6-4, 6-5) suggested a late generation for the two medial populations, the Li and the VTA, peaking at E11.5 and E12.5. Surprisingly, there were hardly any TH+ cells strongly labelled by BrdU cells in the RR and SN regions. Although we have difficulties classifying the weak BrdU positive cells in the RR and SN as being born on any specific

embryonic day, it is clear that there is significant overlapping between the birth of different mDA populations, and that our results on the birthdate of the VTA agrees with data obtained by Bayer et al., 1995. Moreover, we were not yet able to detect any cells double positive for both β-gal and BrdU due to the sparse labelling by tamoxifen treatment. Therefore, the birthdates of the medial progenitors remain to be determined.

Furthermore, the gene expression profile in the progenitors changes during mDA neuron generation. The level of Shh starts to be reduced at E10.5 and this reduction is evident at E11.5. The expression levels of Lmx1b and En1 decrease at E11.5. This timing coincides with the peak of generation for Li and VTA populations. It will be interesting to know if the downregulations of Shh, Lmx1b and En1 are responsible for the production of distinct mDA neuronal subtypes.

3.4.3.2 Do mDA progenitors along the AP axis develop into different subpopulations?

Besides the medial and lateral differences in gene expression within the mDA progenitor region, we have also observed progressive AP changes in the levels and domains of Bmp7 and Raldh1 expressions. Moreover, En1 is expressed in the midbrain but not the caudal diencephalon (McMahon et al., 1992). These differences in gene expression along the AP axis may possibly lead to different fates of mDA progenitors.

Our studies using the ArxLacZ embryos have also indicated that Arx expression is absent from the most rostral TH+ cells at E12.5. Further experiments are required to confirm whether it is due to a degradation of the β-gal protein by examining these embryos at earlier stages such as E11.5 and on sagittal sections. If the ArxLacZ is not expressed in the rostral mDA progenitor domain, it will serve as another difference in the gene expression profile of mDA progenitors that leads to heterogeneity of these neurons. However, the transient expression of β-gal in the Arx-expressing progenitor cells would not permit tracing of their long-term fate.

We then turned to the permanent labelling of the En1 expressing cells in the midbrain by crossing the En1-Cre (Kimmel et al., 2000) with R26RLacZ mice. As expected, the progenies of En1 expressing cells were roughly restricted posterior to the midbrain and diencephalic boundary, with the exception of the ventral midbrain region (data not shown). Since En1 is expressed in postmitotic mDA neurons, the En1-Cre mouse line labels all mDA neurons. This suggests that labelling early En1-expressing cells by the tamoxifen inducible En1-CreERT1 (Sgaier et al., 2005) will allow the

midbrain specific cells to be followed. More interestingly, En1-CreERT1 and En2-CreERT2 mice have been shown to label progressively smaller domains in the posterior midbrain by tamoxifen treatment at E9.5 and E10.5 (Sgaier et al., 2005). These mouse lines will provide valuable information as to whether mDA progenitors along the AP axis have different contributions to the mDA neuronal subpopulations. However, tamoxifen treatment should be administered before E9.5 in order to avoid labelling of postmitotic neurons. Unfortunately, we were unable to obtain these lines for our analysis.

We have recently obtained embryos which contain a BAC transgene for Pax2-Cre (Ohyama and Groves, 2004) and the R26RLacZ reporter to address the question of whether the midbrain progenitors give rise to subsets of mDA neurons. Pax2-Cre allows the tracing of midbrain cells from an early stage because the Cre transcript is already restricted to the MHB at E9.5, and that the LacZ reporter showed a sharp boundary of Pax2 progenies at the midbrain and diencephalic boundary at E9.5 (Ohyama and Groves, 2004). We intended to follow these midbrain restricted cells to E18.5 and analyse their distributions in the mDA neuronal populations. Unfortunately, we were unable to obtain a clear β-gal staining on the sections derived from these embryos. There might have been problem during the shipping of embryos; therefore, no conclusion can be drawn from this mouse line yet.

Taken together, the differential expression along the AP axis may be a possible factor in determining the different fates of mDA subpopulations. It is likely that a combination of positional information along both DV and AP axes, together with the timing of birth coordinate their terminal fates. This can be tested by the intersectional and subtractive genetic fate mapping, which combines gene-specific Cre and Flp recombinases and a dual recombinase-responsive reporter to follow the descendents at both the intersectional region and the subtracted domain with the activity of a single recombinase (Farago et al., 2006).

Here we speculate that the early mDA progenitors have the potential to become any of the different mDA subpopulations. A yet to be identified mechanism induces heterogeneous gene expression within the mDA progenitor domain. This is probably elicited by diffusible molecules from one or more source(s). Each progenitor receives a different quantity of the signalling molecules within a concentration gradient, and is also exposed to these molecules for a different duration of time. Subsequently, cells express different levels of genes relative to the distance from the source(s). The heterogeneity is then exaggerated through time by positive and negative feedback mechanisms. These differential gene expressions along both the DV and AP axes continue to restrict the fates

of the progenitors, determine the properties, migration and finally projection of each neuron.

Chapter 4
Transcriptional regulation of midbrain DA neuron development by Lmx gene family

4.1 Introduction

The development of an organism requires the appropriate specification of progenitors, their expansion by proliferation, and their correct differentiation into distinct cell types. Numerous mechanisms are employed to regulate the expression of genes required for different cellular processes at various levels to ensure the proper development of an organism. These range from controlling the accessibility of the DNA sequences (e.g. by DNA methylation and alteration of the chromatin structure), the transcription of DNA sequences into RNA, RNA splicing, RNA stability, translation of mRNA into proteins, and post-translational modifications (such as phosphorylation).

Transcriptional regulation of gene expression, a main level at which developmental processes are coordinated, involves the interactions of specific transcription factors with their co-factors, the target promoter, enhancer and/or silencer elements. Transcription factors integrate extrinsic influences from different signalling pathways as well as intrinsic information within a cell, and act in combination to direct specific gene expression. Thus, transcription factors integrate information from the environment and control the expression of genes that ultimately dictate the identity and specific function of the cell types generated in the developing embryo.

4.1.1 LIM-homeodomain transcription factors

Transcription factors may consist of individual or multiple domains for DNA binding, transcriptional activation or repression, dimerisation, ligand recognition, and polymerase interaction. LIM-homeodomain (LIM-HD) transcription factors, including the Lhx, Islet (Isl) and Lmx families, are characterised by having two protein-binding

LIM domains located at the N-terminus, a centrally located DNA-binding homeodomain (HD), and a transcription activation domain at the C-terminus (Figure 4-1) (Curtiss and Heilig, 1998; Hobert and Westphal, 2000; Johnson et al., 1997). There are 12, 7 and 6 LIM-HD genes in the mammalian, *Caenorhabditis elegans* and *Drosophila melanogaster* genomes respectively (Zhao et al., 2006a), divided into six subgroups (Lhx1/5, Lhx2/9, Lhx3/4, Lhx6/8, Islet and Lmx) based on the amino acid sequence similarities between the homeodomains. Most of these subgroups are represented by one gene in invertebrates and two closely related genes in mice, possibly reflecting a gene duplication event during evolution. Zebrafish and *Xenopus laevis* occasionally contain a third member in each subgroup of the LIM-HD protein. Additionally, *C. elegans* has an extra member, Mec-3, which has no identified homologue in other species.

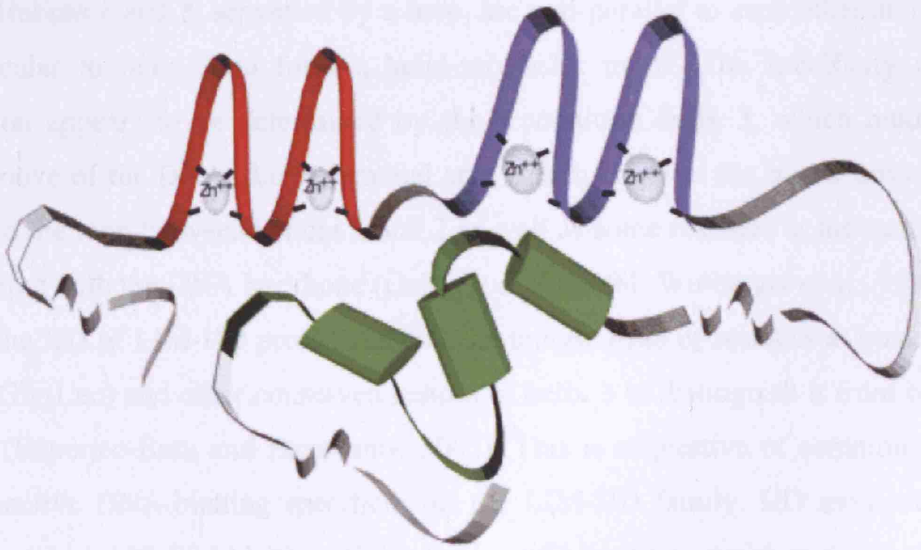

Figure 4-1 Hypothetical configuration of LIM-HD protein, suggesting an intramolecular association of the LIM and HD regions.

LIM1-, LIM2-, and homeodomains are depicted in red, blue, and green, respectively. The broken gray lines indicate that the lengths of these regions vary between different proteins. Each LIM domain coordinates two zinc ions. (Curtiss and Heilig, 1998)

HDs are found in homeobox transcription factors in animals, plants and fungi (Bürglin, 1994). Homeobox transcription factors typically induce a cascade of genes by specifically binding to their promoter regions, and play fundamental roles in the genetic control of development, such as body plan specification, pattern formation and cell fate determination (Hanes et al., 1994; Lewis, 1978; Yeo et al., 1995).

HD, consisting of 60 amino acids, were first identified as a conserved DNA sequence within the homeotic selector genes (*Ultrabithorax*, *Antennapedia* and *fushi tarazu*) of *Drosophila* (McGinnis et al., 1984; Scott and Weiner, 1984). Mutations in homeotic genes often result in a transformation of one structure of the body into the homologous structure of another body segment. The characteristic DNA-binding helix-turn-helix motif in HD has a very similar overall conformation between different homeobox families across species. For example, structural analysis using either nuclear magnetic resonance (NMR) spectroscopy or X-ray crystallography has revealed that the HD structures of Isl1, MATα2, Msx1 and Pdx1 are highly similar (Hovde et al., 2001; Ippel et al., 1999; Longo et al., 2007; Wolberger et al., 1991). The HD consists of three alpha helices folded into a tight globular structure. A flexible N-terminal arm precedes helix 1. Helices 1 and 2, separated by a loop, are anti-parallel to each other and roughly perpendicular to helix 3 to form a helix-turn-helix motif. The specificity of DNA recognition appears to be determined by the recognition helix 3, which binds in the major groove of the DNA, the N-terminal arm, which contacts the minor groove of the DNA, and the loop between helices 1 and 2 as well as some residues at the start of helix 2 interacting with the DNA backbone (Gehring et al., 1994; Wolberger et al., 1991).

The HD of LIM-HD proteins contains a unique triad of residues at positions 38-40 (Thr-Gly-Leu) and other conserved resides in helix 3 to distinguish it from other HD proteins (Banerjee-Basu and Baxevanis, 2001). This is suggestive of common ancestry and distinctive DNA-binding specificity in the LIM-HD family. HD monomers have approximately a 100-fold higher affinity for specific binding sites than for non-specific DNA, suggesting that additional contributions are required for specificity (Laughon, 1991). To enhance the target specificity, HD proteins usually contain other domains for additional DNA binding such as by the POU and paired domains, or for interactions with other transcriptional modulators such as by the LIM domain.

LIM proteins are originally named by the initials of the three LIM domain-containing transcription factors Lin11, Isl1, and Mec3 (Freyd et al., 1990; Karlsson et al., 1990; Way and Chalfie, 1988). The cysteine-histidine-rich LIM domain, conserved from ascidians to man, has an approximate size of 50-60 amino acids and binds two zinc ions

to form two tandemly repeated zinc fingers ($CX_2CX_{16-23}HX_2C$)-X_2-($CX_2CX_{16-23}CX_2C$/D/H, where X is any amino acid) (Gill, 1995; Hunter and Rhodes, 2005; Sadler et al., 1992). Structural analyses using NMR spectroscopy and X-ray crystallography show that each of the two zinc fingers consists of two orthogonally-arranged anti-parallel β-hairpins (Deane et al., 2004; Perez-Alvarado et al., 1994). Besides associating with the HD, LIM domains are also found alone in LIM-only (LMO) proteins, or in association with other domains including PDZ domains, kinase domains, SH3 domains and GAP domains (Hunter and Rhodes, 2005).

The specific protein-protein interaction properties of LIM domains are demonstrated by *in vitro* binding assays and the yeast two-hybrid systems (Feuerstein et al., 1994). Protein-protein interactions can be mediated by a single LIM domain. The importance of the integrity of the zinc fingers, coordinated by the eight conserved cysteine and histidine residues, is demonstrated by the strong decrease in protein-protein interaction by cysteine-to-serine substitution. Furthermore, the physical interaction has been visualised by X-ray crystal structure of LMO4:Ldb complex, where the LIM domain of LMO4 and LIM-interacting domain (LID) of Ldb1 formed an extensive hydrogen-bonding network to form a tandem β-zipper with a short three-stranded antiparallel β-sheet at each zinc-binding module (Deane et al., 2004).

LIM-HD transcription factors function to regulate gene expression and are involved in crucial developmental events ranging from the establishment of the body axis to the specification of terminal differentiation characteristics of neuronal subtype. While this study focuses on the Lmx subgroup of LIM-HD proteins, knowledge accumulated from other subgroups provides valuable insights into the potential of this important transcription factor family.

4.1.2 Lmx group

Two mammalian members Lmx1a and Lmx1b have been identified in the Lmx (LIM-homeobox) group. In zebrafish, two Lmx1b (Lmx1b.1 and Lmx1b.2) have been identified. At present, there has not been any discovery on a *D. melanogaster* orthologue of Lmx, while *Lim-6* represents the Lmx group in *C. elegans*.

4.1.2.1 Lmx1a

Lmx1a is mapped onto mouse chromosome 1; Locations: 1 H2.3; 1 88.2 cM (NCBI Entrez Gene). *Lmx1a* starts to be expressed from E8.5. In the embryos, its expression can be seen in the roof plate along the neuraxis, the basal plate of the hypothalamus, mDA neurons and choroid plexuses, cortical hemisphere, cerebellar anlage, otic vesicles and notochord posterior to the hindlimb level (Andersson et al., 2006b; Failli et al., 2002; Millen et al., 2004; Millonig et al., 2000; Ono et al., 2007). In adults, *Lmx1a* expression is maintained at low levels in the hippocampus (Failli et al., 2002).

The *Lmx1a* gene has been mapped to the *dreher* (*dr*) locus by positional cloning (Millonig et al., 2000). Mice homozygous for *dr* mutations are characterised by a general developmental delay, skeletal and pigmentation abnormalities, behavioural phenotypes including ataxia, vestibular deficits and hyperactivity, and neurological defects including cerebellar and hippocampal abnormalities (Chizhikov et al., 2006; Lyons and Wahlsten, 1988; Wahlsten et al., 1983). Various *dr* alleles have been described: *dr*, dr^{J}, dr^{2J}, dr^{3J}, dr^{4J}, dr^{5J}, dr^{6J}, dr^{7J}, dr^{8J}, dr^{Kjmi} and dr^{sst} (Bergstrom et al., 1999; Chizhikov et al., 2006; Millonig et al., 2000). Of these spontaneous alleles, dr^{J} ($Lmx1a^{dr}$) has been extensively used in embryological and neurological studies and is the only molecularly defined allele available at the beginning of this study. In the $Lmx1a^{dr}$ mutation, the G-to-A change at neucleotide 245 in exon 2 alters a conserved cysteine (Cys82) within the LIM1 domain to a tyrosine (Figure 4-2). This cysteine is involved in coordinating the zinc that is critical for zinc-finger integrity and function of the LIM1 domain of Lmx1a, which potentially mediates protein-protein interaction (Chizhikov et al., 2006; Millonig et al., 2000).

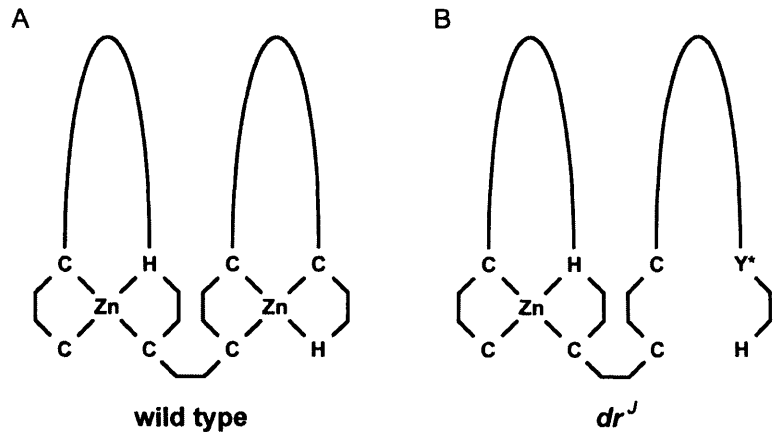

Figure 4-2 Schematic diagram showing the structure of the LIM1 domain of Lmx1a in (A) wild type and (B) *dr*^{J} mouse mutant.

4.1.2.2 Lmx1b

Lmx1b is mapped onto mouse chromosome 2; Locations: 2 B; 2 21.0 cM (NCBI Entrez Gene). Expressed earlier than Lmx1a, Lmx1b is first detected in the anterior embryo in the early head-fold stage at E7.5 (Guo et al., 2007; Smidt et al., 2000). During embryonic development, *Lmx1b* is expressed in the isthmus (Guo et al., 2007), the roof plate (Chizhikov and Millen, 2004a), subthalamic nucleus, posterior hypothalamus (Asbreuk et al., 2002), ventral midbrain DA neurons (Smidt et al., 2000), ventral hindbrain serotonergic neurons (Ding et al., 2003), the dorsal spinal cord (Ding et al., 2004), the eyes (Pressman et al., 2000), the developing ears (Abelló et al., 2007; Giraldez, 1998), kidney, skull and limbs (Cygan et al., 1997). At postnatal day 7 (P7), Lmx1b is expressed in the supramammillary nucleus, ventral premammillary nucleus and posterior hypothalamic area of the hypothalamus; subthalamic nucleus and parasubthalamic nucleus along the cerebral peduncle of the thalamus; substantia nigra and ventral tegmental area in the midbrain; raphe nuclei, parabrachial nuclei, trigeminal nucleus, nucleus of the solitary tract and laminae I-II of the medullary dorsal horn; and dorsal horn of the spinal cord (Dai et al., 2008).

LMX1B mutations in human have been detected in approximately 85% of families with the dominantly inherited nail patella syndrome (NPS) affecting about 1 in 50,000 live births (Bongers et al., 2002; Bongers et al., 2008). NPS is characterised by the pleiotropic developmental defects including dysplasia of the nails, patellar aplasia or

hypoplasia, iliac horns, dysplasia of the elbows, and frequently glaucoma and progressive nephropathy (Bongers et al., 2008; Chen et al., 1998a; Dreyer et al., 1998; Knoers et al., 2000; Vollrath et al., 1998). In mice, limb and renal anomalies similar to human NPS are only observed in homozygous *Lmx1b* mutants, suggesting a difference in dosage sensitivity for this gene between mice and human.

4.1.3 Functions of Lmx family members

Lmx1a and Lmx1b play important roles in various tissues where they are expressed, including the isthmus and the roof plate as sources of signalling molecules, the central nervous system, the eye, the limb, the kidney and the skull.

4.1.3.1 Lmx1b in the Isthmic Organiser (IsO)

Lmx1b, but not *Lmx1a*, is expressed and required for the formation of the IsO. Loss-of-function studies show that *Lmx1b* controls the initiation of *Fgf8* expression, and the maintenance of *Wnt1*, *En1*, *En2* and *Pax2* expressions (Guo et al., 2007). Misexpression studies of Lmx1b in the chick reveal that it induces Wnt1, which in turn induces Fgf8 expression (Matsunaga et al., 2002). Similarly, zebrafish *lmx1b.1* and *lmx1b.2* are both required and sufficient for the expression of IsO genes *wnt1* and *fgf8*, and the integrity of the isthmic constriction and cerebellum (O'Hara et al., 2005). Thus, *Lmx1b* is both required and sufficient for the inductive activity of the IsO during mid/hindbrain development.

4.1.3.2 Lmx1a/b in the roof plate

The roof plate is a transient signalling centre located at the dorsal midline of the neural tube that coordinates the development of the dorsal CNS through the action of BMPs and Wnts. It controls dorsal interneuron specification and differentiation in the developing spinal cord (Helms and Johnson, 2003; Lee and Jessell, 1999; Liem et al., 1997; Muroyama et al., 2002). Both *Lmx1a* and *Lmx1b* are expressed in the roof plate. *Lmx1a* is both sufficient and required for the induction of a functional roof plate,

consequently affecting the development of dorsal interneurons in the spinal cord and granule neurons in the cerebellar cortex, and the dorsal vertebral neural arches (Chizhikov and Millen, 2004b; Millen et al., 2004; Millonig et al., 2000). In the chick, *Lmx1b* acts upstream of *Lmx1a* in roof plate development. In the mouse, *Lmx1a* is the main factor required for roof plate formation, whereas *Lmx1b* is not expressed in the caudal CNS roof plate progenitors (Chizhikov and Millen, 2004a). However, it has been shown that *Lmx1b* can partially rescue roof plate development in *dreher* mice (Chizhikov and Millen, 2004a).

4.1.3.3 Lmx1a in the brain

Consistent with the expression of *Lmx1a* in the neocortex and hippocampus, loss of Lmx1a in *Dreher* mutants results in abnormalities of neuronal migration in the neocortex and a range of variable phenotypes in the hippocampus from the cytoarchitecture to dendritic tree morphology and neuronal circuits (Sekiguchi et al., 1996; Sekiguchi et al., 1994; Sekiguchi et al., 1992). However, without more detailed functional characterisation of *Lmx1a* in these regions, the descriptions of the *dreher* phenotype do not provide information on whether the defects are direct or indirect consequences of the loss of *Lmx1a*.

Dreher mutants also display a broad range of cerebellar abnormalities ranging from almost complete absence of the cerebellum to relatively normal patterns of lamination and foliation (Chizhikov et al., 2006; Sekiguchi et al., 1992; Wahlsten et al., 1983). It remains unclear if the cerebellar defects in Dreher mutants is an indirect effect of the roof plate defect at early stages of embryonic development.

4.1.3.4 Lmx1b in serotonergic neurons

Lmx1b is expressed in the ventral hindbrain, including the floor plate and the serotonergic (5-HT) neurons in the raphe nuclei and adjacent reticular formation (Ding et al., 2003). *Lmx1b* knockout mice studies show that it is required for the differentiation of 5-HT neurons (Cheng et al., 2003; Ding et al., 2003). When *Lmx1b* is conditionally deleted by Pet1-cre, which is expressed in developing and mature 5-HT neurons, 5-HT neurons are initially generated, subsequently lose the neurotransmitter phenotype, and ultimately disappear in the adult hindbrain (Zhao et al., 2006c). These results indicate that *Lmx1b* is required both for the differentiation and maintenance of 5-HT neurons.

Lmx1b also cooperates with other transcription factors to induce 5-HT neurons. Co-transfection of Lmx1b and Pet1 induces 5-HT formation in the ventral spinal cord where Nkx2.2 is endogenously expressed (Cheng et al., 2003). Interestingly, in the absence of Otx2, ectopic Lmx1b expression was sufficient to induce a 5-HT cell fate in the Nkx2.2 expression domain in the ventral midbrain (Vernay et al., 2005).

4.1.3.5 Lmx1b in the spinal cord

In the spinal cord, *Lmx1a* is only expressed in the roof plate but not in any neuronal population in the developing spinal cord. The generation and differentiation of the dI1 interneuron population affected in $Lmx1a^{dr/dr}$ mutants was suggested to be due to the failure of roof plate formation and function, which in turn leads to defects in patterning of the dorsal neural tube (Millen et al., 2004).

Lmx1b is expressed in postmitotic dI5 spinal interneurons, and regulate their differentiation and migration in the dorsal spinal cord (Ding et al., 2004). Lmx1b is also expressed in the postmitotic neurons of the dorsal sensory interneurons that populate laminae I-II of the spinal cord (Dunston et al., 2005). Loss of Lmx1b leads to a failure of cutaneous sensory axon ingrowth into the dorsal horn (Ding et al., 2004)

4.1.3.6 Lmx1b in other tissues

Lmx1b is expressed in the mesenchyme of the eye, and plays an essential role in the regulation of anterior segment development in the murine eye (Pressman et al., 2000). *Lmx1b* expressed in the dorsal mesenchyme of the limb buds is both necessary and sufficient to specify dorsal limb pattern (Chen and Johnson, 2002; Chen et al., 1998a; Riddle et al., 1995; Vogel et al., 1995). In the kidney, *Lmx1b* is expressed exclusively in podocytes. It is important for the glomerular development, and initial differentiation and later maintenance of the podocyte phenotype (Rohr et al., 2002; Suleiman et al., 2007). *Lmx1b* is expressed in the cranial mesenchyme, and is essential for the proper patterning and morphogenesis of the calvaria (Chen et al., 1998b).

4.1.4 Functions of other LIM-HD proteins

Besides members of the Lmx group, other LIM-HD proteins also play important roles in tissue patterning and cell differentiation during embryonic development. In the nervous system, they specify neuronal cell fate by regulating various aspects of neuronal development such as precursor cell proliferation, cell migration, process outgrowth, axonal pathfinding, and synthesis of neurotransmitters.

4.1.4.1 Patterning

Lhx1 (*Lim1*) is required in both primitive streak-derived tissues and the visceral endoderm for head formation. During early stages of mouse embryonic development, *Lhx1* is expressed in the organiser region. Inactivation of *Lhx1* in null mutant embryos display defects in the node and axial mesendoderm development and lack head structures anterior to rhombomere 3 in the hindbrain (Shawlot and Behringer, 1995; Shawlot et al., 1999).

Similarly, the *Xenopus Lhx1* orthologoue *Xlim-1* is expressed in the Spemann organiser, whose major functions include neural induction and dorsalisation of ventral mesoderm (Taira et al., 1994). Ectopically expressing *Xlim-1* with its cofactor into the ventral equatorial region induces secondary axes in the Xenopus embryo.

The *Drosophila Lhx2* orthologoue *apterous* (*ap*) is expressed in the primordium of the dorsal surface of the wing, where it functions to specify the dorsal cell fate (Diaz-Benjumea and Cohen, 1993). Mosaic analyses in the *Drosophila* wing imaginal disc show that the interface between *ap+* and *ap-* clones, with dorsal and ventral identities respectively, induces the formation of an ectopic wing margin, which stimulates growth.

4.1.4.2 Growth and survival

LIM-HD proteins have been shown to control tissue growth by regulating either proliferation or apoptosis. For example, *Lhx2* has been implicated in the growth of the cerebral cortex and the hippocampus. In the cerebral cortex, *Lhx2* is expressed in the ventricular, intermediate, and mantle zones. *Lhx2* knockouts have defects in precursor cell proliferation leading to a hypoplastic neocortex and an aplastic archicortex including the hippocampus (Porter et al., 1997). *Lhx2* has also been shown to regulate cell proliferation in zebrafish forebrain development, and functions as a downstream

regulator of Six3 promoting proliferation in the region (Ando et al., 2005). In the olfactory epithelium, the Lhx2 mutation leads to a slight reduction in proliferation and a marked increase in apoptosis (Hirota and Mombaerts, 2004).

Lhx3 and Lhx4 are required for the proliferation of the Rathke's pouch in the developing pituitary in a gene dosage-dependent manner without a detectable increase in programmed cell death. It has been shown that Lhx3 plays a more important role in this process (Sheng et al., 1997; Sheng et al., 1996). However, a more recent study shows that the growth arrest in *Lhx3* deficient mice is a consequence of increased apoptosis in the pituitary rather than a defect in proliferation (Zhao et al., 2006b). Another group shows that proliferation is slightly reduced and cell death increased in the developing pituitary in *Lhx4* mutants (Raetzman et al., 2002). Despite these controversies, the growth of the developing pituitary is clearly dependent on both Lhx3 and Lhx4.

4.1.4.3 Cell fate specification in the vertebrate brain

Cell fate specification is a multi-step process in which the potential of cells becomes progressively restricted by the expression of specific determinants. This appears to be the major function of LIM-HD transcription factors during embryonic development, with numerous examples across phyla. Most LIM-HD proteins appear to specify neuronal cell fate when cells exit the cell cycle and begin to express determinants that convey specific identities.

Lhx2 is expressed in the cortical neuroepithelium but is absent in the dorsal midline of the forebrain. Elegant *Lhx2* null mosaic analyses have shown that Lhx2 specifies the cortical identity and suppress alternative cortical hem fate (Mangale et al., 2008). Lhx2 is required for the cortical expression of Emx1, Foxg1 and Pax6, while suppressing hem markers Lmx1a, Wnt2b and Wnt3a in a cell-autonomous manner (Mangale et al., 2008). Lhx2 is also involved in the thalamocortical axon pathfinding (Lakhina et al., 2007).

Lhx5 is expressed in hippocampal precursor cells, and is required for the differentiation of GluR1 positive pyramidal cells in Ammon's horn, GAD67 positive interneurons, and calretinin positive Cajal-Retzius cells in the hippocampus. In *Lhx5* mutants, hippocampal neuronal precursor cells were specified and proliferated, but many of them fail to either exit the cell cycle or to differentiate and migrate properly (Zhao et al., 1999).

In the cerebral cortex, Lhx6 is expressed in the medial ganglionic eminence (MGE) as cells exit the cell cycle and migrate tangentially toward the striatum and cortex (Grigoriou et al., 1998; Liodis et al., 2007). Its expression becomes restricted to subsets of cortical GABAergic interneurons expressing the calcium-binding protein parvalbumin and somatostatin. Loss-of-function studies show that *Lhx6* is not required for the GABAergic neurotransmitter identity of cortical interneurons, but is required for the specification of neuronal subtypes in the neocortex and the hippocampus where it is expressed. It is also required for the normal tangential and radial migration of GABAergic interneurons in the cortex (Liodis et al., 2007).

Lhx8 is expressed in the MGE and preoptic area in the developing basal telencephalon. Lhx8 is required for the differentiation of subsets of cholinergic interneurons, including hippocampal and cortical projection neurons in the septum and nucleus basalis respectively, without affecting their initial specification. It is also required for the cholinergic projection to the hippocampus (Zhao et al., 2003).

4.1.4.4 Cell fate specification in the vertebrate spinal cord

The roles of LIM-HD transcription factors in the specification of motor neuron (MN) in the ventral spinal cord are well studied. Several LIM-HD proteins are expressed in MNs and are required for their differentiation. Each of them has distinct and sometimes redundant roles during the differentiation process, ranging from early cell fate specification to the later determination of axon projections.

Isl1 is expressed in all classes of postmitotic MN in the spinal cord, and acts as an early determinant of their differentiation (Pfaff et al., 1996). In the absence of Isl1, the MN progenitors fail to adopt a MN fate and undergo apoptosis instead of converting into the adjacent interneurons (Pfaff et al., 1996).

The MN can be divided into subclasses based on the location of their cell bodies that eventually organise into five longitudinally oriented motor columns occupying distinct domains along the rostral caudal axis, and establish different axonal pathways towards the peripheral targets (Tanabe and Jessell, 1996). These MN subtypes are defined by the combinatorial expression of LIM-HD proteins prior to their segregation into the different motor columns and establishment of axon projections (Tsuchida et al., 1994).

Lhx3 and Lhx4 are transiently expressed in a subset of MNs that extend axons ventrally (v-MNs) from the neural tube during their final progenitor cell division. As v-

MNs become topographically organised and extend axons in the periphery, Lhx3/4 are only maintained in the medial motor column ($MMCm^{v}$) innervating the ventral body wall muscles, and are rapidly down-regulated in other motor columns (Sharma et al., 1998). *Lhx3* and *Lhx4* coordinately specify the fate of v-MNs. Motor neurons convert to a dorsal fate in *Lhx3/4* double knockouts. Conversely, when Lhx3 is misexpressed, v-MNs are generated at the expense of dorsal-exiting motor neurons (d-MNs) (Sharma et al., 1998).

Lhx1 (Lim1) is expressed by a lateral subset of the lateral motor column (LMCl). Lhx1 is not required for the specification of these neurons, but instead functions to ensure that these neurons select a dorsal axonal trajectory into the limb. Lhx1 also promotes the extension of LMCl axons into the distal limb (Kania et al., 2000). In addition to the importance of LIM-HD proteins in the developing neurons, Lmx1b expressed by the target of LMCl neurons in the dorsal limb mesenchymal cells is also essential for the LMCl axons to select a dorsal trajectory in the developing limb (Kania et al., 2000).

Besides the columnar organisation of spinal MN subtypes, these cells can also be subdivided by the targets they innervate. Somatic MNs directly innervate skeletal muscles, whereas visceral MNs indirectly innervate smooth muscles of the viscera by synapsing onto neurons located in ganglia. Both Isl1 and Isl2 are initially expressed by all postmitotic spinal MNs, and Isl2 is only maintained in somatic but not visceral motor neurons after their diversification. Interestingly, the transient expression of Isl2 in visceral MNs is critical for the determination of complete visceral motor neuron character. In *Isl2* mutants, the visceral MNs of the sympathetic preganglionic motor column (PGC) display a mixed identity with both PGC and somatic characters, settle in aberrant locations, and exhibit defects in their peripheral axonal trajectory (Thaler et al., 2004). Zebrafish Isl2 is also required for the positioning, axonal pathfinding and neurotransmitter expression by the Isl2 positive primary motor neurons (Segawa et al., 2001).

In the dorsal spinal cord, Lhx1 and Lhx5 are not required for the initial specification of the dI4, dI6 and dIL^{A} inhibitory interneurons where they are expressed. Instead, they coordinately regulate the differentiation of these GABAergic inhibitory interneurons by consolidating the expression of *Pax2*, which controls the transcription of the inhibitory-neurotransmitter-specific genes such as *Viaat*, *Gad1*, *Gad2* and *GlyT2* (Pillai et al., 2007).

4.1.4.5 Cell fate specification other parts of the body

Besides playing important roles in specifying neuronal cell fate, LIM-HD proteins are also required for the specification of other cell types. *Lhx2* is required for eye development, where lens, globe or retina are absent in *Lhx2* homozygous mutant embryos (Porter et al., 1997). Lhx2 is expressed in the progenitors of the olfactory epithelium and gradually decreases in immature and mature neurons. Lhx2 is required for the terminal differentiation into olfactory sensory neurons without affecting neurogenesis (Hirota and Mombaerts, 2004).

Isl1 is expressed in nascent, developing and adult retinal ganglion cells (RGCs). Isl1 is dispensable for the generation and migration of RGCs, but required for their axon growth and pathfinding, and survival (Pan et al., 2008).

Lhx3 and Lhx4 are both expressed in the developing pituitary, where the expression of Lhx3 is more wide spread and that of Lhx4 is more spatially and temporally restricted. Lhx3 and Lhx4 coordinately control the development of Rathke's pouch from the oral ectoderm, whereas the commitment of precursor cells in Rathke's pouch to a pituitary organ fate is controlled by Lhx3 (Sheng et al., 1997).

4.2 Aim

The importance of LIM-HD transcription factors during embryonic development, their pivotal roles in cell fate specification and the expressions of Lmx1a and Lmx1b in the ventral midbrain area from E8.5 have led us to hypothesize that these two members of the LIM-HD transcription factors may play important roles in the development of mDA neurons. Although a study on *Lmx1b* knockout mice has demonstrated an essential role of *Lmx1b* in the proper specification and maintenance of mDA neurons (Smidt et al., 2000), *Lmx1b* has also been shown to control the expression of IsO genes essential for the development of the midbrain and hindbrain region (Matsunaga et al., 2002; O'Hara et al., 2005). Moreover, its role in maintaining mDA neurons is also questioned due to its regulation of En1 expression during early somite stages and the requirement of En1 in the maintenance of mDA neurons. Indeed, our initial studies have shown a loss of the IsO in *Lmx1b* knockout embryos. The aim of this study is to investigate the specific roles of *Lmx1a* and *Lmx1b* in the molecular specification of mDA neurons by the spontaneous *Lmx1a* mutant *dreher* and a condition mutant of *Lmx1b*, in which the IsO is functional.

4.3 Results

4.3.1 Lmx1a and Lmx1b are expressed in the midbrain dopaminergic progenitors and neurons

From whole mount *in situ* hybridisation, *Lmx1a* and *Lmx1b* were both expressed in the ventral midbrain and caudal diencephalon where mDA neurons begin to be generated at E10.5 (Figure 4-3A,B). The expression of both Lmx1a and Lmx1b extended beyond the rostral limit of mDA domain, and Lmx1b also extended to the floor plate in the hindbrain.

To study the dynamics of the two genes in detail, double immunohistochemistry was performed on frozen sections of wild type mouse embryos during embryonic development. At E9.5, when mDA neurons started to be born, Lmx1a had a very restricted expression pattern at the ventral midline while Lmx1b was expressed broadly in the ventral midbrain (Figure 4-3C) and caudal diencephalon (data not shown). The Lmx1b expression domain became progressively restricted to the ventral midline. By E10.5 (38-somite stage), Lmx1a and Lmx1b expression domains completely overlapped from the ventral midbrain (Figure 4-3D) to the ventral diencephalon (data not shown). Within the Lmx1a/b expression domain, all the cells expressed both Lmx1a and Lmx1b but at different levels.

At E11.5, when mature mDA neurons emerged, the expression of Lmx1a remained strong in both the mDA progenitors and postmitotic neurons. In contrast, Lmx1b expression was attenuated in the mDA progenitors, but remained at a high level in postmitotic neurons (Figure 4-3E). The same expression pattern of Lmx1a and Lmx1b was observed at E12.5 (Figure 4-3F). At this stage, the majority of the mDA neurons are born and being actively generated (Bayer et al., 1995). The mDA progenitors (strong Lmx1a weak Lmx1b), immature neurons (strong Lmx1a strong Lmx1b TH-) and mature neurons (Lmx1a+ Lmx1b+ TH+) are well distributed on transverse sections of the mouse midbrain and caudal diencephalon. This is the stage chosen to analyse cells at different stages during mDA development in studies. Interestingly, Lmx1b appeared to have stronger expression in the more lateral than medial region within the postmitotic mDA neurons (Figure 4-3F'). This raises the possibility that differences in the level of Lmx1b have an effect on the specification and migration of mDA subpopulations.

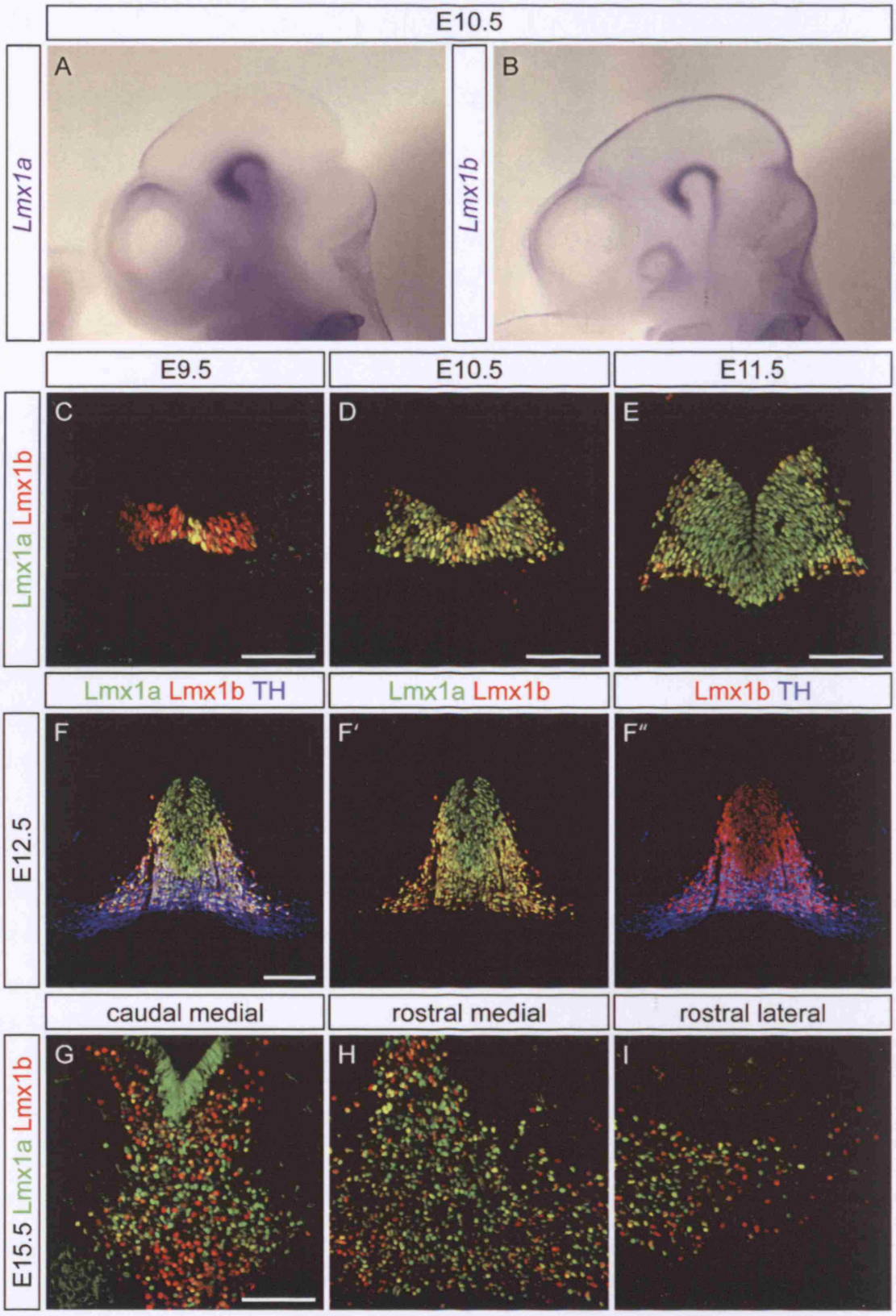
E10.5
Lmx1a
A
Lmx1b
B
E9.5
E10.5
E11.5
Lmx1a Lmx1b
C
D
E
Lmx1a Lmx1b TH
Lmx1a Lmx1b
Lmx1b TH
E12.5
F
F′
F″
caudal medial
rostral medial
rostral lateral
E15.5 Lmx1a Lmx1b
G
H
I

Figure 4-3 Dynamic expression of Lmx1a and Lmx1b in mDA progenitors and neurons.

(A-B) Lmx1a and Lmx1b were expressed in the ventral midbrain and caudal diencephalon at E10.5 by whole mount *in situ* hybridisation. (C) At E9.5, Lmx1b was expressed more broadly than Lmx1a in the ventral midbrain. (D) At E10.5, Lmx1a and Lmx1b expression domains completely overlapped in the ventral midbrain and caudal diencephalon. At E11.5 (E) and E12.5 (F), Lmx1a expression was high in the whole mDA domain, while Lmx1b was expressed at high level in postmitotic neurons and at low level in the progenitors. (G-I)) At E15.5, Lmx1a was strongly expressed in the mDA progenitor region, while Lmx1b was only weakly expressed. Lmx1a and Lmx1b were expressed in different levels in the postmitotic neurons. Scale bars correspond to 100μm.

At E15.5 when mDA neurons are no longer generated, Lmx1a continued to be expressed at a high level in the ventricular zone while Lmx1b expression was maintained at a very low level in the ventricular zone. Lmx1a and Lmx1b expression levels were not uniform in the TH+ neuronal populations, but it appeared that the gross level of Lmx1a/b protein was similar. Cells that expressed Lmx1a strongly had a low Lmx1b expression level, and vice versa. Lmx1b was expressed more strongly in relatively lateral mDA neurons, while Lmx1a was stronger in more medial mDA populations. However, there was no clear spatial correlation in cells with differential Lmx1a/b expression levels at this stage.

All the neurons in the floor plate and basal plate region of the midbrain expressed at least one of the LIM-HD transcription factors (Figure 4-4). Lmx1a/b were expressed by the mDA neurons in the ventral midline region. Islet-1 (Isl1) expressing oculomotor neurons were present lateral to the mDA neurons. Lhx1/5 expressing neurons, stained by the Lim1/2 antibody, encompassed the remaining neurons of the basal plate and extended more dorsally to the alar plate where their expression became scattered.

Most LIM-HD transcription factors are only expressed in postmitotic neurons and play important roles in neuronal cell fate specification (Sharma et al., 1998; Thaler et al., 2002; Tsuchida et al., 1994; Zhao et al., 2007). Both *Lmx1a* and *Lmx1b* were expressed in the mDA neurons in addition to their progenitors. Moreover, the progenitor expression pattern of Lmx1a/b (in particular Lmx1a) correlated spatially and temporally with the birth of the mDA neurons. This raised the possibility that *Lmx* genes might have a functional significance in the specification of both the mDA progenitors and neurons. Moreover, the difference in expression between Lmx1a and Lmx1b suggested that the two genes might play different roles during mDA neuron development and in defining specific subpopulations. The functions of these two genes in mDA neuron development were studied by the spontaneous *Lmx1a* mutant dr^J and a conditional knockout mutant of *Lmx1b*.

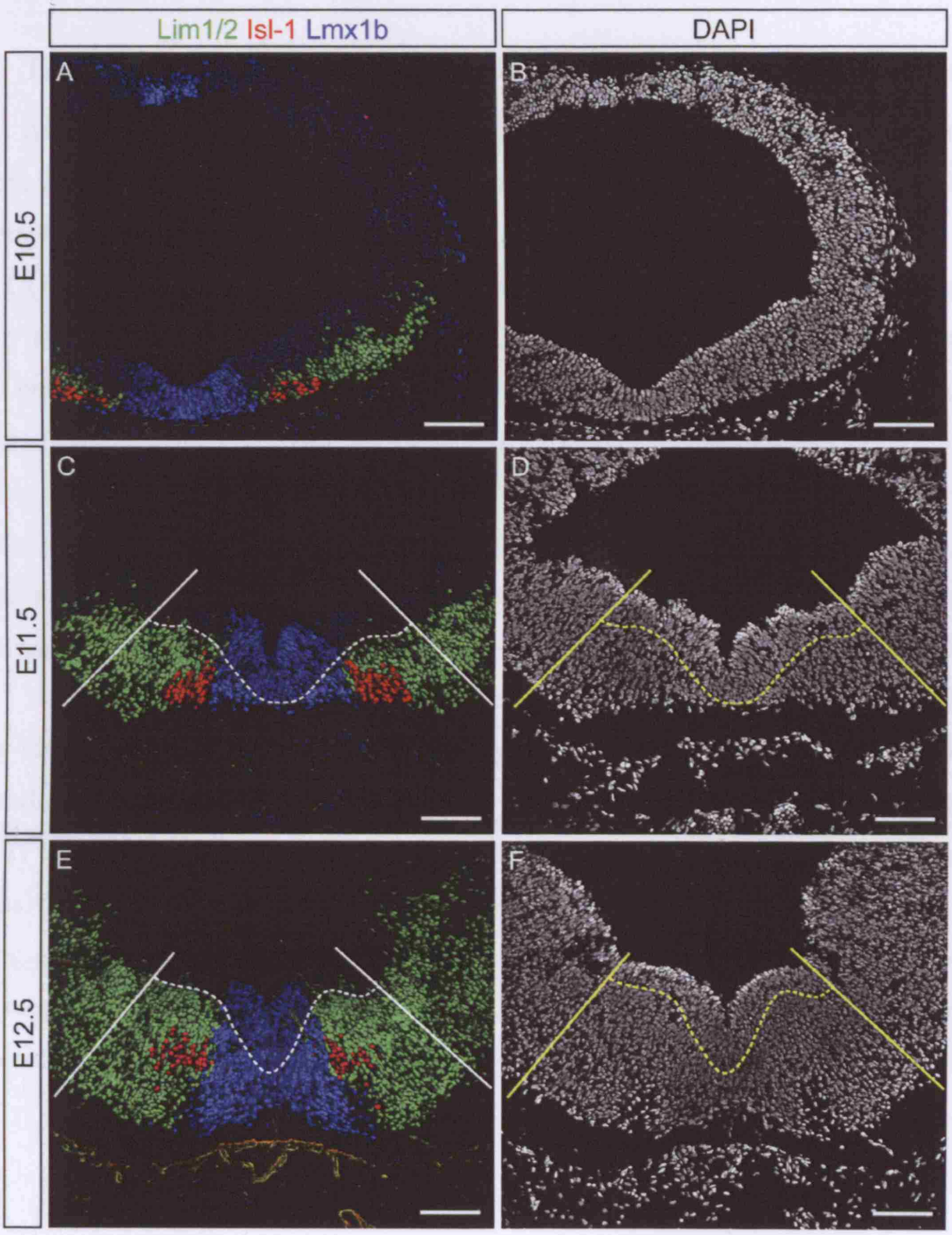

Figure 4-4 Postmitotic neurons in the floor plate and basal plate of midbrain express Lmx1b, Isl1 and Lim1/2 in a complementary manner.

(A-C) Lmx1b, Isl1 and Lim1/2 were expressed in a complementary manner in the postmitotic neurons in the floor plate and basal plate in wild type embryos from E10.5 to E12.5. (A'-C') DAPI staining was performed on the same section to visualise all the cells. The ventricular zone, marked by dotted lines, was distinguished by the boundary between strong and weak Lmx1b expression or Lim1/2 expression boundary. Solid lines demarcate the alar and basal plate boundary. Scale bars correspond to 100μm.

4.3.2 The *Lmx1a* mutant *dreher* has a moderate reduction in mDA neurons

At E12.5, the *Lmx1a* mutant dr^J ($Lmx1a^{dr/dr}$) expressed mDA specific progenitor markers Lmx1a and *Msx1* (Figures 4-5A,B and 4-18A,B), immature mDA neuronal markers Lmx1b, Nurr1, *En1*, and mature mDA neuronal markers *Pitx3*, AADC, TH, VMAT (Figures 4-5D-K and 4-27F,G). The Lmx1a antibody is able to detect the mutant protein with a single amino acid change at Cys82Tyr. Quantification of TH+ mature mDA neurons from the whole region revealed a 46.12% reduction in $Lmx1a^{dr/dr}$ compared with their wild type littermates (Figure 4-5C). The expression of mDA markers ranging from transcription factors (Lmx1b, Nurr1, *En1* and *Pitx3*) to genes involved in neurotransmitter phenotype (AADC, TH and VMAT) suggests that although the number of neurons is reduced, the remaining neurons are specified towards dopaminergic fate.

To understand if the loss of *Lmx1a* affects the late differentiation processes such as the migration and projection, E18.5 embryos and an adult $Lmx1a^{dr/dr}$ mouse were analysed. The $Lmx1a^{dr/dr}$ mutant continued to display a reduction in mDA neurons at E18.5 (Figure 4-28A,B,M,N) and at 3 months of age (Figure 6-8). The reduction was not obviously confined to any of the major mDA populations such as the Li, RRF, VTA and SN, suggesting that the mutation of *Lmx1a* did not affect the migration and generation of these subpopulations of mDA neurons. The projection to the striatum was also normal (Ono et al., 2007).

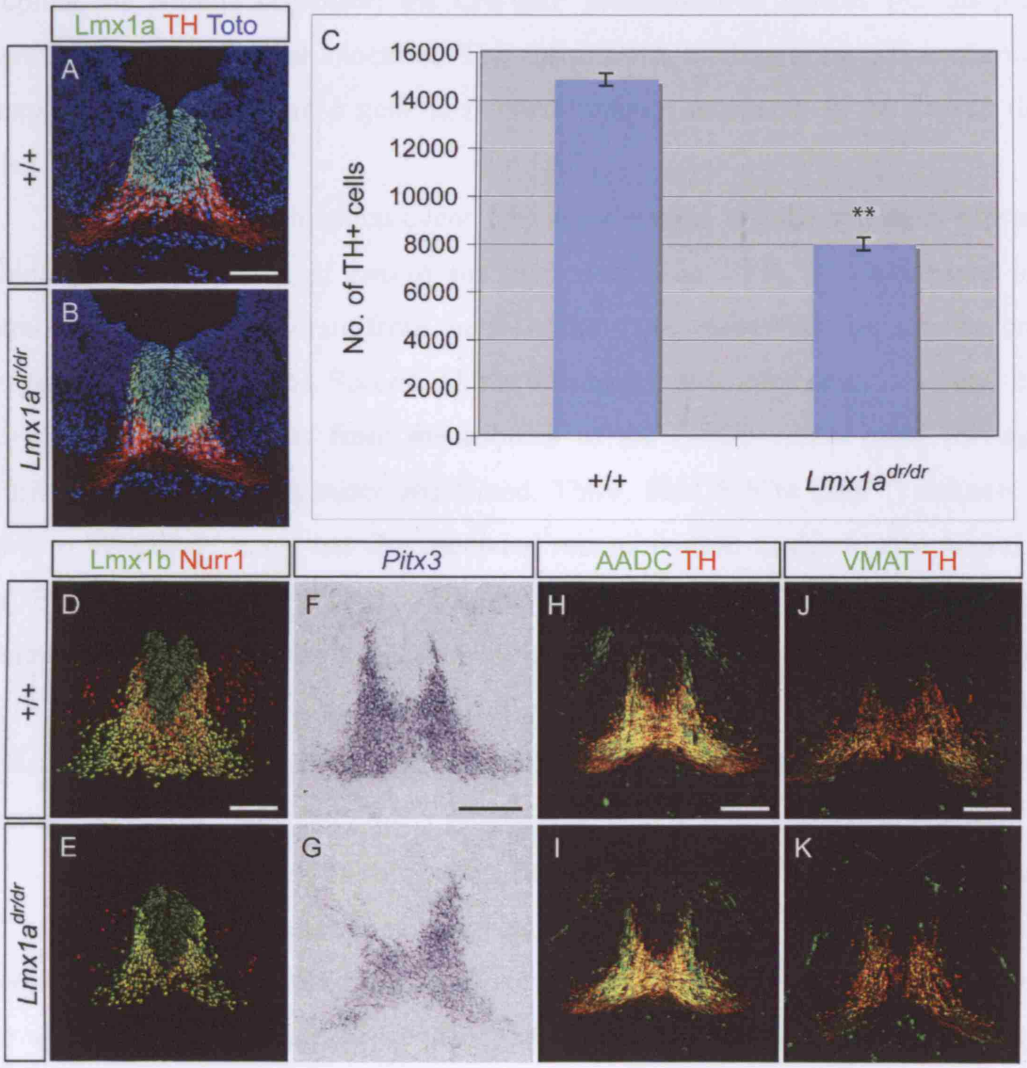

Figure 4-5 Specification of mDA neurons is not affected in *Lmx1a*$^{dr/dr}$ mutants at E12.5.

(A,B) *Lmx1a*$^{dr/dr}$ mutants expressed mDA progenitor marker Lmx1a and mature mDA neuronal marker TH. (C) The number of TH+ cells in the whole ventral midbrain and caudal diencephalon region was reduced by 46.12% from 14838±1627 in wild type to 7994±1651 in *Lmx1a*$^{dr/dr}$ mutants, n=3. Two-tailed Student's t-Test shows that the difference between wild type and mutant embryos was statistically significant. *$p<0.05$; **$p<0.01$; ***$p<0.001$. Expressions of postmitotic mDA markers Lmx1b, Nurr1 (D,E), Pitx3 (F,G), AADC (H,I) and VMAT (J,K) were not affected in *Lmx1a*$^{dr/dr}$ embryos. Scale bars correspond to 100μm.

4.3.3 Conditional deletion of *Lmx1b* in the ventral midline by Shh^{cre}

To study the specific effect of *Lmx1b* on mDA neuron development without disrupting the isthmic organiser, the Cre-loxP recombaintion system was adopted to generate *Lmx1b* conditional knockout. The entire DNA binding homeodomain encoded by exons 4 to 6 of the *Lmx1b* gene is flanked by loxP sequences in the *Lmx1b* floxed allele (Zhao et al., 2006c).

To drive the recombination event, *Shh* was the most specific and early expressing candidate for the deletion of *Lmx1b* for several reasons. First, it is expressed in the ventral midline of the midbrain from the 5-somite stage, more than two days before the emergence of mDA neurons. Second, *Shh* is only expressed in the anterior ventral neural tube and in the floor plate from the isthmus to the caudal neural tube, leaving the majority of the isthmic organiser unaffected. Third, ShhGFPCre (Shh^{cre}) animals were shown to effectively carry out Cre mediated recombination in the ventral neural tube from E9.0 in ShhGFPCre;R26RLacZ embryos (Figure 3-10K), prior to mDA neuron generation, and to contribute to all subpopulations of mDA neurons in the adult. Thus, *Lmx1b* should be deleted specifically in the ventral neural tube where all mDA populations are developed from, and before their generation although functional Lmx1b proteins may persist in the early mDA progenitors.

Shh^{cre} mice were mated with $Lmx1b^{flox/flox}$ ($Lmx1b^{f/f}$) mice to generate Shh^{cre};$Lmx1b^{f/+}$ mice. These mice were subsequently mated with $Lmx1b^{f/f}$ mice to generate Shh^{cre};$Lmx1b^{f/f}$ mice. Homozygous *Lmx1b* conditional mutant Shh^{cre};$Lmx1b^{f/f}$ mice were born at the expected frequency and were morphologically indistinguishable from their wild type littermates. The Shh^{cre};$Lmx1b^{f/f}$ mice survived to adulthood, were fertile, and did not show any behavioural defects at least until 18 months of age. In contrast, *Lmx1b* null mice, which lack the LIM2 domain, HD and most of the C-terminal region of *Lmx1b*, die within 24 hours of birth (Chen et al., 1998a).

Shh^{cre};$Lmx1b^{f/f}$ embryos were also morphologically indistinguishable from their wild type littermates. At E10.5, the morphology of the isthmus and the expression of *Erm*, readout of Fgf signalling, appeared normal (Figure 4-6). Thus, Fgf signalling from the IsO is normal in *Lmx1b* condition mutants.

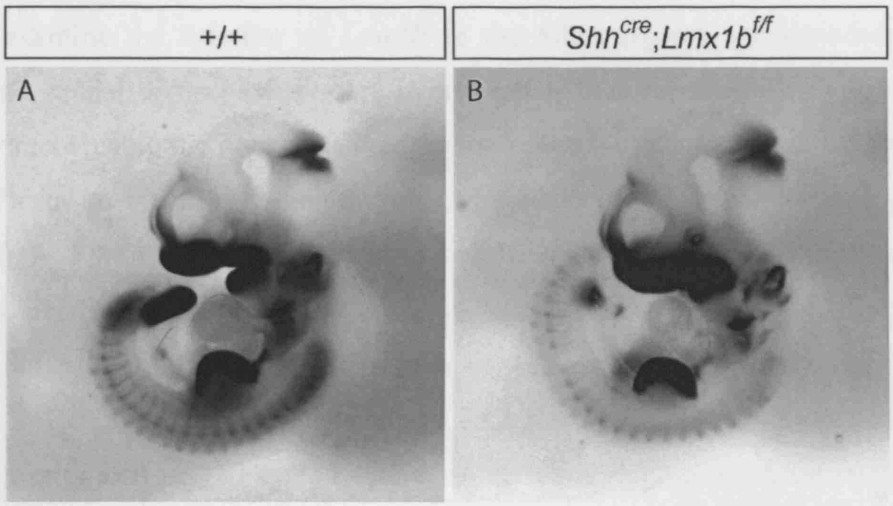

Figure 4-6 *Lmx1b* conditional mutants are indistinguishable from wild type littermates.

The expression pattern of *Erm* is similar between wild type (A) and $Shh^{cre};Lmx1b^{f/f}$ (B) embryos at 33-34 somite stages.

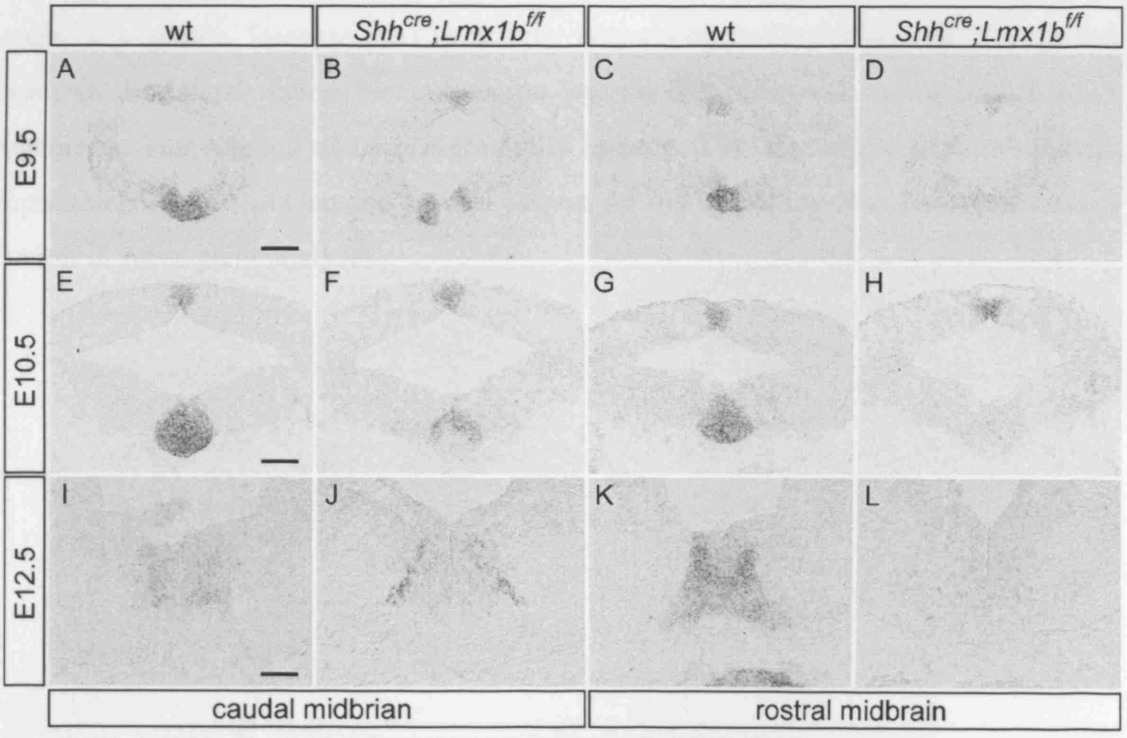

Figure 4-7 *Lmx1b* is deleted in the majority of the midbrain floor plate in *Lmx1b* conditional mutants before the generation of mDA neurons.

(A,C,E,G,I,K) *Lmx1b* transcripts were detected in the ventral midline of wild type embryos in the midbrain. (A,B,E,F,I,J) In $Shh^{cre};Lmx1b^{f/f}$ embryos, *Lmx1b* transcript was only detected as two lateral stripes in the caudal midbrain, and was undetectable in the rostral midbrain at E9.5, E10.5 and E12.5. Scale bars correspond to 100μm.

To examine the deletion of *Lmx1b* in the mDA region, cross-sections of the midbrain and caudal diencephalon were hybridised with a complementary RNA probe specifically recognising the region flanked by loxP sequences in the *Lmx1b* floxed allele (Figure 4-7) due to the Lmx1b antibody being able to recognise the truncated protein (Figure 4-8). At E9.5 in $Shh^{cre};Lmx1b^{f/f}$ embryos, before the generation of mDA neurons, *Lmx1b* was deleted in the majority of its expression domain, except for the lateral margins at the caudal midbrain. When Lmx1b expression became restricted to the mDA progenitors at E10.5, the two lateral stripes of Lmx1b-expressing cells were still present, but the proportion of Lmx1b+ cells relative to the whole region had been reduced. The number of caudal lateral *Lmx1b*-expressing cells had further reduced at E12.5.

To better understand this incomplete deletion of *Lmx1b*, the Cre activity in Shh^{cre};R26RLacZ embryos was visualised with an antibody raised against β-gal (Figure 4-8). The region where Shh^{cre} was active encompassed the whole Lmx1b expression domain, where it was very broad in the rostral, but only slightly broader than Lmx1b in the caudal midbrain. Because the Cre activity was strong in the medial, while weak and mosaic in the lateral region, recombination was inefficient in the caudal lateral mDA progenitors. The deletion of *Lmx1b* gradually improved at later stages of development. Emphases had been put on the central region of the midbrain with complete *Lmx1b* deletion in subsequent analyses.

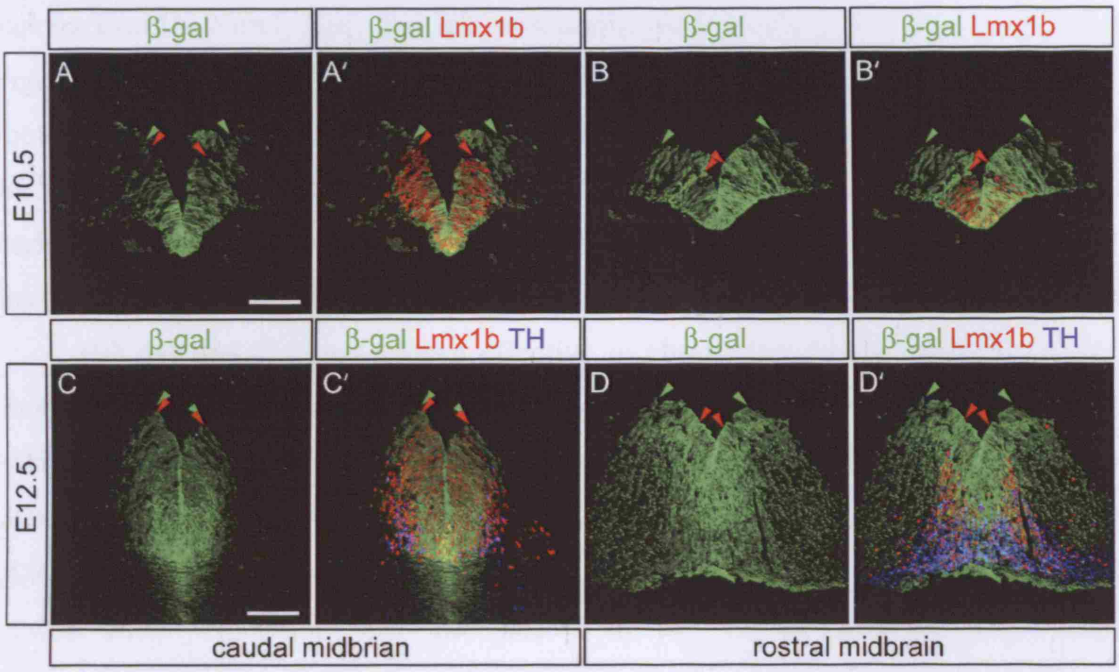

Figure 4-8 Mosaic and weak Cre activity in the lateral Shh domain in the midbrain of Shh^{cre};R26RLacZ embryos.

(A,B) Double immunostaining of β-gal and Lmx1b in Shh^{cre};R26RLacZ embryos at E10.5. (C,D) Triple immunostaining of β-gal, Lmx1b and TH in Shh^{cre};R26RLacZ embryos at E12.5. The borders of β-gal and Lmx1b expression are marked by green arrows and red arrows respectively. Scale bars correspond to 100μm.

4.3.4 Expression of Lmx1b in mDA neurons is not required for their generation and maintenance

At E12.5, *Shh*^{cre};*Lmx1b*$^{f/f}$ embryos expressed the mDA specific progenitor markers Lmx1a and *Msx1* (Figures 4-9A,B and 4-18A,E), early postmitotic neuronal markers Lmx1b, Nurr1, *En1*, and late postmitotic markers *Pitx3*, AADC, TH, VMAT (Figures 4-9D-K and 4-27F,J). Quantification of the TH+ mature mDA neurons from the whole region confirmed that the generation of mDA neurons was not compromised in *Shh*^{cre};*Lmx1b*$^{f/f}$ embryos (Figure 4-9C). It is surprising that *Pitx3* was detected in *Lmx1b* conditional mutants because has been described as being absent in mDA neurons of *Lmx1b* null mutants (Smidt et al., 2000).

HD deletion has been proven effective in eliminating *Lmx1b* function in mid-hindbrain boundary and serotonergic neuron development (Guo et al., 2007; Zhao et al., 2006c). To assess the efficacy of the HD deletion to disable *Lmx1b* function in mDA neuron development, embryos carrying β-actin-Cre and *Lmx1b*$^{f/f}$ were analysed. The mDA phenotypes of these embryos resembled those of *Lmx1b* null embryos (data not shown). *Pitx3* expression was also absent in the ventral midbrain and caudal diencaphalon. Taken together, these data suggest that *Lmx1b* is neither required for the specification of mDA neurons nor the expression of *Pitx3* in *Lmx1b* conditional mutants.

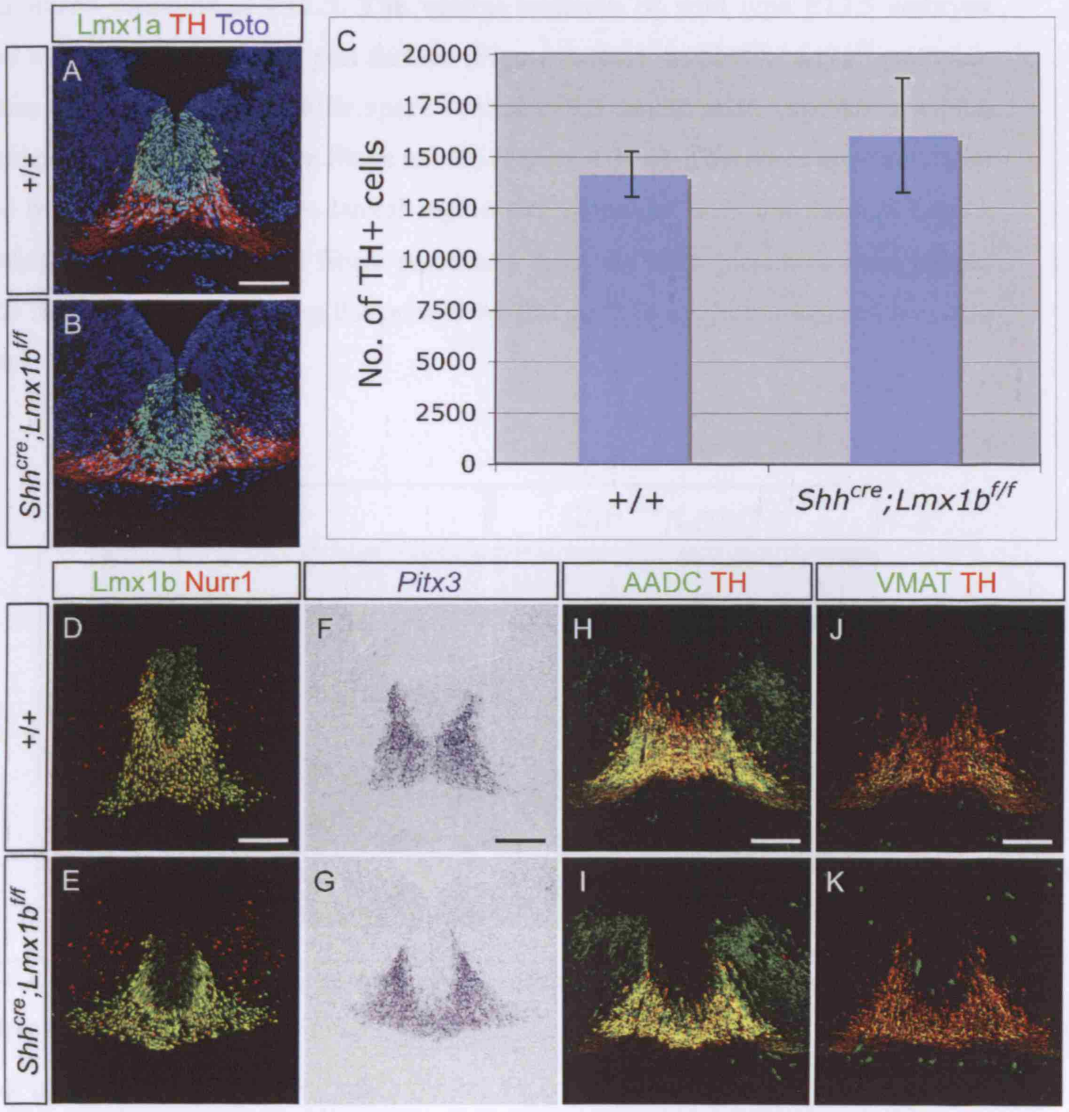

Figure 4-9 The specification of mDA neurons is not affected in *Lmx1b* conditional mutants at E12.5.

(A,B) *Shh*^{cre};*Lmx1b*$^{f/f}$ embryos expressed mDA progenitor marker Lmx1a and mature mDA neuronal marker TH. (C) There is no statistically significant difference in the number of TH+ cells in the whole ventral midbrain and caudal diencephalon region between wild type and *Shh*^{cre};*Lmx1b*$^{f/f}$ embryos. The cell counts represent mean ± SD of triplicate. Two-tailed Student's t-Test shows that the differences between wild type and mutant embryos were not statistical significance. Postmitotic mDA markers Lmx1b, Nurr1 (D,E), Pitx3 (F,G), AADC (H,I) and VMAT (J,K) were all expressed in *Shh*^{cre};*Lmx1b*$^{f/f}$ embryos. Scale bars correspond to 100μm.

A change in the morphology of the caudal ventral midbrain was observed in $Shh^{cre};Lmx1b^{f/f}$ embryos at E12.5. The ventral midbrain of wild type E12.5 embryos adopted a concave shape at the pial surface (Figure 4-10A). In $Shh^{cre};Lmx1b^{f/f}$ embryos, there was an expansion of acellular space ventral to the caudal mDA population, which was also poorly filled with nerve fibres (n>10) (Figure 4-10B). This space appeared to be flanked by a constriction in the lateral region that coincided with the residual *Lmx1b* expressing cells. Moreover, the fibres emanating from the floor plate area were guided towards the lateral edges, raising the possibility that Lmx1b might be required for axon guidance.

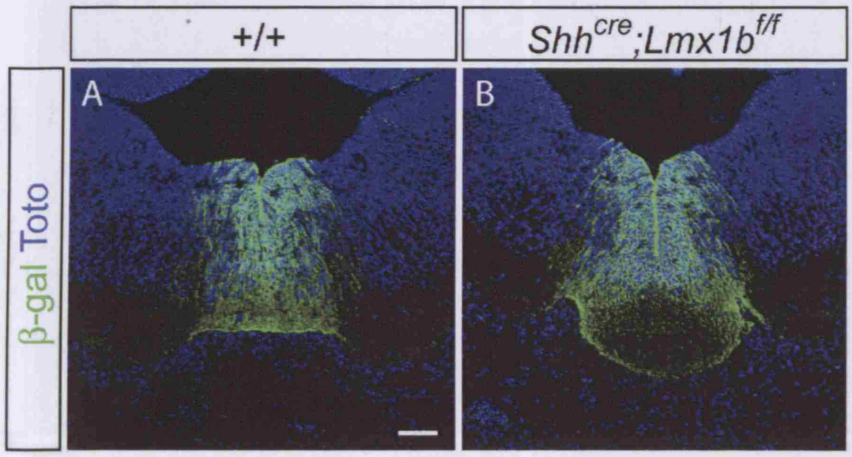

Figure 4-10 Lmx1b conditional mutants have an abnormal morphology in the caudal ventral midbrain at E12.5.

Scale bar corresponds to 100μm.

In the *Lmx1b* null mutants, TH+ neurons fail to survive beyond E16 (Smidt et al., 2000). In contrast, there was no obvious reduction in TH+ mDA subpopulations at any position along rostral-caudal extent of the *Lmx1b* conditional mutants at E18.5 (Figure 6-9,10). Therefore, *Lmx1b* is not required for the survival of mDA neurons. This data also argues against a role of *Lmx1b* in specifying mDA neuronal subpopulations despite its preferential expression in the lateral postmitotic neurons.

The distribution of mDA neurons in *Shh*^{cre};*Lmx1b*$^{f/f}$ embryos was slightly altered in comparison with the wild type at E18.5 (Figures 4-11, 6-9, 6-10). In the Li and caudal VTA subpopulations, cells migrated around an area devoid of cells (Figure 4-11B') similar to the space observed at E12.5. The minor migration defect in *Lmx1b* conditional mutant is a likely consequence of the morphological change in the caudal midbrain at early embryonic stages.

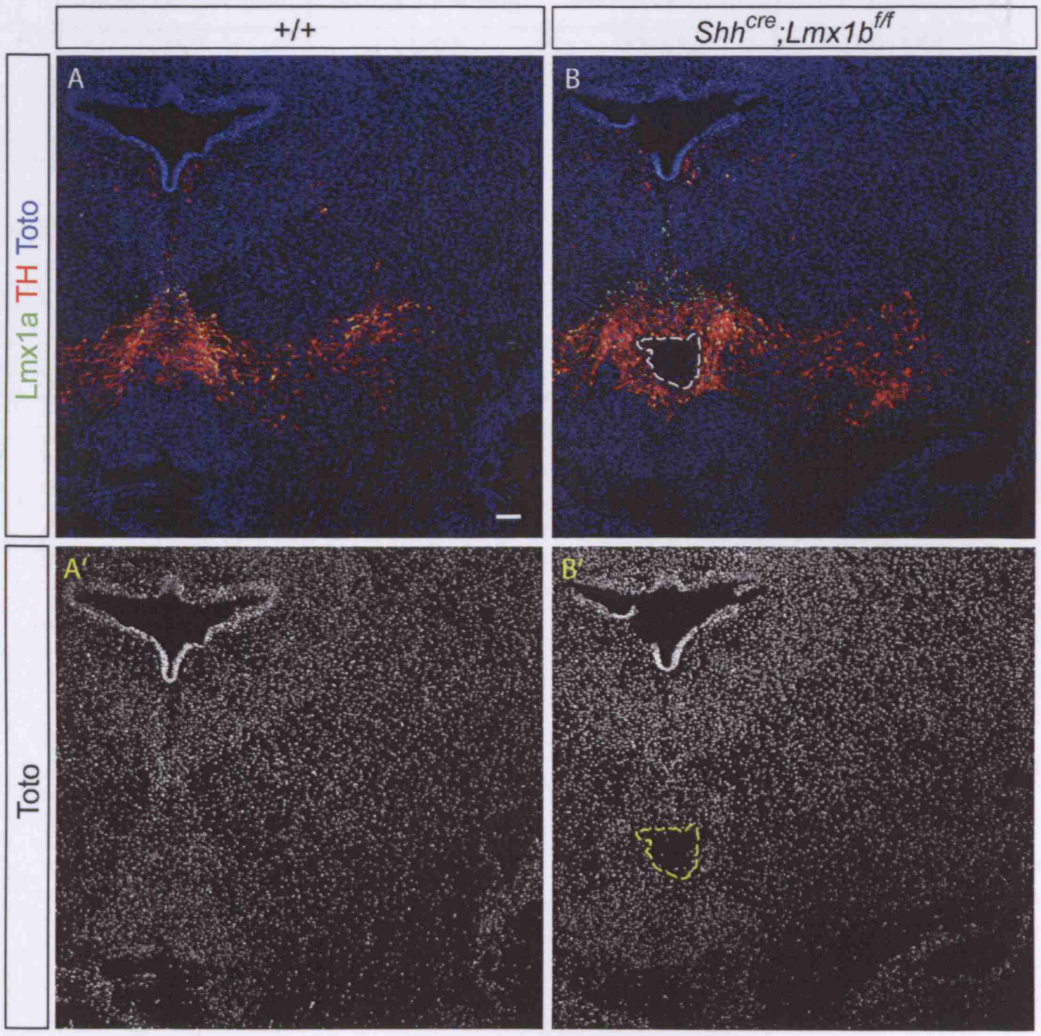

Figure 4-11 *Lmx1b* conditional mutants have an abnormal area devoid of cells at E18.5.

(A) The Li subpopulation was organised into a triangular shape in wild type embryos. (B) The organisation of Li in *Shh*^{cre};*Lmx1b*$^{f/f}$ embryos was interrupted by a sparsely populated area marked by dotted line. Scale bar corresponds to 100μm.

4.3.5 Generation of *Lmx1a/b* double mutants

The murine Lmx1a and Lmx1b proteins have highly similar functional domains, annotated by UniProtKB/Swiss-Prot and aligned by BLASTP version 2.2.18 matrix BLOSUM62 (Table 4-1, Figure 4-12). Lmx1a and Lmx1b share a 64% homology in their amino acid composition. The protein binding LIM1 and LIM2 domains show 67% and 83% identity respectively. The homeodomains of Lmx1a and Lmx1b are identical, suggesting that they can bind to the same target genes.

Gene	Total length (aa)	LIM1 position	LIM2 position	HD position
Lmx1a	382	33-92	92-154	195-154
Lmx1b	372	33-83	92-145	196-255

Table 4-1 The positions of the functional domains in *Lmx1a* and *Lmx1b* as annotated in UniProtKB/Swiss-Prot.

Lmx1a: http://beta.uniprot.org/uniprot/Q9JKU8

Lmx1b: http://beta.uniprot.org/uniprot/O88609

A

```
Lmx1a  MLDGLKMEENFQSAIETSASFSSLLGRAVSPKSVCEGCQRVISDRFLLRLNDSFWHEQCV  60
       MLDG+KMEE+  +     A+   LLG       +VCEGCQR ISDRFL+R+N+S WHE+C+
Lmx1b  MLDGIKMEEH--ALRPGPATLGVLLGSDCPHPAVCEGCQRPISDRFLMRVNESSWHEECL  58

Lmx1a  QCASCKEPLETTCFYRDKKLYCKYHYEKLFAVKCGGCFEAIAPNEFVMRAQKSVYHLSCF  120
       QCA+C++ L T+C++RD+KLYCK  Y++LFA KC GC E IAP EFVMRA + VYHL CF
Lmx1b  QCAACQQALTTSCYFRDRKLYCKQDYQQLFAAKCSGCMEKIAPTEFVMRALECVYHLGCF  118

Lmx1a  CCCVCERQLQKGDEFVLKEGQLLCKGDYEKERELLSLVSPAASDSGKSDDEESLCKSAHG  180
       CCCVCERQL+KGDEFVLKEGQLLCKGDYEKE++LLS VSP  SDS KS+DE+   K A G
Lmx1b  CCCVCERQLRKGDEFVLKEGQLLCKGDYEKEKDLLSSVSPDESDSVKSEDEDGDMKPAKG  178

Lmx1a  AG---KGASEDGKDHKRPKRPRTILTTQQRRAFKASFEVSSKPCRKVRETLAAETGLSVR  237
        G   KG+ +DGKD +RPKRPRTILTTQQRRAFKASFEVSSKPCRKVRETLAAETGLSVR
Lmx1b  QGSQSKGSGDDGKDPRRPKRPRTILTTQQRRAFKASFEVSSKPCRKVRETLAAETGLSVR  238

Lmx1a  VVQVWFQNQRAKMKKLARRQQQQQQDQQNTQRLTSAQTNGSG--NAGMEGIMNPYTTL-P  294
       VVQVWFQNQRAKMKKLARR QQQQ+          ++Q  G    ++ MEG+M  YT L P
Lmx1b  VVQVWFQNQRAKMKKLARRHQQQQEQ-------QNSQRLGQEVLSSRMEGMMASYTALAP  291

Lmx1a  TPQQLLAIEQSVY-NSDPFRQGLTPPQMPGDHMHPYGAEPLFHDLDSDDTSLSNLGDCFL  353
         QQ++A+EQS Y +SDPF+QGLTPPQMPG+        + +FH     DTSL++L DCFL
Lmx1b  PQQQIVAMEQSPYGSSDPFQQGLTPPQMPGN-------DSIFH-DIDSDTSLTSLSDCFL  343

Lmx1a  ATSEAGPLQSRVGNPIDHLYSMQNSYFTS  382
        +S+ G LQ+RVGNPID LYSMQ+SYF S
Lmx1b  GSSDVGSLQARVGNPIDRLYSMQSSYFAS  372
```

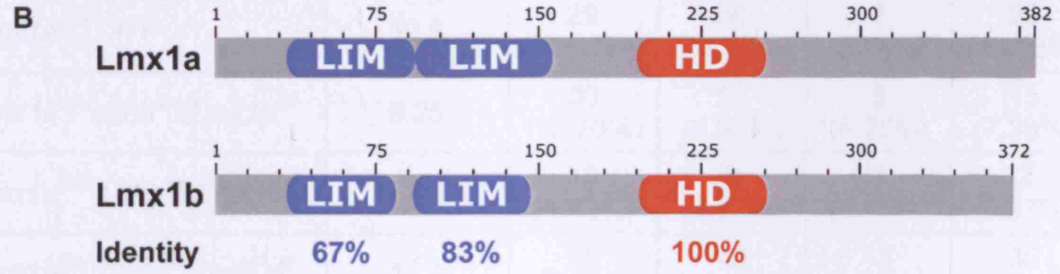

Figure 4-12 Comparison of amino acid sequence and functional domains in Lmx1a and Lmx1b.

(A) Amino acid sequence alignment of Lmx1a and Lmx1b. LIM1 domain, LIM2 domain and HD are highlighted in yellow, blue and pink respectively. The conserved residues essential for the integrity of the zinc finger structures are in bold fonts. (B) Schematic diagrams of Lmx1a and Lmx1b showing the distribution and amino acid identity of the LIM domains and HD.

Three lines of evidence suggest that Lmx1a and Lmx1b may have redundant functions in mDA neuron development. First, Lmx1a and Lmx1b proteins have high identity in their functional domains. Second, Lmx1a/b are co-expressed in mDA progenitors and neurons during their generation. Third, single mutants of either *Lmx1a* or *Lmx1b* do not show any severe phenotype in mDA neuron development, and continue to express Lmx1b and Lmx1a respectively.

To test for functional redundancy in *Lmx1a/b* genes, double heterozygous ($Lmx1a^{dr/+}$;Shh^{cre};$Lmx1b^{f/+}$) animals were first generated by crossing $Lmx1a^{dr/+}$ with Shh^{cre};$Lmx1b^{f/+}$ mice. *Lmx1a/b* double mutant ($Lmx1a^{dr/dr}$;Shh^{cre};$Lmx1b^{f/f}$) embryos and animals were produced by crossing $Lmx1a^{dr/+}$;Shh^{cre};$Lmx1b^{f/+}$ males with $Lmx1a^{dr/+}$;$Lmx1b^{f/f}$ females. The expected and actual frequencies of the nine possible genotypes are shown in Table 4-2.

Genotype	Expected frequency (%)	Number of animals (frequency in %)			
		E10.5	E12.5	E18.5	P21
+/+;+/+	12.5	38 (12.93%)	25 (10.33%)	12 (15.00%)	26 (12.62%)
$Lmx1a^{dr/+}$; +/+	25	79 (26.87%)	72 (29.75%)	25 (31.25%)	47 (22.82%)
$Lmx1a^{dr/dr}$; +/+	12.5	29 (9.86%)	30 (12.40%)	7 (8.75%)	29 (14.08%)
$Lmx1a^{dr/dr}$;Shh^{cre};$Lmx1b^{f/+}$	6.25	30 (10.20%)	12 (4.96%)	5 (6.25%)	15 (7.28%)
$Lmx1a^{dr/dr}$; Shh^{cre};$Lmx1b^{f/f}$	6.25	13 (4.42%)	9 (3.72%)	3 (3.75%)	2 (0.97%)
$Lmx1a^{dr/+}$; Shh^{cre};$Lmx1b^{f/f}$	12.5	38 (12.93%)	45 (18.60%)	12 (15.00%)	35 (16.99%)
+/+; Shh^{cre};$Lmx1b^{f/f}$	6.25	18 (6.12%)	10 (4.13%)	2 (2.50%)	14 (6.80%)
+/+; Shh^{cre};$Lmx1b^{f/+}$	6.25	15 (5.10%)	14 (5.79%)	7 (8.75%)	20 (9.71%)
$Lmx1a^{dr/+}$; Shh^{cre};$Lmx1b^{f/+}$	12.5	34 (11.56%)	25 (10.33%)	7 (8.75%)	18 (8.74%)
No. of embryos/animals	--	294	242	80	206
No. of litters	--	35	34	9	25

Table 4-2 Frequencies of all genotypes from $Lmx1a^{dr/+}$;Shh^{cre};$Lmx1b^{f/+}$ and $Lmx1a^{dr/+}$;$Lmx1b^{f/f}$ intercross at embryonic stages E10.5, E12.5, E18.5 and postnatal stage P21.

The actual frequencies for obtaining each genotype roughly correlated with the Mendelian ratio. However, the frequencies for obtaining *Lmx1a/b* double mutants were consistently lower than expected at all stages. Moreover, the survival of double mutants was strongly compromised after birth. From the 25 litters of mice collected, 100 males and 106 females survived to P21, of which only 2 mice were *Lmx1a/b* double mutants (Table 4-2 and Figure 4-13A). One of these double mutants did not survive the weaning process. The other one, which was born in a small litter of 7 pups, was not weaned and managed to survive until P28.

Mice carrying a single wild type allele of *Lmx1a* (*Lmx1a*$^{dr/+}$;*Shh*^{cre};*Lmx1b*$^{f/f}$) survived to adulthood, did not display any morphological and behavioural defects, and were fertile. Mice losing both copies of *Lmx1a* (*Lmx1a*$^{dr/dr}$, and *Lmx1a*$^{dr/dr}$;*Shh*^{cre};*Lmx1b*$^{f/+}$ and *Lmx1a*$^{dr/dr}$;*Shh*^{cre};*Lmx1b*$^{f/f}$) all showed the classical *dreher* phenotype of head-tossing, ataxia, circulating behaviour and abdominal white patches of fur (Lyons and Wahlsten, 1988; Wahlsten et al., 1983). Due to the severity of *Lmx1a*$^{dr/dr}$ phenotype, mice carrying 2 *dreher* alleles were not kept beyond P28.

The size of the mutants was variable. The *Lmx1b* conditional mutation did not affect of the size of both *Shh*^{cre};*Lmx1b*$^{f/f}$ and *Lmx1a*$^{dr/+}$;*Shh*^{cre};*Lmx1b*$^{f/f}$ mutants. *Lmx1a*$^{dr/dr}$ single mutants were noticeably smaller, consistent with the general retardation of overall body growth reported in mutants of another *Lmx1a* allele *dr*$^{sst/sst}$ (Lyons and Wahlsten, 1988). *Lmx1a*$^{dr/dr}$;*Shh*^{cre};*Lmx1b*$^{f/+}$ mice were smaller than *Lmx1a*$^{dr/dr}$ single mutants, and *Lmx1a*$^{dr/dr}$;*Shh*^{cre};*Lmx1b*$^{f/f}$ double mutants were about half the size of phenotypically normal littermates (Figure 4-14). Thus, *Lmx1a/b* mutations lead to growth retardation. This is likely an indirect effect of inability to compete for nursing due to the behavioural defects since growth retardation was more severe in large litters with many normal siblings.

The sole surviving *Lmx1a/b* double mutant and mice from five selected genotypes were perfused at P28. The brain morphologies are shown in Figure 4-13B-G. Similar to previous report on *dreher* mutants (Lyons and Wahlsten, 1988), the six *Lmx1a*$^{dr/dr}$ brains analysed at P28 showed highly variable cerebellar abnormality ranging from only slight reduction in the foliation to an almost complete absence of the cerebellum. The sole surviving *Lmx1a/b* double mutant displayed an almost complete absence of cerebellar structures (Figure 4-13E). Post-mortem examination of the other *Lmx1a/b* double mutant showed less severe cerebellar abnormality.

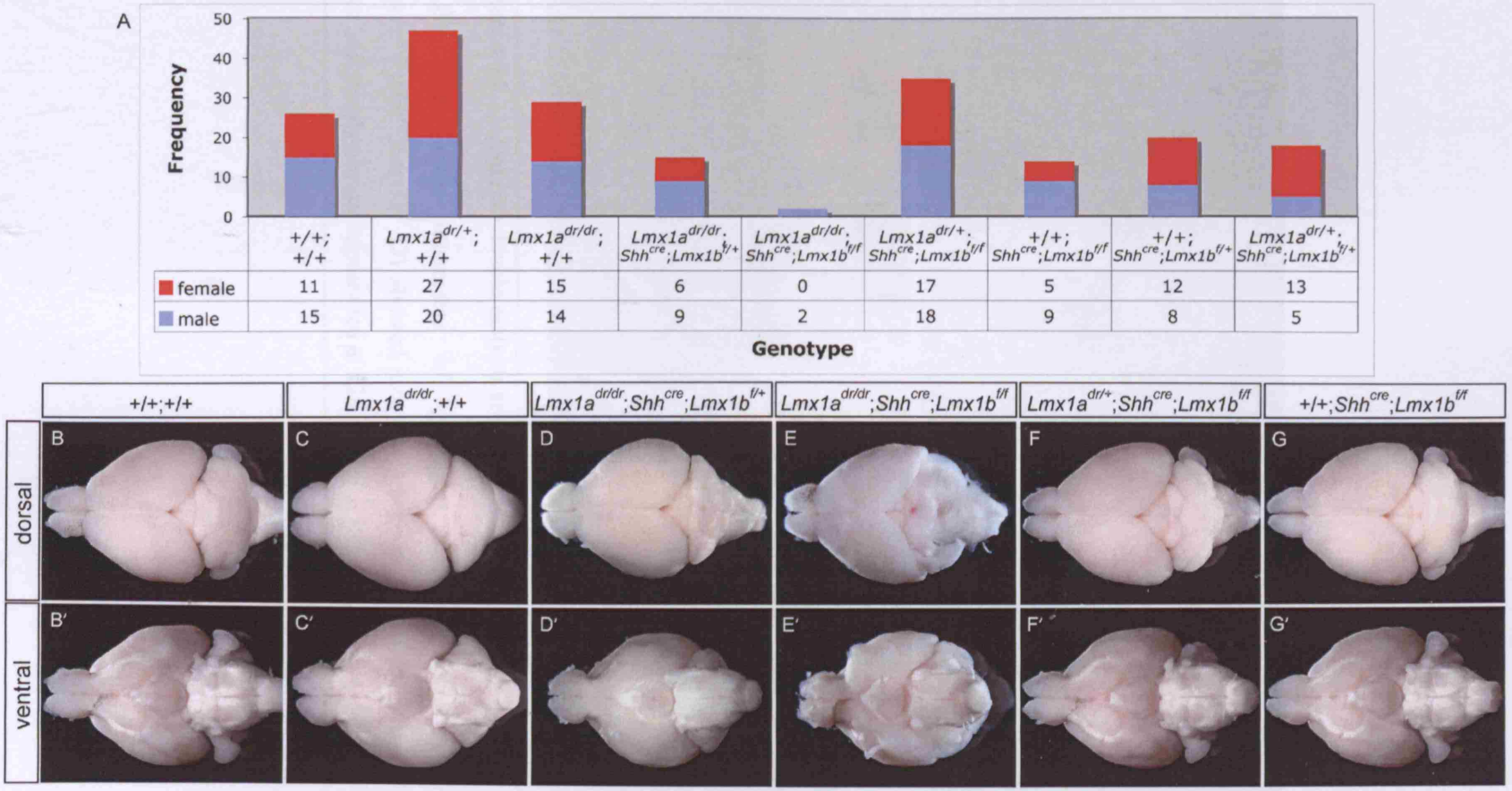

Figure 4-13 Survival and brain morphologies of postnatal *Lmx1a/b* mutants.

(A) Graphical representation of the survival of all nine genotypes of *Lmx1a/b* mutants at P21. (B-G) Brain morphologies of six genotypes at P28 in both dorsal and ventral views.

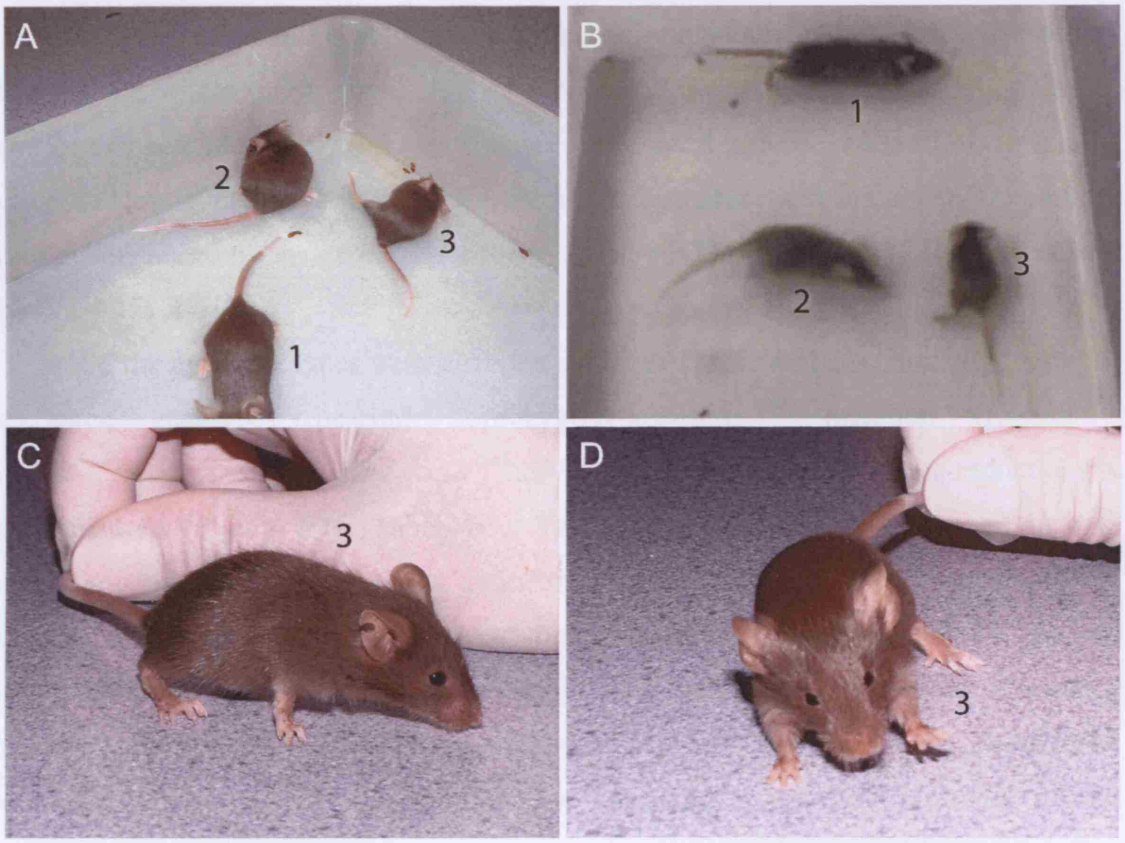

Figure 4-14 *Lmx1a/b* double mutants are smaller in size.

(A,B) Three male littermates of genotypes $Lmx1a^{dr/+}$ (1), $Lmx1a^{dr/dr}$ (2) and $Lmx1a^{dr/dr}$;Shh^{cre};$Lmx1b^{f/f}$ (3) showed size differences at P28. (C,D) $Lmx1a^{dr/dr}$;Shh^{cre};$Lmx1b^{f/f}$ mice had grossly normal appearance at P28.

4.3.6 Lmx1a/b have redundant functions in mDA neuron development

Due to the rapid growth in both the mDA progenitors and neurons between E10.5 and E12.5, and the significant variation in the size of embryos collected between litters with normal mating, 3 hours timed matings were set up for better stage control of embryos to allow more accurate comparisons between litters.

Changes in the mDA progenitors, immature and mature neurons were assessed by studying the whole mDA population of the nine different genotypes at E12.5. mDA progenitors were identified by co-expression of the mDA specific marker Lmx1a and the active cell cycle marker Ki67 (Figure 4-15A-I). Immature and mature mDA neurons were distinguished by the expression profile of Nurr1+TH- and Nurr1+TH+ respectively (Figure 4-15J-R).

Of the nine genotypes with different doses of *Lmx1a* and *Lmx1b* genes, embryos of three genotypes bearing homozygous $Lmx1a^{dr/dr}$ mutation ($Lmx1a^{dr/dr}$, $Lmx1a^{dr/dr}$;Shh^{cre};$Lmx1b^{f/+}$ and $Lmx1a^{dr/dr}$;Shh^{cre};$Lmx1b^{f/f}$) displayed strong reductions in mDA neurons (Figure 4-16, Table 4-3). There was a proportionate decrease in both mDA progenitors and neurons by reducing the *Lmx1b* gene dosage on $Lmx1a^{dr/dr}$ background. Similar to the previous *Lmx1b* single conditional mutant studies, Shh^{cre};$Lmx1b^{f/f}$ embryos displayed an insignificant increase in mDA neurons. Removing an *Lmx1a* allele from Shh^{cre};$Lmx1b^{f/f}$ embryos led to a mild reduction in the whole mDA population. These results suggest that *Lmx1a* plays a key role in mDA neuron development, and that *Lmx1b* can partially compensate for the loss of *Lmx1a* in mDA neuron specification.

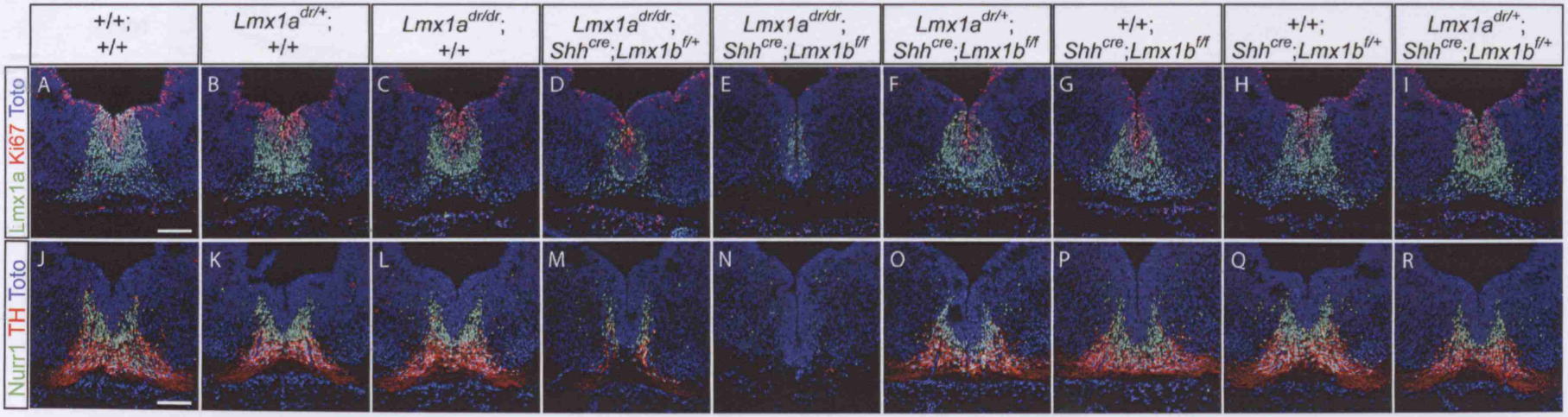

Figure 4-15 Lmx1a/b are required for the development of mDA neurons.

(A-I) mDA progenitors were identified as Lmx1a/Ki67 double positive cells at E12.5. (J-R) Immature and mature mDA neurons were distinguished by Nurr1+TH- and Nurr1+TH+ expression at E12.5. Scale bars correspond to 100μm.

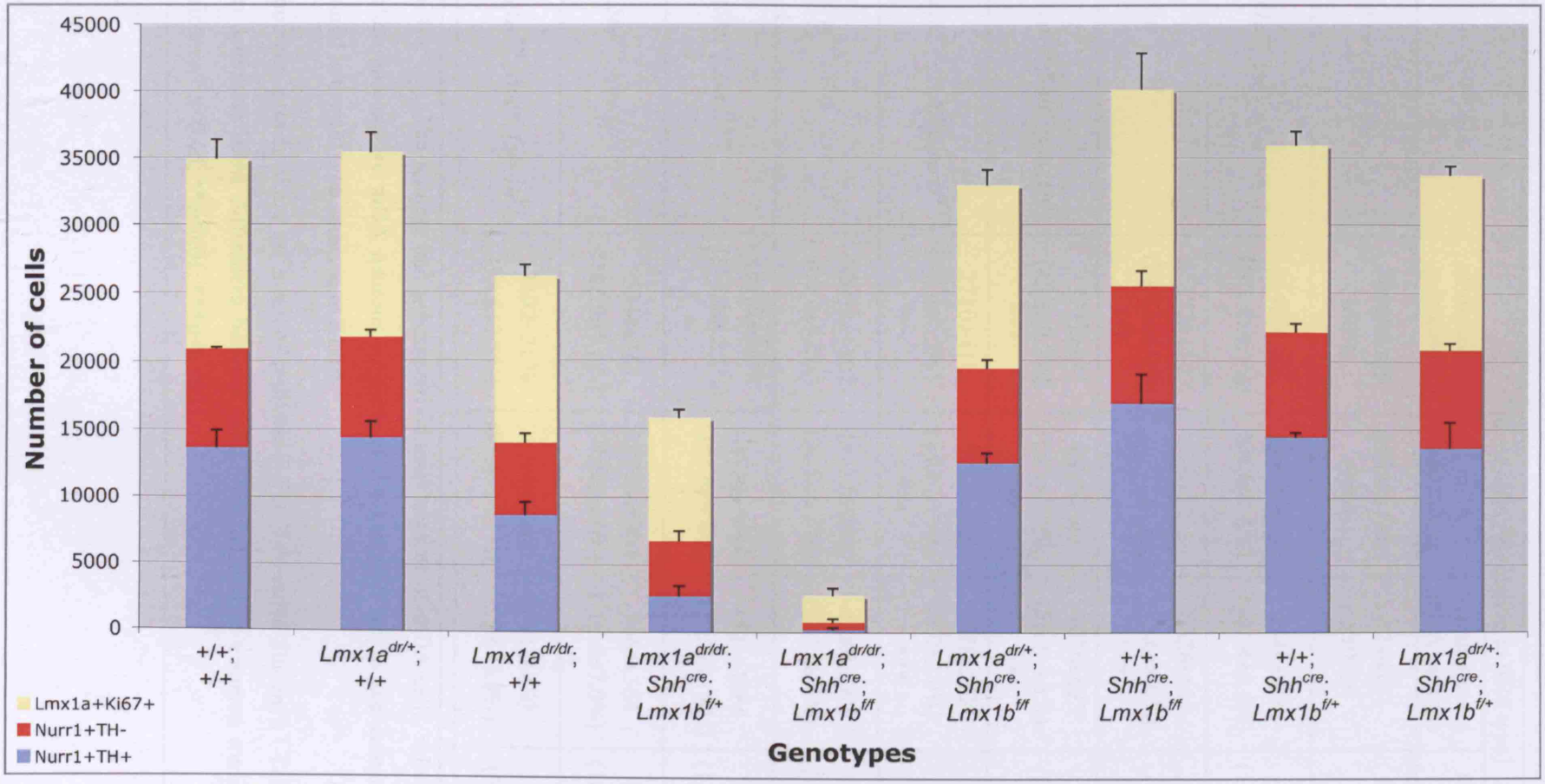

Figure 4-16 Quantification of mDA progenitors (Lmx1a+Ki67+), and immature (Nurr1+TH-) and mature (Nurr1+TH+) mDA neurons in the midbrain and caudal diencephalic region of *Lmx1a/b* compound mutants at E12.5. The cell counts represent mean ± SD of triplicate.

Genotype	No. of cells (% relative to wild type)			
	whole mDA population	mDA progenitors	immature mDA neurons	mature mDA neurons
+/+;+/+	34920±484 (100%)	14020±1386 (100%)	7244±54 (100%)	13656±1222 (100%)
Lmx1a$^{dr/+}$;+/+	35408±806 (101.4±3.7%)	13684±1437 (97.6±0.6%)	7344±429 (101.4±5.5%)	14380±1132 (105.3±17.6%)
Lmx1a$^{dr/dr}$;+/+	26132±1349 (74.83±4.9%) ***	12116±798 (86.4±3.1%)	5328±617 (73.6±8.0%) **	8688±885 (63.6±4.5%) **
Lmx1a$^{dr/dr}$;*Shh*^{cre};*Lmx1b*$^{f/+}$	15772±34 (45.2±0.7%) ***	8980±564 (64.1±5.4%) **	4076±693 (56.3±9.1%) **	2716±710 (19.9±3.6%) ***
Lmx1a$^{dr/dr}$;*Shh*^{cre};*Lmx1b*$^{f/f}$	2780±471 (8.0±1.5%) ***	2012±465 (14.4±4.5%) ***	578±202 (8.0±2.9%) ***	190±103 (1.4±0.7%) ***
Lmx1a$^{dr/+}$;*Shh*^{cre};*Lmx1b*$^{f/f}$	32952±1502 (94.4±3.0%)	13572±1094 (96.8±2.9%)	6860±567 (94.7±8.4%)	12520±658 (91.7±12.2%)
+/+;*Shh*^{cre};*Lmx1b*$^{f/f}$	40132±3674 (114.9±12.1%) *	14720±2664 (105.0±9.6%)	8524±1066 (117.7±13.8%)	16888±2034 (123.7±15.3%)
+/+;*Shh*^{cre};*Lmx1b*$^{f/+}$	35944±161 (102.9±1.0%)	13816±1004 (98.5±14.0%)	7664±564 (105.8±7.0%)	14464±296 (105.9±11.4%)
Lmx1a$^{dr/+}$;*Shh*^{cre};*Lmx1b*$^{f/+}$	33692±2138 (96.5±7.5%)	12840±649 (91.6±11.1%)	7212±460 (99.6±6.9%)	13640±1866 (99.9±14.2%)

Table 4-3 The number and percentage of total number of mDA cells, mDA progenitors, immature and mature mDA neurons in each of the *Lmx1a/b* single and compound mutants compared with wild type embryos at E12.5.

The numbers presented are the mean of triplicate ± SD. Two-tailed Student's t-Test was carried out to determine if the differences between wild type and mutant embryos were of statistical significance. *$p<0.05$; **$p<0.01$; ***$p<0.001$.

Subsequent studies focused on understanding the defects in *Lmx1a*$^{dr/dr}$, *Lmx1a*$^{dr/dr}$;*Shh*^{cre};*Lmx1b*$^{f//+}$ and *Lmx1a*$^{dr/dr}$;*Shh*^{cre};*Lmx1b*$^{f/f}$ mutants embryos in comparison with wild type and *Shh*^{cre};*Lmx1b*$^{f/f}$ single mutants as controls.

The reduction in the mDA progenitors and neurons appeared to be uniform at all rostral caudal levels in both the *Lmx1a*$^{dr/dr}$ and *Lmx1a*$^{dr/dr}$;*Shh*^{cre};*Lmx1b*$^{f/+}$ mutants (Figure 4-17). However, in *Lmx1a/b* double mutants, defects in both progenitors and postmitotic neurons were less severe in the caudal midbrain. This appears to relate to the incomplete deletion of *Lmx1b* in *Lmx1b* conditional mutants. Similar to *Lmx1b* single conditional mutants, *Lmx1a/b* double mutants only had barely detectable levels of *Lmx1b* transcript in the most caudal section of the midbrain at E12.5. However, previous studies on the dynamics of the *Lmx1b* deletion in the single mutants revealed a stronger level of *Lmx1b* transcript at E10.5 (Figure 4-7). Hence, the early *Lmx1b* expression in the caudal lateral midbrain might be sufficient for the generation of the few TH+ neurons.

Most of the TH+ neurons in the *Lmx1a*$^{dr/dr}$;*Shh*^{cre};*Lmx1b*$^{f/+}$ embryos and all of the TH+ neurons in *Lmx1a*$^{dr/dr}$;*Shh*^{cre};*Lmx1b*$^{f/f}$ embryos were located in the lateral region. However, this lateral distribution was not restricted to the caudal midbrain. Moreover, preliminary studies showed that the pattern of TH+ cells in *Lmx1a*$^{dr/dr}$;*Lmx1b*$^{+/-}$ embryos (Figure 6-11M) was similar to that of *Lmx1a*$^{dr/dr}$;*Shh*^{cre};*Lmx1b*$^{f/+}$ (Figure 4-15M). Therefore, this is likely a phenotype inherent to the loss of *Lmx1a/b*.

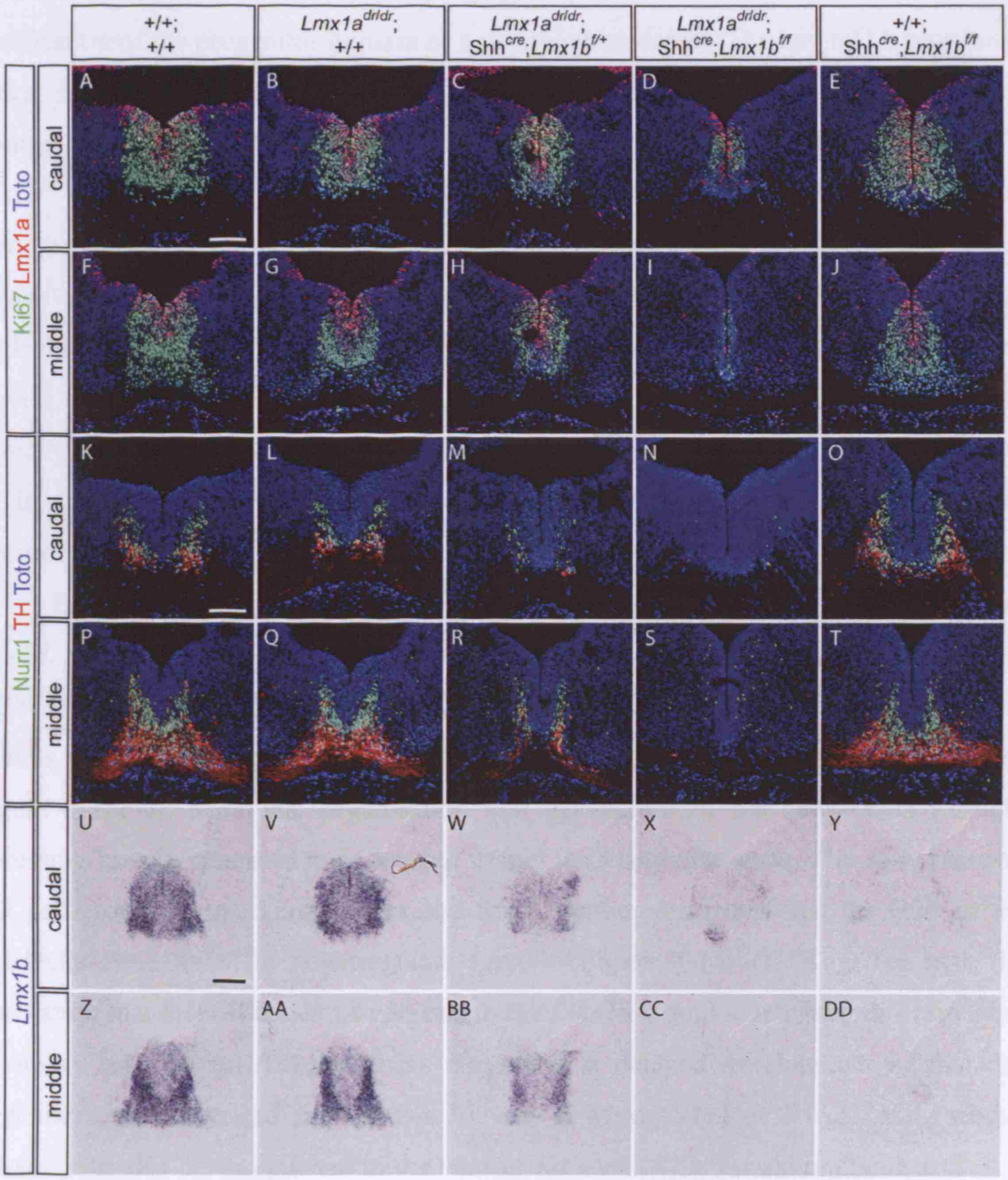

Figure 4-17 *Lmx1a/b* double mutants displayed less severe phenotype in the caudal midbrain.

Double immunohistochemistry of Lmx1a/Ki67 (A-J) and Nurr1/TH (K-T) at E12.5 showed that more mDA progenitors and postmitotic neurons were present in the caudal midbrain. This correlated to the residual *Lmx1b* expression (U-DD). Scale bars correspond to 100μm.

4.3.7 Lmx1a/b play a redundant role in the specification of mDA progenitors

The reduction in the mDA progenitor population could be due to a mis-specification of the progenitor domain or a proliferation defect. The key mDA progenitor marker Lmx1a appeared to be expressed in a normal domain in all nine genotypes, although the number of Lmx1a expressing cells was significantly reduced in *Lmx1a*$^{dr/dr}$, *Lmx1a*$^{dr/dr}$;*Shh*^{cre};*Lmx1b*$^{f/+}$ and *Lmx1a*$^{dr/dr}$;*Shh*^{cre};*Lmx1b*$^{f/f}$ embryos at E12.5. The other mDA progenitor specific marker *Msx1* was used to examine whether the mDA progenitors are correctly specified. The RNA expression pattern of *Msx1* in all *Lmx1a/b* single and compound mutants, except for *Lmx1a*$^{dr/dr}$;*Shh*^{cre};*Lmx1b*$^{f/f}$, were similar to that of wild type embryos (Figure 4-18A-E). This suggests that the mDA progenitors are correctly specified in embryos carrying at least one copy of either *Lmx1a* or *Lmx1b*, but not in *Lmx1a/b* double mutant embryos. Despite the fact that the caudal midbrain appeared less severely affected, Msx1 expression is lost in all rostral caudal extent.

Besides the only two known mDA specific progenitor markers, the expression of Lmx1b, which is normally weakly expressed in mDA progenitors, was also studied at E12.5. Lmx1b was strongly expressed in the whole mDA domain in the *Lmx1a/b* double mutants, while the expression pattern was not affected in all other genotypes examined (Figure 4-18F-J). From the organisation and orientation of the cells, cells strongly expressing Lmx1b appeared to be located within the ventricular zone. The co-expression with pan-progenitor markers, Nestin and Sox2, further confirmed that the cells in the ventricular zone failed to downregulate Lmx1b (Figure 4-18F-O). Together with the observation that there is a lack of neurons in the *Lmx1a/b* double mutants, this raises the possibility that the mDA progenitors may have a delayed development or that the progenitors were arrested before *Lmx1b* was downregulated at E11.5. *En1*, whose expression is also downregulated in the ventricular zone of the ventral midbrain at E11.5, was thus examined (Figure 4-27F-J). The successful downregulation of *En1* expression in the ventricular zone of the *Lmx1a/b* double mutants at E12.5 argues against a developmental delay in mDA progenitors.

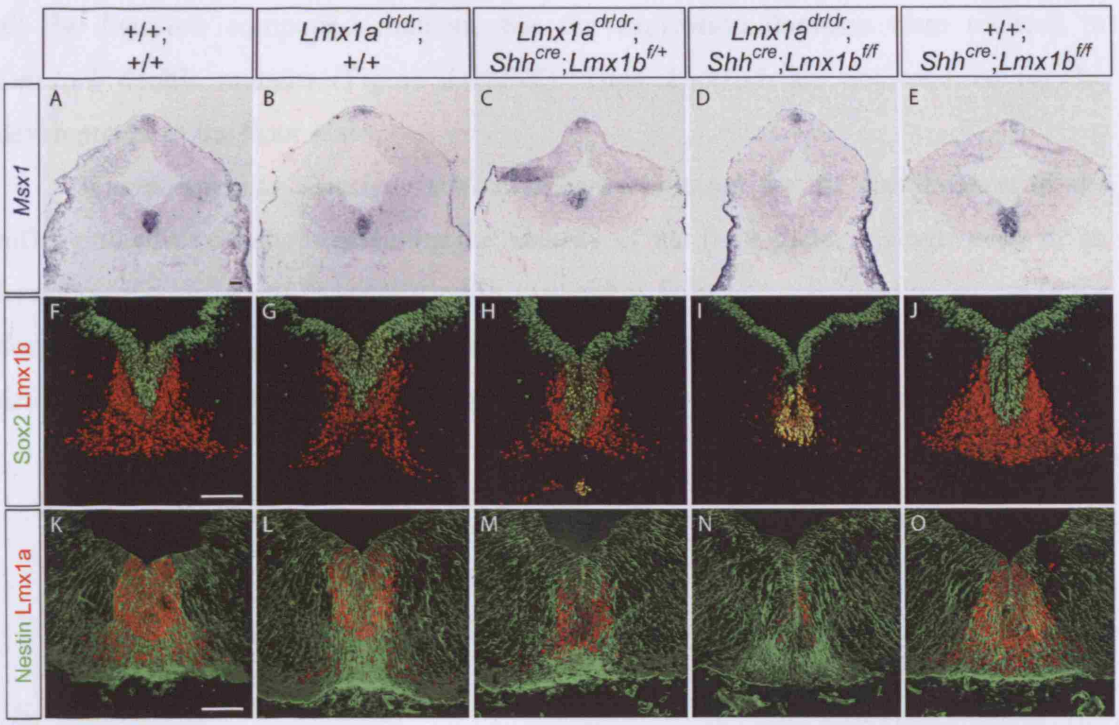

Figure 4-18 Lmx1a/b are co-ordinately required for the correct specification of mDA progenitors.

Msx1 RNA expression in mDA progenitors(A-E), and double immunohistochemistry of Sox2/Lmx1b (F-J) and Nestin/Lmx1a (K-O) at E12.5. Scale bars correspond to 100μm.

Since mDA neurons are generated in the floor plate, the identity of the floor plate was also examined. At E12.5 in the midbrain of wild type embryos, the transcript of the classical floor plate marker *Shh* is strongly expression in the ventricular zone of the basal plate, but weakly expressed in the ventricular zone of the floor plate and some postmitotic neurons. The expression patterns of *Shh* transcript were similar in the wild type and Shh^{cre};$Lmx1b^{f/f}$ embryos at E12.5 (Figure 4-19A,E). The downregulation of *Shh* transcript was less evident in $Lmx1a^{dr/dr}$ and $Lmx1a^{dr/dr}$;Shh^{cre};$Lmx1b^{f/+}$ embryos (Figure 4-19B,C). There was a complete failure to downregulate *Shh* transcript in the *Lmx1a/Lmx1b* double mutants at E12.5 (Figure 4-19D).

The aristaless related homeobox gene Arx, secreted extracellular matrix protein Slit2 and the Wnt pathway scaffolding protein Axin2 have restricted expression domains within the floor plate (Holmes et al., 1998; Kitamura et al., 2002; Saarimaki-Vire et al., 2007). The expression of *Arx*, *Slit2* and *Axin2* were all detected in the ventral midline of

all the *Lmx1a/b* compound mutants, but the expression domains were reduced in *Lmx1a/b* double mutants (Figure 4-19F-T). Thus, *Lmx1a/b* are not required for the development of the floor plate.

Taken together, *Lmx1a/b* are redundantly required for the specification of the mDA progenitors without affecting the identity of the floor plate. A single copy of an Lmx1 gene is sufficient to specify mDA progenitor fate. The consistent reduction in the domains of all mDA progenitor and floor plate markers suggests that proliferation defects exist in the *Lmx1a/b* double mutants.

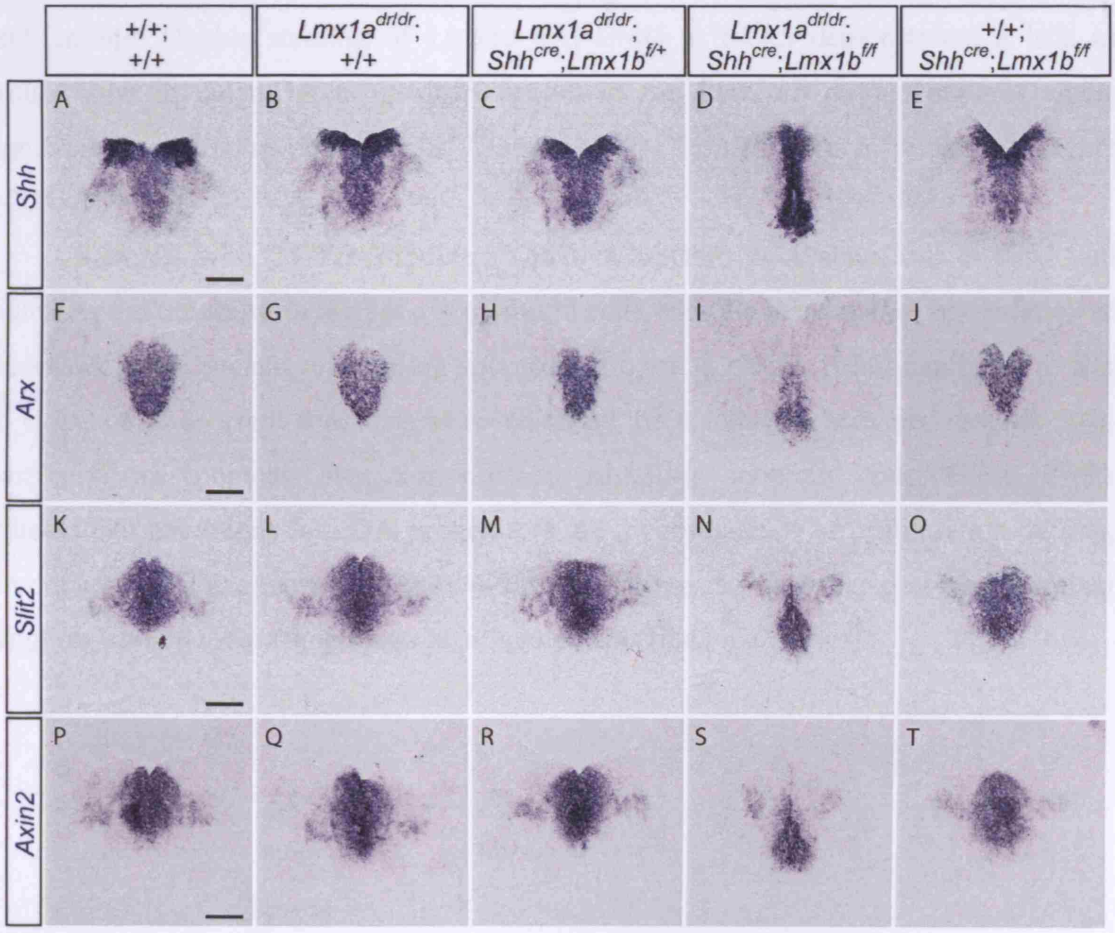

Figure 4-19 Floor plate specification is normal in *Lmx1a/b* compound mutants.

Shh (A-E), *Arx* (F-J), *Slit2* (K-O) and *Axin2* (P-T) transcripts were detected in all *Lmx1a/b* compound mutants at E12.5. Scale bars correspond to 100μm.

4.3.8 Lmx1a/b are required for the proliferation of the mDA progenitors

Despite the correct specification of mDA progenitors in both *Lmx1a*$^{dr/dr}$ and *Lmx1a*$^{dr/dr}$;*Shh*^{cre};*Lmx1b*$^{f/+}$ embryos, there was a significant reduction in the number of progenitors observed. The whole mDA population was compared in *Lmx1a/b* compound mutants to assess the accumulative effect of *Lmx1a/b* on proliferation until E12.5. The reduction in the mDA population correlated to the gene dosage of *Lmx1a/b* (Table 4-3).

The reduction in the number of Lmx1a+ cells could be due to a decrease in proliferation or an increase in cell death, or both. Short pulse BrdU incorporation assays were performed to examine cells in S-phase of the cell cycle as an indication of proliferation. Double staining of Lmx1a and BrdU at E12.5 demonstrated a lack of proliferation in the mDA progenitors region in the *Lmx1a/b* double mutants and a significant reduction in both *Lmx1a*$^{dr/dr}$ and *Lmx1a*$^{dr/dr}$;*Shh*^{cre};*Lmx1b*$^{f/+}$ embryos (Figure 4-20A-E).

Staining with TOTO-3-iodide (Toto), a nucleic acid stain and a dead cell indicator, did not show an increase in pyknotic cells with the irreversible condensation of chromatin in the nucleus undergoing apoptosis (Figure 4-20F-J). Additionally, there was no evidence of aberrant apoptosis as revealed by the staining in activated caspase-3 (p-Caspase3), an apoptosis execution protease revealing apoptotic cells. These results indicate that reductions in mDA progenitors are a consequence of proliferation defects, but not attributed to apoptosis (Figure 4-20F-J). Apoptosis was detected in the trigeminal ganglion from the same embryo as positive controls (data not shown).

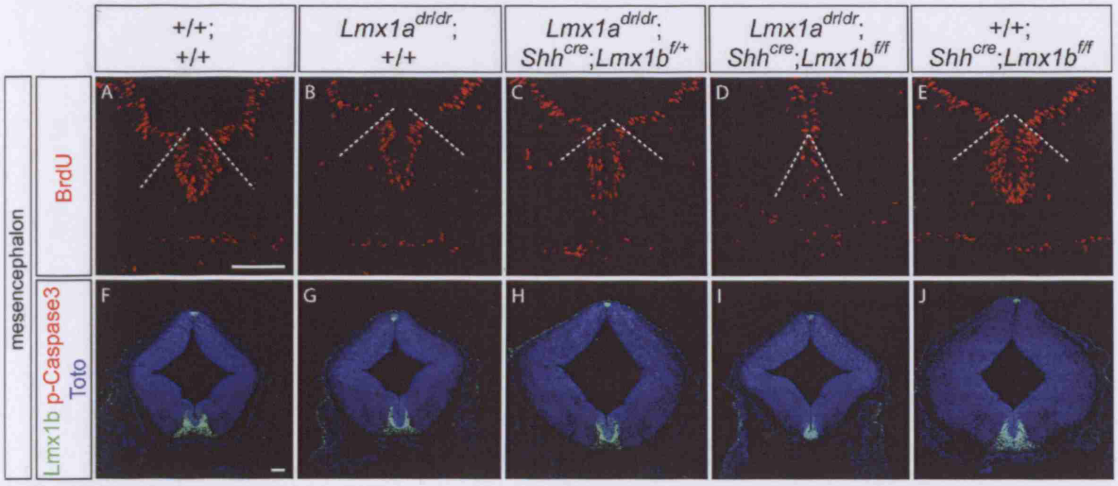

Figure 4-20 (A-E) One hour BrdU incorporation was slightly reduced in the mDA progenitors but not in the dorsal neural tube of *Lmx1a/b* double mutants. (E-J) Double staining of Lmx1b and p-Caspase3 showed a lack of apoptosis in wild type and *Lmx1a/b* mutants. (K-O) Apoptosis was detected in the fore limb buds from the same embryo as positive controls. Scale bars correspond to 100μm.

Because proliferation was already strongly affected at E12.5, the effect of *Lmx1a/b* on the mDA progenitor proliferation was further studied at an earlier stage of mDA neuron development. At E10.5, before the generation of the mature mDA neurons, the vast majority of the Lmx1a+ cells were still within the ventricular zone.

Short pulse BrdU incorporation assays showed that there was a reduction in the proliferation in *Lmx1a/b* compound mutants at E10.5 (Figure 4-21A-E). Similar to E12.5, the lack of p-Caspase3 immunohistochemistry in the mDA domain of the *Lmx1a/b* single and compound mutants at E10.5 (Figure 4-21F-J) suggests that there is no cell death in the region. Moreover, the number of Lmx1a+ cells in the whole midbrain and caudal diencephalon was reduced in *Lmx1a/b* double mutants. Therefore, proliferation in the Lmx1a-expressing mDA progenitors was quantified.

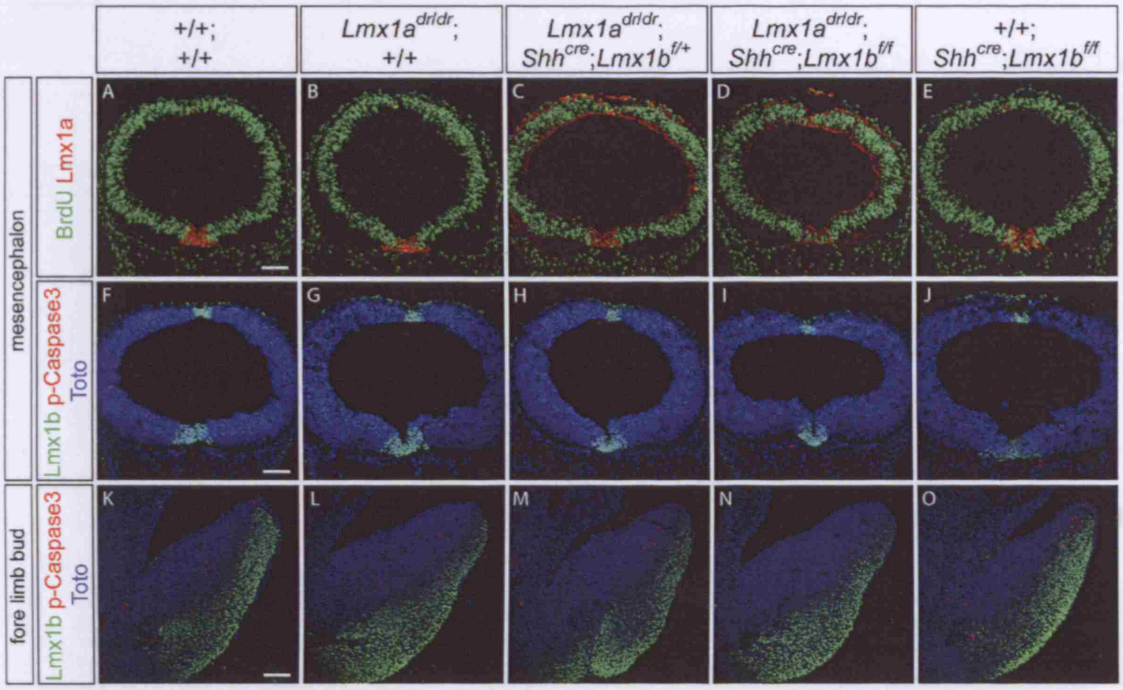

Figure 4-21 *Lmx1a/b* compound mutants have mild proliferation defect at E10.5.

(A-E) One hour BrdU incorporation was slightly reduced in the mDA progenitors but not in the dorsal neural tube of *Lmx1a/b* double mutants. (E-J) Double staining of Lmx1b and p-Caspase3 showed a lack of apoptosis in wild type and *Lmx1a/b* mutants. (K-O) Apoptosis was detected in the fore limb buds from the same embryo as positive controls. Scale bars correspond to 100μm.

Quantifications were made on mDA progenitors in active cell cycle (Lmx1a+Ki67+) (Figure 4-22A-E), mDA progenitors in S-phase of the cell cycle (Lmx1a+Ki67+BrdU+) (Figure 4-22F-J), and non-dividing mDA progenitors/neurons (Lmx1a+Ki67-) at E10.5 (Figure 4-22K). As expected, the proliferation defects were much milder than at E12.5. There was however a statistically significant reduction in mDA progenitors in *Lmx1a/b* double mutants at this stage (Table 4-4). The reductions in the number of cells in S-phase of the cell cycle were stronger than those of mDA progenitors. Because the total number of Lmx1a-expressing cells was reduced in the mutants, the fraction of cells in S-phase of cell cycle within the population of cells in active cell cycle was also compared. All *Lmx1a/b* mutants showed a reduction in the percentage of cells in S-phase compared with wild type. *Lmx1a/b* double mutants had a strong reduction in the proportion of cells in S-phase, with only 41.0% of cells in S-phase comparing with the 59.7% in wild type embryos (Table 4-4). This may imply that *Lmx1a/b* are redundantly and continuously required for the proliferation of mDA progenitors by facilitating the progression of the cell cycle.

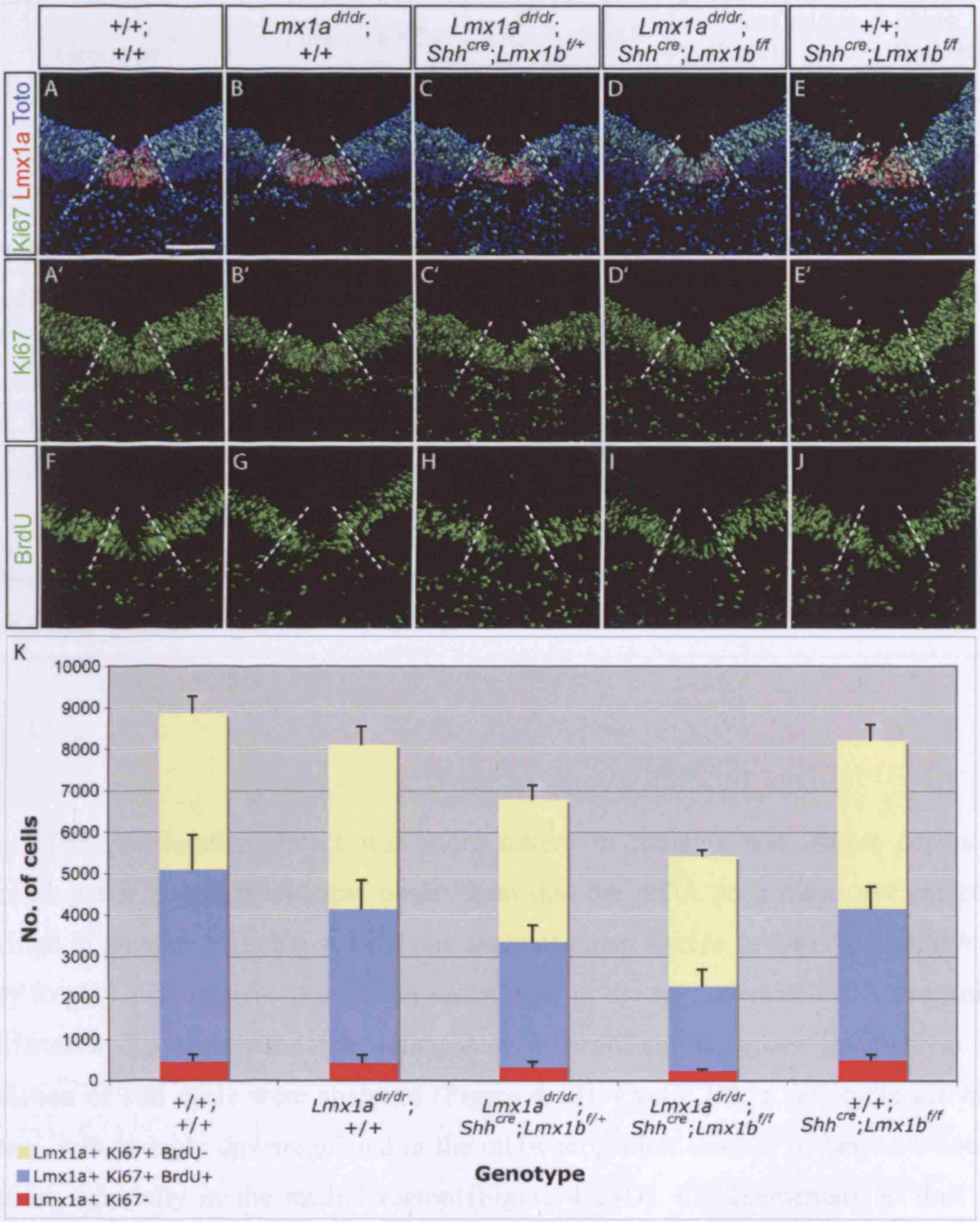

Figure 4-22 *Lmx1a/b* compound mutants have proliferation defects at E10.5.

(A-E) mDA progenitors in active cell cycle expressed both Lmx1a and Ki67. (F-J) mDA progenitor cells in S-phase of the cell cycle are double positive for Lmx1a and BrdU. The Lmx1a+ region is demarcated by dotted lines. (K) Quantification of proliferating cells in the Lmx1a+ domain of whole midbrain and caudal diencephalon at E10.5. The cell counts represent mean ± SD of triplicate. Scale bars correspond to 100μm.

Genotype	Lmx1a+Ki67+ cells	Lmx1a+BrdU+ cells	% of cells in S-phase (Lmx1a+ Ki67+ BrdU+/ Lmx1a+ Ki67+)
+/+;+/+	8397±1341	4628±815	55.0±2.4%
Lmx1a$^{dr/dr}$;+/+	7677±1504	3709±680	48.4±1.8% *
Lmx1a$^{dr/dr}$;*Shh*^{cre};*Lmx1b*$^{f/+}$	6455±862	3007±396 *	46.6±0.3% **
Lmx1a$^{dr/dr}$;*Shh*^{cre};*Lmx1b*$^{f/f}$	5173±1179 *	2021±404 **	39.4±6.2% **
+/+; *Shh*^{cre};*Lmx1b*$^{f/f}$	7715±815	3651±512	50.6±4.6%

Table 4-4 The proportion of cells in S-phase of the cell cycle is reduced in Lmx1a/b mutants at E10.5.

The numbers shown are the mean ± SD of triplicate. Two-tailed Student's t-Test was carried out to determine if the differences between wild type and mutant embryos were of statistical significance. *p<0.05; **p<0.01; ***p<0.001.

The proliferation defect was more severe in mutants with fewer copies of *Lmx1a/b* gene. Together with the observation that the mDA progenitors are correctly specified in mutants retaining at least one allele of either *Lmx1a* or *Lmx1b*, *Lmx1a/b* are likely to play a direct gene dosage dependent role in the regulation of mDA progenitor proliferation. To understand the deficiencies in proliferation, genes involved in the regulation of cell cycle were analysed (Figure 4-23). Cyclin D2, a cell cycle activator protein, was strongly downregulated in the mDA progenitor domain of *Lmx1a/b* double mutants, especially in the medial region (Figure 4-23D). Complementary to this, the expression of cyclin-dependent kinase inhibitor p27^{Kip1}, which regulates cell cycle exit, was elevated in the mDA progenitors of *Lmx1a/b* double mutants (Figure 4-23I).

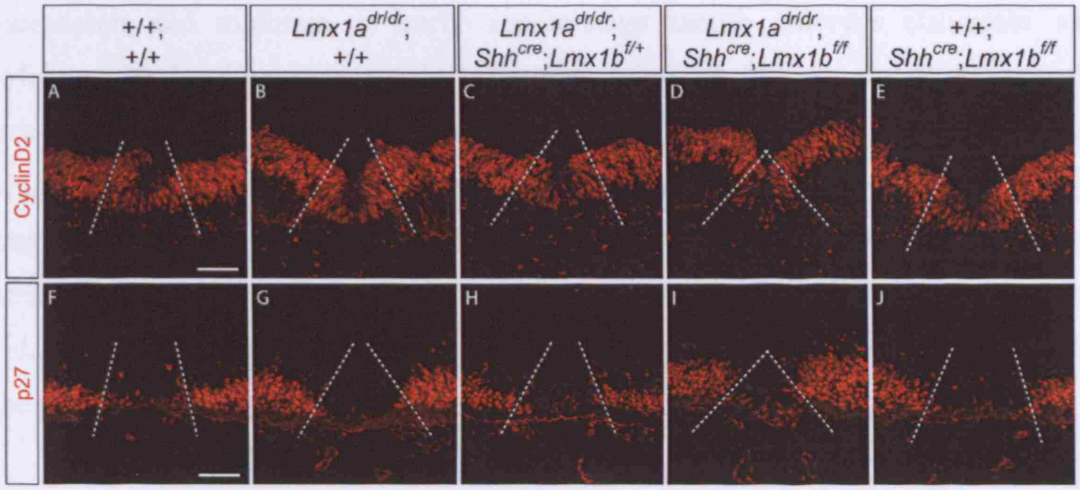

Figure 4-23 Inhibition of cell cycle progression in *Lmx1a/b* double mutants at E10.5.

Expression of Cyclin D2 was strongly reduced (A-E) and expression of p27 was upregulated (F-J) in *Lmx1a/b* double mutants. Lmx1b+ (A-E) and Lmx1a+ (F-J) regions are demarcated by dotted lines. Scale bars correspond to 100μm.

To investigate whether *Lmx1a/b* regulate signalling molecules that are implicated in proliferation, the expression patterns of *Wnt1*, *Shh* and *Bmp7*, which are endogenously expressed in the mDA domain, were analysed.

Wnt1 has been shown to increase the proliferation of isolated mDA precursors from rat ventral midbrain cultures by up-regulating cyclins D1 and D3 and down-regulating the expression of p27 and p57 (Castelo-Branco et al., 2003). In addition, ectopic expression of Wnt1 enhances the proliferation of neural precursors in the ventral spinal cord by regulating cyclins D1 and D2 through β-catenin signalling (Dickinson et al., 1994; Megason and McMahon, 2002). At E10.5, *Wnt1* expression was specifically lost in the region where both Lmx1a and Lmx1b were non-functional (Figure 4-24A-D). However, the expression of *Wnt1* was not affected in *Lmx1a*$^{dr/dr}$, which also showed reduction in proliferation. These suggest that *Lmx1a/b* specifically and redundantly regulate *Wnt1* expression in the lateral mDA domain. The loss of anterior *Wnt1* expression in *Lmx1a/b* double mutants may be responsible for much stronger reduction in proliferation in *Lmx1a/b* double mutants compared with other mutants, but not for the milder proliferation defects in other *Lmx1a/b* mutants.

Shh is required for the expression of cyclin D1 and the growth of the diencephalon and midbrain in early somite-stage mouse embryos (Ishibashi and McMahon, 2002). Complementarily, over-expression of Shh in the Wnt1 domain increases proliferation in the developing spinal cord (Rowitch et al., 1999). In cerebellar granule neuron precursors, Shh indirectly induces cyclin D1, cyclin D2 and cyclin E through the synthesis of intermediate proteins (Kenney and Rowitch, 2000). In the ventral midbrain, the expression patterns of *Shh* remained unaffected in any of the *Lmx1a/b* mutants analysed at E10.5 (Figure 4-24E-H), suggesting that *Shh* is not related to the proliferation defects in the mutants.

The roles of Bmps in proliferation are highly context dependent. BMP7 is required for germ cell proliferation in the gonads (Ross et al., 2007), and it stimulates proliferation of the mesenchyme of the lacrimal glands (Dean et al., 2004). In the nervous system, BMP counteracts the proliferation promoted by Wnt in spinal cord neuroepithelium, but ectopic BMP7 promotes the growth of the ventral hindbrain during early embryonic development (Arkell and Beddington, 1997; Ille et al., 2007). In all the *Lmx1a/b* mutants analysed, the ventral midbrain *Bmp7* expression patterns were not significantly different from those of wild type embryos at E10.5 (Figure 4-24I-L), suggesting that *Lmx1a/b* does not regulate proliferation of mDA neurons through the action of Bmp7.

Taken together, Lmx1a/b are required in a dose-dependent manner for the proliferation of mDA progenitors, where Lmx1a plays a more important role during this process. Lmx1a/b appear to have an additional redundant role in controlling the progression of the cell cycle in mDA progenitors through Wnt1, which regulates the key cell cycle proteins Cyclin D2 and p27.

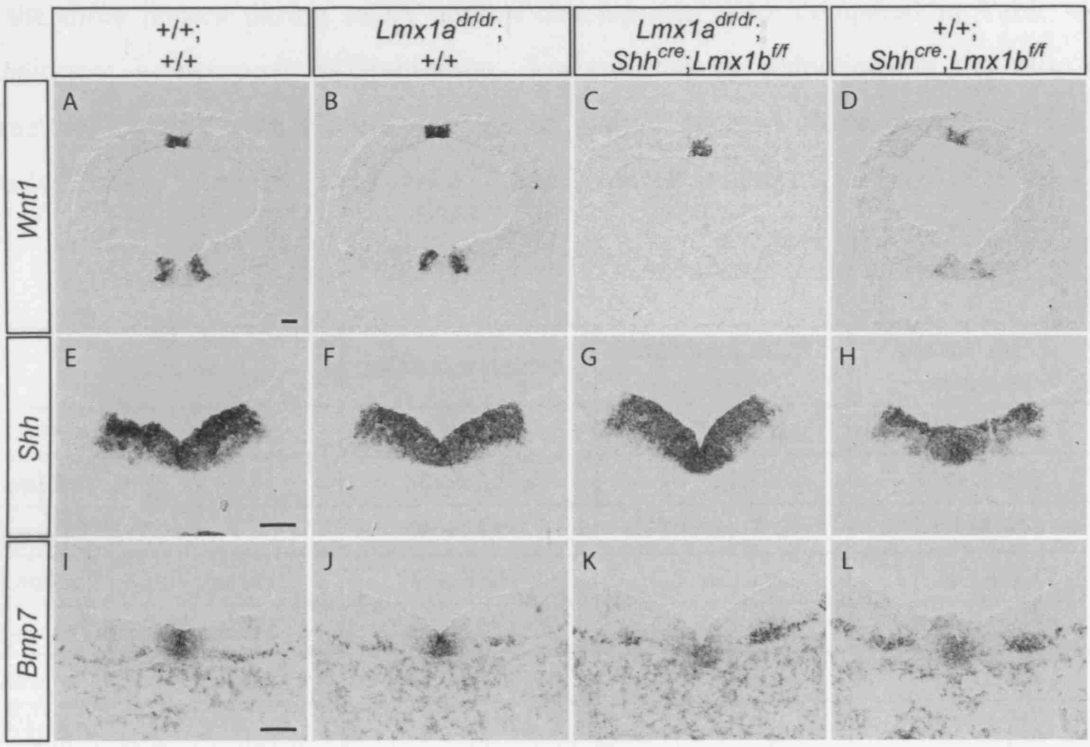

Figure 4-24 Lmx1a/b redundantly regulate *Wnt1* expression in the ventral midbrain.

(A-D Expression of *Wnt1* was lost in the ventral region where both Lmx1a and Lmx1b were non-functional at E10.5. Expression of *Shh* (E-H) and *Bmp7* (I-L) were unaffected in *Lmx1a/b* single and double mutants. Scale bars correspond to 100μm.

4.3.9 Lmx1a/b are required for neurogenesis in mDA progenitors

The data presented in Figure 4-16 and Table 4-3 show that there were stronger reductions in immature and mature mDA neurons than mDA progenitors in *Lmx1a*$^{dr/dr}$, *Lmx1a*$^{dr/dr}$;*Shh*^{cre};*Lmx1b*$^{f/+}$ and *Lmx1a*$^{dr/dr}$;*Shh*^{cre};*Lmx1b*$^{f/f}$ embryos at E12.5. To understand if these correspond to an additional role of *Lmx1a/b* in the specification of mDA neuronal fate independent of the loss of progenitors, the fractions of cells in each of the three phases during mDA neuron development were compared in Table 4-5. Impairment in neuronal differentiation, demonstrated by reductions in the ratio of immature together with mature neurons or mature neurons alone, was observed in *Lmx1a*$^{dr/dr}$;*Shh*^{cre};*Lmx1b*$^{f/+}$ and *Lmx1a*$^{dr/dr}$;*Shh*^{cre};*Lmx1b*$^{f/f}$ embryos.

Genotype	mDA progenitors	immature mDA neurons	mature mDA neurons
+/+;+/+	40.1±3.8%	20.7±0.3%	39.1±3.6%
Lmx1a$^{dr/+}$;+/+	38.6±2.5%	20.7±1.7%	40.6±1.2%
Lmx1a$^{dr/dr}$;+/+	46.4±4.0%	20.4±1.7%	33.2±2.3%
Lmx1a$^{dr/dr}$;*Shh*^{cre};*Lmx1b*$^{f/+}$	56.9±5.9% *	25.8±3.1%	17.2±3.4% **
Lmx1a$^{dr/dr}$;*Shh*^{cre};*Lmx1b*$^{f/f}$	72.4±9.0% **	20.8±7.0%	6.8±4.9% ***
Lmx1a$^{dr/+}$;*Shh*^{cre};*Lmx1b*$^{f/f}$	41.2±0.8%	20.8±1.3%	38.0±1.1%
+/+; *Shh*^{cre};*Lmx1b*$^{f/f}$	36.7±5.7%	21.2±2.8%	42.1±3.2%
+/+;*Shh*^{cre};*Lmx1b*$^{f/+}$	38.4±1.9%	21.3±1.1%	40.2±1.9%
Lmx1a$^{dr/+}$;*Shh*^{cre};*Lmx1b*$^{f/+}$	38.1±3.3%	21.4±1.5%	40.5±3.7%

Table 4-5 The relative percentage of cells in progenitor, immature and mature neuron stages within the whole mDA population from each genotype at E12.5.

The numbers of cells are presented in Table 4-3. The percentage shown are the mean of triplicate ± SD. Two-tailed Student's t-Test was carried out to determine if the differences between wild type and mutant embryos were of statistical significance. *p<0.05; **p<0.01; ***p<0.001.

Neuronal differentiation can be uncoupled into the acquisition of neuronal fate and specification of neuronal subtype identities (Bertrand et al., 2002). Therefore, the roles of *Lmx1a/b* in neurogenesis and mDA neuronal cell fate specification were studied separately using proneural proteins and postmitotic mDA neuronal markers respectively.

In the ventral midbrain, the expression of the proneural gene Ngn2 is not restricted to the mDA region, and is found in both the ventricular zone and the intermediate zone adjacent it. *Ngn2* is specifically required for the differentiation of the mDA progenitors (Andersson et al., 2006a; Kele et al., 2006). At E12.5, Ngn2 expression in mDA region was decreased in $Lmx1a^{dr/dr}$, $Lmx1a^{dr/dr}$;Shh^{cre};$Lmx1b^{f/+}$ and $Lmx1a^{dr/dr}$;Shh^{cre};$Lmx1b^{f/f}$ embryos (Figure 4-25A-E,K and Table 4-6). As the number of mDA progenitors was reduced in these mutants, the percentage of Ngn2+ cells relative to mDA progenitors in each of the wild type mutants was compared (Table 4-6). Although there were strong reductions in Ngn2 expressing cells after normalising with the mDA progenitor numbers, the reductions from the duplicate experiments were not statistically significant. Therefore, the experiments have to be repeated to determine if Lmx1a/b are required for the expression of Ngn2 in mDA domain.

Another proneural gene Mash1, which is expressed in mDA progenitors, has a broad expression pattern in the ventricular zone in the midbrain and diencephalic region. It can partially compensate for the loss of Ngn2 in the differentiation of mDA neurons although it is not required for the differentiation of the mDA progenitor cells in the presence of Ngn2 (Kele et al., 2006). The expression of Mash1 was reduced in the same manner as Ngn2 in *Lmx1a/b* mutants (Figure 4-25F-J). Since Mash1 expression in the mDA progenitors is reduced in $Ngn2^{-/-}$ embryos (Kele et al., 2006), it is not possible to dissociate whether this reduction of Mash1 is a direct effect of *Lmx1a/b* or not. However, the deficiency in Mash1 is likely to limit the potential for recovery in the mDA neurons at later stages of development.

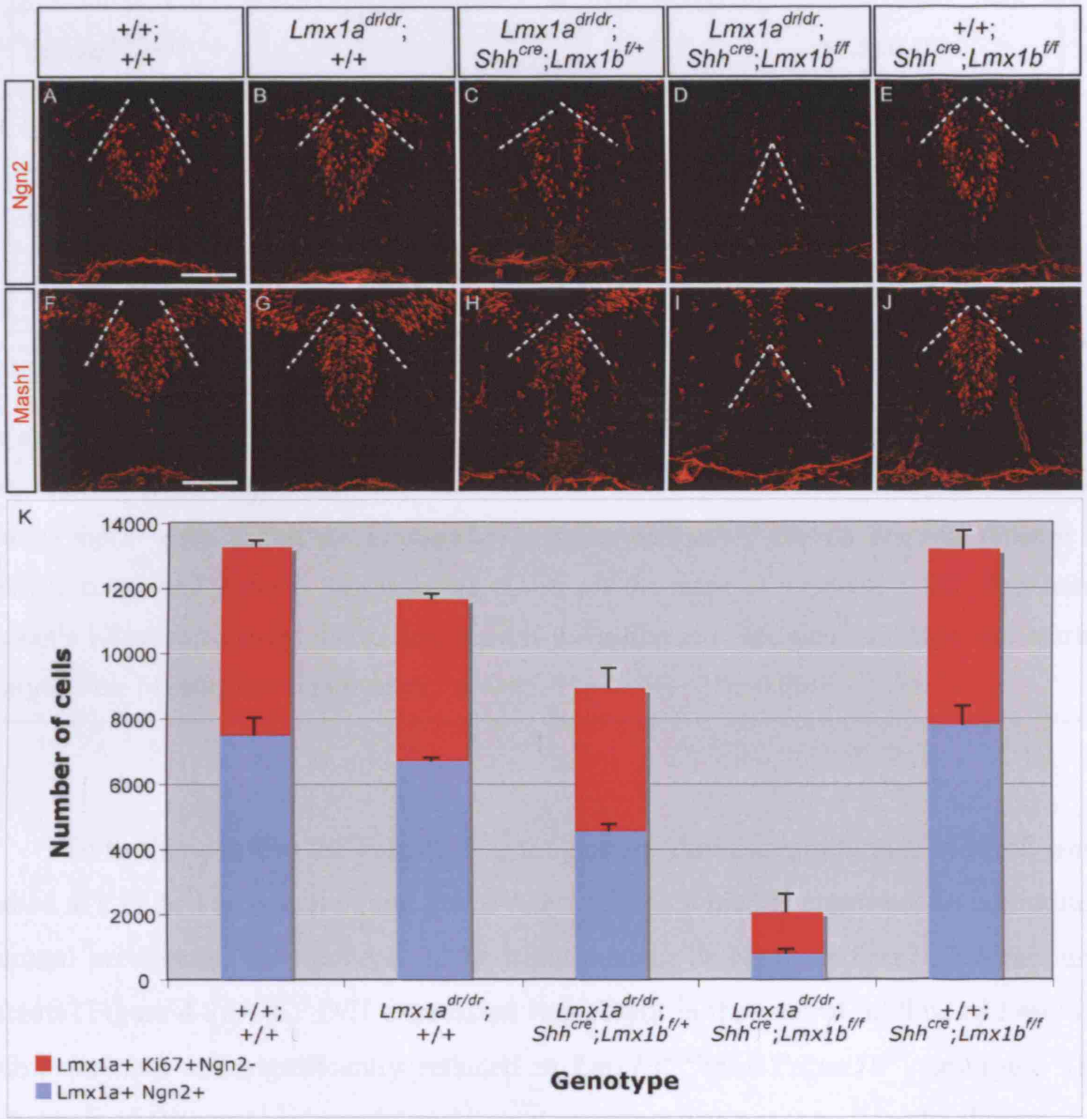

Figure 4-25 Lmx1a/b co-ordinately regulate neurogenesis.

The expression of proneural genes Ngn2 (A-E) and Mash1 (F-J) were reduced in *Lmx1a/b* compound mutants. Dashed lines mark the border of Lmx1a+ domain. (K) Quantification of Ngn2+ cells in Lmx1a+ mDA progenitor domain. The cell numbers shown are the mean ± SD of duplicate. Scale bars correspond to 100μm.

Genotype	Lmx1a+Ngn2+ cells (% compared with wild type)	Lmx1a+Ngn2+/ Lmx1a+Ki67+
+/+;+/+	7494±518 100%	56.4±0.9%
Lmx1a$^{dr/dr}$;+/+	6702±76 89.4±5.2%	57.5±0.4%
Lmx1a$^{dr/dr}$;*Shh*^{cre};*Lmx1b*$^{f/+}$	4542±195 60.6±1.6% *	50.9±2.3%
Lmx1a$^{dr/dr}$;*Shh*^{cre};*Lmx1b*$^{f/f}$	783±115 10.4±2.3% **	39.0±6.6%
+/+; *Shh*^{cre};*Lmx1b*$^{f/f}$	7812±560 104.2±14.7%	59.3±4.2%

Table 4-6 Lmx1a/b regulate Ngn2 expression.

The numbers of Lmx1a+Ngn2+ cells in *Lmx1a/b* compound mutants are reduced relative to wild type. After normalising with the reduction in mDA progenitors, the proportions of Lmx1a+Ngn2+ cells within the Lmx1a+Ki67+ mDA progenitor domain are still reduced in *Lmx1a/b* compound mutants. The numbers shown are the mean of duplicate ± SD. Two-tailed Student's t-Test was carried out to determine if the differences between wild type and mutant embryos were of statistical significance. *p<0.05; **p<0.01; ***p<0.001.

To further confirm the defects in neurogenesis, downstream targets of Ngn2 were studied at E12.5. The Notch ligand *Delta-like 1* (*Dll1*), which is expressed in committed neuronal precursors, was reduced in the same manner as Ngn2 in *Lmx1a/b* compound mutants (Figure 4-26A-E). *Dll1* expression was absent in the ventral midline of *Lmx1a/b* double mutants and significantly reduced in *Lmx1a*$^{dr/dr}$;*Shh*^{cre};*Lmx1b*$^{f/+}$ embryos. The expression of *Dll1* in *Lmx1a* and *Lmx1b* single mutants was not significantly altered.

Another Notch ligand *Delta3*, expressed in committed neuronal precursors, was almost absent in the medial mDA region of *Lmx1a/b* double mutants and reduced in *Lmx1a*$^{dr/dr}$;*Shh*^{cre};*Lmx1b*$^{f/+}$ embryos at E12.5. However, its expression was not significantly reduced in *Lmx1a* single mutant embryos (Figure 4-26F-J).

Hes5, a repressor type bHLH gene and effector of Notch signalling, which is strongly expressed in the ventricular zone of the midbrain, with the exception of the roof plate (Figure 4-26K-O), was absent in mDA region of *Lmx1a/b* double mutants. Its expression was reduced in the medial region within the ventral midline of the *Lmx1a*$^{dr/dr}$;*Shh*^{cre};*Lmx1b*$^{f/+}$ embryos, but was not significantly changed in either *Lmx1a* or *Lmx1b* single mutants.

Id proteins act as dominant-negative regulator of proneural protein by sequestering E proteins and preventing them from forming functional heterodimers with proneural proteins, thereby inhibiting cell differentiation (Yokota, 2001). *Id3*, which is expressed in the ventricular zone of the floor plate and basal plate region, was not affected in all the *Lmx1a/b* mutants (Figure 4-26P-T), indicating that the neurogenesis defect is not a result of ectopic expression of *Id3*.

From the observation that the loss of *Dll1* and *Hes5* expression in the Lmx1a/b double mutants resembles the absence of *Dll1* and *Hes5* expression described for the *Ngn2*$^{-/-}$ embryos, we can postulate that Lmx1a/b may play a role in controlling the activity of the proneural gene Ngn2 in a dose-dependent manner.

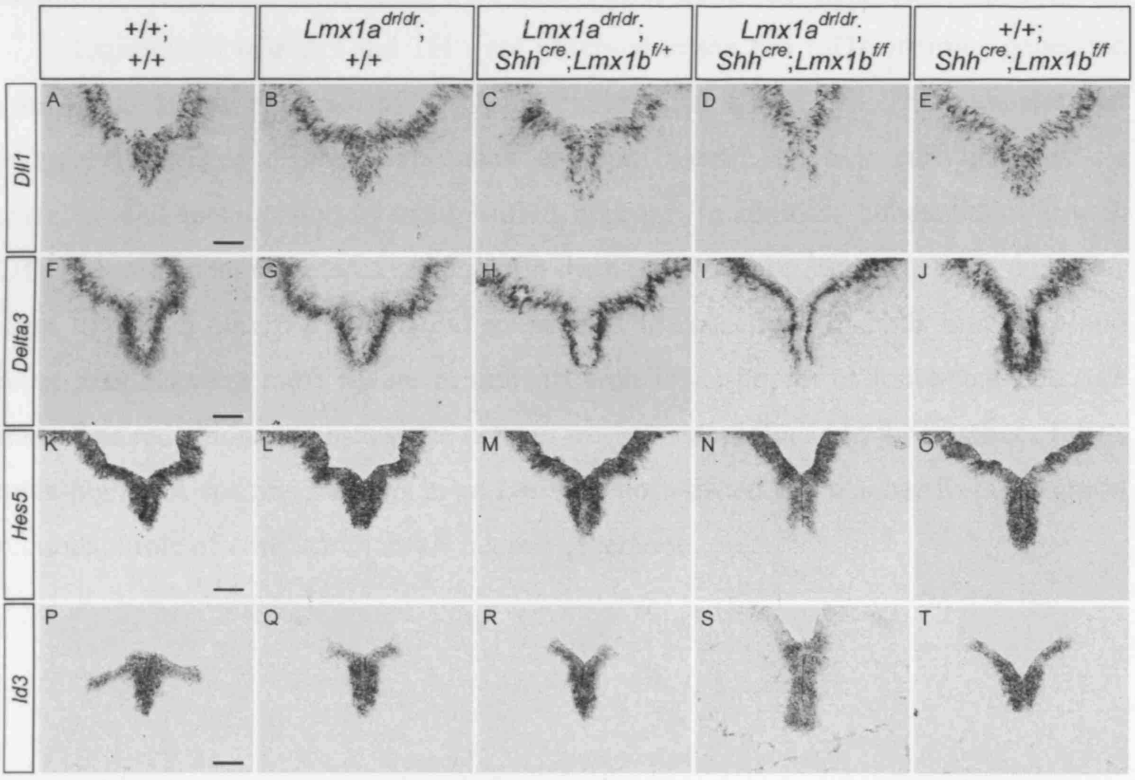

Figure 4-26 The expression of Ngn2 downstream targets are specifically lost in the mDA domain of *Lmx1a/b* double mutants at E12.5.

The expression of Notch ligands *Dll1* (A-E) and *Delta3* (F-J) and Notch effector *Hes5* (K-O) were reduced in *Lmx1a*$^{dr/dr}$;*Shh*^{cre};*Lmx1b*$^{f/+}$ embryos, and absent in the ventral midline of *Lmx1a/b* double mutants. In contrast, the expression of *Id3* (P-T), a negative regulator of proneural proteins, was maintained. Scale bars correspond to 100μm.

4.3.10 Lmx1a/b are required in a dose dependent manner for the specification of mDA neurons

Lmx1b, Nurr1 and En1 are expressed in both immature and mature mDA neurons, while Pitx3 and TH expressions are only expressed in mature mDA neurons. En1 was not only expressed strongly in postmitotic mDA neurons, but also expressed in a much lower level in the mDA progenitors and adjacent progenitors and some postmitotic neurons. In *Lmx1a/b* mutants at E12.5, postmitotic Lmx1b and *En1* expressions were reduced in the same manner as Nurr1 (Figure 4-27A-J). Likewise, the reduction in *Pitx3* was similar to that in TH (Figure 4-27K-T). Thus, all known postmitotic mDA markers analysed were clearly affected by the mutations of *Lmx1a/b*.

Expressions of *Pitx3* and TH were observed in the few mDA neurons generated in the caudal lateral midbrain of *Lmx1a/b* double mutants at E12.5. This indicates that the highly restricted residual expression of Lmx1b until E12.5 is sufficient for the generation and specification of mature mDA neurons. In addition, counterstaining with TOTO-3-iodide demonstrated a reduction in the number of postmitotic cells in the mDA region of E12.5 *Lmx1a/b* compound mutants. The reductions in both immature and mature neurons were more severe in mutants with fewer copies of functional *Lmx1a/b* alleles. The reductions in postmitotic cells in the ventral midline and the number of cells expressing mDA specific markers in an *Lmx1a/b* dose-dependent manner further support a redundant role of *Lmx1a/b* in mDA neuron generation.

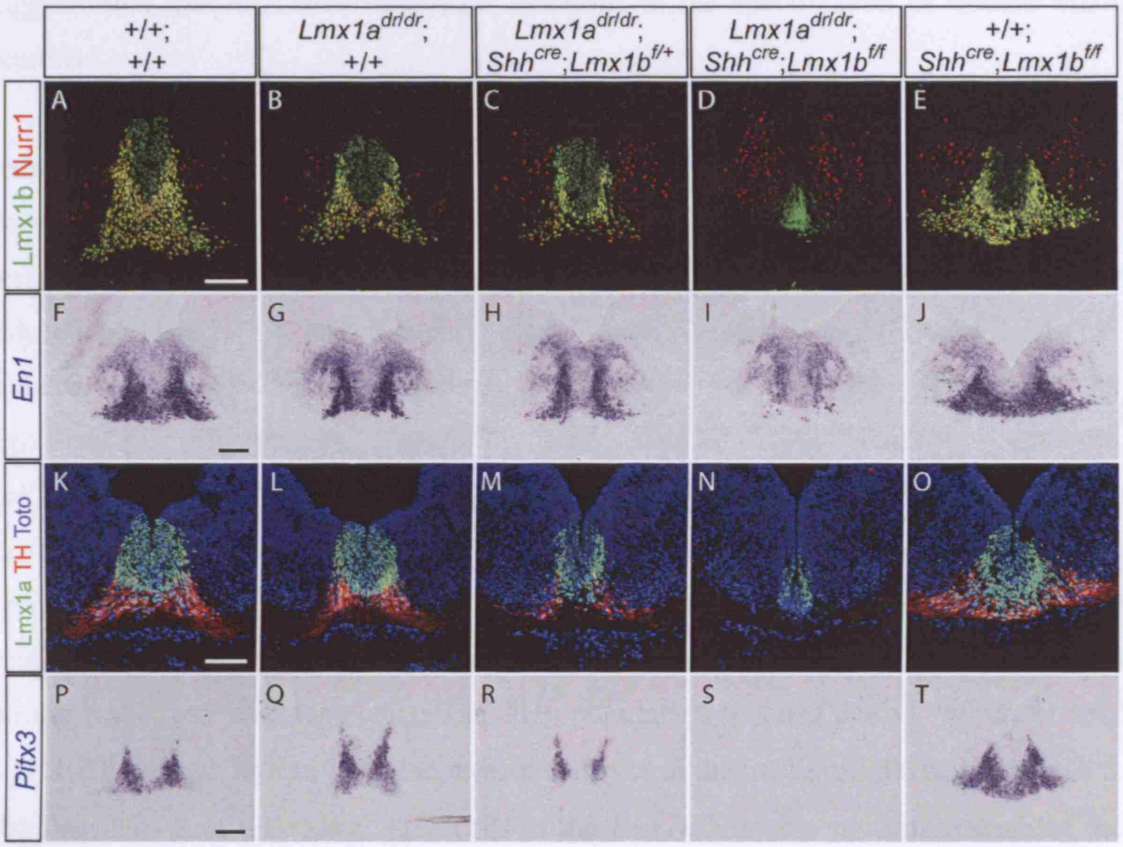

Figure 4-27 Lmx1a/b are required for the differentiation of mDA neurons.

(A-E) Nurr1 was strongly expressed in postmitotic mDA neurons. Lmx1b (A-E) and *En1* (F-J) were expressed weakly in the ventricular zone, and strongly in postmitotic mDA neurons at E12.5. (K-O) Lmx1a and TH double staining to reveal mature neurons in the mDA domain. (P-T) *Pitx3* was expressed in mature mDA neurons. Scale bars correspond to 100μm.

However, the reduction in the proportion of mature mDA neurons in *Lmx1a*$^{dr/dr}$, *Lmx1a*$^{dr/dr}$;*Shh*^{cre};*Lmx1b*$^{f/+}$ and *Lmx1a*$^{dr/dr}$;*Shh*^{cre};*Lmx1b*$^{f/f}$ embryos at E12.5 point to additional specification defects in the postmitotic neurons (Table 4-5). Some cells that had undergone neurogenesis and acquired immature mDA marker expression failed to progress with their differentiation and fail to express the mature mDA markers. Most of these cells failed to migrate ventrally from within the intermediate zone. Moreover, a minority of the Lmx1b positive cells near the edge of the mDA neuronal domain were not positive for Nurr1 in mutants with homozygous deletion of *Lmx1a*. Thus, many

postmitotic neurons were not fully specified for mDA fate. Again, the severity of mDA neuronal specification defect was enhanced by removing more *Lmx1a/b* alleles. This suggests that *Lmx1a/b* have redundant functions in the specification of mature mDA neurons.

To study if Lmx1a/b are required for the maintenance and migration of the mDA neurons as a late specification event, *Lmx1a/b* mutants were analysed at E18.5. At this stage in the wild type embryos, mDA neurons have migrated extensively to their destinations. At E18.5, the numbers of Lmx1a+TH+ neurons were still significantly reduced in $Lmx1a^{dr/dr}$ and $Lmx1a^{dr/dr}$;Shh^{cre};$Lmx1b^{f/+}$ and $Lmx1a^{dr/dr}$;Shh^{cre};$Lmx1b^{f/f}$ mutants (Figure 4-28). Nevertheless, the distributions of TH+ populations not significantly affected in $Lmx1a^{dr/dr}$ and $Lmx1a^{dr/dr}$;Shh^{cre};$Lmx1b^{f/+}$ embryos. Shh^{cre};$Lmx1b^{f/f}$ and $Lmx1a^{dr/+}$;Shh^{cre};$Lmx1b^{f/f}$ embryos displayed a similar disruption in the Li and VTA region described in section 4.3.4. Although the ventral midbrain of *Lmx1a/b* double mutants was severe reduced in size and cells in the mDA region were much less densely populated, they were able to migrate a considerable distance and in a similar fashion as wild type cells. The TH+ population spanned across 960μm in wild type and 672μm in *Lmx1a/b* double mutant embryos in the rostral caudal extent at E18.5. The distribution of the rostral TH+ cells in the *Lmx1a/b* double mutants resembled the mid-rostral VTA and SN subpopulations in wild type embryos (compare Figure 4-28M and P). This implies that the rostrally located mDA populations are generated in *Lmx1a/b* double mutants.

We then studied the identities of the TH+ cells in the *Lmx1a/b* double mutants. Raldh1 (Ahd2) is expressed in a subset of mDA neurons in the SN and in the ventral and lateral VTA (Jacobs et al., 2007). By comparing adjacent sections at E18.5, the TH+ cells in *Lmx1a/b* double mutants appeared to bias towards the *Raldh1*+ subpopulations. This suggests that the TH+ cells in *Lmx1a/b* double mutants are likely to be the SN and/or ventral and lateral VTA subpopulations.

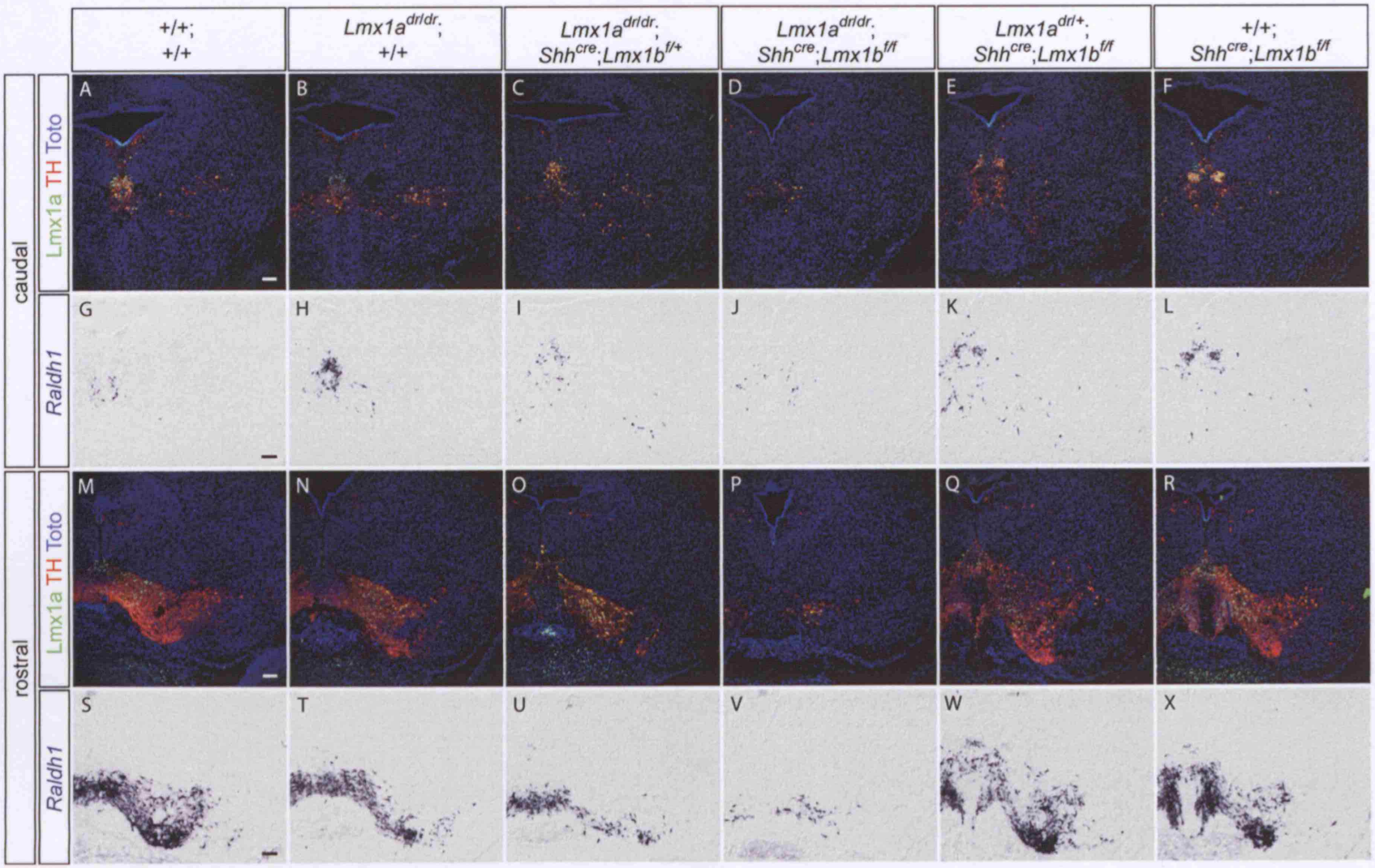
+/+; +/+
Lmx1a^dr/dr; +/+
Lmx1a^dr/dr; Shh^cre;Lmx1b^f/+
Lmx1a^dr/dr; Shh^cre;Lmx1b^f/f
Lmx1a^dr/+; Shh^cre;Lmx1b^f/f
+/+; Shh^cre;Lmx1b^f/f
caudal
rostral
Lmx1a TH Toto
Raldh1
A
B
C
D
E
F
G
H
I
J
K
L
M
N
O
P
Q
R
S
T
U
V
W
X

Figure 4-28 mDA neurons survived and migrated in *Lmx1a/b* double mutants.

(A-F, M-R) The whole mDA population was shown by Lmx1a and TH double staining at E18.5. (G-L, S-X) Raldh1 transcript was shown on adjacent sections of (A-F, M-R) to compare the subpopulation of mDA neurons in the SN and ventral and lateral VTA. Scale bars correspond to 100μm.

4.4 Discussion

4.4.1 Functional redundancy between Lmx1a and Lmx1b in mouse

4.4.1.1 Discrepancies in the function of Lmx in mDA neuron development between the mouse and chick models

Results from this study corroborate with the two recent studies showing that Lmx1a is specifically expressed in the mDA progenitors and neurons, and plays an important role in their development (Andersson et al., 2006b; Ono et al., 2007). However, there are some major discrepancies arising from the analyses performed in the chick and the mouse. In chick, transfection of Lmx1a cDNA and siRNA showed that Lmx1a is both sufficient and required for the generation of DA neurons, and that Lmx1b expressed in the mDA progenitors cannot compensate for the loss of Lmx1a (Andersson et al., 2006b). In contrast to the almost complete elimination of DA neurons by Lmx1a siRNA knockdown in chick, *Lmx1a*$^{dr/dr}$ mouse mutants only display a moderate reduction of mDA neurons [this study and (Ono et al., 2007)]. The possible reasons for the discrepancies are discussed below.

4.4.1.2 Lmx1a and Lmx1b have different potencies in mDA neuron generation

The first possible explanation for the discrepancies is that *Lmx1a* and *Lmx1b* may have different potencies in mDA neuron generation between mouse and chick, similar to that observed in the roof plate development (Chizhikov and Millen, 2004a). The severely compromised development of mDA neurons in *Lmx1b* null mutant mice indicates a more important role of *Lmx1b* over *Lmx1a* in the mouse mDA neuron development. Due to the obvious defects of the isthmus in the *Lmx1b* knockout embryos and well-documented function of Lmx1b in IsO development, we decided to use a conditional approach to investigate the specific functions of Lmx1b in mDA neuron development. In line with the down-regulation of Lmx1b expression in the mDA progenitors during mDA neuron development, *Lmx1b* is not required for the generation of mDA neurons. This argues against a cell-autonomous role of *Lmx1b* in mDA neuron development.

The importance of *Lmx1b* in mDA neuron development therefore lies in its early role in the initiation and maintenance of the inductive activity of the IsO, which patterns

the caudal midbrain and rostral hindbrain area (Guo et al., 2007). Preliminary data on double mutants of *Lmx1a*^{dr} and *Lmx1b* knockout further suggest that Lmx1a/b have an additional and redundant role in maintaining both the roof plate and floor plate of the midbrain (data not shown), underscoring the early patterning roles of Lmx1a/b.

Therefore, Lmx1b plays a non-cell-autonomous role during early embryonic development to pattern the midbrain area from the isthmus, and is required co-ordinately with Lmx1a for the integrity of the roof plate and floor plate. Similar to the chick system, Lmx1b does not play a dominant cell-autonomous role over Lmx1a during murine mDA neuron development.

4.4.1.3 *Lmx1a*$^{dr/dr}$: a potential hypomorph?

The second possible explanation is that the point mutation in the LIM1 domain of *Lmx1a*^{dr} does not act as a null allele in the generation of mDA neurons although it has been suggested to resemble the theoretical null phenotype in cerebellar development (Chizhikov et al., 2006). However, the effectiveness of this allele in cerebellar development should not be extrapolated to the mDA system.

There are controversies as to whether LIM domains influence DNA binding and the transcriptional regulation of LIM-HD proteins. LIM domain deletion in hamster Lmx1a increases transcriptional activity as seen in the yeast two-hybrid system (Johnson et al., 1997), while the LIM domains of *C. elegans* MEC-3 and rat Isl1 inhibit DNA binding (Sanchez-Garcia and Rabbitts, 1993; Xue et al., 1993). Ectopic expression of Xlim-1 carrying a LIM domain mutation more effectively initiates secondary axis formation in the ventral equatorial region of *Xenopus* embryos than the wild type Xlim-1 (Taira et al., 1994). Furthermore, the deletion of the LIM domain of Lhx3 increases the binding to and activation of mouse αGSU promoter (Bach et al., 1997; Bach et al., 1995). It has also been suggested that the LIM domains may interact with the HD to inhibit DNA-binding in the absence of a LIM binding partner, and that the inhibition is relieved by interacting with another protein (Figure 4-30) (Curtiss and Heilig, 1998). Therefore, mutation of the LIM1 domain in *Lmx1a*^{dr} allele may potentially enhance the transcriptional activity of Lmx1a.

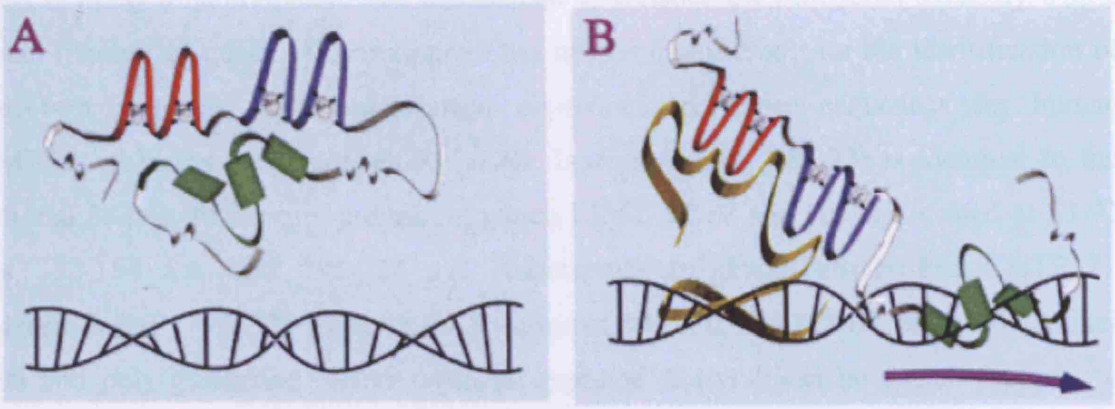

Figure 4-29 Proposed mechanisms of intramolecular interaction of the LIM and HD regions that prevent association of the HD with DNA, thus preventing transcriptional activation (Curtiss and Heilig, 1998).

On the contrary, there are also studies showing that LIM domains are essential for the function of LIM-HD. The LIM domain does not constrain DNA binding of Isl1 to the proglucagon gene promoter and functions as positive regulator of proglucagon gene transcription in the endocrine pancreas (Wang and Drucker, 1995). The LIM2 domain is absolutely required for the transcriptional activity of the *Drosophila* Lhx2 orthologue Apterous (Ap), whereas the LIM1 domain is only required for full Ap activity (Rincón-Limas et al., 2000).

Studies on the mechanisms of the actions of LIM-HD transcription factors are described in section 6.3 and summarised in Figure 6-12. In short, they regulate different target genes by either directly interacting with other transcription factors, or indirectly via the Ldb co-factors. Some of the protein interactions do not involve LIM domains. For example, a 30-residue Lhx3-binding domain on Isl1 can bind to Lhx3 in an identical manner as the LIM-interacting domain (LID) of Ldb1 (Bhati et al., 2008), and C. *elegans* MEC-3 forms heterodimer with UNC-86 via its C-terminal region (Xue et al., 1993). These uncommon interactions argue against an absolute role of the LIM domains in mediating cooperative function of LIM-HD proteins.

The differences in the ability of LIM domains to inhibit DNA binding and transactivation of target genes may have a physiological significance. Isoforms generated by alternative splicing have been identified in Lhx3 and Lhx9. The three human LHX3 isoforms display different biochemical and functional properties (Sloop et al., 1999).

This is likely a naturally evolved mechanism to enhance the functional diversity with a small number of genes. Although there has not been any report on the identification of Lmx1a/b isoforms, three unreviewed provisional reference sequences for human LMX1A isoforms are annotated in NCBI. Isoform a (NP_796372) is identical to the original 382a.a. full length protein, in which LIM1, LIM2 and HD are located at 33-92 a.a., 92-154 a.a. and 195-254 a.a. respectively (UniProtKB/Swiss-Prot Q8TE12). Isoform b (NP_796373) contains the C-terminal 133 a.a. of LMX1A where glutamine-rich and poly-glutamine regions with no reported function can be found. Isoforms c (NP_001028679) containing 100 a.a. of LMX1A, in which no functional domain has been identified.

Therefore, the requirement of a particular domain in the function of a gene cannot be generalised. The involvement of LIM domain in LIM-HD proteins appears to be highly context dependent. Thus, it is still unclear if *Lmx1a*^{dr} acts as a hypomorph in mDA neuron development until a null mutant is available.

There are a few drawbacks of using *Lmx1a*^{dr} to study the functions of Lmx1a in mDA neuron development. First, as suggested above, it may be a hypomorph. Second, it would not be possible to dissociate the ataxic phenotype from the cerebellar defects from any behavioural studies caused by the loss of DA neurons. Finally, the lengthy and arduous genotyping significantly slows down functional studies. These prompted us to consider generating a conditional *Lmx1a* mutant instead of an *Lmx1a* null mutant to study its function better.

There are two general considerations in the design of the Lmx1a conditional allele. Firstly, the removal of LIM domain may enhance transcriptional activity of some LIM-HD protein, including Lmx1a (Johnson et al., 1997), or it may prevent protein-protein interactions (German et al., 1992). Secondly, although the removal of the HD should eliminate the DNA binding ability and thus the transcriptional activity of Lmx1a, it is unclear if the truncated protein is able to perform other functions independent of its DNA binding ability, such as affecting the formation of transcriptional complex of other proteins. Therefore, it would be best to prevent the formation of the whole Lmx1a protein instead of removing the well-characterised functional domains such as the LIM domain or HD for unambiguous loss of function studies.

4.4.1.4 Lmx1a and Lmx1b play redundant roles in mDA neuron generation

The third possible explanation is that Lmx1a and Lmx1b may have redundant functions in mDA neuron development due to their sequence homology and overlapping expression patterns. There are many examples of functional redundancy between the LIM-HD pairs in the developing embryos. Lhx3/4 coordinately control the differentiation of a spinal motor neuron subtype (Sharma et al., 1998). The proliferation defects in Rathke's pouch is dependent on the gene dosage of Lhx3/4, and Lhx3 plays a more dominant role (Sheng et al., 1997). Lhx1/5 also play redundant roles in the differentiation of Purkinje cell differentiation in the developing cerebellum and the maintenance of GABAergic neurotransmitter phenotype in the dorsal interneurons of the spinal cord (Pillai et al., 2007; Zhao et al., 2007).

Mutational studies on different dosage of *Lmx1a/b* genes clearly demonstrate that Lmx1a/b are required in a gene dosage dependent manner during the mDA neuron development. Lmx1a plays more important roles in most, if not all, of the mDA neuron specification and differentiation processes. Although the expression of Lmx1b is not restricted to mDA progenitors prior to mDA neuron generation and is also downregulated during the development of mDA neurons, it is sufficient to partially compensate for the loss of Lmx1a in mDA neuron development.

The inability of Lmx1b to fully compensate for the loss of Lmx1a may be due to a requirement of cofactor(s) for the function of Lmx1a in mDA neuron development. The transcriptional regulation of LIM-HD proteins is highly dependent on (1) the interaction with other factors that bind to the same target gene, (2) specific co-factors or co-repressors that bind to the LIM domain and possibly other domains, and (3) the presence of other factors competing for co-factor binding. Since the amino acid sequences of LIM1 and LIM2 domains are only 67% and 83% identical respectively, Lmx1a and Lmx1b may bind to different cofactors and/or co-repressors, or may have different affinities to the factors involved in mDA neuron development. Therefore, identifying factors that interact with Lmx1a and Lmx1b for the development of mDA neurons will greatly enhance the understanding of this process. Taken together, there is partial functional redundancy between Lmx1a/b in the development of mDA neurons.

4.4.2 Lmx1a/b in mDA progenitor specification

4.4.2.1 Lmx1a/b redundantly regulate the expression of mDA progenitor marker *Msx1*

The specification of mDA progenitors is now better understood when two mDA progenitor specific markers Lmx1a and Msx1 were identified during the preparation of this thesis (Andersson et al., 2006b). Lmx1a is the only gene specifically expressed in the whole dorsoventral extent of mDA progenitor domain. The expression of Msx1 is excluded from the lateral mDA progenitors. Using *Lmx1a/b* compound mouse mutants, we show that Lmx1a/b are required for the expression of *Msx1*, thus the specification of mDA progenitors, in a redundant manner. In chick, Lmx1a is both sufficient and required for the expression of Msx1, and Lmx1b expression in the mDA progenitors is not able to compensate for the loss of Lmx1a (Andersson et al., 2006b). Unlike the unique role of Lmx1a in the mDA progenitor specification in chick, a single copy of either *Lmx1a* or *Lmx1b* is sufficient for *Msx1* expression in mouse.

This may be due to the identical HD in Lmx1a and Lmx1b proteins; therefore, they can bind to the same transcriptional targets. It will be interesting to know if the functional domains of chick Lmx1a and Lmx1b are more divergent than in mouse that lead to the inability of Lmx1b to compensate for the lack of Lmx1a. The overall amino acid sequences between mouse and chick Lmx1b are 88% identical, with 98% identity in LIM1 domain, 96% identity in LIM2 domain and 100% identity in HD, indicating that Lmx1b is highly conserved between the two species. Unfortunately, the sequence of chick Lmx1a is not available to answer this question. One has to note that there has not been any evidence from the literature that Lmx1a/b can bind to *Msx1* regulatory sequences. Thus, it remains unclear if Lmx1a/b directly regulate Msx1 expression.

Alternatively, Msx1 may be indirectly regulated by Lmx1a/b. Msx1 has been shown to be regulated by the Bmp pathway (Bei and Maas, 1998; Suzuki et al., 1997). Overexpression studies in the chick dorsal spinal cord show that the ability of Lmx1a/b to induce Msx1/s expression is dependent on Bmp signalling (Chizhikov and Millen, 2004a). In the roof plate of $Lmx1a^{dr/dr}$ mutants, elements of the Bmp signalling pathway *growth differentiation factor 7* (*Gdf7*) and *bone morphogenetic protein 6* (*Bmp6*) are lost 2 days before the disappearance of *Msx1* expression (Millen et al., 2004). However, in the ventral midbrain *Lmx1a/b* double mutants, *Msx1* expression is absent, while *Bmp7*

expression is maintained. This implies that the presence of *Bmp7* is insufficient to maintain the expression of *Msx1* in the midbrain.

4.4.2.2 Lmx1a/b regulate the expression of *Wnt1* in lateral mDA progenitors

The role of Lmx1b in regulating *Wnt1* expression is well-documented. Lmx1b maintains the expression of *Wnt1* in the mouse isthmus (Guo et al., 2007). Misexpression of Lmx1b in the chick dorsal midbrain can induce ectopic Wnt1 expression independent of Fgf8 (Matsunaga et al., 2002). Overexpression of Lmx1b in the chick dorsal spinal cord also induces the expression Wnt1 (Chizhikov and Millen, 2004a). On the other hand, the $Lmx1a^{dr/dr}$ mutation does not abolish the expression of Wnt1 in the roof plate (Millen et al., 2004). These all point to a unique role of Lmx1b in the regulation of Wnt1 expression.

Surprisingly, we were not able to detect a loss of *Wnt1* expression in the ventral midbrain in the *Lmx1b* conditional mutant at both E10.5 (Figure 4-25) and E12.5 (data not shown). The expression of *Wnt1* in lateral mDA progenitors is only lost in regions where both Lmx1a/b were non-functional in the double mutant. Moreover, gain-of-functions studies in the mouse have shown that both Lmx1a and Lmx1b are able to induce the expression of *Wnt1*, where the induction by Lmx1b is more potent (W. Lin, unpublished data). These data suggest that unlike in other regions of the CNS, the expression of *Wnt1* in the ventral midbrain is co-ordinately regulated by both Lmx1a and Lmx1b in a cell autonomous manner. While Wnt1 is shown to regulate the proliferation of DA precursors *in vitro* (Castelo-Branco et al., 2003), its *in vivo* function(s) in the lateral mDA progenitor domain have not yet been documented.

4.4.2.3 Is there a change in progenitor fate?

We have established that the fate of mDA progenitor is not correctly specified by demonstrating a loss of *Msx1* expression in *Lmx1a/b* double mutants. Misexpression of Msx1 has been shown to suppress the expression of Nkx6.1 in the chick ventral midbrain progenitors, and Nkx6.1 is required for the generation of motor neurons (Andersson et al., 2006b). Since Msx1 functions to suppress alternative cell fate in the mDA progenitor domain, a loss of Msx1 in the Lmx1a/b may induce a switch of progenitor cell fate. Preliminary data showed that Nkx6.1 did not appear to have expanded (Figure 6-6), but this requires further confirmation.

4.4.3 The role of Lmx1a/b in the proliferation of mDA progenitors

Our data strongly indicate a role for Lmx1a/b in regulating the proliferation of mDA progenitors in a gene dosage-dependent manner, in which Lmx1a plays a more important role. However, neither Lmx1a nor Lmx1b alone have been previously shown to promote proliferation. Lmx1b overexpression does not alter cell proliferation in neural progenitors in both chick and subdissected E9.25 mouse neural tubes *in vitro* (Chizhikov and Millen, 2004a). Contrary to a role in promoting proliferation, the proliferation rate of the spinal cord roof plate progenitors was found to be threefold higher in *Lmx1a*$^{dr/dr}$ mutant embryos (Chizhikov and Millen, 2004b). Moreover, overexpression of *Lmx1a* in chick spinal cord withdraws neural progenitors from the cell cycle with at least 18 hours of delay, and does not alter the cell fate of the differentiated cells (Chizhikov and Millen, 2004b).

These context dependent and delayed effects have led us to speculate that Lmx1a/b may play an indirect role in proliferation. Gain- and loss-of-function of Lmx1a and Lmx1b have been shown to alter the expressions of the Bmps and Wnt1 (Chizhikov and Millen, 2004b; Guo et al., 2007; Matsunaga et al., 2002; Millen et al., 2004). These pathways integrate to regulate the balance of proliferation and differentiation of neural progenitors, in which BMP antagonises Wnt-dependent proliferation, whereas Wnt counteracts BMP-dependent neuronal differentiation in the spinal cord progenitors (Ille et al., 2007).

4.4.3.1 Lmx1a/b may regulate the proliferation of mDA progenitors via *Wnt1*

The loss of *Wnt1* expression in *Lmx1a/b* double mutants may correlate to the strong proliferation defects in these embryos. Wnt1 has been shown to promote the proliferation of mDA precursors *in vitro* and spinal cord precursor cells (Castelo-Branco et al., 2003; Dickinson et al., 1994; Megason and McMahon, 2002). Conversely, misexpression of Lmx1b in the dorsal midbrain induces Wnt1 expression and causes enlargement of the midbrain (Adams et al., 2000; Matsunaga et al., 2002).

The mitogenic Wnt1 activity in the CNS is transduced through β-catenin, a nonredundant signalling component in the canonical Wnt signalling pathway (Megason and McMahon, 2002). β-catenin has been shown to control the proliferation of neuronal progenitors in the CNS (Chenn and Walsh, 2002; Zechner et al., 2003). Moreover, the

canonical Wnt pathway also promotes proliferation and maintenance of retinal progenitor cells in post-embryonic *Xenopus* (Denayer et al., 2008).

Transfection of dominant active β-catenin in the chick spinal cord upregulates transcription of the G1 cyclins (cyclin D1 and cyclin D2) but not the G2/M cyclins (cyclin A1 or cyclin B3) in neural precursors (Megason and McMahon, 2002). In addition, the β-catenin/LEF-1 complex binds to the LEF-1 consensus sequence of the cyclin D1 promoter in electrophoretic mobility shift assays (Shtutman et al., 1999). These suggest that the effects of Wnt signalling on proliferation and cell cycle regulation are mediated through β-catenin signalling.

Despite the loss of *Wnt1* expression, the expression of *axin2*, which is a direct target and negative regulator of the canonical Wnt signalling pathway, is maintained in *Lmxa/b* double mutants. This indicates that canonical Wnt signalling is not disrupted in the mDA region, and argues against a major contribution in the proliferation defects of *Lmx1a/b* double mutants. The persistence of canonical Wnt signalling may be attributed to the presence of other Wnt protein such as Wnt3a in the region. Therefore, it is also necessary to investigate the expression of other members of the Wnt signalling pathway.

Although the expression of axin2 is a good indication of the presence of canonical Wnt signalling in the mDA region of *Lmx1a/b* double mutants, we wonder if a reduction in the level of canonical Wnt signalling is related to the strong reduction in proliferation in mDA progenitors. We are in the process of testing if constitutive expression of β-catenin can rescue the proliferation defects in the *Lmx1a/b* double mutants. The serines and threonine in β-catenin, encoded by exon 3, are phosphorylated by glycogen synthase kinase 3β (GSK3β) leading to the degradation of β-catenin. This can be conditionally removed by Cre recombinase to generate stabilised β-catenin proteins (β-catCA) (Harada et al., 1999). By introducing a β-catCA allele into the *Lmx1a/b* double mutant background, canonical Wnt signalling will be constitutively activated in the same cells where Lmx1b is non-functional.

4.4.3.2 *Lmx1a/b* mutants have Wnt1-independent proliferation defects

It remains unclear whether canonical Wnt signalling is responsible for the proliferation defects in *Lmx1a/b* double mutant. The presence of *Wnt1* expression in these mutants combined with the gene-dosage dependent effects of Lmx1a/b on the

proliferation of the mDA progenitor cells is suggestive that Lmx1a/b may play a more prominent role, possibly independent to Wnt1 function.

Besides Lmx1a/b, Lhx2 has also been shown to be required for proliferation in the forebrain (Ando et al., 2005; Porter et al., 1997). To date, no mechanism has been suggested for the regulation of proliferation by LIM-HD. From the changes in the cell cycle regulators cyclin D2 and p27 in Lmx1a/b double mutants, the simplest model is a direct regulation of these genes by the transcription factors Lmx1a/b, possibly in conjunction with other co-factors. This can be verified by chromatin immunoprecipitation (ChIP). Other targets of Lmx1a/b, related to cell cycle regulation, can be obtained by combining ChIP with microarray technology (ChIP-on-CHIP). Moreover, performing a thorough survey on the effect of *Lmx1a/b* mutations on cell cycle regulators will be necessary.

In addition, the roles of *Lmx1a/b* in proliferation and cell cycle regulation can be studied by gain-of-function studies to investigate if Lmx1a/b are sufficient to induce proliferation. However, chick ventral midbrain and dorsal spinal cord electroporated with Lmx1a do not show aberrant tissue growth (Andersson et al., 2006b; Chizhikov and Millen, 2004b). With the discrepancies in mDA neuron development between mouse and chick models in mind, the inability of Lmx1a to induce proliferation may not apply to mouse. This can be verified by performing gain-of-function studies in various part of the mouse neural tube including the ventral midline of the midbrain. Since the ability of Lmx1a to control proliferation is affected by a point mutation disrupting the protein interacting LIM domain, the presence of co-factors or co-repressors of Lmx1a/b at the right stoichiometry for the proper complex formation may also be critical.

4.4.4 Lmx1a/b regulate the neurogenesis of mDA progenitors

Our results concur with the mild neurogenesis defects reported in *Lmx1a* single mutants (Ono et al., 2007), and further provide evidence that Lmx1a/b are indispensable in the neurogenesis of mDA progenitors by regulating Ngn2 expression in a redundant manner. Although the other proneural protein Mash1 in mDA progenitor domain is affected in the same manner as Ngn2 in Lmx1a/b mutants, we were not able to dissociate if the reduction in Mash1 was directly affected by Lmx1a/b or as a consequence of the loss of Ngn2. In order to answer this question, we will need to investigate if Ngn2 is able to rescue Mash1 expression in these mutants, or to show whether Mash1 is a direct target of Lmx1a/b.

4.4.4.1 Lmx1a/b regulate the expression of Ngn2

Ngn2 is the major proneural gene required for the differentiation of mDA progenitors (Andersson et al., 2006a; Kele et al., 2006). By showing that Lmx1a is sufficient and required for the expression of Msx1 in chick and that premature expression of Msx1 is sufficient to induce Ngn2 expression and neuronal differentiation in the mouse ventral midbrain, Andersson et al. proposed a genetic cascade where Lmx1a regulate Msx1, which in turn regulate Ngn2 to promote neuronal differentiation (Figure 4-30) (Andersson et al., 2006b).

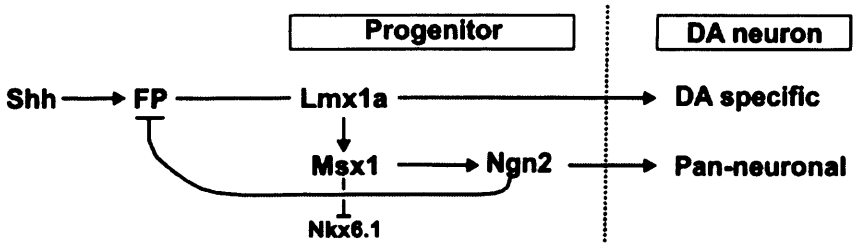

Figure 4-30 Model of DA neuron specification.

Shh induces floor plate (FP) cells and Lmx1a. The induction of Lmx1a may be indirect. Lmx1a, in turn, induces Msx1 in DA progenitors and activates DA cell-specific properties in differentiating cells. Msx1 suppresses Nkx6.1 and alternative cell fates and induces Ngn2 expression. The Msx1 mediated induction of Ngn2 results in the suppression of FP characteristics and induction of panneuronal differentiation. Since Lmx1a only induces DA neurons in the ventral progenitors, it is likely that ongoing Shh signalling, or a Shh-induced activity, operates in parallel to Lmx1a (Andersson et al., 2006b).

This model is likely to represent a simplified scenario that may not be entirely applicable to the mouse model. Firstly, unlike the loss of Msx1 expression in chick Lmx1a knockdown experiments (Andersson et al., 2006b), *Msx1* expression and the progenitor identity are not affected in *Lmx1a* single mutant (this study). Secondly, in *Msx1* knockout mouse embryos, there is only a 40% reduction in the number of Ngn2+ progenitors and Nurr1+ DA neurons, and Nkx6.1 expression is not completely extinguished (Andersson et al., 2006b). The authors attributed these to the presence of Msx2 and Lmx1a in the DA progenitors. In view of this, we have recently obtained Msx1/2 double mutant embryos from B. Robert verify this. Thirdly, our results show that the expression of Ngn2 is related to the gene dosage of Lmx1a/b. Although Lmx1a clearly plays a more important role in regulating the expression of Ngn2, its expression is only abolished in the medial mDA domain of *Lmx1a/b* double mutants. Lastly, Msx1 expression is maintained in $Lmx1a^{dr/dr}$ and $Lmx1a^{dr/dr}$;Shh^{cre};$Lmx1b^{f/+}$ mutants that also display reduction in Ngn2 expression, although the absence of Msx1 expression in Lmx1a/b double mutant correlates with a much more severe reduction in Ngn2 expression. These suggest that Lmx1a/b co-ordinately regulate the expression of Msx1, which serves as an important regulator for the neurogenesis in mDA progenitors, and that Lmx1a/b may also regulate Ngn2 expression through an Msx1-independent mechanism.

4.4.4.2 Does Lmx1a/b cooperate with Ngn2?

Besides regulating the expression of Ngn2, there is also a possibility that Lmx1a/b may cooperate with Ngn2 to promote mDA neuron differentiation. Lmx1a has been shown to specifically interact with the bHLH protein E47 but not with Mash1, NeuroD and Id1, and synergistically activate insulin I enhancer *in vitro* (Johnson et al., 1997; Ohneda et al., 2000). From this information, we can speculate that Lmx1a/b may synergistically promote mDA neuron differentiation by interacting with the bHLH protein Ngn2 or a heterodimer of Ngn2:E47. Therefore, it will be interesting to investigate if Lmx1a/b can bind to Ngn2 or Ngn2:E47 complex, and synergistically activate DA specific markers.

Alternatively, Lmx1a/b may form complexes mediated by Ldb as suggested by the enhancement of *in vitro* transcriptional activity of Lmx1a by cotransfection of Ldb1 (Andersson et al., 2006b). Lmx1a, Ldb1 and Ngn2 may be able to form a high order

complex similar to Figure 6-12C to synergistically promote mDA neuron differentiation, where additional factors may also by involved.

4.4.5 Lmx1a/b regulate the terminal differentiation of mDA neurons

We have shown that the differentiation into TH expressing mature mDA neurons is more severely affected than the differentiation into Nurr1 positive immature neurons. In the absence of Lmx1a, some prospective mDA neurons in the lateral region have been found to have mixed identities by expressing the mDA marker Nurr1 and ectopically expressing Lhx1/5 at the same time [data not shown and (Ono et al., 2007)]. These cells fail to express the mature mDA markers Pitx3 and TH (Ono et al., 2007). In addition, Nurr1 and TH expression can be induced by overexpressing Lmx1a or Lmx1b into the ventral midbrain where Foxa2 is expressed (W. Lin, unpublished data). This implies that Lmx1a/b control the expression of late mDA neuronal markers independent of neurogenesis.

4.4.5.1 Lmx1b is not required for *Pitx3* expression in a cell autonomous manner

Lmx1b has been proposed to regulate the expression of Pitx3 in a previous *Lmx1b* knockout study (Smidt et al., 2000). However, these mutants lose Wnt1 expression prior to 4-somite stage, lack a functional IsO (Guo et al., 2007), and display a very similar phenotype as the *Wnt1*$^{-/-}$ mutant (Prakash et al., 2006; Simon et al., 2003). Using an *Lmx1b* conditional mutant with a functional IsO, we demonstrated that Lmx1b is not required for the expression of Pitx3 in a cell autonomous manner. Furthermore, *Pitx3* expression was observed in the mature mDA neurons in all mutants with different gene dosage of *Lmx1a/b*. This is further supported by the strong expression of Raldh1, whose expression is severely affected by Pitx3 deficiency (Jacobs et al., 2007), in all the *Lmx1a/b* mutants. Unfortunately, we were unable to obtain a Pitx3 antibody to verify if Pitx3 is expressed in all TH+ neurons or if it is partially lost. Moreover, it was not possible to determine whether Lmx1a/b are redundantly required for the expression of *Pitx3* because mature mDA neurons were not generated where both *Lmx1a/b* genes were non-functional. Therefore, we only provide evidence to argue against a direct regulation of Pitx3 by Lmx1b in the genetic cascade for mDA neurons development.

4.4.5.2 Do Lmx1a/b suppress an alternative fate?

The expression of LIM-HD has been shown to be important in distinguishing between cell fates of motor neuron and interneuron in the vertebrate spinal cord. The loss of Lhx3/4 shifts the cell fate of motor neurons from ventrally to dorsally projecting motor neuronal subtypes (Sharma et al., 1998). The presence and absence of Isl1 in the ventral spinal cord distinguishes MNs from V2 interneurons (Thaler et al., 2002).

However, in the mDA system, only very few cells with mixed identities were observed in the lateral postmitotic mDA region in the absence of Lmx1a, and this was not detected in Lmx1b conditional mutants. These may imply that Lmx1a/b do not act as a binary switch between alternative cell fate in the ventral midbrain. A possible explanation is that this is a consequence of the compensation between the two closely related Lmx1a and Lmx1b.

In the *Lmx1a/b* double mutant, there appears to be some postmitotic neurons situated near the ventral midline that do not express any mDA mature and immature neuronal markers. Due to the time constrain and the difficulty in obtaining double mutant embryos, we have not yet investigated if these very few postmitotic neurons have switched to adjacent cell fates of either Isl1+ oculomotor neurons or Brn3a+ red nucleus neurons. If there is a fate switch in these postmitotic neurons, it is likely due to a role of Lmx1a/b in specifying the postmitotic cell fate because our preliminary data have ruled out the expansion of adjacent Nkx6.1 or Nkx2.2 expression into the ventral midline (Figure 6-6). However, in the *Lmx1a/b* double mutants, it will not be possible to pinpoint the role of Lmx1a/b in termination differentiation of mDA neurons due to the loss of mDA progenitor identities and the expression of Ngn2, which plays a role in mDA neuronal cell fate specification (Kele et al., 2006).

An alternative explanation is the timing of Lmx1b deletion by ShhCre, as hinted by the expression of Lmx1b and the phenotype in the Lmx1b null mutants. The Lmx1b expression is detected in the anterior embryo in the early head fold stage at E7.5 and in the presumptive midbrain hindbrain boundary region at E8.5 (Guo et al., 2007). From the characterisation of ShhCre mouse line in chapter 3, β-gal protein only started to be detected weakly at E9.0 and strongly at E9.5. It is conceivable that if Lmx1b protein ceases to be produced from E9.0, it may not be entirely eliminated when the earliest neurons are born from around E9.5 (Bayer et al., 1995). It would be very useful if we can

produce an antibody that can distinguish the normal Lmx1b protein from the truncated one to establish the timing for the elimination of Lmx1b protein.

In the Lmx1b null mutant, there is a strong reduction in TH+ mDA neurons, almost complete lost of Isl+ oculomotor neurons and a ventral expansion of Brn3a+ red nucleus neurons (Figure 6-7). Although the phenotype of this mutant is complicated by a disrupted IsO, this observation gives us an idea that loss of Lmx1b may directly or indirectly lead to a switch to alternative fate.

4.4.5.3 Do Lmx1a/b play a role in mDA neuron migration?

Due to the postnatal lethality of *Lmx1a/b* double mutants, the late phenotype of *Lmx1a/b* mutants was examined at E18.5. The migrations of mDA neurons in *Lmx1a* and *Lmx1b* single mutants grossly normal. It is surprising that the very few TH+ neurons generated in the *Lmx1a/b* double mutants are able to migrate to populate the ventral midbrain in a similar pattern as the wild type embryos despite the severe reduction in cell density. This is suggestive that neither Lmx1a/b play a role in the migration of mDA neurons. However, Lmx1b is not completely deleted in the caudolateral midbrain on or before E12.5. This has raised two interesting questions. Are the TH+ cells generated in the rostral midbrain where both Lmx1a/b are non-functional? Alternatively, are these cells generated from the caudolateral midbrain where functional Lmx1b protein is expressed briefly during early mDA neuron development, and migrate extensively to the rostral midbrain?

It is currently not possible to answer these questions from the analysis of marker gene expression. Therefore, we have tried to introduce the R26RLacZ reporter allele into *Lmx1a/b* double mutants to understand if Cre recombinase has been active in the TH+ cells. $Lmx1a^{dr/+};Shh^{cre};Lmx1b^{f/+}$ mice were crossed with R26RLacZ mice to generate $Lmx1a^{dr/+};Shh^{cre};Lmx1b^{f/+}$;R26RLacZ males. These males were then crossed with $Lmx1a^{dr/+};Lmx1b^{f/f}$ females to generate $Lmx1a^{dr/dr};Shh^{cre};Lmx1b^{f/f}$;R26RLacZ double mutants with a LacZ reporter. However, due to the extremely low frequencies of $Lmx1a^{dr/dr};Shh^{cre};Lmx1b^{f/f}$;R26RLacZ embryos, no embryo of the correct genotype has been collected so far. Therefore, the origin of the mDA neurons in *Lmx1a/b* double mutants remains unresolved.

Additionally, the examination of the sole *Lmx1a/b* double mutant at P28 will provide information on whether the TH+ neurons are able to survive postnatally. This

will allow the identification of the mDA subpopulations using the markers Calbindin and Girk2.

4.4.5.4 Do Lmx1a/b play a role in axon pathfinding in mDA neuron?

Axon pathfinding represents the most frequently reported function of LIM-HD proteins from *C. elegans*, *Drosophila* to mice. This study focuses on the role of Lmx1a/b in the molecular specification of mDA. Because of the important roles of Lmx1a/b in the early progenitor and postmitotic neuron specification events, it is not possible to study the specific function of Lmx1a/b in the late event of axon pathfinding with the mutant mice used in this study. The generation of Lmx1a/b conditional mutants where these genes are deleted in postmitotic neurons will be ideal to answer this question. However, it appears that neurons start to extend processes soon after they have exited the cell cycle. Therefore, Nestin-Cre, which is active in the progenitor cells from about E10.5, is a good candidate for this purpose. Otx2 and Foxa2 are inactivated in the ventral midbrain region between E11.5 and E12.5 in Nestin-Cre driven conditional deletion of Otx2 and Foxa2 respectively (Ferri et al., 2007; Vernay et al., 2005). By further introducing R26RLacZ alleles to the mutants, the mutant cells can be located. Furthermore, the trans-synaptic neural pathways can be visualised by introducing a reporter carrying the plant lectin wheat germ agglutinin to study whether the neural pathways are affected (Farago et al., 2006; Yoshihara et al., 1999).

4.4.6 The LIM code

LIM-HD transcription factors are widely expressed in the central nervous system. Their differential and combinatorial expression patterns correlate with distinct neuronal populations. The dorsal interneurons of the spinal cord can be distinguished by the differential expression of LIM-HD proteins (Helms and Johnson, 2003), and each motor neuronal subtype in the ventral spinal cord expresses a unique combination of LIM-HD proteins (Tsuchida et al., 1994). A similar LIM-HD code has been proposed to control the development of the forebrain (Bachy et al., 2002; Nakagawa and O'Leary, 2001).

LIM-HD code has not been described in the developing midbrain. We have shown that mDA neurons, oculomotor neurons and the rest of the neurons in the basal plate express Lmx1a/b, Isl1 and Lhx1/5 respectively. Lhx2 is expressed in the outer layers of dorsal midbrain (Porter et al., 1997). Lhx3 appears to be expressed in the dorsal midbrain (Bach et al., 1997). Lhx4 appears to be expressed in the oculomotor neurons (Li et al., 1994). Lhx6, 7 and 9 are not expressed in the midbrain of E10.5 mouse embryos (Failli et al., 2000; Grigoriou et al., 1998). Therefore, a detailed study of the expression patterns of all LIM-HD proteins will be necessary to understand if a LIM-HD code exits in the midbrain.

The differential expression of Lmx1a/b in the mature mDA neurons had led us to hypothesize that Lmx1a/b might specify different subpopulation of mDA neurons. However, specific loss of anatomically distinct mDA subpopulations could not be detected in *Lmx1a*$^{dr/dr}$ and *Lmx1b* conditional mutants. This has to be confirmed by the analysis of postnatal expression of mDA subpopulation specific markers Girk2 and Calbindin.

Chapter 5
Conclusions and future perspectives

The degeneration of the pigmented dopaminergic neurons in the substantia nigra pars compacta of the midbrain is the hallmark of Parkinson's disease. The quest for restorative cell replacement therapies for this debilitating neurodegenerative disease has led to intensive research in the generation of these neurons from embryonic stem cells. This requires a thorough understanding of the development of these neurons from their origin to specification in the embryonic brain.

Despite a constantly improving understanding on the origin of these neurons by indirect inference and speculations on the origins of their subpopulations, the exact origin of the mDA neurons and their subpopulations in the embryonic brain had not yet been demonstrated when this study began. Similarly, the early induction of mDA neurons by the diffusible molecules Shh, Fgf8, Wnt1 and TGF-β, and the roles of several factors, such as Lmx1b, En1/2, Nurr1 and Pitx3, on their development have been documented prior to this study. Yet, the specific determinants for early specification of mDA neurons appeared to remain unidentified for two reasons. First, Lmx1b and En1 are required for the maintenance of a functional isthmic organiser, which is the source of Fgf8 and Wnt1. Second, Nurr1 and Pitx3 are only expressed in postmitotic neurons. Of these factors, Lmx1b has a transient but specific expression in the presumptive mDA progenitor region. Therefore, this study aimed at: (1) identifying the origin of mDA neurons and their subpopulations by genetic fate mapping studies, and (2) examining the specific roles of Lmx1b and the other family member of the same family, Lmx1a, in mDA neuron specification.

Here we provide direct evidence that the mDA neurons are exclusively derived from the floor plate with a LacZ reporter mouse line of Arx, which is specifically expressed in the ventricular zone of the floor plate. This argues against a previously proposed model that mDA neurons are generated from both the floor plate and basal plate. A floor plate origin has also been suggested by two independent groups studying Lmx1a and Corin during this study. However, neither of these studies was able to show a direct lineage relationship between floor plate and mDA neurons.

Without a suitable mouse line, we can only provide indirect evidence to suggest that the anterior limit of mDA progenitors lies at the boundary between the rostral and caudal diencephalon using a transgenic Lmx1aCre mouse line, in which there is no Cre activity in the midbrain and caudal diencephalon. We therefore suggest the prospect of providing stronger evidence by using specific midbrain and caudal diencephalic enhancers shown to be present in *Shh* and *Wnt1* genes or a prospective mDA specific enhancer in *Lmx1a* gene. Incorporating the data from a study showing that cells originate from the mid-hindbrain boundary do not become mDA neurons, we suggest that mDA neurons are generated from the floor plate of the midbrain and caudal diencephalon.

We have tested the hypothesis that different subpopulations of mDA neurons are derived from genetically and spatially distinct progenitors. We show that mDA progenitors display differential expression of Bmp7, Msx1, Raldh1 and Wnt1, as well as a mild difference in the level of Arx. Within a small window, a narrow medial group of progenitors expressing Shh can be labelled from around E8.0 to E8.5 by tamoxifen induced fate mapping using the ShhCreER^{T2} mouse line. These early-labelled cells can generate mDA neurons in all the anatomically distinct subpopulations in the PAG, Li, RR, VTA and SN at E18.5. Lateral mDA progenitors labelled from around E11.75 to E13.5 have a more restricted fate of medially located mDA populations in the Li, VTA and a few medial SN neurons. Our results strongly suggest that the medial cells in the ventral midline can give rise to all major subpopulations of mDA neurons. This argues against the simple popular model that subpopulations of mDA neurons originate from distinct subsets of medial and lateral progenitors. The differences in the destiny of early medial and late lateral labelling have prompted us to re-examine the birth-date of mDA neurons. Our preliminary data corroborate with the previously published data and argue against a strict temporal cue for the generation of mDA subpopulation.

We propose two other possibilities for the generation of mDA subpopulations. First, there may be an anteroposterior difference in the fate of mDA neurons. Our attempt to test this hypothesis by the midbrain specific Pax2-Cre has failed due to technical problems. Therefore, we will continue to test this hypothesis by overcoming this problem. We also suggest the potential of the tamoxifen inducible En1-CreERT1 and En2-CreERT2 mouse lines for progressively tracing more restricted domains along the AP axis in the midbrain. Second, the different populations of mDA neurons can be generated by a complex combinatorial influence between AP and DV spatial factors as

well as the timing of birth of these neurons. This can be addressed by the intersectional and subtractive genetic fate mapping, and requires the generation of appropriate mouse lines carrying Cre and Flp recombinases along the AP and DV axes.

In the development of the mDA neurons, the two closely related members of the LIM-HD transcription factors Lmx1a and Lmx1b are specifically expressed in the mDA progenitors and neurons. This study demonstrates that unlike the exclusive role of Lmx1a in the chick model, Lmx1a/b are redundantly required in multiple steps during mDA development, from patterning the midbrain, specifying the fate of mDA progenitors, regulating the proliferation of mDA progenitors, controlling neurogenesis, to specifying mDA neuronal cell fate. Therefore, the molecular mechanisms should not be extrapolated across species without verification, although the key developmental regulations are usually highly conserved across phyla.

Our results indicate that Lmx1a/b play an essential role in the specification of mDA progenitors by being required for the expression of Msx1. Since we have shown that mDA neurons are derived from floor plate cells, we have also examined the identity of the floor plate and showed that the floor plate is intact. Therefore, Lmx1a/b specifically regulate the expression of Msx1 and the specification of mDA progenitors.

Furthermore, we show that Lmx1a/b regulate the proliferation of mDA progenitors by directly or indirectly regulating the expression of cell cycle molecules cyclin D2 and p27. Our results indicate that although the loss of Wnt1 expression in the double mutant may account for the striking proliferation defect in *Lmx1a/b* double mutants, Lmx1a/b appear to have a dose-dependent effect in the presence of Wnt1. We are currently testing whether constitutive activation of canonical Wnt signalling can rescue the proliferation phenotype in the *Lmx1a/b* double mutants. We also suggest carrying out a more thorough analysis of cell cycle regulators to gain insights into the possible role of Lmx1a/b in regulating the proliferation of mDA progenitors. It would be necessary to verify any potential downstream targets of Lmx1a/b by chromatin immunoprecipitation studies.

We have presented data to show that Lmx1a/b are required for the expression of Ngn2 and the neurogenesis of mDA neurons. This corroborates with the two recent reports showing that Ngn2 is regulated by Lmx1a. The avian study suggests that Msx1 is

the mediator for this regulation. However, the reduction in Ngn2 expression correlates with the gene dosage of *Lmx1a/b* in the presence of Msx1, suggesting an Msx1-independent regulation by Lmx1a/b. It is however noted that the Ngn2 expression is severely reduced in *Lmx1a/b* double mutants, in which Msx1 expression is lost. Therefore, Msx1 may still play in important role in the regulation of Ngn2 in the mouse. Finally, our data suggest that a loss of Lmx1a/b prevents some prospective mDA neurons to adopt the mature mDA fate. Further experiments are required to fully characterise the role of Lmx1a/b in the late specification of mDA neurons.

Taken together, the generation of mDA neurons is an intricately regulated process. Most of the factors involved in early specification process, like Foxa1/2, En1/2 and Lmx1a/b, play redundant roles in mDA neuron development. It is still unclear how the different subpopulations of mDA neurons are generated from the early progenitors, and at which stage during their development that the fate of different subpopulations are determined. However, it is conceivable that the progressive restriction of mDA cell fate will involve a multitude of factors integrating extrinsic and intrinsic information to ensure the correct number and cell types to be generated.

Chapter 6
Appendix

6.1 Supplementary data for Chapter 3

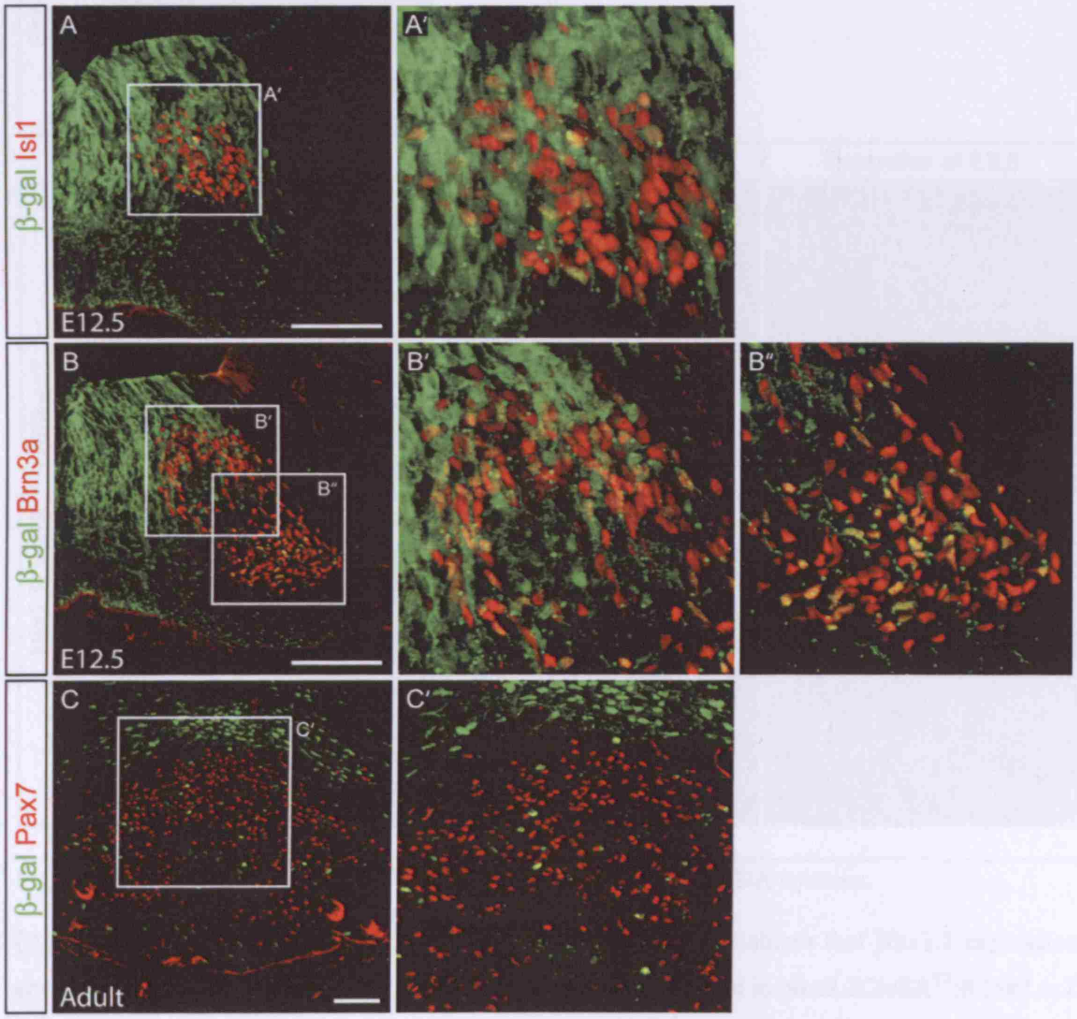

Figure 6-1 Shh expressing cells give rise to some neurons in the (A) oculomotor complex, (B) red nucleus and (C) interpeduncular fossa.

Double immunostaining of β-gal and Isl1 (A), β-gal and Brn3a (B) and β-gal and Pax7. Scale bars correspond to 100μm.

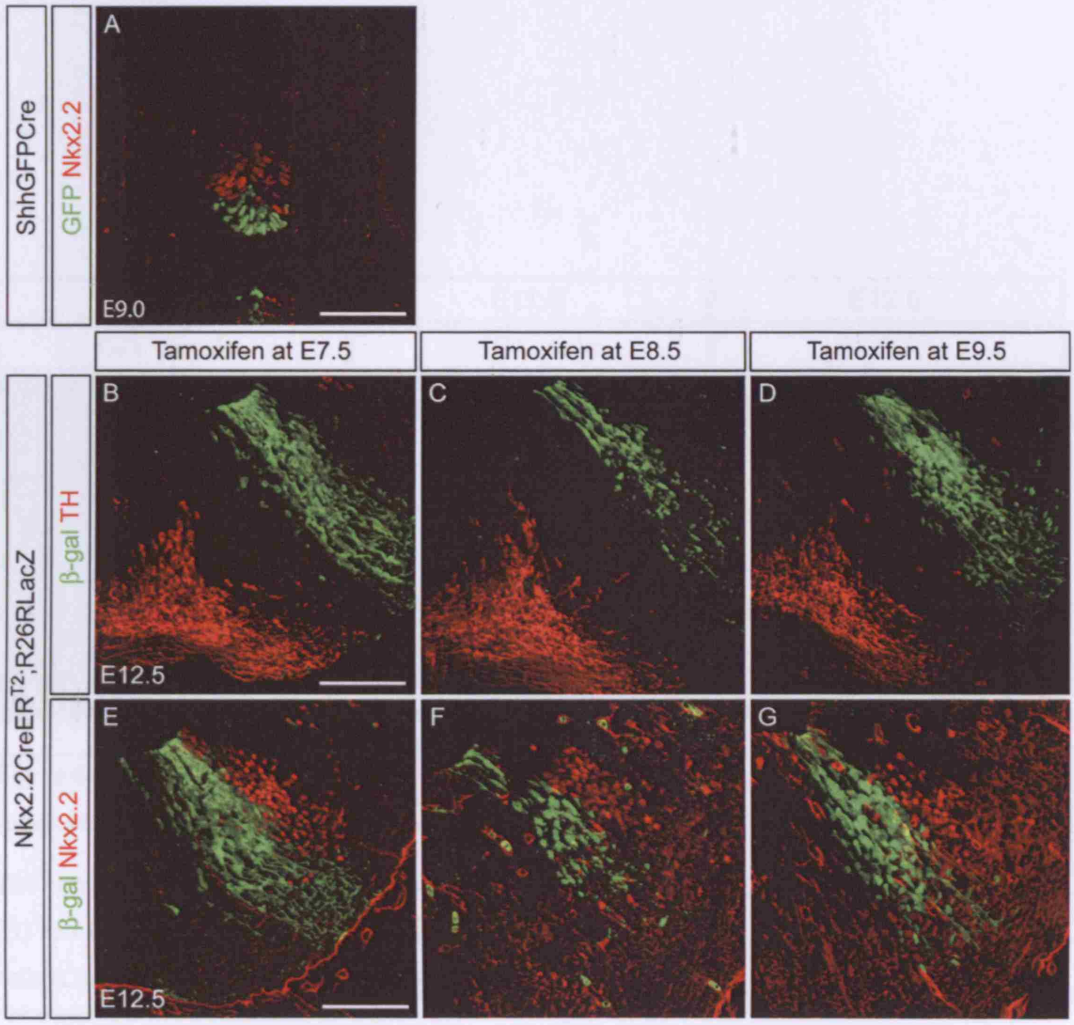

Figure 6-2 The Nkx2.2CreER^{T2} mouse line does not label mDA neurons.

(A) Double staining of GFP and Nkx2.2 in ShhGFPCre embryo shows that Nkx2.2 expression abuts the small Shh domain at E9.0. None of the domains labelled in Nkx2.2CreER^{T2};R26RLacZ embryos by tamoxifen administration at E7.5 (B,E), E8.5 (C,F) and E9.5 (D,G) overlaps with the TH+ mDA neurons at E12.5. No labelling was obtained from tamoxifen treatment at E6.5 from four experiments (data not shown). The domains labelled with Nkx2.2CreER^{T2} are located near the alar/basal plate boundary just ventral to (E,F) or partially overlapping with (G) the endogenous Nkx2.2 domain at E12.5. Scale bars correspond to 100μm.

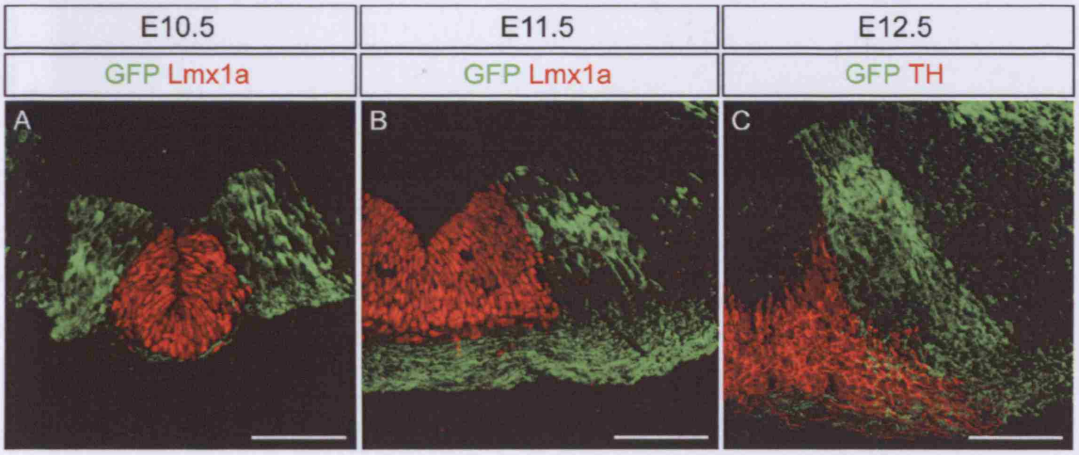

Figure 6-3 GFP reporter driven by zebrafish *ngn1* promoter and upstream regulatory sequences does not mark mDA region.

The expression of mDA progenitor marker Lmx1a does not overlap with *-8.4ngn1:gfp* at E10.5 (A) and E11.5 (B). No co-localisation in the cell bodies was observed in TH and GFP expressing cells (C). Scale bars correspond to 100μm.

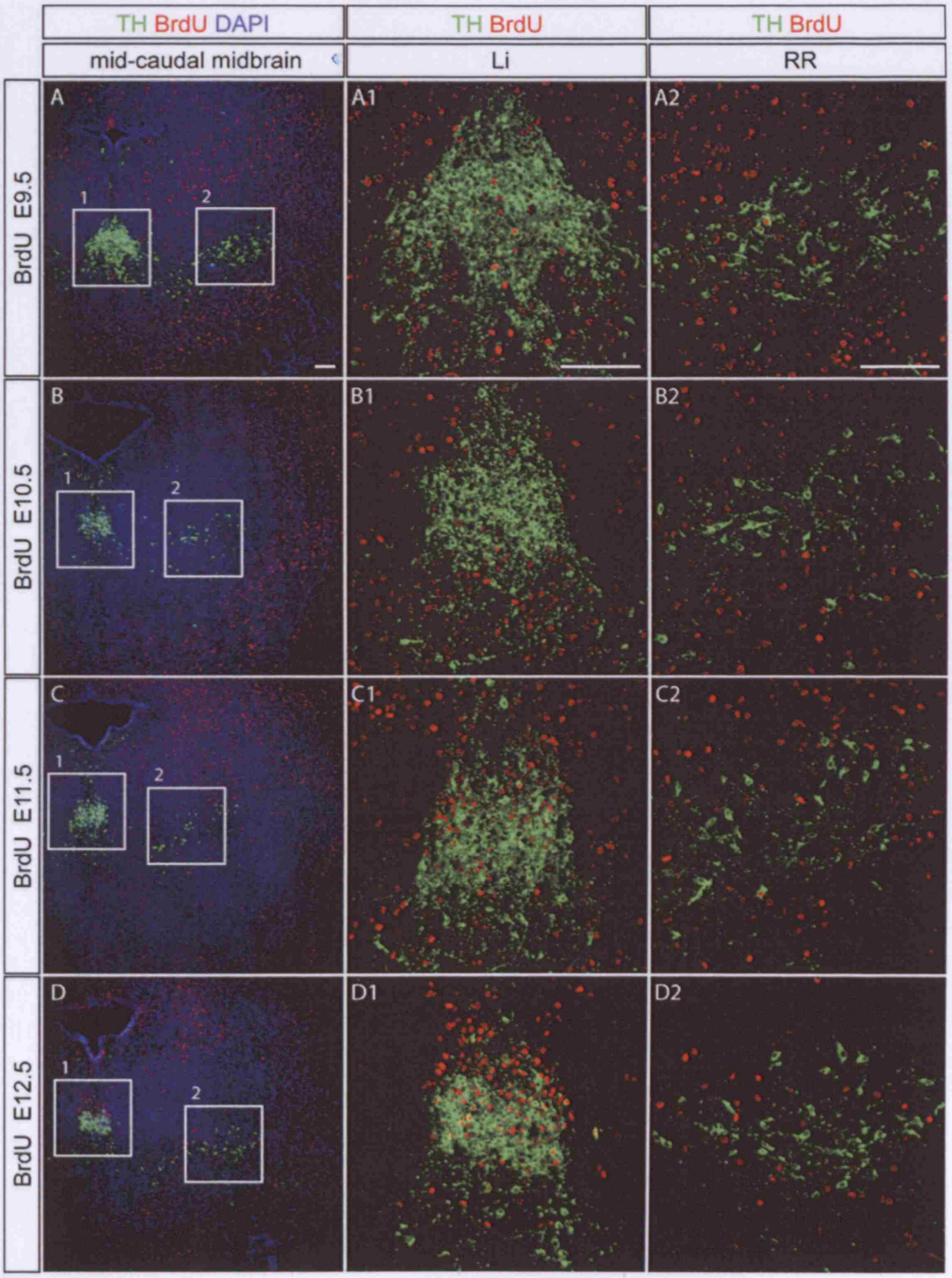

Figure 6-4 BrdU birthdating of the Li and RR populations.

Three pulses of BrdU at 2 h intervals were given to pregnant females from 3 h timed mating from E9.5 to E12.5 as indicated. Embryos were harvested at E18.5. Mid-rostral midbrain sections were analysed by double immunostaining of TH and BrdU for the Li (1) and RR (2) subpopulations. Scale bars correspond to 100μm.

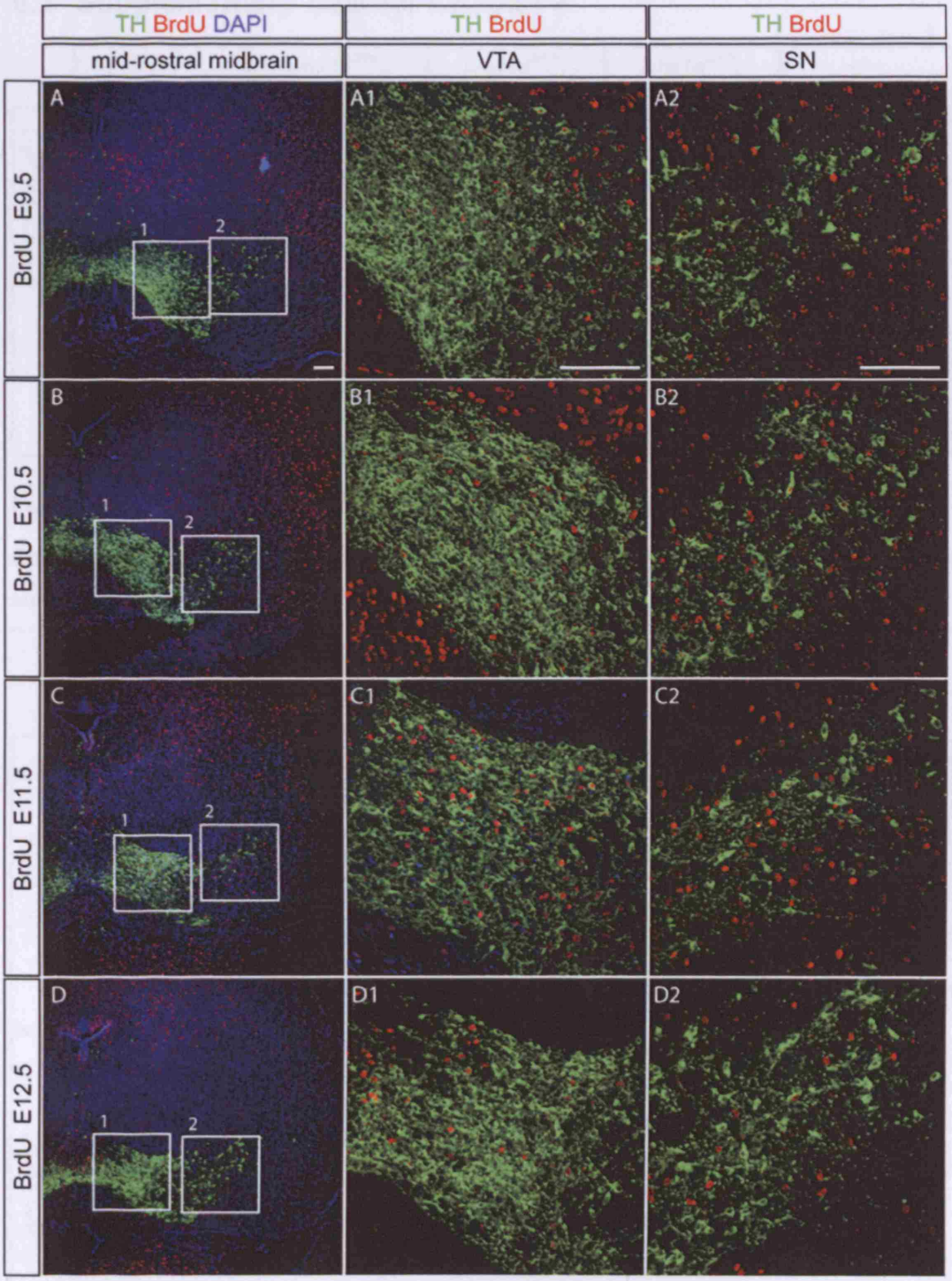

Figure 6-5 BrdU birthdating of the VTA and SN populations.

Three pulses of BrdU at 2 h intervals were given to pregnant females from 3 h timed mating from E9.5 to E12.5 as indicated. Embryos were harvested at E18.5. Mid-rostral midbrain sections were analysed by double immunostaining of TH and BrdU for the VTA (1) and SN (2) subpopulations. Scale bars correspond to 100μm.

6.2 Supplementary data for Chapter 4

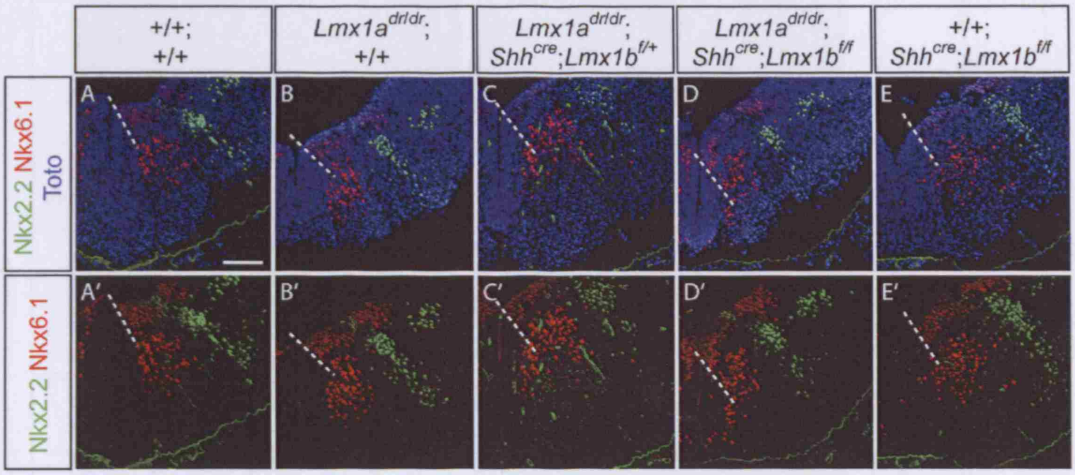

Figure 6-6 No change of progenitor cell fate in *Lmx1a/b* mutants.

Double staining of Nkx2.2 and Nkx6.1 in wild type and Lmx1a/b mutants carrying different number of Lmx1a or Lmx1b gene copies at E12.5. Scale bar corresponds to 100μm.

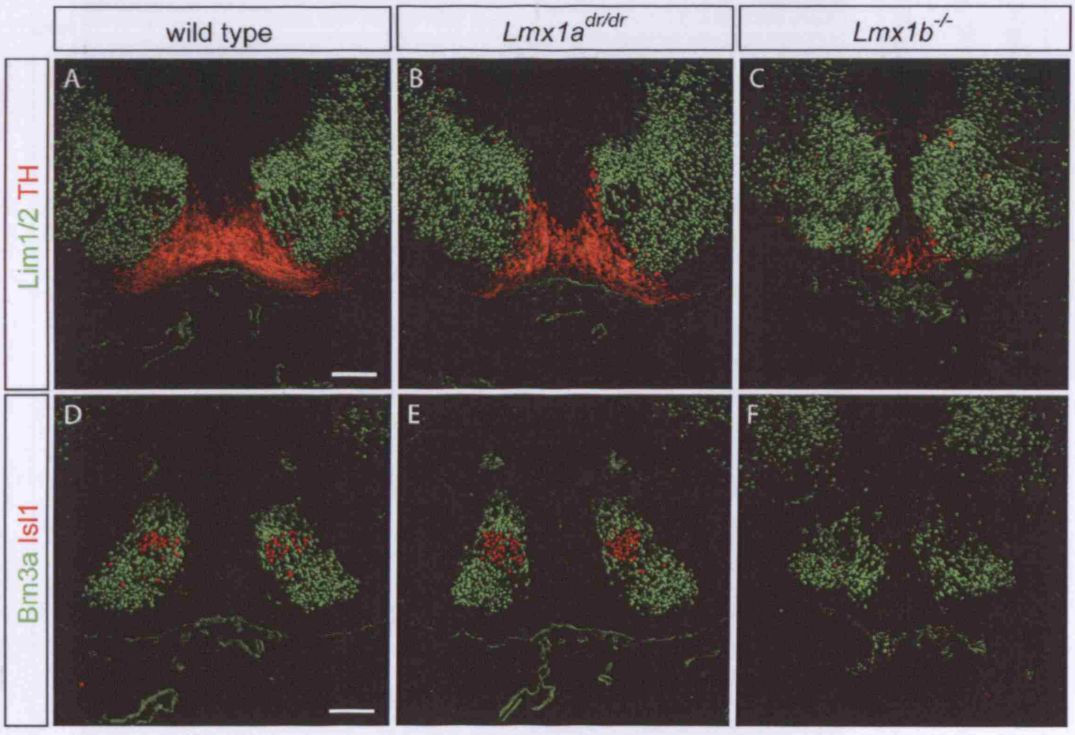

Figure 6-7 Neuronal populations in the ventral midbrain in *Lmx1a*$^{dr/dr}$ and *Lmx1b*$^{-/-}$ mutants.

Double immunostaining of Lmx1/2 and TH (A-C), and Brn3a and Isl1 (D-F) in wild type (A,D, Lmx1a$^{dr/dr}$ (B,E) and Lmx1b$^{-/-}$ (C,F) embryos at E12.5. Scale bars correspond to 100μm.

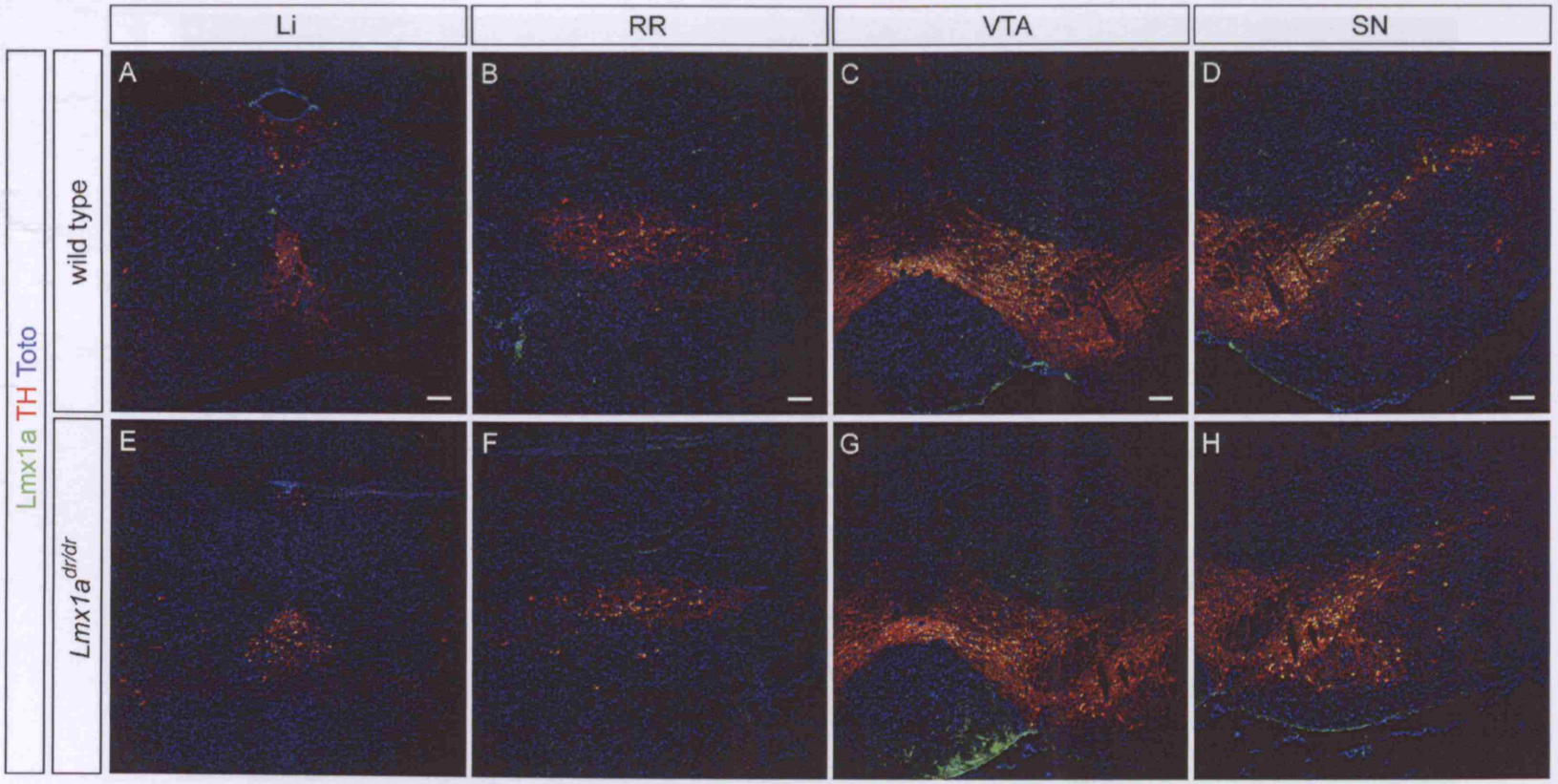

Figure 6-8 Mutation in Lmx1a does not affect the survival and migration of mDA neurons to various subpopulations in the adult.

Double staining of Lmx1a and TH in wild type (A-D) and *Lmx1a*$^{dr/dr}$ (E-H) adult mice. The mDA populations in the Li (A,E) and RR (B,F) in the mid-caudal and VTA (C,G) and SN (D,H) in the mid-rostral midbrain are shown. Scale bars correspond to 100μm.

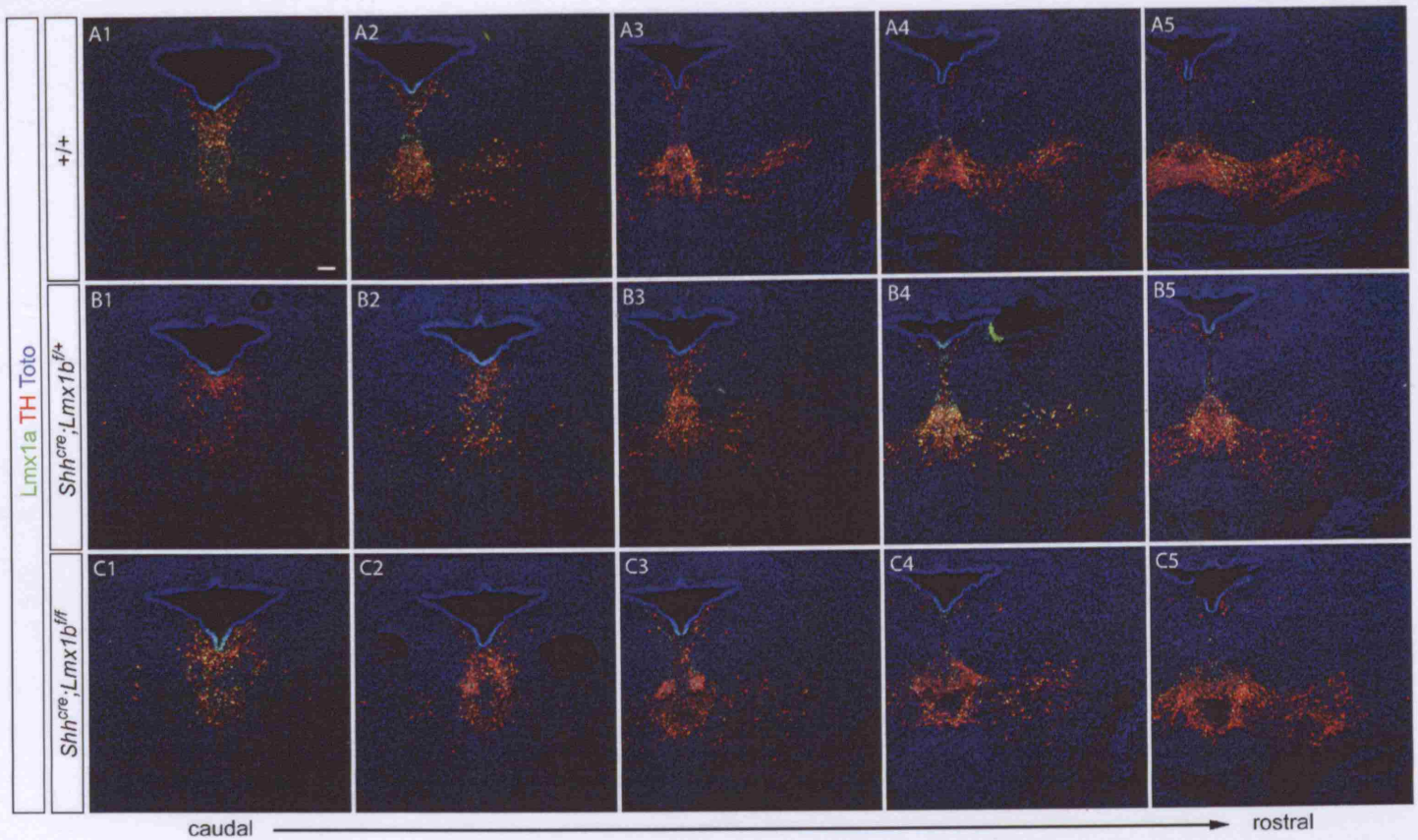

Figure 6-9 The distribution of mDA neurons is slightly affected in the mid-caudal midbrain of *Lmx1b* conditional mutant.

Double immunostaining of Lmx1a and TH with TOTO-3-iodide (Toto) as counterstain in wild type (A), heterozygous (B) and homozygous (C) *Lmx1b* conditional mutants. The full series of caudal midbrain is shown from caudal (1) to rotral (5) regions. Scale bars correspond to 100μm.

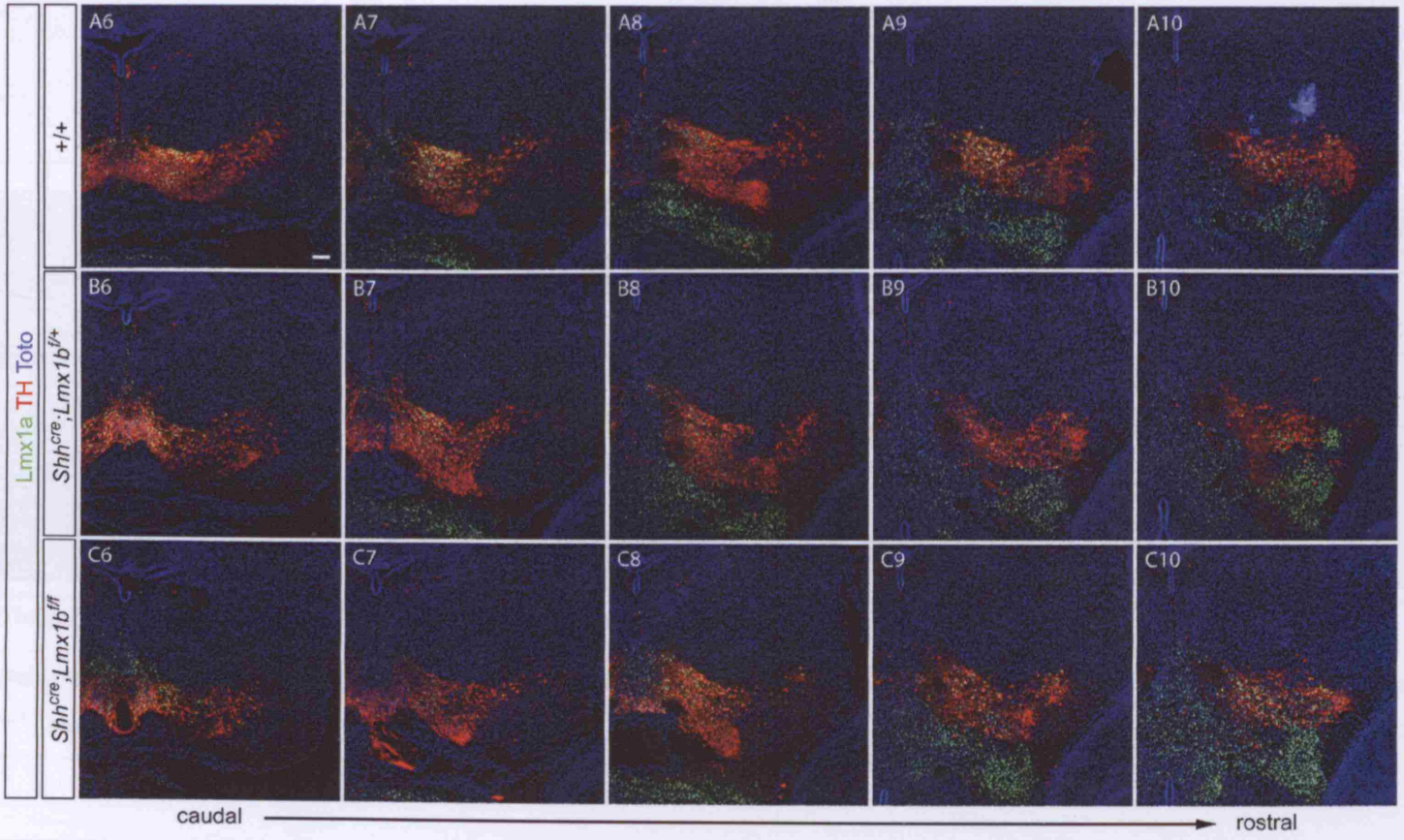

Figure 6-10 The distribution of mDA neurons is slightly affected in the middle midbrain region of *Lmx1b* conditional mutant.

Double immunostaining of Lmx1a and TH with TOTO-3-iodide (Toto) as counterstain in wild type (A), heterozygous (B) and homozygous (C) *Lmx1b* conditional mutants. The full series of caudal midbrain is shown from caudal (6) to rostral (10) regions. Scale bars correspond to 100μm.

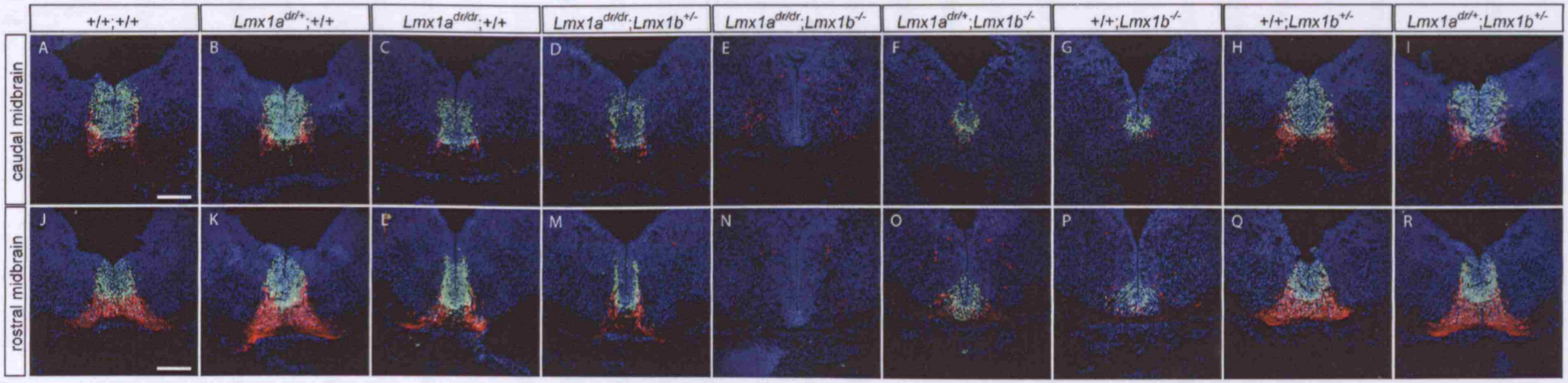

Figure 6-11 The mDA phenotype of *Lmx1a*$^{dr/dr}$ and *Lmx1b*$^{-/-}$ compound mutant.

Double immunostaing of Lmx1a (green) and TH (red) with Toto counterstain (blue) on caudal midbrain (A-I) and rostral midbrain (J-R) at E12.5. *Lmx1a*$^{dr/dr}$ and *Lmx1a*$^{dr/dr}$; *Lmx1b*$^{+/-}$ mutants show similar patterns of Lmx1a+ TH- mDA progenitors and Lmx1a+ TH+ mDA neurons. Scale bars correspond to 100μm.

6.3 Supplementary information on the mechanisms of LIM-HD actions

Combinatorial control of gene expression is a common mechanism in eukaryotic transcriptional control involving the cooperative interactions of multiple transcription factors and regulatory sequences in the genome. This mechanism enhances the number of regulatory decisions to be made through the cooperation of a small number of transcription factors, and allows effective integration of different signalling pathways during development to generate highly complex organisms (Remenyi et al., 2004).

Courey has reviewed three types of coo`perative interactions among transcription factors (Courey, 2001). The first type involves interactions of transcription factors at the enhancer to assemble a large nucleoprotein complex called 'enhancesome', which is thought to be stabilised by multiple protein-protein and protein-DNA interactions while integrating multiple inputs to regulate the activity of a promoter. The second type of cooperative interactions between transcription factors enhances target specificity. For example, Exd/Pbx and Hox proteins bind cooperatively to composite DNA elements containing binding sites for both proteins. The third type of cooperative interaction does not require cooperative binding to DNA. For example, many glucocorticoid receptor (GR) target genes harbour multiple GR response elements, and molecules of GR bound to these multiple elements act synergistically after DNA binding.

The highly versatile function of LIM-HD proteins in a wide variety of tissues and that some of the functions rely on the combination with other factors strongly suggest that LIM-HD regulate transcription in combination with other factors. In fact, there are ample of examples where LIM-HD proteins interact with and act synergistically with proteins from various families such as the bHLLH (Johnson et al., 1997), POU-HD (Bach et al., 1995; Xue et al., 1993), PAIRED-HD (Bach et al., 1997), and a member of the Iroquois complex (de Navascues and Modolell, 2007). Moreover, LIM-HD can also mediate indirect interactions via co-factors Ldb and RLIM to mediate transcriptional activation and repression respectively. The different types of interactions are described in the following sections are summarised in Figure 6-12.

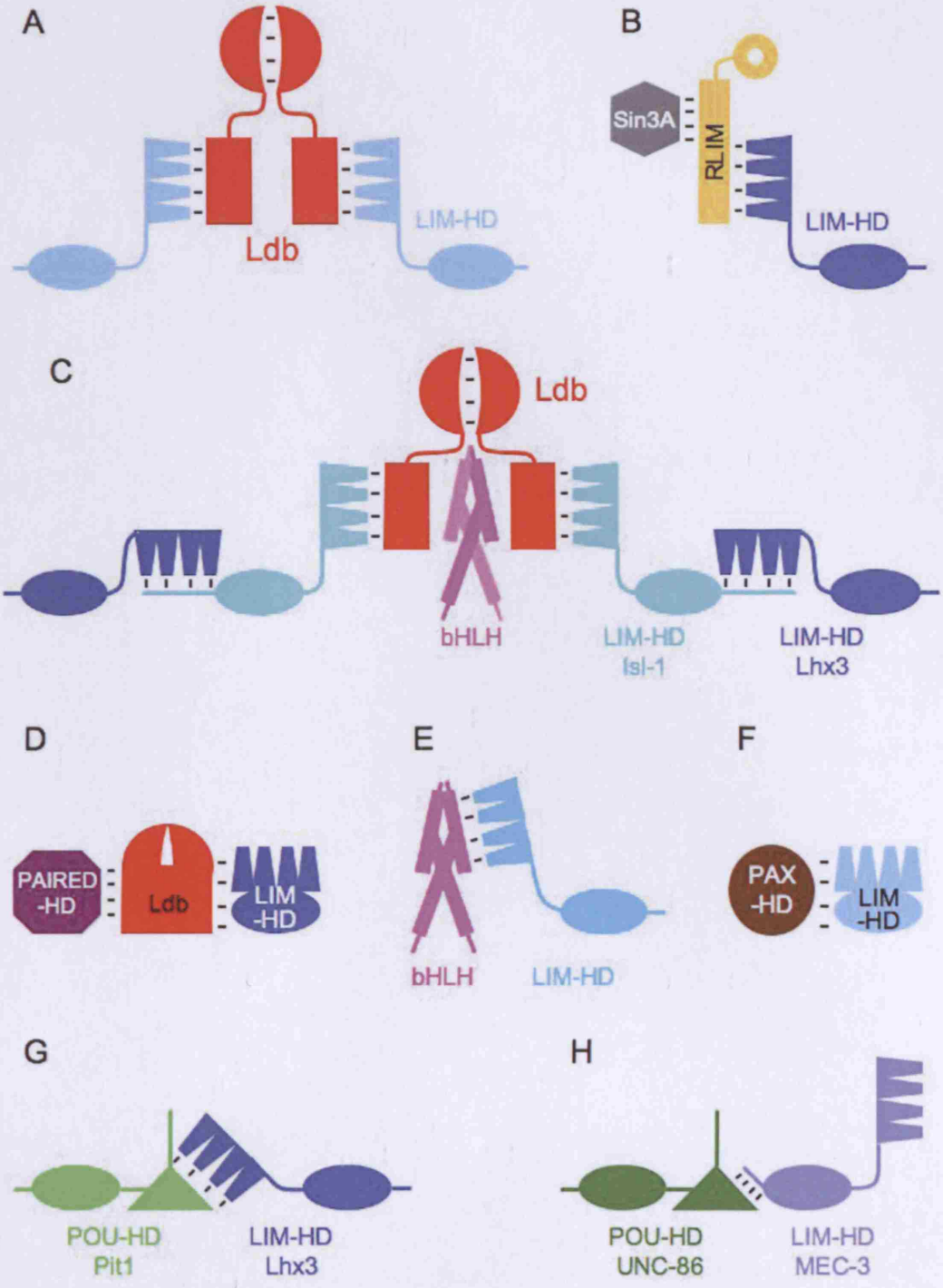

Figure 6-12 Schematic diagram showing the proposed interactions between LIM-HD transcription factors and other proteins.

(A-D) Indirect interactions mediated by Ldb. (E-H) Direct interactions with various proteins. (A) The LIM domains of LIM-HD proteins interact with the LID of Ldb cofactors, which self-dimerise to form a tetramer (Agulnick et al., 1996; Jurata and Gill, 1997; Jurata et al., 1998; Segawa et al., 2001). (B) Rlim binds to the LIM domains of Lhx3 and recruits the Sin3A/histone

deacetylase co-repressor complex (Bach et al., 1999; Hobert and Westphal, 2000). (C) Hexamer of 2Ldb:2Isl1:2Lhx3, where the LIM domains of Isl1 bind to the LID of Ldb and the LIM domains of Lhx3 interact with the 30-residue Lhx3-binding domain on Isl1 (Bhati et al., 2008; Thaler et al., 2002). Ngn2 interacts with the hexamer complex through Ldb (Lee and Pfaff, 2003; Ma et al., 2008). (D) Both Lhx3 and Pitx1 interact with Ldb (Bach et al., 1997; Hobert and Westphal, 2000). (E) The LIM domain of Lmx1a/b interact with the bHLH region of E47 (German et al., 1992; Johnson et al., 1997). (F) The HD of human LMX1B interact with PAX2 (Marini et al., 2005). (G) The LIM domain of Lhx3 interacts with the POU domain of Pit-1 (Bach et al., 1997; Bach et al., 1995). (H) The POU domain of *C. elegans* UNC-86 interact with the acidic domain adjacent to the carboxyl end of the HD of MEC-3 (Xue et al., 1993).

6.3.1 Transcription activation mediated by cofactor Ldb

LIM domain-binding protein 1 (Ldb1), also known as Nuclear LIM interactor (NLI), cofactor of LIM-HD protein 2 (CLIM2), or the *Drosophila* orthologue Chip, was identified as a LIM interacting protein in cDNA expression library screen, yeast two-hybrid system, and co-immunoprecipitation (Agulnick et al., 1996; Bach et al., 1997; Jurata et al., 1996). Suggested by one of its name NLI, Ldb1 binds to nuclear LIM proteins but not cytoplasmic LIM proteins (Jurata et al., 1996). Ldb1 is ubiquitously expressed at E8.5 (Ostendorff et al., 2006), and widely expressed within the central and peripheral nervous systems in mouse embryos (Jurata et al., 1996). The expression becomes progressively stronger in regions of the developing embryo in which the LIM-HD transcripts are abundant (Bach et al., 1997). Another member of the same family, Ldb2/CLIM1, is expressed in a more restricted fashion than Ldb1/NLI/CLIM (Bach et al., 1997).

Ldb1 has an N-terminal dimerisation domain for homodimersation, a nuclear localisation sequence, and a C-terminal LIM interacting domain (LID), which binds with high affinity to the LIM domains of nuclear LIM domain proteins including LIM-HD and LMO proteins (Jurata and Gill, 1997; Jurata et al., 1996; Matthews and Visvader, 2003).

Ldb1 preferentially associates with LIM1 of LMO2 and Isl1, but LIM2 of Lmx1 and mec-3 in *in vitro* binding assays (Jurata and Gill, 1997; Jurata et al., 1996).

However, if Lmx1 and Ldb1 are present in equimolar amounts, both LIM domains are required for Ldb1 interaction (Jurata and Gill, 1997). Similarly, both intact LIM domains are required for strong binding between Ldb1 and Xlim-1 (Agulnick et al., 1996). The X-ray crystal structure of Ldb1 in a complex with the nuclear LIM protein LMO4 further demonstrates that the elongated LID of Ldb1 binds across the entire length of both LIM domains of LMO4 to form a tandem β-zipper to give a rod-shaped complex (Deane et al., 2004). Furthermore, both LIM domains of Lmx1 are required for the Ldb1 supershifts in electrophoretic mobility shift assays (EMSA), indicating both LIM domains are required for the formation of the Lmx1-Ldb1 complex, which binds to the target DNA element (Jurata and Gill, 1997).

The functional significance of complex formation between LIM-HD proteins and Ldb1 is shown in vertebrate embryonic development. Xlim-1 and XLdb1 are endogenously expressed in the dorsal region of the *Xenopus* gastrula (Taira et al., 1994). While injection of either Xlim-1 or XLdb1 alone has little effect on embryo development, co-injection of Xlim-1 and XLdb1 synergistically induce partial secondary axes or a dorsalised phenotype in Xenopus embryos (Agulnick et al., 1996). This provides evidence for functional interactions between Xlim-1 and XLbd1.

6.3.2 Stoichiometry for LIM-HD and Ldb complex

Tetrameric complex formation between 2 Ldb1 and 2 LIM-HD proteins is suggested in various members of the LIM-HD family across species (Figure 4-3A). The LIM domain of LIM-HD proteins binds to the LIM-interacting domain (LID) of Ldb, which self-dimerises via its dimerisation domain to form a tetramer (Agulnick et al., 1996; Segawa et al., 2001).

Hamster Lmx1a and murine Ldb1 form a 2Ldb1:2Lmx1a complexs *in vitro* with the two Lmx1a proteins bridged by the Ldb1 homodimer (Jurata and Gill, 1997; Jurata et al., 1998). Excess Ldb1 inhibits Lmx1a DNA binding, suggesting that the correct ratio of both proteins is required for DNA binding *in vitro* (Jurata and Gill, 1997). Both zebrafish Isl1 and Isl2 can form tetrameric complex bridged by an Ldb1 homodimer (Segawa et al., 2001). The physical binding between LIM and LID domains for Isl2-Ldb1 tetramer formation in zebrafish is required for the development of the optic vesicles and MHB, and the axonal outgrowth of primary sensory neurons into the periphery. Misexpressions of either LIM domain of Isl2 or LID domain of Ldb1 that interferes with Isl2-Ldb1

binding induce the same phenotypes as Isl2 antisense morpholino knockdown (Segawa et al., 2001). The correct levels of Apterous and Chip is critical for the dorsoventral compartmentalisation in *Drosophila* wing, providing further evidence that the stoichiometry of Ap and CHIP is critical (Fernández-Fúnez et al., 1998; Rincón-Limas et al., 2000).

Thaler *et al.* elegantly showed that cell-type specific protein-protein interactions leading to the formation different complexes induces specific gene expression and promotes the development of certain neuronal identity. In the chick spinal cord, tetramers of 2Ldb1:2Lhx3 induce Chx10 expression and direct V2 interneuron generation, whereas hexamers of 2Ldb1:2Isl1:2Lhx3 induce Isl2 expression and trigger MN differentiation (Thaler et al., 2002). This group further proposed a model coupling neurogenesis and MN cell fate specification (Lee and Pfaff, 2003). The 2Ldb1:2Isl1:2Lhx3 hexamer forms higher order complex with heterodimers of bHLH proteins of either NeuroM:E47 or Ngn2:E-protein via interaction between Ldb and the phosphorylated C-terminal of Ngn2 (Figure 4-3C) (Lee and Pfaff, 2003; Ma et al., 2008).

The activity of LIM-HD is also determined by the relative levels of LIM-HD, Ldb and LIM-only (LMO) proteins. The *Dorsophila* LMO has been shown to compete with Apterous for binding its co-factor Chip and negatively regulate its activity (Milán and Cohen, 1999; Milán et al., 1998).

6.3.3 Transcription repression mediated by cofactor RLIM

The RING finger LIM domain-binding protein (RLIM), containing a RING finger motif at its C-terminal, is encoded by the gene Rnf12 (Bach et al., 1999). RLIM is ubiquitously expressed at E8.5, with higher expression in the develop neural tube (Ostendorff et al., 2006). In the spinal cord, RLIM is expressed in most postmitotic neurons and the progenitor region throughout the whole neural tube at E11.5. Its expression becomes restricted to the dorsal ventricular zone and ventral postmitotic neurons at E12.5. The expression level of RLIM becomes weaker from E13.5. RLIM binds to the LIM domains of nuclear LIM proteins Lhx2, Lhx3, Isl1, Lmo2 and LIM kinase 1, while only binds weakly or does not bind to the LIM domains of the cytoplasmic LIM proteins CRP, enigma, paxillin and zyxin. RLIM also interacts with Ldb *in vitro*.

RLIM inhibits the functional activity of LIM-HD transcription factors. For example, it inhibits the transcriptional activity of Lhx3 on the pituitary trophic hormones prolactin, thyroid-stimulating hormone β-subunit (TSH-β) and glycoprotein hormone α-subunit (α-GSH) by interacting with their LIM domains in transient transfection assays (Bach et al., 1999). It also inhibits the formation of Lhx3/Ldb2/DNA complex as well as the synergistic action of Lhx3 with Pit1 or Lhx3 with Pitx1 (Bach et al., 1999).

Two mechanisms have been suggested for the action of RLIM on modulating the transcriptional regulation of LIM-HD. The first one involves the binding of RLIM to LIM-HD proteins and the recruitment of Sin3A/histone deacetylase co-repressor complex, which mediates transcription repression (Figure 4-3B). The evidences are that RLIM can bind to both LIM-HD protein and Sin3A, and that anti-Sin3A and anti-HDAC2 antibodies block the repressor ability of RLIM (Bach et al., 1999).

In the second mechanism, RLIM modulates the actions of Ldb on LIM-HD factors by competing for binding to the LIM domains of LIM-HD and by a ubiquitination/degradation-dependent exchange in cofactor occupation on LIM-HD proteins on DNA. RLIM is shown to act as an E3 ubiquitin ligase targeting Ldb to proteolytic degradation through the 26S proteasome pathway (Ostendorff et al., 2002). Thus, RLIM competes with Ldb for DNA-bound LIM-HD proteins by poly-ubiquitinating and targeting Ldb for degradation. This mechanism is confirmed *in vivo* in *Xenopus* that XRnf12/RLIM also mediates ubiquitination and proteasome-dependent degradation of Ldb1 (Hiratani et al., 2003).

The mutual interactions between LIM-HD, Ldb and RLIM conferring proper Xlim-1/Ldb1 stoichiometry has been suggested to be important for their function in the *Xenopus* organiser (Hiratani et al., 2003). Transient increases in Xlim-1 or the LIM-only protein LMO2 inhibit RLIM-mediated turnover of Ldb1 levels *in vivo* (Hiratani et al., 2003; Ostendorff et al., 2002).

The balance appears to be controlled by single-stranded DNA-binding proteins (Ssbp or Ssdp), which bind to Ldb1/Chip (Chen et al., 2002; van Meyel et al., 2003). Ssdps regulate the abundance of LIM protein and Ldb by interacting with Ldb and prevent Ldb and LIM proteins from binding to RLIM, thus inhibiting the RLIM mediated ubiquitination/proteasomal degradation (Xu et al., 2007).

Ssdp1 also contains an activation domain and is able to enhance transcriptional activation by the Lim-Ldb1 complex in a dose-dependent manner in transfected cells (Nishioka et al., 2005). In the mouse, Ssdp1 interacts genetically with Lim1 and Ldb1 in

both head development and body growth (Nishioka et al., 2005). These suggest that Ssdp1 function as an essential activator component of Lim1 complex through interaction with Ldb1.

6.3.4 Interaction with Paired-like HD

Lhx3 (P-Lim) and the paired-like HD protein Pitx1 (Ptx1, P-Otx) both interact with Ldb on DNA to enhance transcriptional activation (Figure 4-3D) (Bach et al., 1997). The LIM domains of Lhx3 are required for the coactivator function of Ldb with Lhx3, whereas the domain for the interaction between Pitx1 and Ldb has not been investigated. Cotransfections of Lhx3, Pitx1 and Ldb2 result in a strongly synergistic activation in the mouse αGSU gene promoter. Surprisingly, this synergistic activation is also observed when Lhx3-ΔLIM is used instead of the full length Lhx3, demonstrating that the LIM domain is not required. Therefore, the exact interactions among Lhx3, Ldb and Pitx3 remain unclear.

6.3.5 Interaction with bHLH proteins

LIM-HD proteins are also found to interact directly with various groups of protein. The LIM2 domain of Lmx1a and Lmx1b (previously Lmx1.1 and Lmx1.2 respectively) interacts with the bHLH region of class I bHLH protein E47 (Pan1-1 in hamster) to synergistically activate the insulin I E2A3/4 minienhancer in transfected fibroblasts (Figure 4-3E) (Dreyer et al., 2000; German et al., 1992; Johnson et al., 1997; Ohneda et al., 2000). The specificity of Lmx1a-E47 interaction is demonstrated by the fact that Lmx1a does not interact with class II bHLH proteins NeuroD1, Mash1 and MyoD or class V bHLH protein Id1 in *in vitro* protein-protein interaction assays (Ohneda et al., 2000). The specificity of the LIM domains for the interaction is illustrated by the loss of transcriptional synergy between Lmx1a and E47 by replacing with the LIM domains of Lmx1a with those of Isl1 (German et al., 1992). The transcriptional synergy between LMX1B and E47 is proportionately decreased by the addition of LDB1 (Dreyer et al., 2000). Despite the interaction and synergistic activation, Lmx1a and E47 do not bind DNA synergistically in EMSA (German et al., 1992). The

proteins (Wadman et al., 1994)

6.3.6 Interaction with PAX-HD

The HD of human LMX1B is shown to interact with PAX2 by hybrid system and coimmunoprecipitation studies (Figure 4-3F) (Mari However, the mechanism of interaction has not been studied.

6.3.7 Interaction with POU-HD

The LIM domain of Lhx3 specifically interacts with the P pituitary-specific POU-domain transcription factor Pit-1 (Figure 4-3G LIM domain is not required for the basal transactivation function of Lhx for synergistic activation of specific Pit-1 distal target genes, such as pr stimulating hormone β-subunit (TSHβ) and the *pit-1* enhancer itself. T synergy does not appear to act by improving the cooperative DNA b Lhx3 and Pit-1 on a series of DNA response element, nor is it affected b al., 1997; Bach et al., 1995).

In *C. elegans*, the POU-HD protein UNC-86 is expressed in precursors and neurons, and the LIM-HD protein MEC-3 is present in The POU domain of UNC-86 appears to interact with the acidic domain carboxyl end of the HD instead of the LIM domain of MEC-3 to inc binding affinity and the stability of the binding (Figure 4-3H) (Xue et al.,

Isl1 and POU-HD protein Brn3b were shown to simultaneously ganglion cells (RGCs) specific promoters (*Brn3b*, *Shh*, *Brn3a* and *Isl2* immunoprecipitation (ChIP) assays. There is a more severe defect i

differentiation of RGC in *Isl1* and *Brn3b* compound null mice. Complementarily, Isl1 and Brn3b synergistically regulate the expression of Brn3a in an *in vitro* transactivation assay (Pan et al., 2008).

Taken together, LIM-HD transcription factors can bind to various types of transcription factors directly and indirectly using the LIM domain or other regions in the protein. The indirect interactions mediated by Ldb cofactors and RLIM corepressor leading to transcriptional activation and repression respectively are further modulated by other interacting proteins like Ssdps. The dynamic cooperations allow LIM-HD proteins to perform a wide variety of functions in different tissues during the highly organised embryonic development.

Chapter 7

References

Abelló, G., Khatri, S., Gir·ldez, F. and Alsina, B. (2007). Early regionalization of the otic placode and its regulation by the Notch signaling pathway. *Mechanisms of Development* **124**, 631-645.

Abi-Dargham, A., Rodenhiser, J., Printz, D., Zea-Ponce, Y., Gil, R., Kegeles, L. S., Weiss, R., Cooper, T. B., Mann, J. J., Van Heertum, R. L. et al. (2000). Increased baseline occupancy of D2 receptors by dopamine in schizophrenia. *Proc Natl Acad Sci U S A* **97**, 8104-9.

Adams, K. A., Maida, J. M., Golden, J. A. and Riddle, R. D. (2000). The transcription factor Lmx1b maintains Wnt1 expression within the isthmic organizer. *Development* **127**, 1857-1867.

Agarwala, S. and Ragsdale, C. W. (2002). A role for midbrain arcs in nucleogenesis. *Development* **129**, 5779-5788.

Agarwala, S., Sanders, T. A. and Ragsdale, C. W. (2001). Sonic Hedgehog Control of Size and Shape in Midbrain Pattern Formation. *Science* **291**, 2147-2150.

Agid, O., Mamo, D., Ginovart, N., Vitcu, I., Wilson, A. A., Zipursky, R. B. and Kapur, S. (2007). Striatal Vs Extrastriatal Dopamine D2 Receptors in Antipsychotic Response - A Double-Blind PET Study in Schizophrenia. *Neuropsychopharmacology* **32**, 1209-1215.

Agulnick, A. D., Taira, M., Breen, J. J., Tanaka, T., Dawid, I. B. and Westphal, H. (1996). Interactions of the LIM-domain-binding factor Ldbl with LIM homeodomain proteins. *Nature* **384**, 270-272.

Akazawa, C., Sasai, Y., Nakanishi, S. and Kageyama, R. (1992). Molecular characterization of a rat negative regulator with a basic helix-loop-helix structure predominantly expressed in the developing nervous system. *J. Biol. Chem.* **267**, 21879-21885.

Alberi, L., Sgado, P. and Simon, H. H. (2004). Engrailed genes are cell-autonomously required to prevent apoptosis in mesencephalic dopaminergic neurons. *Development* **131**, 3229-36.

Andersson, E., Jensen, J. B., Parmar, M., Guillemot, F. and Bjorklund, A. (2006a). Development of the mesencephalic dopaminergic neuron system is compromised in the absence of neurogenin 2. *Development* **133**, 507-516.

Andersson, E., Tryggvason, U., Deng, Q., Friling, S., Alekseenko, Z., Robert, B., Perlmann, T. and Ericson, J. (2006b). Identification of Intrinsic Determinants of Midbrain Dopamine Neurons. *Cell* **124**, 393-405.

Ando, H., Kobayashi, M., Tsubokawa, T., Uyemura, K., Furuta, T. and Okamoto, H. (2005). Lhx2 mediates the activity of Six3 in zebrafish forebrain growth. *Developmental Biology* **287**, 456-468.

Angrist, B., Sathananthan, G., Wilk, S. and Gershon, S. (1974). Amphetamine psychosis: Behavioral and biochemical aspects. *Journal of Psychiatric Research* **11**, 13-23.

Arkell, R. and Beddington, R. S. (1997). BMP-7 influences pattern and growth of the developing hindbrain of mouse embryos. *Development* **124**, 1-12.

Asbreuk, C. H. J., Vogelaar, C. F., Hellemons, A., Smidt, M. P. and Burbach, J. P. H. (2002). CNS Expression Pattern of Lmx1b and Coexpression with Ptx Genes Suggest Functional Cooperativity in the Development of Forebrain Motor Control Systems. *Molecular and Cellular Neuroscience* **21**, 410-420.

Astradsson, A., Cooper, O., Vinuela, A. and Isacson, O. (2008). Recent advances in cell-based therapy for Parkinson disease. *Neurosurgical FOCUS* **24**, E6.

Bach, A., Lallemand, Y., Nicola, M.-A., Ramos, C., Mathis, L., Maufras, M. and Robert, B. (2003). Msx1 is required for dorsal diencephalon patterning. *Development* **130**, 4025-4036.

Bach, I., Carriere, C., Ostendorff, H. P., Andersen, B. and Rosenfeld, M. G. (1997). A family of LIM domain-associated cofactors confer transcriptional synergism between LIM and Otx homeodomain proteins. *Genes Dev.* **11**, 1370-1380.

Bach, I., Rhodes, S. J., Pearse Rv, II, Heinzel, T., Gloss, B., Scully, K. M., Sawchenko, P. E. and Rosenfeld, M. G. (1995). P-Lim, a LIM Homeodomain Factor, is Expressed During Pituitary Organ and Cell Commitment and Synergizes with Pit-1. *Proceedings of the National Academy of Sciences* **92**, 2720-2724.

Bach, I., Rodriguez-Esteban, C., Carriere, C., Bhushan, A., Krones, A., Rose, D. W., Glass, C. K., Andersen, B., Belmonte, J. C. I. and Rosenfeld, M. G. (1999). RLIM inhibits functional activity of LIM homeodomain transcription factors via recruitment of the histone deacetylase complex. *Nat Genet* **22**, 394-399.

Bachy, I., Failli, V. and Retaux, S. (2002). A LIM-homeodomain code for development and evolution of forebrain connectivity. *NeuroReport* **13**, A23-27.

Bäckman, C., Perlmann, T., Wallén, Å., Hoffer, B. J. and Morales, M. (1999). A selective group of dopaminergic neurons express Nurr1 in the adult mouse brain. *Brain Research* **851**, 125-132.

Bai, G., Sheng, N., Xie, Z., Bian, W., Yokota, Y., Benezra, R., Kageyama, R., Guillemot, F. and Jing, N. (2007). Id Sustains Hes1 Expression to Inhibit Precocious Neurogenesis by Releasing Negative Autoregulation of Hes1. *Developmental Cell* **13**, 283-297.

Banerjee-Basu, S. and Baxevanis, A. D. (2001). Molecular evolution of the homeodomain family of transcription factors. *Nucl. Acids Res.* **29**, 3258-3269.

Bayer, S. A., Wills, K. V., Triarhou, L. C. and Ghetti, B. (1995). Time of neuron origin and gradients of neurogenesis in midbrain dopaminergic neurons in the mouse. *Exp Brain Res* **105**, 191-199.

Bei, M. and Maas, R. (1998). FGFs and BMP4 induce both Msx1-independent and Msx1-dependent signaling pathways in early tooth development. *Development* **125**, 4325-4333.

Bergstrom, D. E., Gagnon, L. H. and Eicher, E. M. (1999). Genetic and Physical Mapping of the Dreher Locus on Mouse Chromosome 1. *Genomics* **59**, 291-299.

Berry, N., Jobanputra, V. and Pal, H. (2003). Molecular genetics of schizophrenia: a critical review. *J Psychiatry Neurosci* **28**, 415-29.

Bertrand, N., Castro, D. S. and Guillemot, F. (2002). Proneural genes and the specification of neural cell types. *Nat Rev Neurosci* **3**, 517-530.

Bettenhausen, B., Hrabe de Angelis, M., Simon, D., Guenet, J. L. and Gossler, A. (1995). Transient and restricted expression during mouse embryogenesis of Dll1, a murine gene closely related to Drosophila Delta. *Development* **121**, 2407-2418.

Bezard, E., Dovero, S., Prunier, C., Ravenscroft, P., Chalon, S., Guilloteau, D., Crossman, A. R., Bioulac, B., Brotchie, J. M. and Gross, C. E. (2001). Relationship between the Appearance of Symptoms and the Level of Nigrostriatal Degeneration in a Progressive 1-Methyl-4-Phenyl-1,2,3,6-Tetrahydropyridine-Lesioned Macaque Model of Parkinson's Disease. *J. Neurosci.* **21**, 6853-6861.

Bhati, M., Lee, C., Nancarrow, A. L., Lee, M., Craig, V. J., Bach, I., Guss, J. M., Mackay, J. P. and Matthews, J. M. (2008). Implementing the LIM code: the structural basis for cell type-specific assembly of LIM-homeodomain complexes. *EMBO J*, doi: 10.1038/emboj.2008.123.

Björklund, A. and Dunnett, S. B. (2007). Dopamine neuron systems in the brain: an update. *Trends in Neurosciences* **30**, 194-202.

Björklund, A. and Lindvall, O. (1984). Dopamine-containing systems in the CNS. In *Handbook of chemical neuroanatomy*, (ed. A. Björklund and T. Hökfelt), pp. 55-122. Amsterdam: Elsevier.

Blader, P., Plessy, C. and Strahle, U. (2003). Multiple regulatory elements with spatially and temporally distinct activities control neurogenin1 expression in primary neurons of the zebrafish embryo. *Mechanisms of Development* **120**, 211-218.

Bongers, E., Gubler, M.-C. and Knoers, N. (2002). Nail-patella syndrome. Overview on clinical and molecular findings. *Pediatric Nephrology* **17**, 703-712.

Bongers, E. M. H. F., de Wijs, I. J., Marcelis, C., Hoefsloot, L. H. and Knoers, N. V. A. M. (2008). Identification of entire LMX1B gene deletions in nail patella syndrome: evidence for haploinsufficiency as the main pathogenic mechanism underlying dominant inheritance in man. *Eur J Hum Genet.*

Bradberry, C. W., Barrett-Larimore, R. L., Jatlow, P. and Rubino, S. R. (2000). Impact of Self-Administered Cocaine and Cocaine Cues on Extracellular Dopamine in Mesolimbic and Sensorimotor Striatum in Rhesus Monkeys. *J. Neurosci.* **20**, 3874-3883.

Branda, C. S. and Dymecki, S. M. (2004). Talking about a Revolution: The Impact of Site-Specific Recombinases on Genetic Analyses in Mice. *Developmental Cell* **6**, 7-28.

Brennan, A. R. and Arnsten, A. F. T. (2008). Neuronal Mechanisms Underlying Attention Deficit Hyperactivity Disorder. *Annals of the New York Academy of Sciences* **1129**, 236-245.

Brunet, J.-F. and Ghysen, A. (1999). Deconstructing cell determination: proneural genes and neuronal identity. *BioEssays* **21**, 313-318.

Bürglin, T. R. (1994). A Comprehensive Classification of Homeobox Genes. In *Guidebook to the Homeobox Genes*, (ed. D. Duboule), pp. 25-71. Oxford: Oxford University Press.

Burke, R. E. (2003). Postnatal Developmental Programmed Cell Death in Dopamine Neurons. *Ann NY Acad Sci* **991**, 69-79.

Buss, R. R., Sun, W. and Oppenheim, R. W. (2006). Adaptive roles of programmed cell death during nervous system development. *Annual Review of Neuroscience* **29**, 1-35.

Campos, L. S., Duarte, A. J., Branco, T. and Henrique, D. (2001). *mDll1* and *mDll3* expression in the developing mouse brain: Role in the establishment of the early cortex. *Journal of Neuroscience Research* **64**, 590-598.

Castellanos, F. X. (1997). Toward a pathophysiology of attention-deficit/hyperactivity disorder. *Clin Pediatr (Phila)* **36**, 381-93.

Castelo-Branco, G., Wagner, J., Rodriguez, F. J., Kele, J., Sousa, K., Rawal, N., Pasolli, H. A., Fuchs, E., Kitajewski, J. and Arenas, E. (2003). Differential regulation of midbrain dopaminergic neuron development by Wnt-1, Wnt-3a, and Wnt-5a. *PNAS* **100**, 12747-12752.

Chen, H. and Johnson, R. L. (2002). Interactions between dorsal-ventral patterning genes lmx1b, engrailed-1 and wnt-7a in the vertebrate limb. *Int J Dev Biol* **46**, 937-41.

Chen, H., Lun, Y., Ovchinnikov, D., Kokubo, H., Oberg, K. C., Pepicelli, C. V., Can, L., Lee, B. and Johnson, R. L. (1998a). Limb and kidney defects in Lmx1b mutant mice suggest an involvement of LMX1B in human nail patella syndrome. *Nat Genet* **19**, 51-55.

Chen, H., Ovchinnikov, D., Pressman, C. L., Aulehla, A., Lun, Y. and Johnson, R. L. (1998b). Multiple calvarial defects in *lmx1b* mutant mice. *Developmental Genetics* **22**, 314-320.

Chen, L., Segal, D., Hukriede, N. A., Podtelejnikov, A. V., Bayarsaihan, D., Kennison, J. A., Ogryzko, V. V., Dawid, I. B. and Westphal, H. (2002). Ssdp proteins interact with the LIM-domain-binding protein Ldb1 to regulate development. *Proceedings of the National Academy of Sciences of the United States of America* **99**, 14320-14325.

Cheng, L., Chen, C.-L., Luo, P., Tan, M., Qiu, M., Johnson, R. and Ma, Q. (2003). Lmx1b, Pet-1, and Nkx2.2 Coordinately Specify Serotonergic Neurotransmitter Phenotype. *J. Neurosci.* **23**, 9961-9967.

Chenn, A. and Walsh, C. A. (2002). Regulation of Cerebral Cortical Size by Control of Cell Cycle Exit in Neural Precursors. *Science* **297**, 365-369.

Chinta, S. J. and Andersen, J. K. (2005). Dopaminergic neurons. *The International Journal of Biochemistry & Cell Biology* **37**, 942-946.

Chizhikov, V., Steshina, E., Roberts, R., Ilkin, Y., Washburn, L. and Millen, K. J. (2006). Molecular definition of an allelic series of mutations disrupting the mouse *Lmx1a* (*dreher*) gene. *Mammalian Genome* **17**, 1025-1032.

Chizhikov, V. V. and Millen, K. J. (2004a). Control of Roof Plate Development and Signaling by Lmx1b in the Caudal Vertebrate CNS. *J. Neurosci.* **24**, 5694-5703.

Chizhikov, V. V. and Millen, K. J. (2004b). Control of roof plate formation by Lmx1a in the developing spinal cord. *Development* **131**, 2693-2705.

Collombat, P., Mansouri, A., Hecksher-Sorensen, J., Serup, P., Krull, J., Gradwohl, G. and Gruss, P. (2003). Opposing actions of Arx and Pax4 in endocrine pancreas development. *Genes Dev.* **17**, 2591-2603.

Colombo, E., Galli, R., Cossu, G., Gécz, J. and Broccoli, V. (2004). Mouse orthologue of ARX, a gene mutated in several X-linked forms of mental retardation and epilepsy, is a marker of adult neural stem cells and forebrain GABAergic neurons. *Developmental Dynamics* **231**, 631-639.

Conlon, R. A. and Herrmann, B. G. (1993). Detection of messenger RNA by in situ hybridization to postimplantation embryo whole mounts. *Methods Enzymol* **225**, 373-83.

Courey, A. J. (2001). Cooperativity in transcriptional control. *Current Biology* **11**, R250-R252.

Crossley, P. H. and Martin, G. R. (1995). The mouse Fgf8 gene encodes a family of polypeptides and is expressed in regions that direct outgrowth and patterning in the developing embryo. *Development* **121**, 439-451.

Crossley, P. H., Martinez, S. and Martin, G. R. (1996). Midbrain development induced by FGF8 in the chick embryo. *Nature* **380**, 66-68.

Curtiss, J. and Heilig, J. S. (1998). DeLIMiting development. *BioEssays* **20**, 58-69.

Cygan, J. A., Johnson, R. L. and McMahon, A. P. (1997). Novel regulatory interactions revealed by studies of murine limb pattern in Wnt-7a and En-1 mutants. *Development* **124**, 5021-5032.

Dahlström, A. and Fuxe, K. (1964). Evidence for the existence of monoamine-containing neurons in the central nervous system. I.

Demonstration of monoamines in the cell bodies of brain stem neurons. *Acta Physiol. Scand Suppl* **232**, 1-55.

Dai, J.-X., Hu, Z.-L., Shi, M., Guo, C. and Ding, Y.-Q. (2008). Postnatal ontogeny of the transcription factor *Lmx1b* in the mouse central nervous system. *The Journal of Comparative Neurology* **509**, 341-355.

Danielian, P. S. and McMahon, A. P. (1996). Engrailed-1 as a target of the Wnt-1 signalling pathway in vertebrate midbrain development. *Nature* **383**, 332-4.

Davis, C. A. and Joyner, A. L. (1988). Expression patterns of the homeo box-containing genes En-1 and En-2 and the proto-oncogene int-1 diverge during mouse development. *Genes Dev* **2**, 1736-44.

de Navascues, J. and Modolell, J. (2007). tailup, a LIM-HD gene, and Iro-C cooperate in Drosophila dorsal mesothorax specification. *Development* **134**, 1779-1788.

Dean, C., Ito, M., Makarenkova, H. P., Faber, S. C. and Lang, R. A. (2004). Bmp7 regulates branching morphogenesis of the lacrimal gland by promoting mesenchymal proliferation and condensation. *Development* **131**, 4155-4165.

Deane, J. E., Ryan, D. P., Sunde, M., Maher, M. J., Guss, J. M., Visvader, J. E. and Matthews, J. M. (2004). Tandem LIM domains provide synergistic binding in the LMO4:Ldb1 complex. *EMBO J* **23**, 3589-98.

Demyanenko, G. P., Shibata, Y. and Maness, P. F. (2001). Altered distribution of dopaminergic neurons in the brain of L1 null mice. *Developmental Brain Research* **126**, 21-30.

Denayer, T., Locker, M., Borday, C., Deroo, T., Janssens, S., Hecht, A., van Roy, F., Perron, M. and Vleminckx, K. (2008). Canonical Wnt Signaling Controls Proliferation of Retinal Stem/progenitor Cells in Post-embryonic Xenopus Eyes. *Stem Cells*, 2007-0900.

Di Chiara, G., Bassareo, V., Fenu, S., De Luca, M. A., Spina, L., Cadoni, C., Acquas, E., Carboni, E., Valentini, V. and Lecca, D. (2004). Dopamine and drug addiction: the nucleus accumbens shell connection. *Neuropharmacology* **47 Suppl 1**, 227-41.

Diaz-Benjumea, F. J. and Cohen, S. M. (1993). Interaction between dorsal and ventral cells in the imaginal disc directs wing development in Drosophila. *Cell* **75**, 741-52.

Dickinson, M. E., Krumlauf, R. and McMahon, A. P. (1994). Evidence for a mitogenic effect of Wnt-1 in the developing mammalian central nervous system. *Development* **120**, 1453-71.

Ding, Y.-Q., Marklund, U., Yuan, W., Yin, J., Wegman, L., Ericson, J., Deneris, E., Johnson, R. L. and Chen, Z.-F. (2003). Lmx1b is essential for the development of serotonergic neurons. *Nat Neurosci* **6**, 933-938.

Ding, Y.-Q., Yin, J., Kania, A., Zhao, Z.-Q., Johnson, R. L. and Chen, Z.-F. (2004). Lmx1b controls the differentiation and migration of the superficial dorsal horn neurons of the spinal cord. *Development* **131**, 3693-3703.

Dreyer, S. D., Morello, R., German, M. S., Zabel, B., Winterpacht, A., Lunstrum, G. P., Horton, W. A., Oberg, K. C. and Lee, B. (2000). LMX1B transactivation and expression in nail-patella syndrome. *Hum. Mol. Genet.* **9**, 1067-1074.

Dreyer, S. D., Zhou, G., Baldini, A., Winterpacht, A., Zabel, B., Cole, W., Johnson, R. L. and Lee, B. (1998). Mutations in LMX1B cause abnormal skeletal patterning and renal dysplasia in nail patella syndrome. *Nat Genet* **19**, 47-50.

Dunston, J. A., Reimschisel, T., Ding, Y.-Q., Sweeney, E., Johnson, R. L., Chen, Z.-F. and McIntosh, I. (2005). A neurological phenotype in nail patella syndrome (NPS) patients illuminated by studies of murine Lmx1b expression. *Eur J Hum Genet* **13**, 330-335.

Durstewitz, D. and Seamans, J. K. (2008). The Dual-State Theory of Prefrontal Cortex Dopamine Function with Relevance to Catechol-O-Methyltransferase Genotypes and Schizophrenia. *Biological Psychiatry* **In Press, Corrected Proof**.

Echelard, Y., Epstein, D. J., St-Jacques, B., Shen, L., Mohler, J., McMahon, J. A. and McMahon, A. P. (1993). Sonic hedgehog, a member of a family of putative signaling molecules, is implicated in the regulation of CNS polarity. *Cell* **75**, 1417-1430.

Eells, J. B. (2003). The control of dopamine neuron development, function and survival: insights from transgenic mice and the relevance to human disease. *Curr Med Chem* **10**, 857-70.

Egan, M. F. and Weinberger, D. R. (1997). Neurobiology of schizophrenia. *Curr Opin Neurobiol* **7**, 701-7.

Epstein, D. J., McMahon, A. P. and Joyner, A. L. (1999). Regionalization of Sonic hedgehog transcription along the anteroposterior axis of the mouse central nervous system is regulated by Hnf3-dependent and -independent mechanisms. *Development* **126**, 281-292.

Failli, V., Bachy, I. and Retaux, S. (2002). Expression of the LIM-homeodomain gene Lmx1a (dreher) during development of the mouse nervous system. *Mechanisms of Development* **118**, 225-228.

Failli, V., Rogard, M., Mattei, M.-G., Vernier, P. and Rétaux, S. (2000). Lhx9 and Lhx9[alpha] LIM-Homeodomain Factors: Genomic Structure, Expression Patterns, Chromosomal Localization, and Phylogenetic Analysis. *Genomics* **64**, 307-317.

Falck, B., Hillarp, N. A., Thieme, G. and Torp, A. (1962). Fluorescence of catecholamines and related compounds condensed with formaldehyde. *J. Histochem. Cytochem.* **10**, 348-354.

Fallon, J. H. and Moore, R. Y. (1978). Catecholamine innervation of the basal forebrain IV. Topography of the dopamine projection to the basal forebrain and neostriatum. *The Journal of Comparative Neurology* **180**, 545-579.

Fallon, J. H., Riley, J. N. and Moore, R. Y. (1978). Substantia nigra dopamine neurons: separate populations project to neostriatum and allocortex. *Neuroscience Letters* **7**, 157-162.

Farago, A. F., Awatramani, R. B. and Dymecki, S. M. (2006). Assembly of the Brainstem Cochlear Nuclear Complex Is Revealed by Intersectional and Subtractive Genetic Fate Maps. *Neuron* **50**, 205-218.

Farkas, L. M., Dunker, N., Roussa, E., Unsicker, K. and Krieglstein, K. (2003). Transforming growth factor-beta(s) are essential for the development of midbrain dopaminergic neurons in vitro and in vivo. *J Neurosci* **23**, 5178-86.

Feil, R., Wagner, J. r., Metzger, D. and Chambon, P. (1997). Regulation of Cre Recombinase Activity by Mutated Estrogen Receptor Ligand-Binding Domains. *Biochemical and Biophysical Research Communications* **237**, 752-757.

Fernández-Fúnez, P., Lu, C.-H., Rincón-Limas, D. E., García-Bellido, A. and Botas, J. (1998). The relative expression amounts of apterous and its co-factor dLdb/Chip are critical for dorso-ventral compartmentalization in the Drosophila wing. *EMBO J* **17**, 6846-53.

Ferri, A. L., Cavallaro, M., Braida, D., Di Cristofano, A., Canta, A., Vezzani, A., Ottolenghi, S., Pandolfi, P. P., Sala, M., DeBiasi, S. et al. (2004). Sox2 deficiency causes neurodegeneration and impaired neurogenesis in the adult mouse brain. *Development* **131**, 3805-19.

Ferri, A. L. M., Lin, W., Mavromatakis, Y. E., Wang, J. C., Sasaki, H., Whitsett, J. A. and Ang, S.-L. (2007). Foxa1 and Foxa2 regulate multiple phases of midbrain dopaminergic neuron development in a dosage-dependent manner. *Development* **134**, 2761-2769.

Feuerstein, R., Wang, X., Song, D., Cooke, N. E. and Liebhaber, S. A. (1994). The LIM/Double Zinc-Finger Motif Functions as a Protein Dimerization Domain. *Proceedings of the National Academy of Sciences* **91**, 10655-10659.

Flanders, K. C., Ludecke, G., Engels, S., Cissel, D. S., Roberts, A. B., Kondaiah, P., Lafyatis, R., Sporn, M. B. and Unsicker, K. (1991). Localization and actions of transforming growth factor-betas in the embryonic nervous system. *Development* **113**, 183-191.

Flores, J., Galan-Rodriguez, B., Ramiro-Fuentes, S. and Fernandez-Espejo, E. (2005). Role for Dopamine Neurons of the Rostral Linear Nucleus and Periaqueductal Gray in the Rewarding and Sensitizing Properties of Heroin. *Neuropsychopharmacology*.

Freyd, G., Kim, S. K. and Horvitz, H. R. (1990). Novel cysteine-rich motif and homeodomain in the product of the Caenorhabditis elegans cell lineage gene lin-II. *Nature* **344**, 876-879.

Gates, M. A., Coupe, V. M., Torres, E. M., Fricker-Gates, R. A. and Dunnett, S. B. (2004). Spatially and temporally restricted chemoattractive and chemorepulsive cues direct the formation of the nigro-striatal circuit. *European Journal of Neuroscience* **19**, 831-844.

Gates, M. A., Torres, E. M., White, A., Fricker-Gates, R. A. and Dunnett, S. B. (2006). Re-examining the ontogeny of substantia nigra dopamine neurons. *European Journal of Neuroscience* **23**, 1384-1390.

Geffard, M., Buijs, R. M., Seguela, P., Pool, C. W. and Le Moal, M. (1984). First demonstration of highly specific and sensitive antibodies against dopamine. *Brain Research* **294**, 161-165.

Gehring, W. J., Qian, Y. Q., Billeter, M., Furukubo-Tokunaga, K., Schier, A. F., Resendez-Perez, D., Affolter, M., Otting, G. and W,thrich, K. (1994). Homeodomain-DNA recognition. *Cell* **78**, 211-223.

Gerfen, C. R., Herkenham, M. and Thibault, J. (1987). The neostriatal mosaic: II. Patch- and matrix-directed mesostriatal dopaminergic and non-dopaminergic systems. *J. Neurosci.* **7**, 3915-3934.

German, D. C. and Manaye, K. F. (1993). Midbrain dopaminergic neurons (nuclei A8, A9, and A10): Three-dimensional reconstruction in the rat. *The Journal of Comparative Neurology* **331**, 297-309.

German, M. S., Wang, J., Chadwick, R. B. and Rutter, W. J. (1992). Synergistic activation of the insulin gene by a LIM-homeo domain protein and a basic helix-loop-helix protein: building a functional insulin minienhancer complex. *Genes Dev.* **6**, 2165-2176.

Gerrits, M. A. F. M., Petromilli, P., Westenberg, H. G. M., Di Chiara, G. and van Ree, J. M. (2002). Decrease in basal dopamine levels in the nucleus accumbens shell during daily drug-seeking behaviour in rats. *Brain Research* **924**, 141-150.

Gerrits, M. A. F. M. and Van Ree, J. M. (1996). Effect of nucleus accumbens dopamine depletion on motivational aspects involved in initiation of cocaine and heroin self-administration in rats. *Brain Research* **713**, 114-124.

Gibb, W. R. and Lees, A. J. (1991). Anatomy, pigmentation, ventral and dorsal subpopulations of the substantia nigra, and differential cell death in Parkinson's disease. *J Neurol Neurosurg Psychiatry* **54**, 388-96.

Gilbert, S. F. (2003). Developmental Biology: Seventh Edition: Sinauer Associates, Inc.

Gill, G. N. (1995). The enigma of LIM domains. *Structure* **3**, 1285-1289.

Giraldez, F. (1998). Regionalized Organizing Activity of the Neural Tube Revealed by the Regulation of lmx1 in the Otic Vesicle. *Developmental Biology* **203**, 189-200.

Giros, B. and Caron, M. G. (1993). Molecular characterization of the dopamine transporter. *Trends in Pharmacological Sciences* **14**, 43-49.

Golden, G. S. (1972). Embryologic demonstration of a nigro-striatal projection in the mouse. *Brain Research* **44**, 278-282.

Goridis, C. and Rohrer, H. (2002). Specification of catecholaminergic and serotonergic neurons. *Nat Rev Neurosci* **3**, 531-541.

Grigoriou, M., Tucker, A. S., Sharpe, P. T. and Pachnis, V. (1998). Expression and regulation of Lhx6 and Lhx7, a novel subfamily of LIM homeodomain encoding genes, suggests a role in mammalian head development. *Development* **125**, 2063-2074.

Guillemot, F. (1999). Vertebrate bHLH Genes and the Determination of Neuronal Fates. *Experimental Cell Research* **253**, 357-364.

Guo, C., Qiu, H.-Y., Huang, Y., Chen, H., Yang, R.-Q., Chen, S.-D., Johnson, R. L., Chen, Z.-F. and Ding, Y.-Q. (2007). Lmx1b is essential for Fgf8 and Wnt1 expression in the isthmic organizer during tectum and cerebellum development in mice. *Development* **134**, 317-325.

Hanaway, J., McConnell, J. A. and Netsky, M. G. (1971). Histogenesis of the substantia nigra, ventral tegmental area of Tsai and interpeduncular nucleus: An autoradiographic study of the mesencephalon in the rat. *The Journal of Comparative Neurology* **142**, 59-73.

Hanes, S. D., Riddihough, G., Ish-Horowicz, D. and Brent, R. (1994). Specific DNA recognition and intersite spacing are critical for action of the bicoid morphogen. *Mol. Cell. Biol.* **14**, 3364-3375.

Harada, N., Tamai, Y., Ishikawa, T.-o., Sauer, B., Takaku, K., Oshima, M. and Taketo, M. M. (1999). Intestinal polyposis in mice with a dominant stable mutation of the beta-catenin gene. *EMBO J* **18**, 5931-42.

Harfe, B. D., Scherz, P. J., Nissim, S., Tian, H., McMahon, A. P. and Tabin, C. J. (2004). Evidence for an Expansion-Based Temporal Shh Gradient in Specifying Vertebrate Digit Identities. *Cell* **118**, 517-528.

Hasue, R. H. and Shammah-Lagnado, S. J. (2002). Origin of the dopaminergic innervation of the central extended amygdala and accumbens shell: A combined retrograde tracing and immunohistochemical study in the rat. *The Journal of Comparative Neurology* **454**, 15-33.

Hayashi, S. and McMahon, A. P. (2002). Efficient Recombination in Diverse Tissues by a Tamoxifen-Inducible Form of Cre: A Tool for Temporally Regulated Gene Activation/Inactivation in the Mouse. *Developmental Biology* **244**, 305-318.

Helms, A. W. and Johnson, J. E. (2003). Specification of dorsal spinal cord interneurons. *Current Opinion in Neurobiology* **13**, 42-49.

Hermanson, E., Joseph, B., Castro, D., Lindqvist, E., Aarnisalo, P., WallÈn, s., Benoit, G., Hengerer, B., Olson, L. and Perlmann, T. (2003). Nurr1 regulates dopamine synthesis and storage in MN9D dopamine cells. *Experimental Cell Research* **288**, 324-334.

Hiratani, I., Yamamoto, N., Mochizuki, T., Ohmori, S.-y. and Taira, M. (2003). Selective degradation of excess Ldb1 by Rnf12/RLIM confers proper Ldb1 expression levels and Xlim-1/Ldb1 stoichiometry in Xenopus organizer functions. *Development* **130**, 4161-4175.

Hirota, J. and Mombaerts, P. (2004). The LIM-homeodomain protein Lhx2 is required for complete development of mouse olfactory sensory neurons. *Proceedings of the National Academy of Sciences of the United States of America* **101**, 8751-8755.

Hirsch, E., Graybiel, A. M. and Agid, Y. A. (1988). Melanized dopaminergic neurons are differentially susceptible to degeneration in Parkinson's disease. *Nature* **334**, 345-8.

Hobert, O. and Westphal, H. (2000). Functions of LIM-homeobox genes. *Trends in Genetics* **16**, 75-83.

Hökfelt, T., Johansson, O. and Goldstein, M. (1984). Chemical Anatomy of the Brain. *Science* **225**, 1326-1334.

Holland, P. W. H. and Takahashi, T. (2005). The evolution of homeobox genes: Implications for the study of brain development. *Brain Research Bulletin* **66**, 484-490.

Holmes, G. P., Negus, K., Burridge, L., Raman, S., Algar, E., Yamada, T. and Little, M. H. (1998). Distinct but overlapping expression patterns of two vertebrate slit homologs implies functional roles in CNS development and organogenesis. *Mechanisms of Development* **79**, 57-72.

Horn, A. S. (1990). Dopamine uptake: a review of progress in the last decade. *Prog Neurobiol* **34**, 387-400.

Houzelstein, D., Cohen, A., Buckingham, M. E. and Robert, B. (1997). Insertional mutation of the mouse Msx1 homeobox gene by an nlacZ reporter gene. *Mechanisms of Development* **65**, 123-133.

Hovde, S., Abate-Shen, C. and Geiger, J. H. (2001). Crystal Structure of the Msx-1 Homeodomain/DNA Complex. *Biochemistry* **40**, 12013-12021.

Hunter, C. S. and Rhodes, S. J. (2005). LIM-homeodomain genes in mammalian development and human disease. *Mol Biol Rep* **32**, 67-77.

Hynes, M., Porter, J. A., Chiang, C., Chang, D., Tessier-Lavigne, M., Beachy, P. A. and Rosenthal, A. (1995a). Induction of midbrain dopaminergic neurons by Sonic hedgehog. *Neuron* **15**, 35-44.

Hynes, M., Poulsen, K., Tessier-Lavigne, M. and Rosenthal, A. (1995b). Control of neuronal diversity by the floor plate: Contact-mediated induction of midbrain dopaminergic neurons. *Cell* **80**, 95-101.

Hynes, M. and Rosenthal, A. (1999). Specification of dopaminergic and serotonergic neurons in the vertebrate CNS. *Current Opinion in Neurobiology* **9**, 26-36.

Ille, F., Atanasoski, S., Falk, S., Ittner, L. M., Marki, D., Buchmann-Moller, S., Wurdak, H., Suter, U., Taketo, M. M. and Sommer, L. (2007). Wnt/BMP signal integration regulates the balance between proliferation and differentiation of neuroepithelial cells in the dorsal spinal cord. *Developmental Biology* **304**, 394-408.

Inanobe, A., Yoshimoto, Y., Horio, Y., Morishige, K.-I., Hibino, H., Matsumoto, S., Tokunaga, Y., Maeda, T., Hata, Y., Takai, Y. et al. (1999). Characterization of G-Protein-Gated K+ Channels Composed of Kir3.2 Subunits in Dopaminergic Neurons of the Substantia Nigra. *J. Neurosci.* **19**, 1006-1017.

Indra, A. K., Warot, X., Brocard, J., Bornert, J. M., Xiao, J. H., Chambon, P. and Metzger, D. (1999). Temporally-controlled site-specific mutagenesis in the basal layer of the epidermis: comparison of the recombinase activity of the tamoxifen- inducible Cre-ER(T) and Cre-ER(T2) recombinases. *Nucl. Acids Res.* **27**, 4324-4327.

Ippel, H., Larsson, G., Behravan, G., Zdunek, J., Lundqvist, M., Schleucher, J. r., Lycksell, P.-O. and Wijmenga, S. (1999). The solution structure of the homeodomain of the rat insulin-gene enhancer protein Isl-1. Comparison with other homeodomains. *Journal of Molecular Biology* **288**, 689-703.

Ishibashi, M. and McMahon, A. P. (2002). A sonic hedgehog-dependent signaling relay regulates growth of diencephalic and mesencephalic primordia in the early mouse embryo. *Development* **129**, 4807-4819.

Iwawaki, T., Kohno, K. and Kobayashi, K. (2000). Identification of a Potential Nurr1 Response Element That Activates the Tyrosine Hydroxylase Gene Promoter in Cultured Cells. *Biochemical and Biophysical Research Communications* **274**, 590-595.

Jackson-Lewis, V., Vila, M., Djaldetti, R., Guegan, C., Liberatore, G., Liu, J., O'Malley, K. L., Burke, R. E. and Przedborski, S. (2000). Developmental cell death in dopaminergic neurons of the substantia nigra of mice. *The Journal of Comparative Neurology* **424**, 476-488.

Jacob, J., Ferri, A. L., Milton, C., Prin, F., Pla, P., Lin, W., Gavalas, A., Ang, S.-L. and Briscoe, J. (2007). Transcriptional repression coordinates the temporal switch from motor to serotonergic neurogenesis. *Nat Neurosci* **10**, 1433-1439.

Jacobs, F. M. J., Smits, S. M., Noorlander, C. W., von Oerthel, L., van der Linden, A. J. A., Burbach, J. P. H. and Smidt, M. P. (2007). Retinoic acid counteracts developmental defects in the substantia nigra caused by Pitx3 deficiency. *Development* **134**, 2673-2684.

Janec, E. and Burke, R. E. (1993). Naturally Occurring Cell Death during Postnatal Development of the Substantia Nigra Pars Compacta of Rat. *Molecular and Cellular Neuroscience* **4**, 30-35.

Jeong, Y. and Epstein, D. J. (2003). Distinct regulators of Shh transcription in the floor plate and notochord indicate separate origins for these tissues in the mouse node. *Development* **130**, 3891-3902.

Jessell, T. M. (2000). Neuronal specification in the spinal cord: inductive signals and transcriptional codes. *Nat Rev Genet* **1**, 20-29.

Johnson, J. D., Zhang, W., Rudnick, A., Rutter, W. J. and German, M. S. (1997). Transcriptional synergy between LIM-homeodomain proteins and basic helix-loop-helix proteins: the LIM2 domain determines specificity. *Mol. Cell. Biol.* **17**, 3488-3496.

Joyner, A. L., Kornberg, T., Coleman, K. G., Cox, D. R. and Martin, G. R. (1985). Expression during embryogenesis of a mouse gene with sequence homology to the Drosophila engrailed gene. *Cell* **43**, 29-37.

Joyner, A. L. and Martin, G. R. (1987). En-1 and En-2, two mouse genes with sequence homology to the Drosophila engrailed gene: expression during embryogenesis. *Genes Dev* **1**, 29-38.

Joyner, A. L. and Zervas, M. (2006). Genetic inducible fate mapping in mouse: Establishing genetic lineages and defining genetic neuroanatomy in the nervous system. *Developmental Dynamics* **235**, 2376-2385.

Jurata, L. W. and Gill, G. N. (1997). Functional analysis of the nuclear LIM domain interactor NLI. *Mol. Cell. Biol.* **17**, 5688-5698.

Jurata, L. W., Kenny, D. A. and Gill, G. N. (1996). Nuclear LIM interactor, a rhombotin and LIM homeodomain interacting protein, is expressed early in neuronal development. *Proceedings of the National Academy of Sciences* **93**, 11693-11698.

Jurata, L. W., Pfaff, S. L. and Gill, G. N. (1998). The Nuclear LIM Domain Interactor NLI Mediates Homo- and Heterodimerization of LIM Domain Transcription Factors. *J. Biol. Chem.* **273**, 3152-3157.

Kala, K., Jukkola, T., Pata, I. and Partanen, J. (2008). Analysis of the midbrain-hindbrain boundary cell fate using a boundary cell-specific Cre-mouse strain. *genesis* **46**, 29-36.

Kalsbeek, A., Voorn, P., Buijs, R. M., Pool, C. W. and Uylings, H. B. M. (1988). Development of the dopaminergic innervation in the prefrontal cortex of the rat. *The Journal of Comparative Neurology* **269**, 58-72.

Kania, A., Johnson, R. L. and Jessell, T. M. (2000). Coordinate Roles for LIM Homeobox Genes in Directing the Dorsoventral Trajectory of Motor Axons in the Vertebrate Limb. *Cell* **102**, 161-173.

Karlsson, O., Thor, S., Norberg, T., Ohlsson, H. and Edlund, T. (1990). Insulin gene enhancer binding protein Isl-1 is a member of a novel class of proteins containing both a homeo-and a Cys-His domain. *Nature* **344**, 879-882.

Kawano, H., Ohyama, K., Kawamura, K. and Nagatsu, I. (1995). Migration of dopaminergic neurons in the embryonic mesencephalon of mice. *Developmental Brain Research* **86**, 101-113.

Kele, J., Simplicio, N., Ferri, A. L. M., Mira, H., Guillemot, F., Arenas, E. and Ang, S.-L. (2006). Neurogenin 2 is required for the development of ventral midbrain dopaminergic neurons. *Development* **133**, 495-505.

Kenney, A. M. and Rowitch, D. H. (2000). Sonic hedgehog Promotes G1 Cyclin Expression and Sustained Cell Cycle Progression in Mammalian Neuronal Precursors. *Mol. Cell. Biol.* **20**, 9055-9067.

Kim, H.-J., Sugimori, M., Nakafuku, M. and Svendsen, C. N. (2007). Control of neurogenesis and tyrosine hydroxylase expression in neural progenitor cells through bHLH proteins and Nurr1. *Experimental Neurology* **203**, 394-405.

Kimmel, R. A., Turnbull, D. H., Blanquet, V., Wurst, W., Loomis, C. A. and Joyner, A. L. (2000). Two lineage boundaries coordinate vertebrate apical ectodermal ridge formation. *Genes Dev.* **14**, 1377-1389.

Kitamura, K., Yanazawa, M., Sugiyama, N., Miura, H., Iizuka-Kogo, A., Kusaka, M., Omichi, K., Suzuki, R., Kato-Fukui, Y., Kamiirisa, K. et al. (2002). Mutation of ARX causes abnormal development of forebrain and testes in mice and X-linked lissencephaly with abnormal genitalia in humans. *Nat Genet* **32**, 359-369.

Kittappa, R., Chang, W. W., Awatramani, R. B. and McKay, R. D. G. (2007). The foxa2 Gene Controls the Birth and Spontaneous Degeneration of Dopamine Neurons in Old Age. *PLoS Biology* **5**, e325.

Knoers, N. V., Bongers, E. M., van Beersum, S. E., Lommen, E. J., van Bokhoven, H. and Hol, F. A. (2000). Nail-patella syndrome: identification of mutations in the LMX1B gene in Dutch families. *J Am Soc Nephrol* **11**, 1762-6.

Lai, E., Prezioso, V. R., Smith, E., Litvin, O., Costa, R. H. and Darnell, J. E., Jr. (1990). HNF-3A, a hepatocyte-enriched transcription factor of novel structure is regulated transcriptionally. *Genes Dev* **4**, 1427-36.

Lai, E., Prezioso, V. R., Tao, W. F., Chen, W. S. and Darnell, J. E., Jr. (1991). Hepatocyte nuclear factor 3 alpha belongs to a gene family in mammals that is homologous to the Drosophila homeotic gene fork head. *Genes Dev* **5**, 416-27.

Lakhina, V., Falnikar, A., Bhatnagar, L. and Tole, S. (2007). Early thalamocortical tract guidance and topographic sorting of thalamic projections requires LIM-homeodomain gene Lhx2. *Developmental Biology* **306**, 703-713.

Lang, A. E. and Lozano, A. M. (1998a). Parkinson's Disease- First of Two Parts. *N Engl J Med* **339**, 1044-1053.

Lang, A. E. and Lozano, A. M. (1998b). Parkinson's Disease- Second of Two Parts. *N Engl J Med* **339**, 1130-1143.

Laughon, A. (1991). DNA binding specificity of homeodomains. *Biochemistry* **30**, 11357-11367.

Le, W.-d., Xu, P., Jankovic, J., Jiang, H., Appel, S. H., Smith, R. G. and Vassilatis, D. K. (2003). Mutations in NR4A2 associated with familial Parkinson disease. *Nat Genet* **33**, 85-89.

Lee, K. J. and Jessell, T. M. (1999). The specification of dorsal cell fates in the vertebrate central nervous system. *Annual Review of Neuroscience* **22**, 261-294.

Lee, S.-K. and Pfaff, S. L. (2001). Transcriptional networks regulating neuronal identity in the developing spinal cord. *Nat Neurosci.*

Lee, S.-K. and Pfaff, S. L. (2003). Synchronization of Neurogenesis and Motor Neuron Specification by Direct Coupling of bHLH and Homeodomain Transcription Factors. *Neuron* **38**, 731-745.

Levitt, M., Spector, S., Sjoerdsma, A. and Udenfriend, S. (1965). Elucidation of the Rate-Limiting Step in Norepinephrine Biosynthesis in the Perfused Guinea-Pig Heart. *J Pharmacol Exp Ther* **148**, 1-8.

Lewis, E. B. (1978). A gene complex controlling segmentation in Drosophila. *Nature* **276**, 565-570.

Li, H., Witte, D. P., W.Branford, W., Aronow, B. J., Weinstein, M., Kaur, S., Wert, S., Singh, G., Schreiner, C. M., Whitsett, J. A. et al. (1994). Gsh-4 encodes a LIM-

type homeodomain, is expressed in the developing central nervous system and is required for early postnatal survival. *EMBO J* **13**, 2876-85.

Liang, C. L., Sinton, C. M. and German, D. C. (1996). Midbrain dopaminergic neurons in the mouse: co-localization with Calbindin-D28k and calretinin. *Neuroscience* **75**, 523-533.

Liem, K. F., Tremml, G. and Jessell, T. M. (1997). A Role for the Roof Plate and Its Resident TGF[beta]-Related Proteins in Neuronal Patterning in the Dorsal Spinal Cord. *Cell* **91**, 127-138.

Lindvall, O. and Björklund, A. (2004). Cell Therapy in Parkinson's Disease. *NeuroRx* **1**, 382-93.

Lindvall, O., Björklund, A. and Divac, I. (1977). Organization of mesencephalic dopamine neurons projecting to neocortex and septum. *Adv Biochem Psychopharmacol* **16**, 39-46.

Liodis, P., Denaxa, M., Grigoriou, M., Akufo-Addo, C., Yanagawa, Y. and Pachnis, V. (2007). Lhx6 activity is required for the normal migration and specification of cortical interneuron subtypes. *J. Neurosci.* **27**, 3078-3089.

Liu, A. and Joyner, A. L. (2001). EN and GBX2 play essential roles downstream of FGF8 in patterning the mouse mid/hindbrain region. *Development* **128**, 181-191.

Longo, A., Guanga, G. P. and Rose, R. B. (2007). Structural Basis for Induced Fit Mechanisms in DNA Recognition by the Pdx1 Homeodomain. *Biochemistry* **46**, 2948-2957.

Lumsden, A. and Krumlauf, R. (1996). Patterning the Vertebrate Neuraxis. *Science* **274**, 1109-1115.

Lyons, J. P. and Wahlsten, D. (1988). Postnatal Development of Brain and Behavior of Shaker Short-Tail Mice. *Behavior Genetics* **18**, 35.

Ma, Y.-C., Song, M.-R., Park, J. P., Henry Ho, H.-Y., Hu, L., Kurtev, M. V., Zieg, J., Ma, Q., Pfaff, S. L. and Greenberg, M. E. (2008). Regulation of Motor Neuron Specification by Phosphorylation of Neurogenin 2. *Neuron* **58**, 65-77.

Mangale, V. S., Hirokawa, K. E., Satyaki, P. R. V., Gokulchandran, N., Chikbire, S., Subramanian, L., Shetty, A. S., Martynoga, B., Paul, J., Mai, M. V. et al. (2008). Lhx2 Selector Activity Specifies Cortical Identity and Suppresses Hippocampal Organizer Fate. *Science* **319**, 304-309.

Marchand, R. and Poirier, L. J. (1983). Isthmic origin of neurons of the rat substantia nigra. *Neuroscience* **9**, 373-381.

Marín, F., Herrero, M.-T., Vyas, S. and Puelles, L. (2005). Ontogeny of tyrosine hydroxylase mRNA expression in mid- and forebrain: Neuromeric pattern and novel positive regions. *Developmental Dynamics* **234**, 709-717.

Marini, M., Giacopelli, F., Seri, M. and Ravazzolo, R. (2005). Interaction of the LMX1B and PAX2 gene products suggests possible molecular basis of differential phenotypes in Nail-Patella syndrome. *Eur J Hum Genet* **13**, 789-792.

Matsunaga, E., Katahira, T. and Nakamura, H. (2002). Role of Lmx1b and Wnt1 in mesencephalon and metencephalon development. *Development* **129**, 5269-5277.

Matthews, J. M. and Visvader, J. E. (2003). LIM-domain-binding protein 1: a multifunctional cofactor that interacts with diverse proteins. *EMBO Reports* **4**, 1132-7.

Mavromatakis, Y. E. (2006). Role of the forkhead transcription factor *Foxa2* in the development of the ventral mesencephalon: A study using conditional mouse mutants. *PhD thesis*, pp. 347: University of London.

McCaffery, P. and Dräger, U. C. (1994). High levels of a retinoic acid-generating dehydrogenase in the meso-telencephalic dopamine system. *Proc Natl Acad Sci U S A* **91**, 7772-6.

McGinnis, W., Levine, M. S., Hafen, E., Kuroiwa, A. and Gehring, W. J. (1984). A conserved DNA sequence in homoeotic genes of the Drosophila Antennapedia and bithorax complexes. *Nature* **308**, 428-433.

McMahon, A. P., Joyner, A. L., Bradley, A. and McMahon, J. A. (1992). The midbrain-hindbrain phenotype of Wnt-1-/Wnt-1- mice results from stepwise deletion of engrailed-expressing cells by 9.5 days postcoitum. *Cell* **69**, 581-95.

Megason, S. G. and McMahon, A. P. (2002). A mitogen gradient of dorsal midline Wnts organizes growth in the CNS. *Development* **129**, 2087-2098.

Mendez, I., Sanchez-Pernaute, R., Cooper, O., Vinuela, A., Ferrari, D., Bjorklund, L., Dagher, A. and Isacson, O. (2005). Cell type analysis of functional fetal dopamine cell suspension transplants in the striatum and substantia nigra of patients with Parkinson's disease. *Brain* **128**, 1498-1510.

Milán, M. and Cohen, S. M. (1999). Regulation of LIM Homeodomain Activity In Vivo: A Tetramer of dLDB and Apterous Confers Activity and Capacity for Regulation by dLMO. *Molecular Cell* **4**, 267-273.

Milán, M., Diaz-Benjumea, F. J. and Cohen, S. M. (1998). Beadex encodes an LMO protein that regulates Apterous LIM-homeodomain activity in Drosophila wing development: a model for LMO oncogene function. *Genes Dev.* **12**, 2912-2920.

Millen, K. J., Millonig, J. H. and Hatten, M. E. (2004). Roof plate and dorsal spinal cord dI1 interneuron development in the dreher mutant mouse. *Developmental Biology* **270**, 382-392.

Millonig, J. H., Millen, K. J. and Hatten, M. E. (2000). The mouse Dreher gene Lmx1a controls formation of the roof plate in the vertebrate CNS. *Nature* **403**, 764-769.

Miura, H., Yanazawa, M., Kato, K. and Kitamura, K. (1997). Expression of a novel aristaless related homeobox gene 'Arx' in the vertebrate telencephalon, diencephalon and floor plate. *Mechanisms of Development* **65**, 99-109.

Molyneaux, B. J., Arlotta, P., Menezes, J. R. L. and Macklis, J. D. (2007). Neuronal subtype specification in the cerebral cortex. *Nat Rev Neurosci* **8**, 427-437.

Moore, D. J., West, A. B., Dawson, V. L. and Dawson, T. M. (2005). Molecular pathophysiology of Parkinson's disease. *Annual Review of Neuroscience* **28**, 57-87.

Muroyama, Y., Fujihara, M., Ikeya, M., Kondoh, H. and Takada, S. (2002). Wnt signaling plays an essential role in neuronal specification of the dorsal spinal cord. *Genes Dev.* **16**, 548-553.

Nagatsu, T., Levitt, M. and Udenfriend, S. (1964a). Conversion of L-tyrosine to 3,4-dihydroxyphenylalanine by cell-free preparations of brain and sympathetically innervated tissues. *Biochem Biophys Res Commun* **14**, 543-9.

Nagatsu, T., Levitt, M. and Udenfriend, S. (1964b). Tyrosine Hydroxylase. The Initial Step in Norepinephrine Biosynthesis. *J Biol Chem* **239**, 2910-7.

Nakagawa, Y. and O'Leary, D. D. M. (2001). Combinatorial Expression Patterns of LIM-Homeodomain and Other Regulatory Genes Parcellate Developing Thalamus. *J. Neurosci.* **21**, 2711-2725.

Nakamura, S.-i., Ito, Y., Shirasaki, R. and Murakami, F. (2000). Local Directional Cues Control Growth Polarity of Dopaminergic Axons Along the Rostrocaudal Axis. *J. Neurosci.* **20**, 4112-4119.

Nelson, E. L., Liang, C. L., Sinton, C. M. and German, D. C. (1996). Midbrain dopaminergic neurons in the mouse: Computer-assisted mapping. *The Journal of Comparative Neurology* **369**, 361-371.

Niederreither, K., Fraulob, V., Garnier, J. M., Chambon, P. and P., D. (2002). Differential expression of retinoic acid-synthesizing (RALDH) enzymes during fetal development and organ differentiation in the mouse. *Mech Dev* **110**, 165-71.

Nishikawa, S., Goto, S., Yamada, K., Hamasaki, T. and Ushio, Y. (2003). Lack of Reelin causes malpositioning of nigral dopaminergic neurons: Evidence from comparison of normal and *Reln(rl)* mutant mice. *The Journal of Comparative Neurology* **461**, 166-173.

Nishioka, N., Nagano, S., Nakayama, R., Kiyonari, H., Ijiri, T., Taniguchi, K., Shawlot, W., Hayashizaki, Y., Westphal, H., Behringer, R. R. et al. (2005). Ssdp1 regulates head morphogenesis of mouse embryos by activating the Lim1-Ldb1 complex. *Development* **132**, 2535-2546.

Nunes, I., Tovmasian, L. T., Silva, R. M., Burke, R. E. and Goff, S. P. (2003). Pitx3 is required for development of substantia nigra dopaminergic neurons. *PNAS* **100**, 4245-4250.

O'Hara, F. P., Beck, E., Barr, L. K., Wong, L. L., Kessler, D. S. and Riddle, R. D. (2005). Zebrafish Lmx1b.1 and Lmx1b.2 are required for maintenance of the isthmic organizer. *Development* **132**, 3163-3173.

Ohneda, K., Mirmira, R. G., Wang, J., Johnson, J. D. and German, M. S. (2000). The Homeodomain of PDX-1 Mediates Multiple Protein-Protein Interactions in the

Formation of a Transcriptional Activation Complex on the Insulin Promoter. *Mol. Cell. Biol.* **20**, 900-911.

Ohyama, K., Kawano, H., Asou, H., Fukuda, T., Oohira, A., Uyemura, K. and Kawamura, K. (1998). Coordinate expression of L1 and 6B4 proteoglycan/phosphacan is correlated with the migration of mesencephalic dopaminergic neurons in mice. *Developmental Brain Research* **107**, 219-226.

Ohyama, T. and Groves, A. K. (2004). Generation of Pax2-Cre mice by modification of a Pax2 bacterial artificial chromosome. *genesis* **38**, 195-199.

Ono, Y., Nakatani, T., Sakamoto, Y., Mizuhara, E., Minaki, Y., Kumai, M., Hamaguchi, A., Nishimura, M., Inoue, Y., Hayashi, H. et al. (2007). Differences in neurogenic potential in floor plate cells along an anteroposterior location: midbrain dopaminergic neurons originate from mesencephalic floor plate cells. *Development*, dev.02879.

Oo, T. F. and Burke, R. E. (1997). The time course of developmental cell death in phenotypically defined dopaminergic neurons of the substantia nigra. *Developmental Brain Research* **98**, 191-196.

Oo, T. F., Kholodilov, N. and Burke, R. E. (2003). Regulation of Natural Cell Death in Dopaminergic Neurons of the Substantia Nigra by Striatal Glial Cell Line-Derived Neurotrophic Factor In Vivo. *J. Neurosci.* **23**, 5141-5148.

Osborne, P. B., Halliday, G. M., Cooper, H. M. and Keast, J. R. (2005). Localization of immunoreactivity for Deleted in Colorectal Cancer (DCC), the receptor for the guidance factor netrin-1, in ventral tier dopamine projection pathways in adult rodents. *Neuroscience* **131**, 671-681.

Ostendorff, H. P., Peirano, R. I., Peters, M. A., Schluter, A., Bossenz, M., Scheffner, M. and Bach, I. (2002). Ubiquitination-dependent cofactor exchange on LIM homeodomain transcription factors. *Nature* **416**, 99-103.

Ostendorff, H. P., Tursun, B., Cornils, K., Schlüter, A., Drung, A., Güngör, C. and Bach, I. (2006). Dynamic expression of LIM cofactors in the developing mouse neural tube. *Developmental Dynamics* **235**, 786-791.

Pan, L., Deng, M., Xie, X. and Gan, L. (2008). ISL1 and BRN3B co-regulate the differentiation of murine retinal ganglion cells. *Development* **135**, 1981-1990.

Parr, B. A., Shea, M. J., Vassileva, G. and McMahon, A. P. (1993). Mouse Wnt genes exhibit discrete domains of expression in the early embryonic CNS and limb buds. *Development* **119**, 247-261.

Paxinos, G. and Franklin, K. B. J. (2001). The mouse brain in stereoyaxic coordinates. San Diego, Calif.: Academic Press.

Pearson, B. J. and Doe, C. Q. (2004). Specification of temporal identity in the developing nervous system. *Annual Review of Cell and Developmental Biology* **20**, 619-647.

Peng, S.-Y., Wang, W.-P., Meng, J., Li, T., Zhang, H., Li, Y.-m., Chen, P., Ma, K.-T. and Zhou, C.-Y. (2005). ISL1 physically interacts with BETA2 to promote insulin gene transcriptional synergy in non-[beta] cells. *Biochimica et Biophysica Acta (BBA) - Gene Structure and Expression* **1731**, 154-159.

Perez-Alvarado, G. C., Miles, C., Michelsen, J. W., Louis, H. A., Winge, D. R., Beckerle, M. C. and Summers, M. F. (1994). Structure of the carboxy-terminal LIM domain from the cysteine rich protein CRP. *Nat Struct Mol Biol* **1**, 388-398.

Pfaff, S. L., Mendelsohn, M., Stewart, C. L., Edlund, T. and Jessell, T. M. (1996). Requirement for LIM Homeobox Gene Isl1 in Motor Neuron Generation Reveals a Motor Neuron- Dependent Step in Interneuron Differentiation. *Cell* **84**, 309-320.

Pierce, R. C. and Kumaresan, V. (2006). The mesolimbic dopamine system: The final common pathway for the reinforcing effect of drugs of abuse? *Neuroscience & Biobehavioral Reviews* **30**, 215-238.

Pillai, A., Mansouri, A., Behringer, R., Westphal, H. and Goulding, M. (2007). Lhx1 and Lhx5 maintain the inhibitory-neurotransmitter status of interneurons in the dorsal spinal cord. *Development* **134**, 357-366.

Porter, F. D., Drago, J., Xu, Y., Cheema, S. S., Wassif, C., Huang, S. P., Lee, E., Grinberg, A., Massalas, J. S., Bodine, D. et al. (1997). Lhx2, a LIM homeobox gene, is required for eye, forebrain, and definitive erythrocyte development. *Development* **124**, 2935-2944.

Prakash, N., Brodski, C., Naserke, T., Puelles, E., Gogoi, R., Hall, A., Panhuysen, M., Echevarria, D., Sussel, L., Weisenhorn, D. M. V. et al. (2006). A Wnt1-regulated genetic network controls the identity and fate of midbrain-dopaminergic progenitors in vivo. *Development* **133**, 89-98.

Pressman, C. L., Chen, H. and Johnson, R. L. (2000). *Lmx1b*, a LIM homeodomain class transcription factor, is necessary for normal development of multiple tissues in the anterior segment of the murine eye. *genesis* **26**, 15-25.

Puelles, E. (2007). Genetic control of basal midbrain development. *Journal of Neuroscience Research* **85**, 3530-3534.

Puelles, L. and Verney, C. (1998). Early neuromeric distribution of tyrosine-hydroxylase-immunoreactive neurons in human embryos. *The Journal of Comparative Neurology* **394**, 283-308.

Raetzman, L. T., Ward, R. and Camper, S. A. (2002). Lhx4 and Prop1 are required for cell survival and expansion of the pituitary primordia. *Development* **129**, 4229-4239.

Rawal, N., Castelo-Branco, G., Sousa, K. M., Kele, J., Kobayashi, K., Okano, H. and Arenas, E. (2006). Dynamic temporal and cell type-specific expression of Wnt signaling components in the developing midbrain. *Experimental Cell Research* **312**, 1626-1636.

Remenyi, A., Scholer, H. R. and Wilmanns, M. (2004). Combinatorial control of gene expression. *Nat Struct Mol Biol* **11**, 812-815.

Rice, D. S. and Curran, T. (2001). Role of the reelin signaling pathway in central nervous system development. *Annual Review of Neuroscience* **24**, 1005-1039.

Riddle, R. D., Ensini, M., Nelson, C., Tsuchida, T., Jessell, T. M. and Tabin, C. (1995). Induction of the LIM homeobox gene Lmx1 by WNT7a establishes dorsoventral pattern in the vertebrate limb. *Cell* **83**, 631-640.

Rincón-Limas, D. E., Lu, C.-H., Canal, I. and Botas, J. (2000). The level of DLDB/CHIP controls the activity of the LIM homeodomain protein Apterous: evidence for a functional tetramer complex *in vivo*. *EMBO J* **19**, 2602-14.

Rogers, J. H. (1992). Immunohistochemical markers in rat brain: colocalization of calretinin and calbindin-D28k with tyrosine hydroxylase. *Brain Research* **587**, 203-210.

Rohr, C., Prestel, J., Heidet, L., Hosser, H., Kriz, W., Johnson, R. L., Antignac, C. and Witzgall, R. (2002). The LIM-homeodomain transcription factor Lmx1b plays a crucial role in podocytes. *J. Clin. Invest.* **109**, 1073-82.

Rosen, B. and Beddington, R. (1994). Detection of mRNA in whole mounts of mouse embryos using digoxigenin riboprobes. *Methods Mol Biol* **28**, 201-8.

Rosen, B. and Beddington, R. S. (1993). Whole-mount in situ hybridization in the mouse embryo: gene expression in three dimensions. *Trends Genet* **9**, 162-7.

Ross, A., Munger, S. and Capel, B. (2007). Bmp7 regulates germ cell proliferation in mouse fetal gonads. *Sex Dev.* **1**, 127-37.

Roussa, E., Wiehle, M., Dunker, N., Becker-Katins, S., Oehlke, O. and Krieglstein, K. (2006). Transforming growth factor beta is required for differentiation of mouse mesencephalic progenitors into dopaminergic neurons in vitro and in vivo: ectopic induction in dorsal mesencephalon. *Stem Cells* **24**, 2120-9.

Rowitch, D. H., Echelard, Y., Danielian, P. S., Gellner, K., Brenner, S. and McMahon, A. P. (1998). Identification of an evolutionarily conserved 110 base-pair cis-acting regulatory sequence that governs Wnt-1 expression in the murine neural plate. *Development* **125**, 2735-2746.

Rowitch, D. H., St.-Jacques, B., Lee, S. M. K., Flax, J. D., Snyder, E. Y. and McMahon, A. P. (1999). Sonic hedgehog Regulates Proliferation and Inhibits Differentiation of CNS Precursor Cells. *J. Neurosci.* **19**, 8954-8965.

Rubia, K., Overmeyer, S., Taylor, E., Brammer, M., Williams, S. C., Simmons, A. and Bullmore, E. T. (1999). Hypofrontality in attention deficit hyperactivity disorder during higher-order motor control: a study with functional MRI. *Am J Psychiatry* **156**, 891-6.

Saarimaki-Vire, J., Peltopuro, P., Lahti, L., Naserke, T., Blak, A. A., Vogt Weisenhorn, D. M., Yu, K., Ornitz, D. M., Wurst, W. and Partanen, J. (2007). Fibroblast Growth Factor Receptors Cooperate to Regulate Neural Progenitor Properties in the Developing Midbrain and Hindbrain. *J. Neurosci.* **27**, 8581-8592.

Sacchetti, P., Mitchell, T. R., Granneman, J. G. and Bannon, M. J. (2001). Nurr1 enhances transcription of the human dopamine transporter gene through a novel mechanism. *Journal of Neurochemistry* **76**, 1565-1572.

Sadler, I., Crawford, A. W., Michelsen, J. W. and Beckerle, M. C. (1992). Zyxin and cCRP: two interactive LIM domain proteins associated with the cytoskeleton. *J. Cell Biol.* **119**, 1573-1587.

Sakurada, K., Ohshima-Sakurada, M., Palmer, T. D. and Gage, F. H. (1999). Nurr1, an orphan nuclear receptor, is a transcriptional activator of endogenous tyrosine hydroxylase in neural progenitor cells derived from the adult brain. *Development* **126**, 4017-26.

Sanchez-Garcia, I. and Rabbitts, T. H. (1993). Redox Regulation of in Vitro DNA-binding Activity by the Homeodomain of the Isl-1 Protein. *Journal of Molecular Biology* **231**, 945-949.

Sanders, T. A., Lumsden, A. and Ragsdale, C. W. (2002). Arcuate Plan of Chick Midbrain Development. *J. Neurosci.* **22**, 10742-10750.

Sasaki, H. and Hogan, B. L. (1993). Differential expression of multiple fork head related genes during gastrulation and axial pattern formation in the mouse embryo. *Development* **118**, 47-59.

Saucedo-Cardenas, O., Quintana-Hau, J. D., Le, W. D., Smidt, M. P., Cox, J. J., De Mayo, F., Burbach, J. P. and Conneely, O. M. (1998). Nurr1 is essential for the induction of the dopaminergic phenotype and the survival of ventral mesencephalic late dopaminergic precursor neurons. *Proc Natl Acad Sci U S A* **95**, 4013-8.

Schein, J. C., Hunter, D. D. and Roffler-Tarlov, S. (1998). Girk2 Expression in the Ventral Midbrain, Cerebellum, and Olfactory Bulb and Its Relationship to the Murine Mutationweaver. *Developmental Biology* **204**, 432-450.

Schimmel, J. J., Crews, L., Roffler-Tarlov, S. and Chikaraishi, D. M. (1999). 4.5 kb of the rat tyrosine hydroxylase 5' flanking sequence directs tissue specific expression during development and contains consensus sites for multiple transcription factors. *Molecular Brain Research* **74**, 1-14.

Scott, M. P. and Weiner, A. J. (1984). Structural Relationships among Genes That Control Development: Sequence Homology between the Antennapedia, Ultrabithorax, and Fushi Tarazu Loci of Drosophila. *Proceedings of the National Academy of Sciences* **81**, 4115-4119.

Seeman, P., Lee, T., Chau-Wong, M. and Wong, K. (1976). Antipsychotic drug doses and neuroleptic/dopamine receptors. *Nature* **261**, 717-719.

Segawa, H., Miyashita, T., Hirate, Y., Higashijima, S.-i., Chino, N., Uyemura, K., Kikuchi, Y. and Okamoto, H. (2001). Functional Repression of Islet-2 by Disruption of Complex with Ldb Impairs Peripheral Axonal Outgrowth in Embryonic Zebrafish. *Neuron* **30**, 423-436.

Sekiguchi, M., Abe, H., Nagato, Y., Tanaka, O., Guo, H. and Nowakowski, R. S. (1996). The abnormal distribution of mossy fiber bundles and morphological

abnormalities in hippocampal formation of dreherJ (drJ/drJ) mouse. *Developmental Brain Research* **92**, 31-38.

Sekiguchi, M., Abe, H., Shimai, K., Huang, G., Inoue, T. and Nowakowski, R. S. (1994). Disruption of neuronal migration in the neocortex of the dreher mutant mouse. *Developmental Brain Research* **77**, 37-43.

Sekiguchi, M., Shimai, K., Guo, H. and Nowakowski, R. S. (1992). Cytoarchitectonic abnormalities in hippocampal formation and cerebellum of dreher mutant mouse. *Developmental Brain Research* **67**, 105-112.

Sgaier, S. K., Millet, S., Villanueva, M. P., Berenshteyn, F., Song, C. and Joyner, A. L. (2005). Morphogenetic and Cellular Movements that Shape the Mouse Cerebellum: Insights from Genetic Fate Mapping. *Neuron* **45**, 27-40.

Shamim, H., Mahmood, R., Logan, C., Doherty, P., Lumsden, A. and Mason, I. (1999). Sequential roles for Fgf4, En1 and Fgf8 in specification and regionalisation of the midbrain. *Development* **126**, 945-959.

Sharma, K., Sheng, H. Z., Lettieri, K., Li, H., Karavanov, A., Potter, S., Westphal, H. and Pfaff, S. L. (1998). LIM Homeodomain Factors Lhx3 and Lhx4 Assign Subtype Identities for Motor Neurons. *Cell* **95**, 817-828.

Shawlot, W. and Behringer, R. R. (1995). Requirement for Lim1 in head-organizer function. *Nature* **374**, 425-430.

Shawlot, W., Wakamiya, M., Kwan, K. M., Kania, A., Jessell, T. M. and Behringer, R. R. (1999). Lim1 is required in both primitive streak-derived tissues and visceral endoderm for head formation in the mouse. *Development* **126**, 4925-4932.

Shen, Q., Wang, Y., Dimos, J. T., Fasano, C. A., Phoenix, T. N., Lemischka, I. R., Ivanova, N. B., Stifani, S., Morrisey, E. E. and Temple, S. (2006). The timing of cortical neurogenesis is encoded within lineages of individual progenitor cells. *Nat Neurosci* **9**, 743-751.

Sheng, H. Z., Moriyama, K., Yamashita, T., Li, H., Potter, S. S., Mahon, K. A. and Westphal, H. (1997). Multistep Control of Pituitary Organogenesis. *Science* **278**, 1809-1812.

Sheng, H. Z., Zhadanov, A. B., Jr, B. M., Fujii, T., Bertuzzi, S., Grinberg, A., Lee, E. J., Huang, S.-P., Mahon, K. A. and Westphal, H. (1996). Specification of Pituitary Cell Lineages by the LIM Homeobox Gene Lhx3. *Science* **272**, 1004-1007.

Shtutman, M., Zhurinsky, J., Simcha, I., Albanese, C., D'Amico, M., Pestell, R. and Ben-Ze'ev, A. (1999). The cyclin D1 gene is a target of the beta -catenin/LEF-1 pathway. *Proceedings of the National Academy of Sciences* **96**, 5522-5527.

Shults, C. W., Hashimoto, R., Brady, R. M. and Gage, F. H. (1990). Dopaminergic cells align along radial glia in the developing mesencephalon of the rat. *Neuroscience* **38**, 427-436.

Simeone, A. (2000). Positioning the isthmic organizer where Otx2 and Gbx2 meet. *Trends Genet* **16**, 237-40.

Simon, H., Hornbruch, A. and Lumsden, A. (1995). Independent assignment of antero-posterior and dorso-ventral positional values in the developing chick hindbrain. *Current Biology* **5**, 205-214.

Simon, H. H., Bhatt, L., Gherbassi, D., Sgado, P. and Alberi, L. (2003). Midbrain Dopaminergic Neurons: Determination of Their Developmental Fate by Transcription Factors. *Ann NY Acad Sci* **991**, 36-47.

Simon, H. H., Saueressig, H., Wurst, W., Goulding, M. D. and O'Leary, D. D. M. (2001). Fate of Midbrain Dopaminergic Neurons Controlled by the Engrailed Genes. *J. Neurosci.* **21**, 3126-3134.

Sloop, K. W., Meier, B. C., Bridwell, J. L., Parker, G. E., Schiller, A. M. and Rhodes, S. J. (1999). Differential Activation of Pituitary Hormone Genes by Human Lhx3 Isoforms with Distinct DNA Binding Properties. *Mol Endocrinol* **13**, 2212-2225.

Smidt, M. P., Asbreuk, C. H. J., Cox, J. J., Chen, H., Johnson, R. L. and Burbach, J. P. H. (2000). A second independent pathway for development of mesencephalic dopaminergic neurons requires Lmx1b. *Nat Neurosci* **3**, 337-341.

Smidt, M. P., Smits, S. M., Bouwmeester, H., Hamers, F. P. T., van der Linden, A. J. A., Hellemons, A. J. C. G. M., Graw, J. and Burbach, J. P. H. (2004). Early developmental failure of substantia nigra dopamine neurons in mice lacking the homeodomain gene Pitx3. *Development* **131**, 1145-1155.

Smidt, M. P., van Schaick, H. S. A., Lanctot, C., Tremblay, J. J., Cox, J. J., van der Kleij, A. A. M., Wolterink, G., Drouin, J. and Burbach, J. P. H. (1997). A homeodomain gene Ptx3 has highly restricted brain expression in mesencephalic dopaminergic†neurons. *PNAS* **94**, 13305-13310.

Smits, S. M., Burbach, J. P. H. and Smidt, M. P. (2006). Developmental origin and fate of meso-diencephalic dopamine neurons. *Progress in Neurobiology* **78**, 1-16.

Solanto, M. V. (2002). Dopamine dysfunction in AD/HD: integrating clinical and basic neuroscience research. *Behav Brain Res* **130**, 65-71.

Soriano, P. (1999). Generalized lacZ expression with the ROSA26 Cre reporter strain. *Nat Genet* **21**, 70-71.

Specht, L. A., Pickel, V. M., Joh, T. H. and Reis, D. J. (1981a). Light-microscopic immunocytochemical localization of tyrosine hydroxylase in prenatal rat brain. I. Early ontogeny. *The Journal of Comparative Neurology* **199**, 233-253.

Specht, L. A., Pickel, V. M., Joh, T. H. and Reis, D. J. (1981b). Light-microscopic immunocytochemical localization of tyrosine hydroxylase in prenatal rat brain. II. Late ontogeny. *The Journal of Comparative Neurology* **199**, 255-276.

Srinivas, S., Watanabe, T., Lin, C.-S., William, C., Tanabe, Y., Jessell, T. and Costantini, F. (2001). Cre reporter strains produced by targeted insertion of EYFP and ECFP into the ROSA26 locus. *BMC Developmental Biology* **1**, 4.

Suleiman, H., Heudobler, D., Raschta, A.-S., Zhao, Y., Zhao, Q., Hertting, I., Vitzthum, H., Moeller, M. J., Holzman, L. B., Rachel, R. et al. (2007). The podocyte-

specific inactivation of Lmx1b, Ldb1 and E2a yields new insight into a transcriptional network in podocytes. *Developmental Biology* **304**, 701-712.

Suzuki, A., Ueno, N. and Hemmati-Brivanlou, A. (1997). Xenopus msx1 mediates epidermal induction and neural inhibition by BMP4. *Development* **124**, 3037-3044.

Taira, M., Otani, H., Saint-Jeannet, J.-P. and Dawid, I. B. (1994). Role of the LIM class homeodomain protein Xlim-1 in neural and muscle induction by the Spemann organizer in Xenopus. *Nature* **372**, 677-679.

Tanabe, Y. and Jessell, T. M. (1996). Diversity and Pattern in the Developing Spinal Cord. *Science* **274**, 1115-1123.

Thaler, J. P., Koo, S. J., Kania, A., Lettieri, K., Andrews, S., Cox, C., Jessell, T. M. and Pfaff, S. L. (2004). A Postmitotic Role for Isl-Class LIM Homeodomain Proteins in the Assignment of Visceral Spinal Motor Neuron Identity. *Neuron* **41**, 337-350.

Thaler, J. P., Lee, S.-K., Jurata, L. W., Gill, G. N. and Pfaff, S. L. (2002). LIM Factor Lhx3 Contributes to the Specification of Motor Neuron and Interneuron Identity through Cell-Type-Specific Protein-Protein Interactions. *Cell* **110**, 237-249.

Thompson, L., Barraud, P., Andersson, E., Kirik, D. and Bjorklund, A. (2005). Identification of Dopaminergic Neurons of Nigral and Ventral Tegmental Area Subtypes in Grafts of Fetal Ventral Mesencephalon Based on Cell Morphology, Protein Expression, and Efferent Projections. *The Journal of Neuroscience* **25**, 6467-6477.

Tsuchida, T., Ensini, M., Morton, S. B., Baldassare, M., Edlund, T., Jessell, T. M. and Pfaff, S. L. (1994). Topographic organization of embryonic motor neurons defined by expression of LIM homeobox genes. *Cell* **79**, 957-970.

Tzschentke, T. M. (2000). The medial prefrontal cortex as a part of the brain reward system. *Amino Acids* **19**, 211-219.

Van den Heuvel, D. M. A. and Pasterkamp, R. J. (2008). Getting connected in the dopamine system. *Progress in Neurobiology* **85**, 75-93.

van den Munckhof, P., Luk, K. C., Ste-Marie, L., Montgomery, J., Blanchet, P. J., Sadikot, A. F. and Drouin, J. (2003). Pitx3 is required for motor activity and for survival of a subset of midbrain dopaminergic neurons. *Development* **130**, 2535-2542.

van Meyel, D. J., Thomas, J. B. and Agulnick, A. D. (2003). Ssdp proteins bind to LIM-interacting co-factors and regulate the activity of LIM-homeodomain protein complexes in vivo. *Development* **130**, 1915-1925.

Vernay, B., Koch, M., Vaccarino, F., Briscoe, J., Simeone, A., Kageyama, R. and Ang, S.-L. (2005). Otx2 Regulates Subtype Specification and Neurogenesis in the Midbrain. *J. Neurosci.* **25**, 4856-4867.

Verney, C. (1999). Distribution of the catecholaminergic neurons in the central nervous system of human embryos and fetuses. *Microscopy Research and Technique* **46**, 24-47.

Verney, C., Zecevic, N. and Puelles, L. (2001). Structure of longitudinal brain zones that provide the origin for the substantia nigra and ventral tegmental area in human

embryos, as revealed by cytoarchitecture and tyrosine hydroxylase, calretinin, calbindin, and GABA immunoreactions. *The Journal of Comparative Neurology* **429**, 22-44.

Vitalis, T., Cases, O., Engelkamp, D., Verney, C. and Price, D. J. (2000). Defects of Tyrosine Hydroxylase-Immunoreactive Neurons in the Brains of Mice Lacking the Transcription Factor Pax6. *J. Neurosci.* **20**, 6501-6516.

Vogel, A., Rodriguez, C., Warnken, W. and Belmonte, J. C. I. (1995). Dorsal cell fate specified by chick Lmx1 during vertebrate limb development. *Nature* **378**, 716-720.

Vollrath, D., Jaramillo-Babb, V. L., Clough, M. V., McIntosh, I., Scott, K. M., Lichter, P. R. and Richards, J. E. (1998). Loss-of-function mutations in the LIM-homeodomain gene, LMX1B, in nail-patella syndrome. *Hum Mol Genet* **7**, 1091-8.

Voorn, P., Kalsbeek, A., Jorritsma-Byham, B. and Groenewegen, H. J. (1988). The pre- and postnatal development of the dopaminergic cell groups in the ventral mesencephalon and the dopaminergic innervation of the striatum of the rat. *Neuroscience* **25**, 857-887.

Wadman, I., Li, J., O.Bash, R., Forster, A., Osada, H., Rabbitts, T. H. and Baer, R. (1994). Specific in vivo association between the bHLH and LIM proteins implicated in human T cell leukemia. *EMBO J* **13**, 4831-9.

Wahlsten, D., Lyons, J. P. and Zagaja, W. (1983). Shaker short-tail, a spontaneous neurological mutant in the mouse. *J Hered* **74**, 421-425.

Wallén, Å., Zetterström, R. H., Solomin, L., Arvidsson, M., Olson, L. and Perlmann, T. (1999). Fate of Mesencephalic AHD2-Expressing Dopamine Progenitor Cells in Nurr1 Mutant Mice. *Experimental Cell Research* **253**, 737-746.

Wang, M. and Drucker, D. J. (1995). The LIM Domain Homeobox Gene isl-1 Is a Positive Regulator of Islet Cell-specific Proglucagon Gene Transcription. *J. Biol. Chem.* **270**, 12646-12652.

Wang, M. Z., Jin, P., Bumcrot, D. A., Marigo, V., McMahon, A. P., Wang, E. A., Woolf, T. and Pang, K. (1995). Induction of dopaminergic neuron phenotype in the midbrain by Sonic hedgehog protein. *Nat Med* **1**, 1184-1188.

Way, J. C. and Chalfie, M. (1988). mec-3, a homeobox-containing gene that specifies differentiation of the touch receptor neurons in C. elegans. *Cell* **54**, 5-16.

Wilkinson, D. G., Bailes, J. A. and McMahon, A. P. (1987). Expression of the proto-oncogene int-1 is restricted to specific neural cells in the developing mouse embryo. *Cell* **50**, 79-88.

Wilson, P. A. and Hemmati-Brivanlou, A. (1997). Vertebrate Neural Induction: Inducers, Inhibitors, and a New Synthesis. *Neuron* **18**, 699-710.

Wolberger, C., Vershon, A. K., Liu, B., Johnson, A. D. and Pabo, C. O. (1991). Crystal structure of a MAT[alpha]2 homeodomain-operator complex suggests a general model for homeodomain-DNA interactions. *Cell* **67**, 517-528.

Wong, A. H. and Van Tol, H. H. (2003). Schizophrenia: from phenomenology to neurobiology. *Neurosci Biobehav Rev* **27**, 269-306.

Wurst, W., Auerbach, A. B. and Joyner, A. L. (1994). Multiple developmental defects in Engrailed-1 mutant mice: an early mid-hindbrain deletion and patterning defects in forelimbs and sternum. *Development* **120**, 2065-75.

Xu, Z., Meng, X., Cai, Y., Liang, H., Nagarajan, L. and Brandt, S. J. (2007). Single-stranded DNA-binding proteins regulate the abundance of LIM domain and LIM domain-binding proteins. *Genes Dev.* **21**, 942-955.

Xue, D., Tu, Y. and Chalfie, M. (1993). Cooperative Interactions Between the Caenorhabditis elegans Homeoproteins UNC-86 and MEC-3. *Science* **261**, 1324-1328.

Ye, W., Shimamura, K., Rubenstein, J. L., Hynes, M. A. and Rosenthal, A. (1998). FGF and Shh signals control dopaminergic and serotonergic cell fate in the anterior neural plate. *Cell* **93**, 755-66.

Yeo, S. L., Lloyd, A., Kozak, K., Dinh, A., Dick, T., Yang, X., Sakonju, S. and Chia, W. (1995). On the functional overlap between two Drosophila POU homeo domain genes and the cell fate specification of a CNS neural precursor. *Genes Dev.* **9**, 1223-1236.

Yokota, Y. (2001). Id and development. *Oncogene* **20**, 8290-8.

Yoshihara, Y., Mizuno, T., Nakahira, M., Kawasaki, M., Watanabe, Y., Kagamiyama, H., Jishage, K.-i., Ueda, O., Suzuki, H., Tabuchi, K. et al. (1999). A Genetic Approach to Visualization of Multisynaptic Neural Pathways Using Plant Lectin Transgene. *Neuron* **22**, 33-41.

Zechner, D., Fujita, Y., Hulsken, J., Muller, T., Walther, I., Taketo, M. M., Bryan Crenshaw, I. E., Birchmeier, W. and Birchmeier, C. (2003). [beta]-Catenin signals regulate cell growth and the balance between progenitor cell expansion and differentiation in the nervous system. *Developmental Biology* **258**, 406-418.

Zervas, M., Millet, S., Ahn, S. and Joyner, A. L. (2004). Cell Behaviors and Genetic Lineages of the Mesencephalon and Rhombomere 1. *Neuron* **43**, 345-357.

Zhao, S., Maxwell, S., Jimenez-Beristain, A., Vives, J., Kuehner, E., Zhao, J., O'Brien, C., de Felipe, C., Semina, E. and Li, M. (2004). Generation of embryonic stem cells and transgenic mice expressing green fluorescence protein in midbrain dopaminergic neurons. *European Journal of Neuroscience* **19**, 1133-1140.

Zhao, Y., Kwan, K.-M., Mailloux, C. M., Lee, W.-K., Grinberg, A., Wurst, W., Behringer, R. R. and Westphal, H. (2007). LIM-homeodomain proteins Lhx1 and Lhx5, and their cofactor Ldb1, control Purkinje cell differentiation in the developing cerebellum. *Proceedings of the National Academy of Sciences* **104**, 13182-13186.

Zhao, Y., Malik, N. and Westphal, H. (2006a). Functions of LIM-homeodomain proteins in the development of the nervous system. In *Transcription factors in the nervous system*, (ed. G. Thiel), pp. 75-94. Weinheim: Wiley-VCH Verlag GmbH & Co. KGaA.

Zhao, Y., Marin, O., Hermesz, E., Powell, A., Flames, N., Palkovits, M., Rubenstein, J. L. R. and Westphal, H. (2003). The LIM-homeobox gene Lhx8 is required for the development of many cholinergic neurons in the mouse forebrain. *Proceedings of the National Academy of Sciences* **100**, 9005-9010.

Zhao, Y., Morales, D. C., Hermesz, E., Lee, W.-K., Pfaff, S. L. and Westphal, H. (2006b). Reduced expression of the LIM-homeobox gene Lhx3 impairs growth and differentiation of Rathke's pouch and increases cell apoptosis during mouse pituitary development. *Mechanisms of Development* **123**, 605-613.

Zhao, Y., Sheng, H. Z., Amini, R., Grinberg, A., Lee, E., Huang, S., Taira, M. and Westphal, H. (1999). Control of Hippocampal Morphogenesis and Neuronal Differentiation by the LIM Homeobox Gene Lhx5. *Science* **284**, 1155-1158.

Zhao, Z.-Q., Scott, M., Chiechio, S., Wang, J.-S., Renner, K. J., Gereau, R. W. I. V., Johnson, R. L., Deneris, E. S. and Chen, Z.-F. (2006c). Lmx1b Is Required for Maintenance of Central Serotonergic Neurons and Mice Lacking Central Serotonergic System Exhibit Normal Locomotor Activity. *J. Neurosci.* **26**, 12781-12788.

Zhou, Q.-Y. and Palmiter, R. D. (1995). Dopamine-deficient mice are severely hypoactive, adipsic, and aphagic. *Cell* **83**, 1197-1209.